SYNTHESIS AND BIOLOGICAL ACTIVITIES OF IMIDAZOLIUM ACRIDINES AND THEIR SILVER COMPLEXES

OLLA H S SHARHAN

FACULTY OF SCIENCE
UNIVERSITI MALAYA
KUALA LUMPUR

2020

SYNTHESIS AND BIOLOGICAL ACTIVITIES OF IMIDAZOLIUM ACRIDINES AND THEIR SILVER COMPLEXES

OLLA H S SHARHAN

THESIS SUBMITTED IN FULFILMENT OF THE REQUIREMENTS FOR THE DEGREE OF DOCTOR OF PHILOSOPHY

DEPARTMENT OF CHEMISTRY
FACULTY OF SCIENCE
UNIVERSITI MALAYA
KUALA LUMPUR

2020

UNIVERSITI MALAYA

ORIGINAL LITERARY WORK DECLARATION

Name of Candidate: **OLLA HASSAN SALEH SHARHAN**

Matric No**: SHC150050**

Name of Degree: **DOCTOR OF PHILOSOPHY**

Title of Thesis ("This work"):

SYNTHESIS AND BIOLOGICAL ACTIVITIES OF IMIDAZOLIUM ACRIDINES AND THEIR SILVER COMPLEXES

Field of Study:

INORGANIC CHEMISTRY

I do solemnly and sincerely declare that:

(1) I am the sole author/writer of this Work;
(2) This Work is original;
(3) Any use of any work in which copyright exists was done by way of fair dealing and for permitted purposes and any excerpt or extract from, or reference to or reproduction of any copyright work has been disclosed expressly and sufficiently and the title of the Work and its authorship have been acknowledged in this Work;
(4) I do not have any actual knowledge nor do I ought reasonably to know that the making of this work constitutes an infringement of any copyright work;
(5) I hereby assign all and every right in the copyright to this Work to the University of Malaya ("UM"), who henceforth shall be owner of the copyright in this Work and that any reproduction or use in any form or by any means whatsoever is prohibited without the written consent of UM having been first had and obtained;
(6) I am fully aware that if in the course of making this Work, I have infringed any copyright whether intentionally or otherwise, I may be subject to legal action or any other action as may be determined by UM.

Candidate's Signature Date:

Subscribed and solemnly declared before,

Witness's Signature Date:

Name:

Designation:

SYNTHESIS AND BIOLOGICAL ACTIVITIES OF IMIDAZOLIUM ACRIDINES AND THEIR SILVER COMPLEXES

ABSTRACT

In the present study, a series of acridine-based imidazolium ligands were synthesized by the Menshutkin reaction and used for the preparation of the silver complexes. The structures were established using NMR and IR spectroscopy as well as high-resolution mass spectrometry. The purity of the ligands was confirmed by CHN elemental analysis, while energy-dispersive X-ray spectroscopy (EDX) was applied for the silver complexes. In view of the luminescent behaviour of acridine, UV-Vis and fluorescence spectra were recorded for ligands and complexes. However, low water solubility constrains potential application as analytical probe. Preliminary *in vitro* cytotoxicity screenings were performed using an MTT assay against three cancer and two non-tumorigenic cell lines. All compounds showed low toxicity on normal cell lines, while the anticancer activity varied with the cancer cell lines. The complexes exhibited higher activities than the ligands. Incorporation of aromatic structures at the imidazolium substituent typically enhances the activity. All compounds were evaluated for antioxidant activity by using DPPH and FRAP assays. However, practically the FRAP results indicated low activities compared to the reference compound (ascorbic acid). The antibacterial activity of benzimidazolium-based acridine salts and their complexes was screened against standard strains of Gram-positive and Gram-negative bacteria using the disc diffusion method as well as minimum inhibitory concentration (MIC) and minimum bactericidal concentration (MBC) assays. Most compounds were effective against the tested bacteria, while the complexes exhibited higher activities than the ligands.

Keyword: 9-aminoacridine derivatives, Menshutkin reaction, N-heterocyclic carbene complex, anticancer, antibacterial

SYNTHESIS DAN AKTIVITI BIOLOGI AKRIDINA IMIDAZOLIUM DAN KOMPLEKS PERAKNYA

ABSTRAK

Di dalam kajian ini, suatu siri sebatian imidazolium berdasarkan akridina telah disintesiskan melalui tindakbalas Menshutkin dan digunakan untuk penyediaan kompleks perak. Strukturnya telah dikenalpasti menggunakan spektroskopi NMR dan IR serta spektroskopi jisim resolusi tinggi. Ketulenan ligan telah dipastikan melalui analisis unsur CHN, sementara itu spektroskopi sinaran-X sebaran tenaga telah digunakan untuk kompleks perak. Spektra UV-Vis dan fluoresen telah direkodkan untuk sebatian ligans dan kompleks Namun, keterlarutan di dalam air yang rendah menghadkan aplikasi sebagai prob analitikal. Penyaringan sitotoksisiti *in vitro* telah dilakukan menggunakan ujian MTT terhadap tiga titisan sel kanser dan dua titisan sel bukan-tumorigenik. Semua sebatian menunjukkan ketoksikan yang rendah terhadap titisan sel kanser yang normal, sementara itu, kepelbagaian aktiviti antikanser dengan titisan sel kanser. Kompleks itu menunjukkan aktiviti yang tinggi berbanding ligans. Penggabungan struktur-struktur aromatik pada penukar ganti imidazolium biasaannya meningkat akan aktiviti tersebut. Semua sebatian dinilai untuk aktiviti antioksidan melalui ujian-ujian DPPH dan FRAP. Namun, secara praktikalnya keputusan ujian FRAP menunjukkan aktiviti yang rendah berbanding sebatian rujukan (asid askorbik). Aktiviti antibakteria untuk garam akridina berdasarkan benzimidazolium dan kompleks tersebut mereka telah disaring terhadap strain bakteria piawai Gram-positif dan Gram-negatif menggunakan kaedah peresapan cakera serta kepekatan perencatan minimum (MIC) dan ujian kepekatan bakterisidal minimal (MBC). Kebanyakan sebatian adalah efektif terhadap ujian bakteria, sementara komplek-komplek menunjukkan aktiviti yang tinggi berbanding ligan.

Katakunci: 9-aminoakridina, tindakbalas Menshutkin, komplek karbena N-heterosiklik, antikanser, antibakteria

ACKNOWLEDGEMENTS

In the name of Allah, most gracious, most merciful. All praise and glory to Allah the Almighty who alone made this thesis to be accomplished. I feel honoured and privileged to glorify his name in the sincerest way through this accomplishment and ask him to accept my efforts.

I would like to dedicate my heartfelt gratitude to my supervisor Professor Dr. Thorsten Heidelberg for his invaluable guidance throughout the entire course of this work. I have no words to thank him for his kind and humble gesture towards my research work, accepting and rectifying my every mistake with great patience and generosity. Without his helping hands, my dream to complete doctorate studies would not have materialized. I am speechless as I speak of his greatness. I would also like to extend my deepest gratitude to my supervisor Professor Dr. Hapipah Mohd Ali and Professor Dr. Najihah for their excellent guidance throughout the entire course of this work. In addition, I would like to express my earnest appreciation for their valuable advices and motivation ever since my Ph. D days in Universiti Malaya. They have always believed in my abilities and trusted me with several projects. Although these projects have been very challenging, they served as stepping-stones for intellectual and professional advancement.

My deepest gratitude and thankful to my parents who I can't thank them as they deserve and my brothers (Obadi, Safi and Hasan) and my sisters (Nawal and Yasar) for their constant motivation, patience, encouragement, and love. Also, I want to thank all friends who have supported me all the way especially Aisha, my home mate Soher, Fatima, Wafa and Boshra who always support me and make my life beautiful. Thanks to the Ministry of Higher Education, Thamar University for the support me to do my PhD.

I am thankful to my colleagues in organic synthesis lab (Dr. Ean Wai, Dr. Abbas, Abdul Qaiyum and NMR and LC-Mass lab staff members and the all staffs in Department of Chemistry-Universiti Malaya for their help during this research work.

In short, sincere acknowledgement is conveyed again for all of above for assisting me to achieve my research goal.

TABLE OF CONTENTS

LIST OF FIGURES

LIST OF SCHEMES

LIST OF TABLES

LIST OF SYMBOLS AND ABBREVIATIONS

Å	:	Angstrom
a.u.	:	Atomic unit
δ	:	Chemical shift
λ_{max}	:	Maximum wavelength
2-bromobenzyl	:	*o* Br-Bn
2PABA	:	2-phenylamino benzoic acid
4-bromobenzyl	:	*p* Br-Bn
4-methylbenzyl	:	*p* Me-Bn
4-nitrobenzyl	:	*p* NO_2-Bn
AA	:	Ascorbic Acid
APT	:	^{13}C-Attached proton test
ATCC	:	American Type Culture Collection
BHT	:	Butylated hydroxytoluene (2,6-bis(1,1-dimethylethyl) -4-methylphenol
Bn	:	Benzyl
bs	:	Broad singlet
CC	:	Central canal
CH_2Cl_2 / DCM	:	Dichloromethane
CHN	:	Elemental Analysis
Compd.	:	Compound
d	:	Doublet
dd	:	Double doublet
ddd	:	Double double doublet
DFT	:	Density Functional Theory
DMF	:	*N*, *N*-dimethylformamide

DMSO	:	Dimethyl sulfoxide
DPPH	:	1,1-Diphenyl-2-picryl-hydrazyl
dt	:	Double triplet
E. coli	:	*Escherichia coli*
EDX	:	Energy dispersive X-ray analysis
eq	:	Equatorial
ESI	:	Electrospray io*n*ization
FBS	:	Fetal Bovine Serum
FRAB	:	Ferric Reducing Antioxidant Power
FTIR	:	Fourier-transform infrared spectroscopy
HRP	:	Horseradish peroxidase
Hz	:	Hertz
IC_{50}	:	Half-maximal inhibitory concentration
J	:	Coupling constant
LCMS	:	Liquid chromatography–mass spectrometry
m	:	Multiple
MeCN	:	Acetonitrile
mp	:	Melting point
MBC	:	Minimum Bactericidal Concentration
MCF-10a	:	non-tumorigenic breast cells
MCF-7	:	Breast cancer cells
MIC	:	Minimum Inhibitory Concentration
MNR	:	Nuclear Magnetic Resonance
MTT	:	3-[4,5-dimethylthiazol-2yl]-diphenyl tetrazolium bromide
NA	:	No activity
NHCs	:	N-heterocyclic carbenes

P. aeruginosa	:	*Pseudomonas aeruginosa*
PBS	:	Phosphate buffered saline
PC-3	:	Prostate adenocarcinoma cells
ppm	:	part per million
s	:	Singlet
S. aureus	:	*Staphylococcus aureus*
S. epidermidis	:	*Staphylococcus epidermidis*
S. typhi	:	*Salmonella typhi*
t	:	Triplet
T1074	:	non-tumorigenic ovarian cells
THF	:	Tetrahydrofuran
TLC	:	Thin Layer Chromatography
UV	:	Ultraviolet
UV-Vis	:	Ultraviolet–visible spectroscopy

LIST OF APPENDICES

CHAPTER 1: INTRODUCTION

1.1 Background

Medicinal compounds have become more important in primary health care especially in developing countries (Mutee et al., 2010). Several pharmacognostic and pharmacological investigations were carried out to develop new drugs or discover new chemical structures for the development of novel therapeutic agents for the treatment of human diseases, such as infectious diseases and cancer (Garcia et al., 2010; Newman et al., 2003). Noteworthy, N-heterocyclic compounds represent a very important class of compounds, which have received considerable attention as core structures and widely used in scientific materials and medicinal chemistry (Zhou et al., 2016b; Gao et al., 2015), leading to an interest in the development of sustainable, convenient, efficient and environmentally benign synthetic methods for the construction of nitrogen-containing heterocycles (Zhou et al., 2016b).

Acridine (a polycyclic compound), is alkaloid that has been found in natural products, and it is one of the abundant compounds that exhibits a biological activity and used for chemotherapy and treatment of many diseases (Benoit et al., 2014; Nowak, 2017; Pereira et al., 2017; Perez et al., 2017). In fact, acridines are used as biological fluorescent probes and anti-bacterial drugs (Afzal et al., 2016; Bongarzone & Bolognesi, 2011; Charmantray & Martelli, 2001; Galdino-Pitta et al., 2013; Kumar et al., 2013b). Since the therapeutic potential is strongly related to its specific interactions with proteins (Demeunynck, 2004), the medicinal effect of acridine compounds has been associated with π-stacking interactions with nucleic acids (Baruah et al., 2002; Liu et al., 2006), leading to concerns of long-term carcinogenic effects of acridine drugs (Byvaltsev et al., 2019). In addition, recent investigations suggest the contribution of interactions with proteins for the therapeutic potential of acridines (Demeunynck, 2004). For such reasons, the synthesis of acridines and their analogues have attracted a great deal of attention to both medicinal

and organic chemists. Moreover, the modification of acridine by metalation is an interesting field for researchers in their quest to discover new potent anticancer and antibacterial agents (Perez et al., 2017). The complexes of silver cations (Ag(I)-complexes) have gained interest due to their anticancer activity (Gandin et al., 2013; Haque et al., 2015b; Hussaini et al., 2019; Ray et al., 2007; Dogan et al., 2011; Subramanya Prasad et al., 2017) and antimicrobial activities (Gok et al., 2014; Hindi et al., 2008; Streciwilk et al., 2014). Ag(I)-complexes with effective *in vivo* and *in vitro* anticancer activity have been established in many literature (Ozdemir et al., 2010; Salman et al., 2013a; Sarı et al., 2017; Wang et al., 2014). The antimicrobial activity of the Ag(I)-N-heterocyclic carbenes (Shahini et al., 2017) is attributed to the effect of Ag^+ against a wide range of microorganisms (Garrison & Youngs, 2005; Shahini *et al.,* 2018). Unlike the complexes based on phosphine-ligands, N-heterocyclic carbenes (NHCs) are strong σ-donors and weak π-acceptors. Therefore, they enable the preparation of complexes comprising a strong M–C bond with transition metal ions. This transfer to high chemical stability in terms of oxygen and water tolerance, comparable to complexes based on phosphine ligands. However, unlike the phosphine analogues, NHC compounds exhibited low toxicity at the same time (Ozdemir et al., 2010).

In addition, Ag(I)-NHCs have received significant attention due to their high stability and slow release of silver ions to the diseased area from Ag(I)-NHC complexes. In fact, combining silver salts with organic ligands may result in complexes with a broad spectrum of antimicrobial activity (Feio et al., 2014; Kora & Rastogi, 2013; Medici et al., 2015; Morones-Ramirez et al., 2013; Nunez et al., 2014). Similarly, imidazolium ligands are heterocyclic compounds with good activity against pathogenic microorganisms. Their activity is increased in the presence of Ag ions (Kalinowska-Lis et al., 2015), leading to the current investigation in which acridine was combined with imidazolium-based heterocyclic carbene complexes. The expansion of the heterocyclic ring hosting the

carbene provides the opportunities for modified biochemical interactions to increase medicinal activity or selectivity for these compounds. Besides simple imidazolium-based NHCs, the benzimidazolium analogues have also gained medicinal interest (Dogan et al., 2011; Subramanya Prasad et al., 2017).

In this study, a series of imidazolium and benzimidazolium-based acridines were synthesized and converted into Ag(I) complexes. The identity of ligands and complexes was confirmed by infrared spectroscopy (IR), nuclear magnetic resonance (NMR) and high-resolution mass spectrometry (HRMS), while analysis of compound purity by elemental analyses and energy dispersive X-ray (EDX) spectrum. In addition, investigations of optical properties (UV-Vis absorption and fluorescence), as well as antioxidant and biological activities addressing bacteria and cancer, round up the investigation.

1.2 Objectives of the thesis

The scope of this research covers synthesis, characterization, as well as the study of the optical properties and biological activities. The objectives are:

i. To synthesize and characterize imidazolium derivatives of acridine.
ii. To prepare Ag(I)- carbene complexes with the ligands.
iii. To evaluate the antioxidant, antibacterial and cytotoxicity of the synthesized ligands and complexes.

1.3 Thesis outline

This thesis is divided into five chapters. Chapter one gives a brief introduction to the research background including the objectives of the study. Chapter two presents a review of related literature and covers the basic theory and experimental background of the biological activity of 9-chloroacridine and its derivatives with imidazolium ligands and metal complexes. Chapter three discusses the experimental methods for the synthesis as depicted in **Figure 1.1** and the characterization applied in this study. This chapter also covers the protocols for biological property studies, such as antioxidant, anticancer and antibacterial activities. Chapter four is subdivided into two sections; the first part emphasizes the synthesis of ligands and their silver complexes, while the second part addresses the biological activity of the compounds. Lastly, the conclusion and recommendations for future work related to this research are provided in chapter five. The experimental data and selected spectra are located in the appendices.

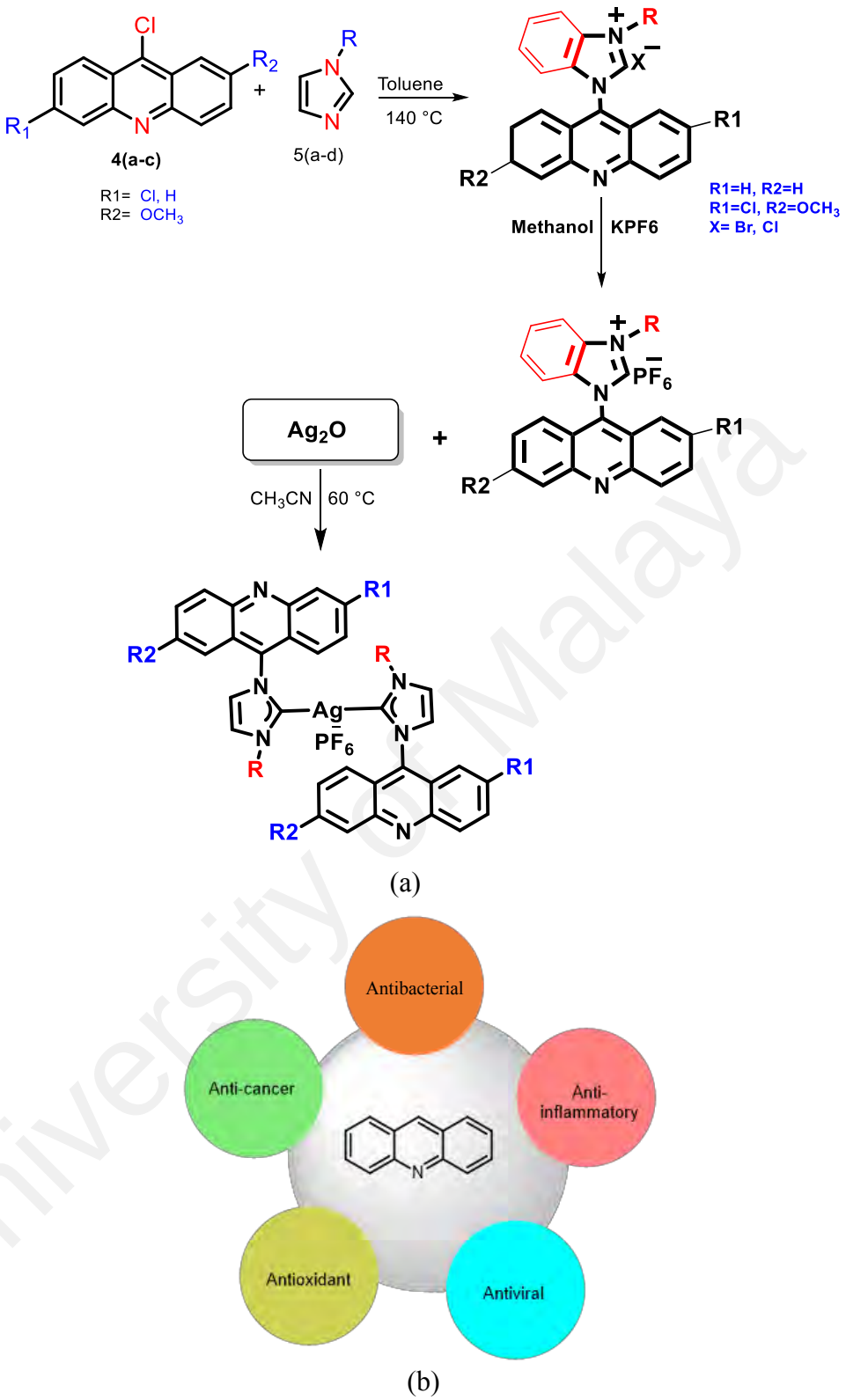

Figure 1.1: Synthetic pathways (a) and optional application of acridine (b)

CHAPTER 2: LITERATURE REVIEW

2.1 Biological background

2.1.1 Antioxidant

Oxidants are reactive molecules that are produced both inside the body and the environment that can react with other cellular molecules in your body such as protein, DNA and lipids. Free radicals such as reactive oxygen species (ROS) are chemically active due to own unpaired electron such as hydroxyl radicals (OH-), hydrogen peroxide (H_2O_2) and superoxide radicals (O^{2-}) (Ahmad et al., 2013). **Figure 2.1** shows how the free radicals grabbing the electrons from rich electronic molecules in order to reach stability (Alfadda & Sallam, 2012; Lobo et al., 2010). These free radicals is produced from extracellular environmental sources such as pollutants, tobacco, smoke, drugs, xenobiotics, and radiation (Valacchi et al., 2012). Excessive production of ROS is associated with pathological situations including glucose homeostasis, inflammation, cellular lifespan, multiple aging-related diseases and cancer. As a result of the previously mentioned reasons, the importance of antioxidant is increasing day by day.

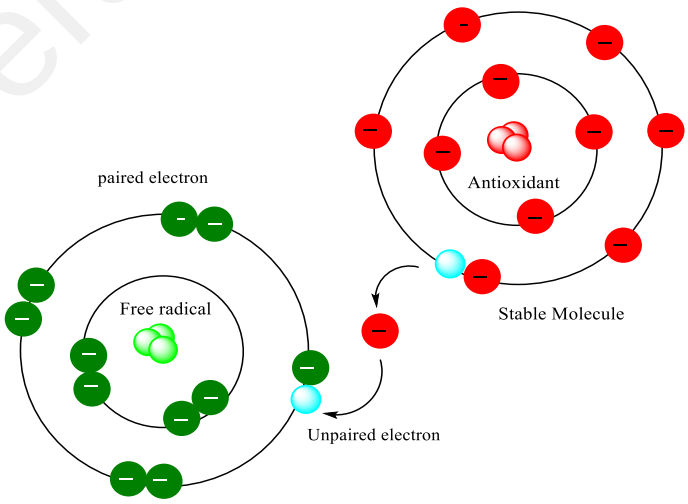

Figure 2.1: Propose structure for free radical as unstable atoms (Lobo et al., 2010)

Antioxidants are natural or synthetic substances that may prevent or delay these damages to cell membranes and other cellular structures. Therefore, antioxidants can be used as food preservatives to protect it from deleterious effects of oxidation reactions. Antioxidants are compounds that can inhibit oxidation reaction producing free radicals (unstable molecules) that may affect the living cells by causing damages in the DNA and as well as oxidizing polyunsaturated fatty acids, amino acids, and the co-factors of some enzymes. Due to their high chemical reactivity, Free radical damage may lead to cancer (Nguyen, 2015; Rippe, 2013). Therefore, antioxidants neutralized the liberated free radicals during the oxidation reactions (Kryston et al., 2011).

For determination of the antioxidant potential of synthetic compounds, many analytical methods have been developed. A variety of analytical methods can be applied to assess the antioxidant activity of compounds (Gupta et al., 2009; Wang et al., 2004; Yehye et al., 2015). The most suitable methods should be selected according to their targeting information, costs and sensitivities. The antioxidant capacity and activity can be measured by ability assay that determine the antioxidants to protect a fluorescent molecules from damage by free radicals (Apak et al., 2007; Turrens, 2003). Common free radical scavenging assays are: ORAC (Oxygen Radical Absorption Capacity) (Dudonne et al., 2009; Ou et al., 2001), ABTS [2,2'-Azino-bis(3-ethylbenzthiazoline-6-sulphonic acid)] (Apak et al., 2016; Cano et al., 2002), Ferric Reducing Antioxidant Power assay (FRAP) and 2,2-diphenyl-1-picrylhydrazyl (DPPH•) radical scavenging assay (Carocho & Ferreira, 2013; Forman et al., 2010; Huang et al., 2005; Sharma & Bhat, 2009; Thaipong et al., 2006). Antioxidant activity is a complex feature, reflecting different mechanistic pathways. These cannot be evaluated using a single test; typically, two commonly applied assays with differing in their working principles are, hence, applied. (Zugic et al., 2016). One of them determines the antioxidant activity by neutralization of coloured DPPH radicals *via* the transfer of hydrogen radicals, leading to

a discolouration that can be measured photometrically (Zugic et al., 2014). The radical-focus of the assay reflects cellular damage processes caused by singlet and triplet oxygen, as well as decomposition of peroxides (Haque et al., 2013b; Sorrenti et al., 2006).

In this study, the compounds were tested on their *in vitro* antioxidant activities using DPPH and FRAP assays. The FRAP assay is a simple, versatile and low-cost test, used to measure the reducing capacity of the ferric tripyridyltriazine complex to ferrous tripyridyltriazine by the transfer of a single electron from an antioxidant compound, according to equation (2.1):

$$[Fe(TPTZ)_2]^{3+} + Ar \xrightarrow{+e} [Fe(TPTZ)_2]^{2+} + Ar^{+\cdot} \qquad \textbf{(2.1)}$$

The reaction of antioxidant with the probe can be monitored by the intense blue colour of $Fe(TPTZ)_2]^{3+}$ with an absorption maximum at 593 nm. Data are reported in terms of FRAP value (Yehye et al., 2015). It is utilized as an indicator to track the endpoint of reactions *i.e.* the reducing capacity. However, the radical scavenging capability of a compound is not directly reflected (Forman et al., 2010; Huang et al., 2005).

The DPPH radical scavenging assay is the most common approach to determine antioxidant activity. DPPH is a stable nitrogen-containing organic free radical capable of accepting an electron or hydrogen radical to become a stable anion or molecule, respectively. However, DPPH molecule is relatively stable due to the delocalization of the unpaired electrons over the entire structure, as shown in **Figure 2.2** (Baydar et al., 2007; Rice-Evans et al., 1996; Valko et al., 2006)**.** When an antioxidant neutralizes the DPPH radical, the colour of the solution changes from deep purple to light yellow at maximum absorption (λmax) of 515 nm, which is reflected in the purple colour of the solution. The molecular absorbance λ_{max} shift to shorter wavelength upon radical

scavenging resulted in a colour change from deep purple to yellow (Carocho & Ferreira, 2013; Sharma & Bhat, 2009).

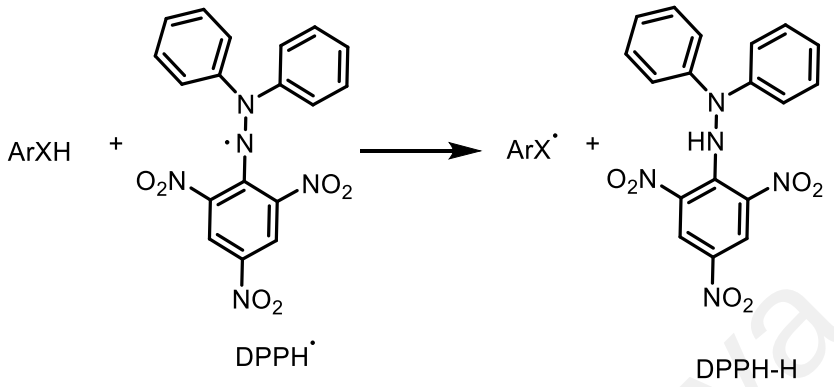

Figure 2.2: The antioxidant (ArXH) with DPPH reactions

Ascorbic acid, or vitamin C, is a hydrophilic antioxidant used as reference compounds. It can effectively reduce the DPPH radical *via* the transfer of an electron. Donation of an additional electron leads to the formation dehydroascorbate, which is not stable and breaks down to threonic and oxalic acids. (Diplock, 1994; Du et al., 2012).

2.1.2 Antibacterial activity

More than 100 years ago, Christian Gram (1884) has classified all bacteria into two large groups, i.e. Gram-negative and Gram-positive. Gram-negative bacteria have a thin cell wall peptidoglycan layer and an outer lipid membrane, whereas Gram-positive bacteria have a thick cell wall peptidoglycan layer and no outer lipid membrane. Typically, Gram-negative are more dangerous bacteria, because their outer membrane is often hidden by a capsule or slime layer, which hides the antigens of the cell (Gram, 1884; Tang et al., 2019). Some examples of common Gram-negative bacteria include *Escherichia coli* and *Salmonella typhi*, while *Staphylococcus aureus*, *Staphylococcus epidermidis* and *Pseudomonas aeruginosa* are common Gram-positive bacteria. *Escherichia coli* (*E. coli*) normally lives in intestines of human and in the gut of some animals. Most types of *E. coli* are harmless and even help keep the digestive tract healthy. *E. coli* can cause very common infection in dividing urinary tract infection, diarrhoea, pneumonia, *etc*. *Salmonella typhi* (*S. typhi)* can cuase typhi fever, gastroenteritis, *etc. Staphylococcus aureus* (*S. aureus*) is the most dangerous type of staphylococcal bacteria that can cause skin, bone, bloodstream and heart valve infections. *Staphylococcus epidermidis* (*S. epidermidis*) cuases opportunistic infections and nosocomial sepsis (Tang et al., 2019).

Antibacterial agents affect the bacteria in four ways: (1) The inhibition or regulation of transglycosylase enzymes that participate in the cell wall biosynthesis: most bacteria produce a cell wall that is partly composed of a macromolecule called peptidoglycan, while human cells contain peptidoglycan. The cell wall functions are to provide structure support and protection for the cell. (2) Affection of the metabolism and repair of nucleic acid: antibiotics can target an enzyme called DNA gyrase in the bacteria. The DNA gyrase relaxes tightly wound chromosomal DNA, thereby allowing DNA replication to proceed. The DNA gyrases also presence humans and differ from the bacterial analogue and are

not affected by the antibiotic. (3) Interference of protein synthesis: the antibiotic inhibits bacterial growth by stopping protein biosynthesis. However, both bacteria and humans carry out protein synthesis on structures called ribosomes. It can cross the membranes of bacteria and accumulate in high concentrations in the cytoplasm. Then it binds to a single site on the ribosome and blocks a key RNA interaction. In human cells, it does not accumulate in sufficient concentrations to stop protein synthesis. (4) Ruination of membrane structure: disrupting the plasma membrane causes rapid depolarization (Chopra et al., 2001; Kohanski et al., 2010).

Many antibacterial agents have been developed and are available in the market, but their effectiveness has deteriorated over the years and failed to solve the problem of multidrug-resistant bacteria (Delhaes et al., 2002; Nicolaou et al., 2009; Youngs et al., 2012). In the light of above, organometallic compounds provide an attractive approach to curb the drug resistance problem and as can add antibacterial activity on top of the interaction of the purely organic parent drugs (Bandow & Metzler-Nolte, 2009; Youngs et al., 2012). Therefore, research on the metal compound as antibacterial is very interesting (Gasser et al., 2011; Peacock & Sadler, 2008).

The recognition of acridines as antimicrobial agents was firstly proposed by Ehrlich and Benda in 1912 (Browning et al., 1922; Wainwright, 2001) and their first clinical use of these agents was started in 1917 (Bongarzone & Bolognesi, 2011; Hamblin & Hasan, 2004; Wainwright, 2001). Microbial resistance to antibiotics has become a worldwide concern. As the number of resistant microbial strains is constantly increasing, the search for new antibacterial compounds becomes an urgent issue in medicinal chemistry (Kalinowska-Lis et al., 2015). Owing to the potential antimicrobial features of silver compounds, this study focuses on the preparation of silver complexes, resulting from the complexation Ag with organic ligands that exhibit antimicrobial properties. This may

result in obtaining complexes with broad spectra of activity (Feio et al., 2014; Kora & Rastogi, 2013; Medici et al., 2015; Morones-Ramirez et al., 2013; Nunez et al., 2014).

2.1.3 Anticancer activity

Cancer is a disorder that can affect any part of the body (Edwards et al., 2005). Cancer is one of the major causes of morbidity and mortality affecting the worldwide population, with about 14 million new cases of cancer-related deaths in 2012 (McGuire, 2016). Uncontrolled cell proliferation may lead to tumour progression. Thus, cancer chemotherapy has become an important focus area of research (Han et al., 2017; Matsuda et al., 2018). Development of cancer is poorly understood and diagnosed late. Cancer can lead to death, however, early detection of it may improve the disorder outcome (Bray et al., 2018; Kumar et al., 2017; Ribeiro et al., 2019). The transformation of healthy cells into cancerous cells through the biological process has become one of the vital research endeavours in the biomedical sciences (Kerru et al., 2017). The cancer therapy has grown over the years and new antitumoral drugs are developed to relieve patients from further suffering (Hanahan & Weinberg, 2011). The investigation on how the normal cells are transformed into malignant cells has become one of the vital research attempts in the biomedical sciences.

Chemotherapy is one of the most common treatment for cancer. It is used to kill cancer cells or stop them from growing and spreading to other parts of the body. Anticancer drugs work by targeting and killing rapidly dividing cells. The uncontrolled cell deviation is a key feature for all cancer types. However, chemotherapy will also affect healthy cells during natural mitosis. Therefore, cells that divide frequently, like hair, is typically affected by chemotherapy. DNA, which is the carrier of genetic information, is a major target for anticancer drugs; anticancer drugs can interfere with transcription and DNA replication, which is a major step in cell division. There are different ways of anticancer

drug binding. The first targets control of transcription factors and polymerases. The second applies small aromatic ligand molecules that bind to DNA double-helical structures. Intercalation can be defined as the process by which compounds containing planar aromatic or heteroaromatic ring systems are inserted between adjacent base pairs perpendicularly to the axis of the helix and without disturbing the overall stacking pattern due to Watson-Crick hydrogen bonding (Goftar et al., 2014). Many biological experiments have suggested that DNA is one of the primary cellular targets for many anticancer agents. Particularly, in cancer cells, DNA can be preferentially damaged, due to the interactions with anticancer agents, therefore inhibition/blockage of cell division causes cell death (Rakesh et al., 2019).

There are various types of common cancer such as breast, prostate and ovarian cancer. Breast cancer is the most common cancer in women worldwide and represents approximately 25% of all cancers in women and leading cause of death in the next few years (Deen et al., 2016; Farghadani et al., 2017; Ferlay et al., 2015; Siegel et al., 2015). Besides, ovarian cancer is responsible for 4% of women deaths from cancer. It has three broad subgroups such as stromal, epithelial and germ cell tumours. Each subgroup has different aetiologies and clinical behaviour. Treatment of malignancies includes a combination of surgery and chemotherapy (Alfarouk et al., 2015), but the relapse of cancer within 2 years of initial treatment remains the big problem.

Prostate cancer is the commonly cancer in men (Alfarouk et al., 2015), and can often be treated successfully. Recently, it was hypothesized that low levels of vitamin D may increase the risk of clinical prostate cancer. Although, some prostate cancers relatively grow slowly; some are quick-growing (Bray et al., 2010; Klotz, 2012).

2.2 Acridine and its derivatives

2.2.1 Biological applications of acridine and its derivatives

Acridine was firstly isolated in 1870 by Carl Grabe and Heinrich Caro and their antimicrobial property were discovered in 1917 by Ehrlich and Benda. The first use of acridine as therapeutic agent for tumours was during the 1970s. Acridine and its derivatives have good potential as pharmaceutical agents due to their remarkable biological activities (Chen et al., 2005; Guo et al., 2009; Kumar et al., 2013b; Rastogi et al., 2002). One of its applications addressed antioxidant behaviour. Makhaeva et al. studied the antioxidant activities of four groups of acridine derivatives, as illustrated in **Figure 2.3**, that demonstrated high radical-scavenging activities (Makhaeva et al., 2017). Dickens *et al.* reported particularly a strong antioxidant activity of 9-amino-acridine-propranolol **9-AAP** (Dickens et al., 2002). Recently, 9-(2-(1-arylethylidene)-hydrazinyl)-acridines were identified as potent antioxidant showing about 50% of the activity of vitamin E (Haider et al., 2019).

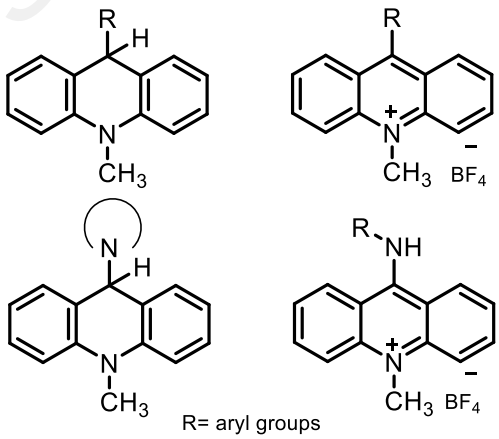

Figure 2.3: **Chemical structures of the acridine derivatives as antioxidants**

Acridine has been clinically used in the treatment of acute non-lymphocytic, lymphocytic and acute myeloid leukemias as a single agent or in combination with other antineoplastic drugs (Guo et al., 2009; Kumar et al., 2013a). The first developed of acridine based therapeutic agent for cancer treatment was specifically designed during the 1970s. Structural modifications on the acridine as depicted in **Figure 2.4**, have given rise to a wider therapeutic window for their anticancer and antibacterial properties, for example, the use of mepacrine (also called as quinacrine) as an alternative to quinine for treating malaria (Dickens et al., 2002; Gamage et al., 1997; Nadaraj et al., 2009).

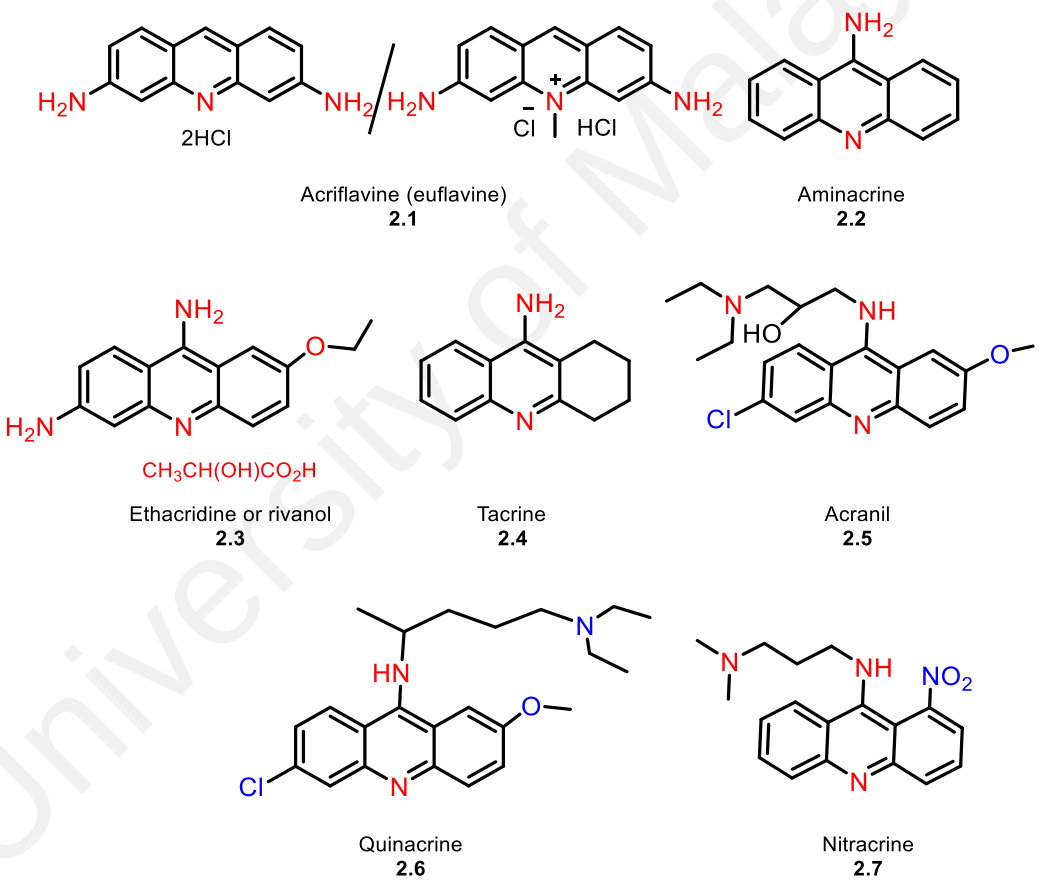

Figure 2.4: Chemical structures of acridine derivatives used as a therapeutic and antibacterial agent

Quinacrine and acranil were tested in clinical trials for different diseases and found to be highly efficient chemotherapeutic agents. They are very well tolerated by children, for whom no toxic effect at all was recorded (Cholewinski et al., 2011).

Among the acridine derivatives, 9-aminoacridines, as shown in **Figure 2.5**, exhibit a good anticancer activity with high selectivity towards tumourous cells. For example, 9-aminoacridine derivatives from testosterone have been designed and used as drugs against various cancers (L.Zhang et al., 2014). Also, pyrazoloacridine (PZA) demonstrated its capability to intercalate into DNA base pairs (Demeunynck, 2004) and it was applied to inhibit DNA topoisomerase II and the treatment of leukaemia disease (Antonini et al., 2001). Furthermore, the methoxy substitution of acridine ring helps to increase the reactivity of the compound towards the human breast carcinoma cell line; both 9-nitro and 9-hydroxyl substituents also exhibited significant tumour selectivity (Adjei, 1999).

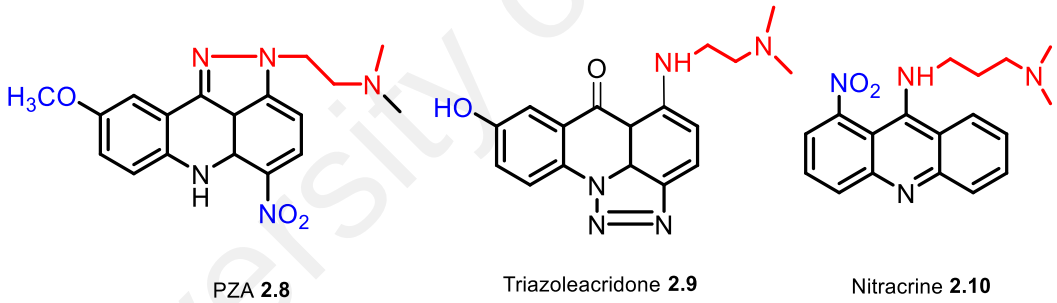

Figure 2.5: Chemical structures of 9-aminoacridine derivatives

In 1990, Cholody's group developed triazoleacridone as antitumor toward a wide range of tumours *in vitro* and *in vivo*. Applications included both mice and human colon carcinomas (Cholody et al., 1990). The 9-hydroxy substitution of triazoleacridone was identified as an important feature, effecting both activity and tumour selectivity (Philippe et al., 2007; Wesierska-Gadek et al., 2004). Nitracrine was used as clinical anticancer agent. Structure-activity relationship (SAR) analysis indicated that the nitro group on the

acridine at position 1 is critical for its anticancer activity (Belmont et al., 2007; Gniazdowski & Szmigiero, 1995).

Amsacrine (m-AMSA) as depicted in **Figure 2.6**, is a well-known antiproliferative agent, which is used to treat certain cancers including acute adult leukaemia (Chilin et al., 2009). The preliminary evaluation indicated a drastic reduction of the anticancer activity upon replacement of the acridine with an analogous quinoline system. Bagueley et al. (1984) modified the structure of m-AMSA to give asulacrine which improved efficacy against leukaemia and solid tumours in phase I/II clinical studies (Baguley et al., 1984; B.Zhang et al., 2014).

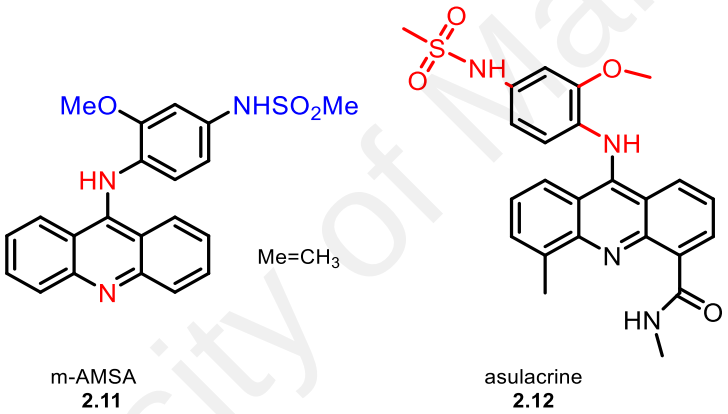

Figure 2.6: Structures of m-AMSA and asulacrine

Besides, 9-amino acridine derivatives partially hydrogenated analogues have been investigated as well. Tetrahydroacridine derivatives with 4-fluorobenzoamide- and 6-hydrazinonicotinamide substituents (**Figure 2.7**) enhanced the biological potency of acridine and reduce its side effects (Sondhi et al., 2013). The 4-fluorobenzoic acid derivatives were much more effective and exhibited good activities against human lung adenocarcinoma (A549) (IC_{50}= 9.6 - 31.3 µM) (Olszewska et al., 2014).

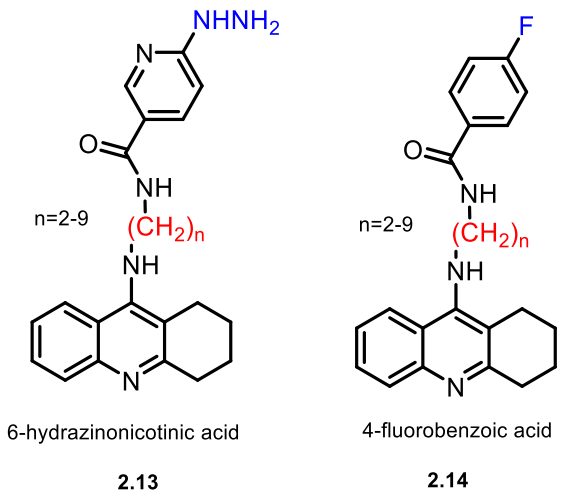

Figure 2.7: Structures of tetrahydro-9-aminoacridine derivatives

Figure 2.8 shows the chemical structure of the carbothioamide-acridine derivatives **2.15**, acridine derivatives-benzimidazole **2.16** and 9-benzylaminoacridine derivatives **2.17** as antiproliferative activity. Compounds **2.15** and **2.16** showed good antiproliferative activity with IC_{50} around 8.74 -41.1 µM (De Almeida et al., 2015; Gao et al., 2015; Liang et al., 2019), as well as good topoisomerase I inhibition activity (Zhang et al., 2016). While compound **2.17** displayed strong topoisomerase II inhibitory activity with low IC_{50} values against HCT-116 cells. The linkers between R-CH_2 groups and acridine maybe affected the bioactivity and the present of chloro and methoxy groups substituted at C-2 and C-6 of acridine ring was evaluated with good *in vitro* antiproliferative activity (Zhang et al., 2016). Another acridine derivatives with 4-carboxamide **2.18** which played interesting in medicinal chemists and appeared in many biologically active. The result indicated that substitution at 4-position may increase the anticancer activity against both the cell lines lung cancer (A-549), IC_{50} (325- 370 µg/ml) and cervical cancer (HeLa), IC_{50} (130-700 µg/ml) (Kumar et al., 2013a; Kumar et al., 2017).

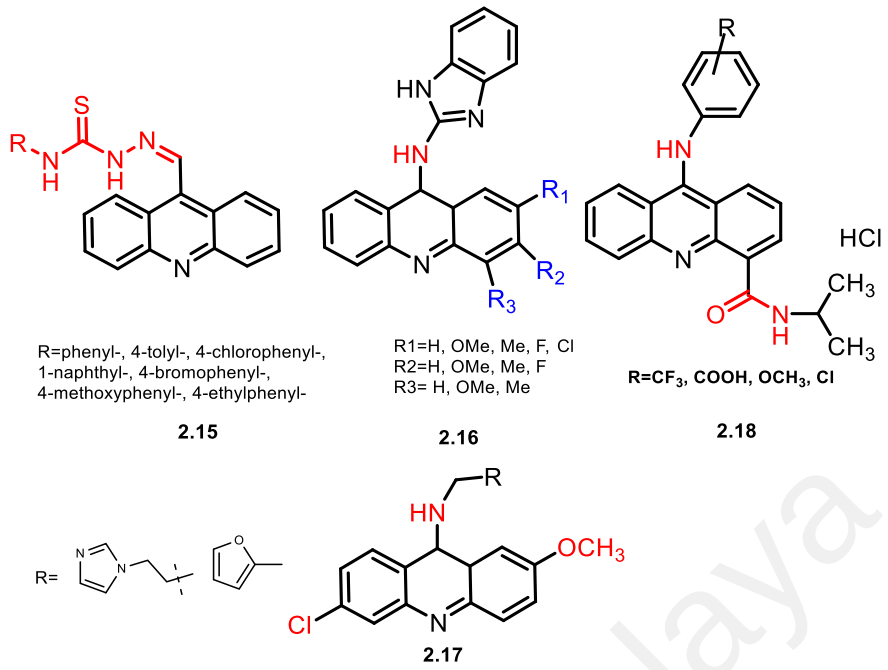

Figure 2.8: Chemical structures of antiproliferative acridine derivatives

Figure 2.9 shows the structural modification of the acridine core. Acridone derivative **2.19** showed good antiproliferative activity against CCRF-CEM cells with IC_{50} at 0.39 µM (Wang et al., 2013). Another acridone derivative, **2.20**, has shown moderate antimicrobial activity against *E.coil*, *S. aureus* and *P. aeruginosa* (Kudryavtseva et al., 2017).

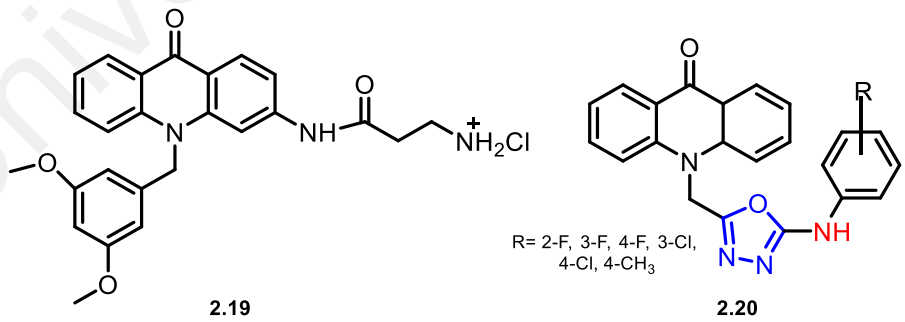

Figure 2.9: Chemical structures of acridone derivatives

In order to enhance the water solubility of acridine derivatives incorporating imidazolium substituents, as shown in **Figure 2.10**, have been reported (Prasad et al., 2016). The nitrogen donor sites at the imidazoliums and acridine played an important role to enhance the hydrogen bonding interaction capability with biomolecules. The compound **2.22** carrying carboxylates in the side arms exhibited particular good activity to reduce TDP-43-YFP aggregations on yeast model.

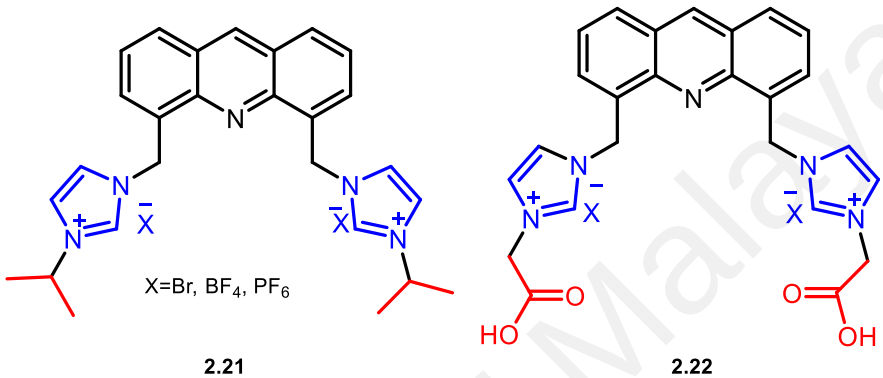

Figure 2.10: Chemical structure of acridine-imidazolium derivatives

In order to increase the anticancer activity of acridine-based drugs, incorporation of metal ions have been reported (Hadjikakou et al., 2008; Movahedi & Rezvani, 2018). The development of metal-containing anticancer compounds has shown a lot of advancement. However, very little awareness has been shown for the development of organometallic antibacterial drugs. Many derivatives of acridine-based complexes (**Figure 2.11**) have been studied on their biological activities. For example, acridine containing platinum-complex **2.23** showed non-crosslinking interaction with DNA (Barry et al., 2003; Baruah et al., 2005). Two other complexes, **2.24 & 2.25**, showed promising active against cancer cell lines (Graham et al., 2012; Ismail et al., 2019).

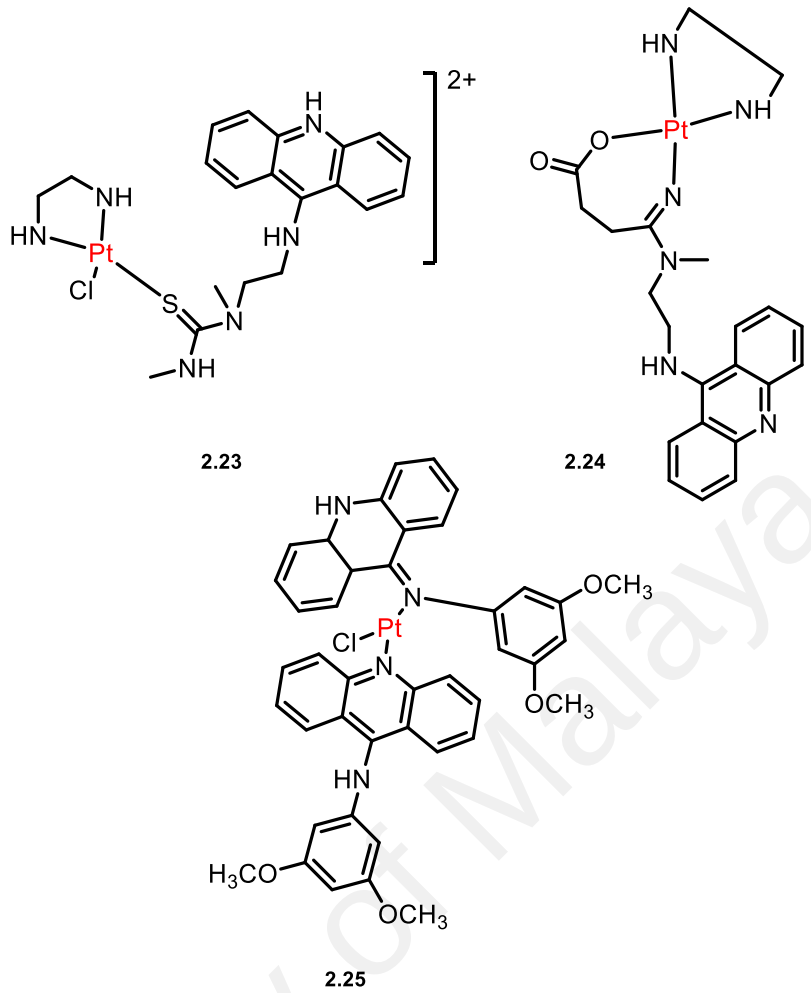

Figure 2.11: Chemical structures of platinum-acridine derivatives

Besides, platinum, ruthenium and palladium complexes, as shown in **Figure 2.12**, have been investigated as well. The Ru(II) complex **2.26** was reported as effective human topoisomerase II inhibitor (Beckford et al., 2011), while palladium(II) complex **2.27** exhibited cytotoxic activity against human lung cancer cell line A549 (Ramachandran et al., 2012). **2.27** showed higher cytotoxic activity (IC_{50}=7-18 μM) than the cisplatin (IC_{50}=25 μM). Moreover, it was also found to be a strong antioxidant against DPPH radicals (IC_{50}=8.56-11.25μM).

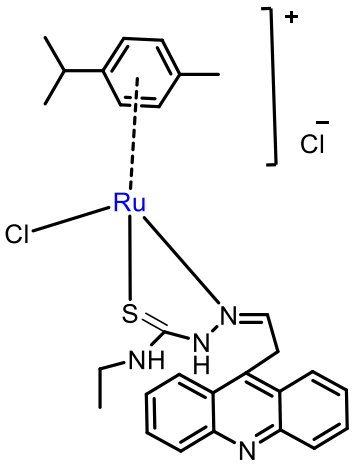

2.26

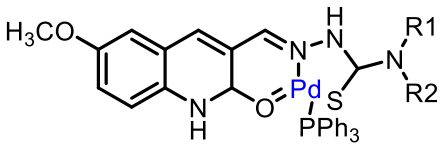

R1= H, Me R2= H, Me, Ph

2.27

Figure 2.12: Chemical structures of acridine-based ruthenium and palladium complexes

The selection of proper ligands is a key factor for the formation of complexes. According to Bu et al. (2004), acridine-based ligands provide potential advantages over than other N-heterocyclic ligands because of the larger conjugated π-systems, leading to π…π stacking interactions which may play important roles in the formations of complexes. Also, the steric hindrance of H atoms of the adjacent benzene rings probably affects the coordination abilities of the acridine (Bu et al., 2004; Guo et al., 2015). Until recently, it has been believed that the N donor of the acridine ring should have difficulty taking part in coordination because of the reasons mentioned above, especially for Ag(I) coordination complexes with different acridine-based ligands (Liu et al., 2006).

2.2.2 Synthesis of acridine and its derivatives

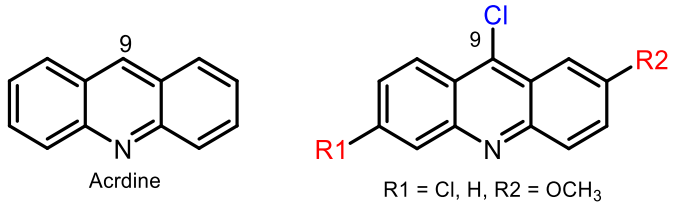

Figure 2.13: Chemical structures of acridine and its derivatives

Acridine (**Figure 2.13**) is an alkaloid with anthracene as the core structure widely used as dyes (Cholewinski et al., 2011), owing to its exhibit good fluorescent properties (Medeiros et al., 1993) that results from the dense π-conjugated system. It is crystallized in light yellow needles and by the blue fluorescence showed by solutions of its salts. The noteworthy medicinal potential of acridines has prompted the development of new acridine derivatives to improve biological activities, particularly in anticancer activity, through chemical syntheses (Belmont & Dorange, 2008; Galdino-Pitta et al., 2013; Gao et al., 2015; Philippe et al., 2007; B.Zhang et al., 2014).

The introduction of substituents onto the acridine can be done during or after the formation of the aromatic ring structure. However, the latter involves the electrophilic substitution on the aromatic ring that can result in structural isomers (Kumar et al., 2012). Therefore, the former approach is more preferred and the two most commonly used reactions for preparing the acridine skeleton are discussed below.

The **Ullmann synthesis** was introduced in 1902 to prepare acridine derivatives by treating aromatic aldehyde or benzoic acid with a primary amine in the presence of strong mineral acids (H_2SO_4 or HCl), followed by dehydrogenation and reduction (Kumar et al., 2012; Ullmann, 1903; Ullmann et al., 1902). The sequence is visualised in **Figure 2.14**.

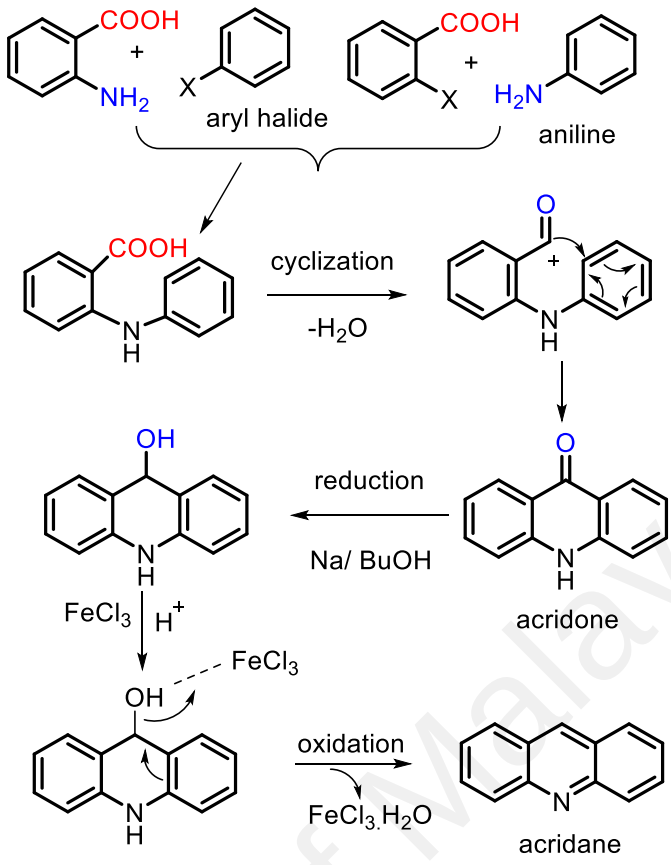

Figure 2.14: Proposed mechanism for formation of acridine compound by Ullmann

The **Bernthsen synthesis**, reacts diphenylamine with a carboxylic acid in the presence of zinc(II) chloride to form 9-substituted acridines (Bernthsen, 1884; Patrick, 2013), as presented in **Figure 2.15.**

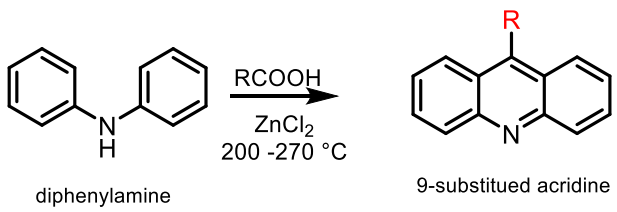

Figure 2.15: Bernthsen synthesis

2.3 Imidazolium-based silver carbenes complexes

2.3.1 Biological applications of N-heterocyclic carbenes and their complexes

N-Heterocyclic carbenes (NHCs) are heterocyclic compounds containing at least one nitrogen atom and carbene carbon within the ring structure (Hopkinson et al., 2014). Typical NHCs are diaminocarbenes, i.e. the carbene is linked two ring nitrogen atoms. They are also called Arduengo carbenes (De Fremont et al., 2009). Wanzlick et al. investigated the reactivity and stability of N-heterocyclic carbenes during the 1960s (Hopkinson et al., 2014; Wanzlick & Schonherr, 1968; Zhong et al., 2017). NHCs compounds are presented with various NHC systems ranging from five to seven-membered rings, including imidazolium. NHCs are a strong σ-donors and weak π-acceptors. Therefore, they can form a strong M–C bond with transition metal ions. NHCs compounds based on the imidazole ring system are excellent ligands for a variety of transition metals (Arduengo et al., 1999; Arduengo III et al., 1991; Weskamp et al., 2000) and main group elements (McGuinness et al., 1998). NHCs are more comparable to typically P-, N- or O-donating ligands than to classical Fischer- or Schrock-type carbenes (Arduengo et al., 1999). They are stable singlet carbenes, due to electronic and steric stabilization, that can act as excellent donor ligands towards 52 elements in the periodic table. Exceptions cover Cd, Tc and Sc (Patil et al., 2011). The electron-donating power of imidazolium-based NHCs, as shown in **Figure 2.16**, increases from benzimidazole over imidazole to imidazoline (Janssen-Muller et al., 2017).

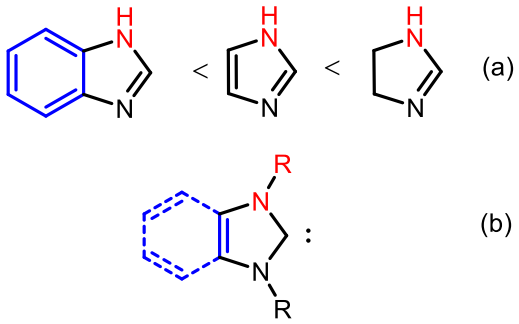

Figure 2.16: (a) Sort order of electron-donating ability (b) position of the carbene carbon

The biological activity of NHCs can be improved by introducing additional bioactive structural elements at the nitrogen (Asekunowo et al., 2017; John & Ghosh, 2010). Particularly benzimidazole, benzodiazepine, imidazole, indazole and triazole are important NHCs for pharmacological and industrial applications. The bioactive groups can be connection to the NHCs via an alkyl linker (Chifotides & Dunbar, 2005). Examples are compounds **2.28** & **2.29** in **Figure 2.17**, for which antibacterial properties have been reported (Achar *et al.,* 2017a & b), as well as compounds **2.30** and **2.31**, which exhibited remarkable antitumor activities (Al-Mohammed et al., 2015a; Coban et al., 2009; Li et al., 2018; Zhou et al., 2016a; Huang et al., 2019).

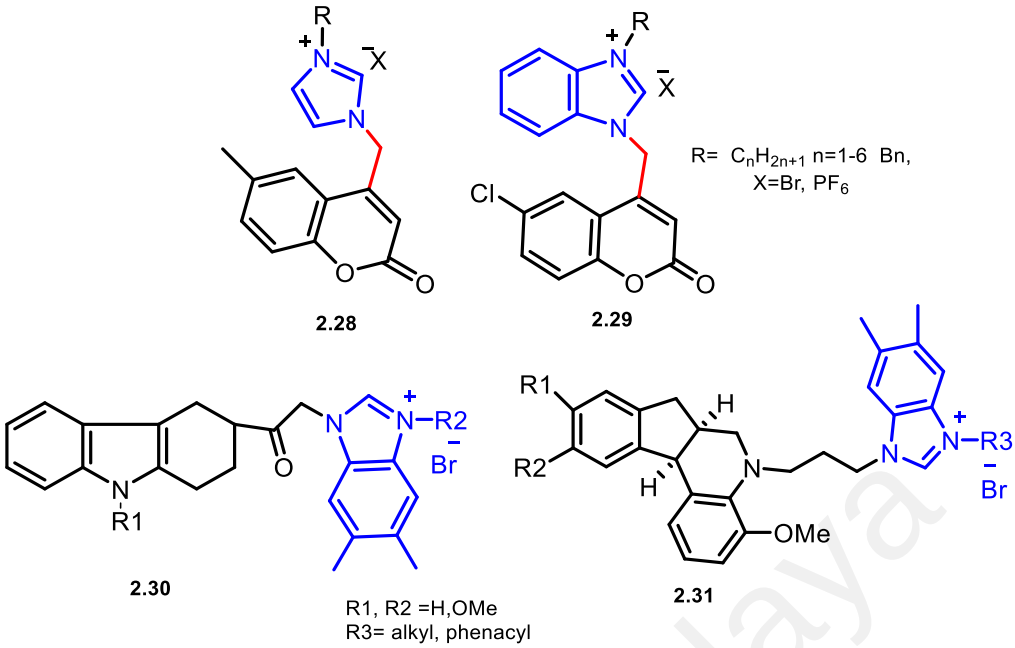

Figure 2.17: Imidazolium-based NHCs with additional bioactive groups

NHCs serve as strong ligands for a variety of cytotoxic metals such as Cu, Au, Ni, Pt, Pd, Ag and Au. Ag appears the most suitable candidate (Hartinger & Dyson, 2009; Mercs & Albrecht, 2010) because of its compatibility with the biological system since it has been used for controlling infections and suppressing fungal, bacterial activities (Fatima *et al.,* 2016; Gautier & Cisnetti, 2012; Haque *et al.,* 2014; Tan *et al.,* 2010). Ag(I)-NHC complexes have a safe history to be used in maintaining human health (Graham, 2005; Teyssot *et al.,* 2009). They have been proven as anticancer and antimicrobial agents in both *in vitro* and *in vivo* studies (Gandin *et al.,* 2013; Oehninger *et al.,* 2013; Shahini *et al.,* 2018; L.Zhang *et al.,* 2014). This is due to the antimicrobial activity of Ag^+ ion.

Ag(I)-benzimidazolium complexes have been tested as potential antibacterial agents against Gram-positive and Gram-negative bacteria. The complexes were showed good activity against *Salmonella Typhimurium*, *Micrococcus luteus*, *Listeria monocytogenes, Escherichia coli* and *Staphylococcus aureus* (Achar et al., 2019; Haque et al., 2018; Mottais et al., 2019; Slimani et al., 2019). **Figure 2.18** shows imidazolium-based Ag-NHCs complexes with remarkable antibacterial activity (Gimeno et al., 2012; Gok et al., 2014; He et al., 2015; Liu & Gust, 2013).

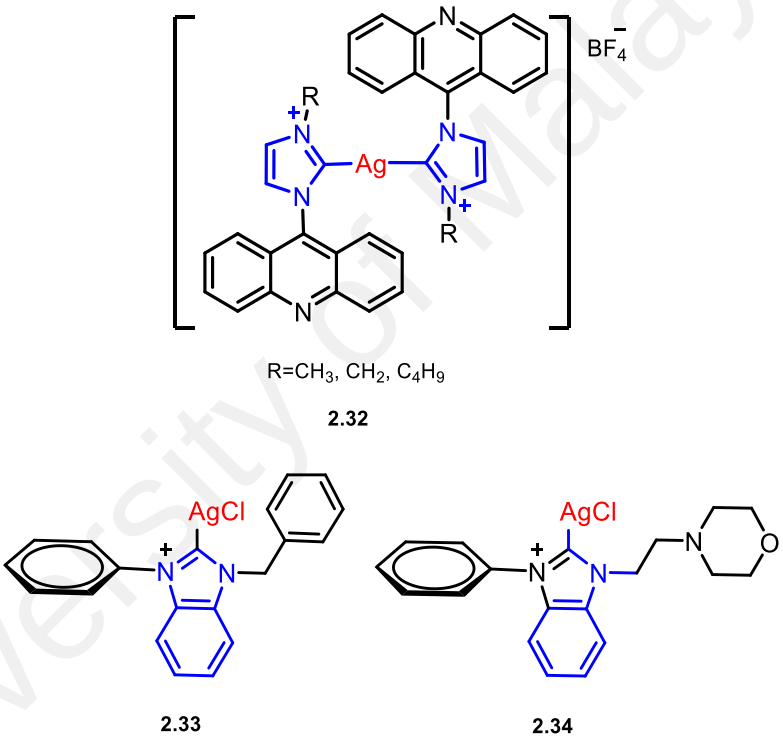

Figure 2.18: Antibacterial of imidazolium-based Ag(I)-NHCs complexes

Ag(I)-mono and di-nuclear complexes, as shown in **Figure 2.19,** have shown good antitumour activity against different cell lines (Baron *et al.,* 2014; Fichtner et al., 2012; Hackenberg & Tacke, 2014; Haque et al., 2013d; Potgieter et al., 2017; Sahin-Bolukbasi & Sahin, 2019; Tacke, 2015).

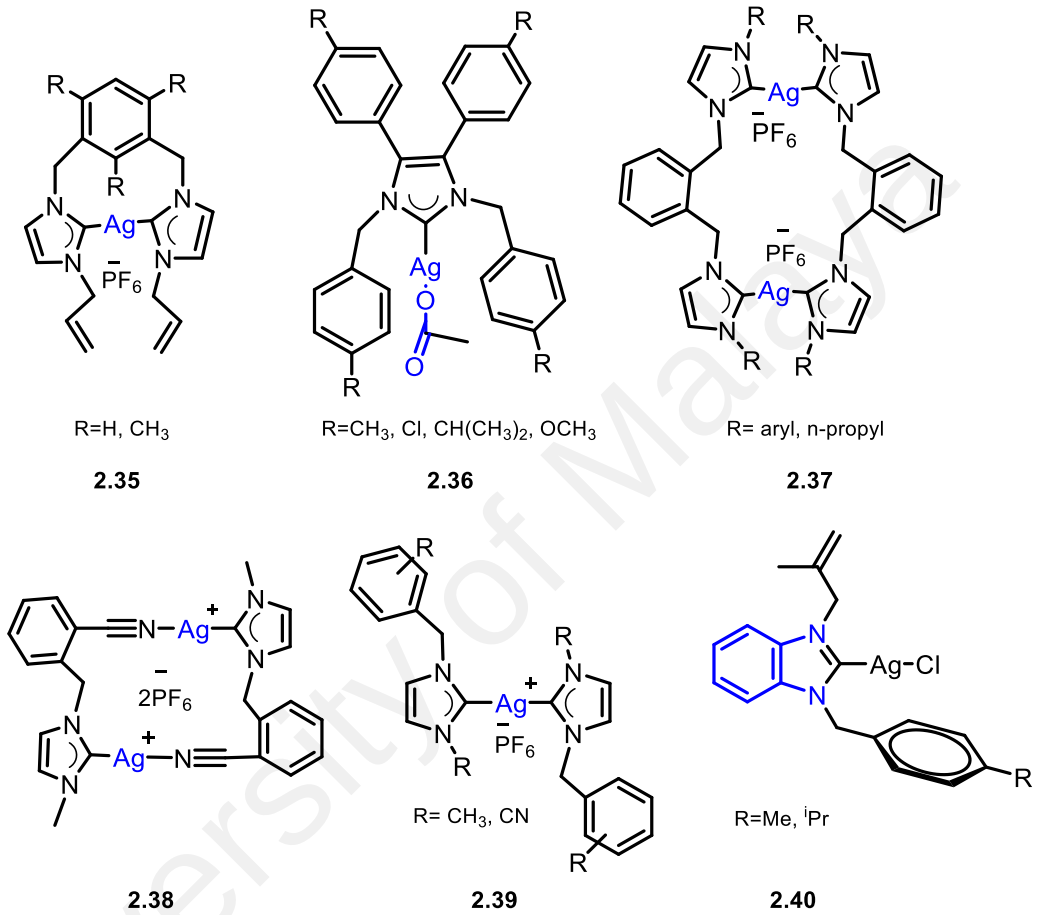

Figure 2.19: Ag(I)-NHC complexes with anticancer activity

2.3.2 Synthesis of imidazolium salts and silver carbenes complexes

Many papers have been published on imidazole and related ligands and their complexing properties. The NHCs ligands are stronger σ-donors than common phosphine ligands. They give rise to a strong metal-carbene bond and even their ligands can be modified through the introduction of electronic directing substituents (Hadei et al., 2005).

NHC precursors can be prepared by nucleophilic substitution of the alkyl or aryl halide by the *N*-deprotonated imidazole, followed by alkylation of the other ring nitrogen, as illustrated in **Figure 2.20**. Unsymmetrical substituted imidazolium salts can be prepared by using different alkylation reagents for two stages.

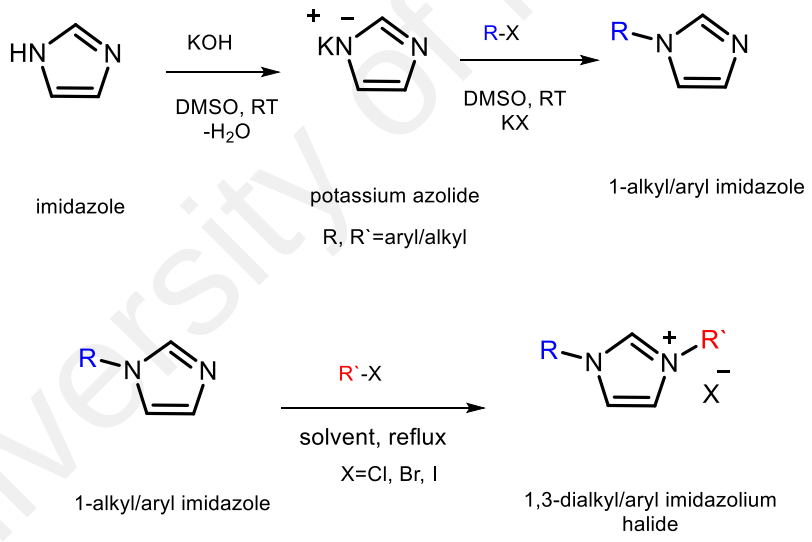

Figure 2.20: Synthesis of imidazolium salts by nucleophilic substitution

Another synthetic approach for symmetric di substituted imidazolium salts involves a multi-component one-step reaction, using glyoxal, primary amine and formaldehyde to yield the imidazolium salt. The reaction proceeds with the formation of Schiff base from a coupling reaction between the amine and the glyoxal, followed by condensation reaction with the formaldehyde, as presented in **Figure 2.21** (Singh & Chowdhury, 2012).

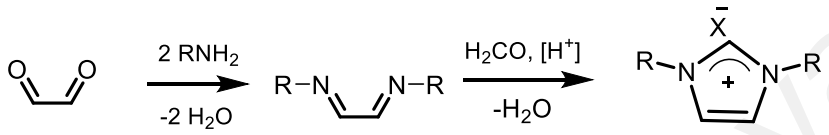

Figure 2.21: One-pot reaction synthesis of imidazolium salts

The synthetic procedure for Ag(I)-NHC complexes has been developed by Ofele and Wanzlick (Ofele, 1968; Weskamp et al., 2000). It applies deprotonation of an imidazolium salt by a basic metal precursor to form the imidazolin-2-ylidene complexes. The complexation is usually done through: the reaction of free NHC with appropriate silver source at ambient temperature (Chianese et al., 2003; Guerret et al., 1997; Haque et al., 2012; Mercs & Albrecht, 2010); the reaction between the silver bases and azolium salts at ambient temperature or the reaction of Ag(I) salts with azolium salts under basic phase transfer condition (Lin & Vasam, 2007), as depicted in **Figure 2.22**.

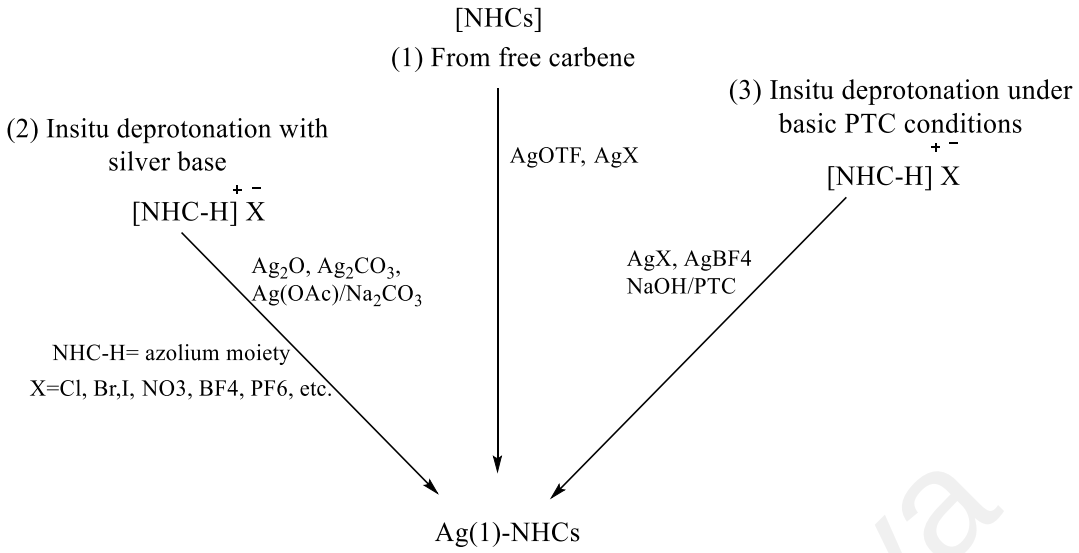

Figure 2.22: Three methods to prepare Ag(I)–NHCs

There is an increased interest in Ag(I)-NHCs complexes due to easy preparation, structural diversity, stability and usefulness in several applications (Li et al., 2011; Salman et al., 2013a; Wang et al., 2014). Acridine-containing Ag(I)-NHC complexes, which are the target compounds of this study, can be synthesized from the acridine imidazolium salts by treatment with Ag_2O. The reaction requires an anion exchange prior to the Ag treatment. The process is shown in **Figure 2.23** (Gimeno et al., 2012; Wang & Lin, 1998).

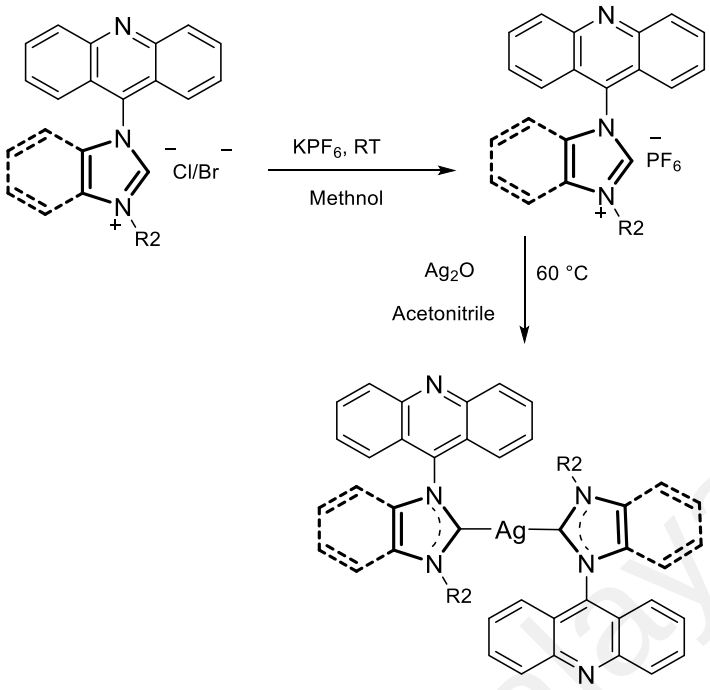

Figure 2.23: Synthesis route of Ag(I)-[benz]imidazolium acridine complexes

CHAPTER 3: METHODOLOGY

3.1 Chemicals and General Techniques

All the reagents and solvents (AR grade) were used as purchased from several commercial sources without prior purification. All chemicals were purchased from commercial sources. Reactions were monitored by thin-layer chromatography (TLC) under UV-light as a visualizing agent, which was performed using pre-coated Silica gel 60 F_{254} aluminium sheets. *N*-substituted imidazole compounds were detected by treating the developed TLCs with basic $KMnO_4$ solution and subsequent heating instead.

3.2 Instrumentation

IR spectra were recorded on a Perkin Elmer using the ATR-FTIR technique 400 spectrometer using at a resolution of 4 cm^{-1} and 8 scans, covering the range from 4000 cm^{-1} to 450 cm^{-1}, while NMR spectra for compounds were recorded on 400 MHz spectrometers, a Bruker Avance III and a JEOL ECX-400. The melting point of solid compounds was determined in an open thin glass capillary tube on a Mel-Temp II (Laboratory Devices, USA) instrument. The compounds were purified by extraction and crystallization. Products were evaporated using Rotavapor (Heidolph HB Digital). Product purities were confirmed by elemental analysis (CHN). Mass spectra were recorded for ESI on Triple-Quadrupole systems from Agilent Technologies model A6490 and High-Resolution Electrospray Ionization Mass Spectroscopy (HRESIMS, ESI-TOF) from Shimadzu were obtained on Agilent 6550 Q-TOF mass spectrometer. Fluorescence spectra were recorded on an Agilent Cary Eclipse spectrometer, while UV-vis spectra were obtained on a Shimadzu UV-2600 spectrophotometer. Powder X-ray diffraction studies PXRD were carried out on a PAN Analytical EMPYREAN using Cu-Kα radiation in the 2θ range of 5° to 50°.

3.2.1 Fourier Transform-Infrared, IR spectroscopy

IR spectroscopy is a technique used to identify the functional groups of the compounds. IR spectroscopy with a diamond ATR accessory was used to collect the Infrared spectra by Perkin Elmer Spectrum 400 FTIR/FT-FIR spectrometer (Waltham, MA, USA), using absorption mode with 8 scans at a resolution ±4 cm^{-1} and a wavenumber range of 4000 to 450 cm^{-1}. For this research, IR was applied to prove the presence of CH_2 aromatic and aliphatic groups in the functionalized imidazolium salts which appeared as a peak at 3100-2800 cm^{-1} and C=N group present a strong peak at 1650 cm^{-1} at room temperature, as shown in **Figure 3.1**.

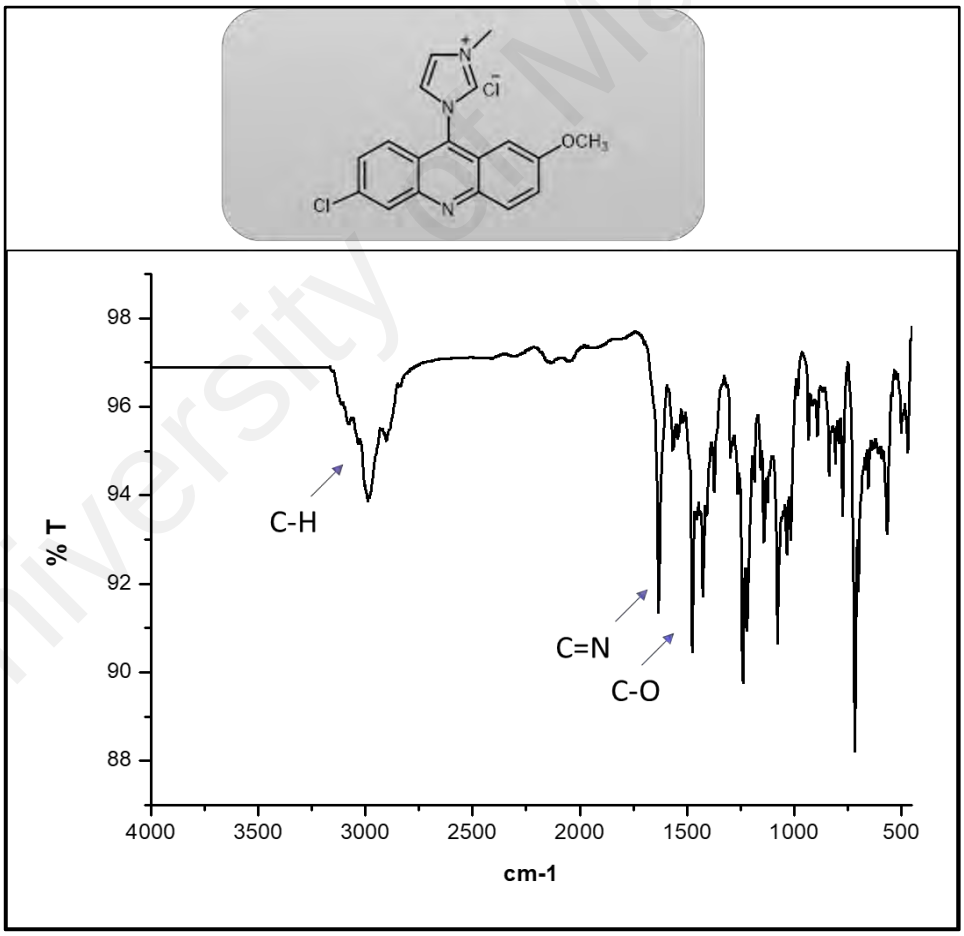

Figure 3.1: IR spectrum

3.2.2 Nuclear Magnetic Resonance NMR spectroscopy

Nuclear magnetic resonance NMR is a technique for identifying and characterizing the structure of organic molecules structure. ^{1}H NMR spectra provide information about the number of protons atoms, chemical environment and configuration of the investigated nuclei, which can be obtained based on the data analysis of signal integration, chemical shift, coupling pattern and coupling constants. Various nuclei can be studied by NMR spectroscopy, but ^{1}H, ^{13}C, ^{19}F and ^{31}P NMR are the most typical nuclei. All compounds were analysed to determine the presence of the proton and carbon through 1D (^{1}H and ^{13}C) experiments. All experiments were carried out at the Chemistry Department, Faculty of Science, University of Malaya. The compounds were dissolved with deuterated dimethyl sulfoxide (DMSO-d_6), chloroform ($CDCl_3$) and acetonitrile-d_3 and transferred to the NMR tube, then placed in the NMR spectrometer for further processing over the scan range 0 to 16 δ ppm and 0 to 250 δ ppm for ^{1}H and ^{13}C NMR studies, respectively. The solvent signals at 7.22 ppm and 77.0 ppm were used as an internal calibration standard for ^{1}H and ^{13}C NMR in $CDCl_3$, respectively, 2.5, 3.11 ppm and 39-40 ppm for ^{1}H and ^{13}C NMR in DMSO and 1.94 ppm and 1.39 & 118 for ^{1}H and ^{13}C NMR in acetonitrile, as shown in **Figure 3.2.**

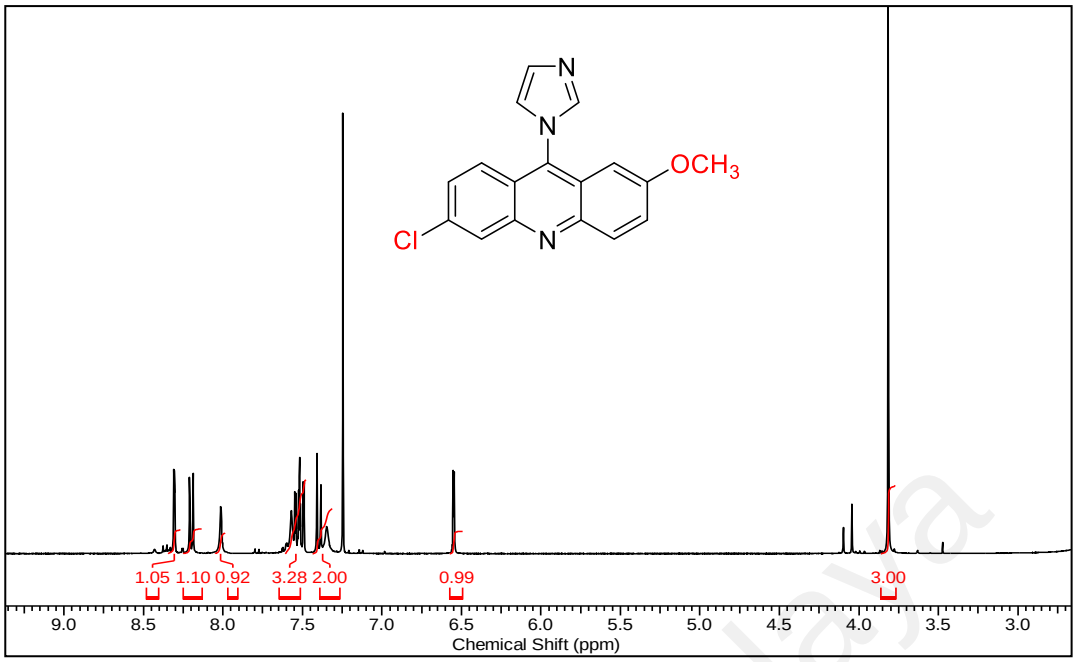

Figure 3.2: ^{1}H NMR spectrum

However, there were some cases such as the aromatic region, where the ^{1}H NMR signals were found not well resolved or overlapped with other signals, causing difficulties in the determination of the coupling constants. A 2D NMR ^{1}H-^{1}H correlation spectroscopy (COSY), as shown in **Figure 3.3**, was employed to indicate which ^{1}H atoms are coupling with each other. ^{13}C NMR spectrum showed all the carbon atoms in the compounds, but it does not differentiate between quaternary carbon (C), methine (CH), methylene (CH_2) and methyl (CH_3) signals. Therefore, the APT-NMR (Attached Proton Test) experiment was applied instead, in which both CH and CH_3 will appear as positive signals, while quaternary C and CH_2 are the negative signals in the spectrum, as illustrated in **Figure 3.4.** The assignments of carbon signals were based on 2D NMR heteronuclear single quantum coherence spectroscopy (HSQC), which provides a correlation of carbons and their attached protons, as shown in **Figure 3.5.** Heteronuclear multiple bond correlation (HMBC) spectrum, which enables the correlation between carbons and protons that are separated by two to three bonds, as shown in **Figure 3.6**.

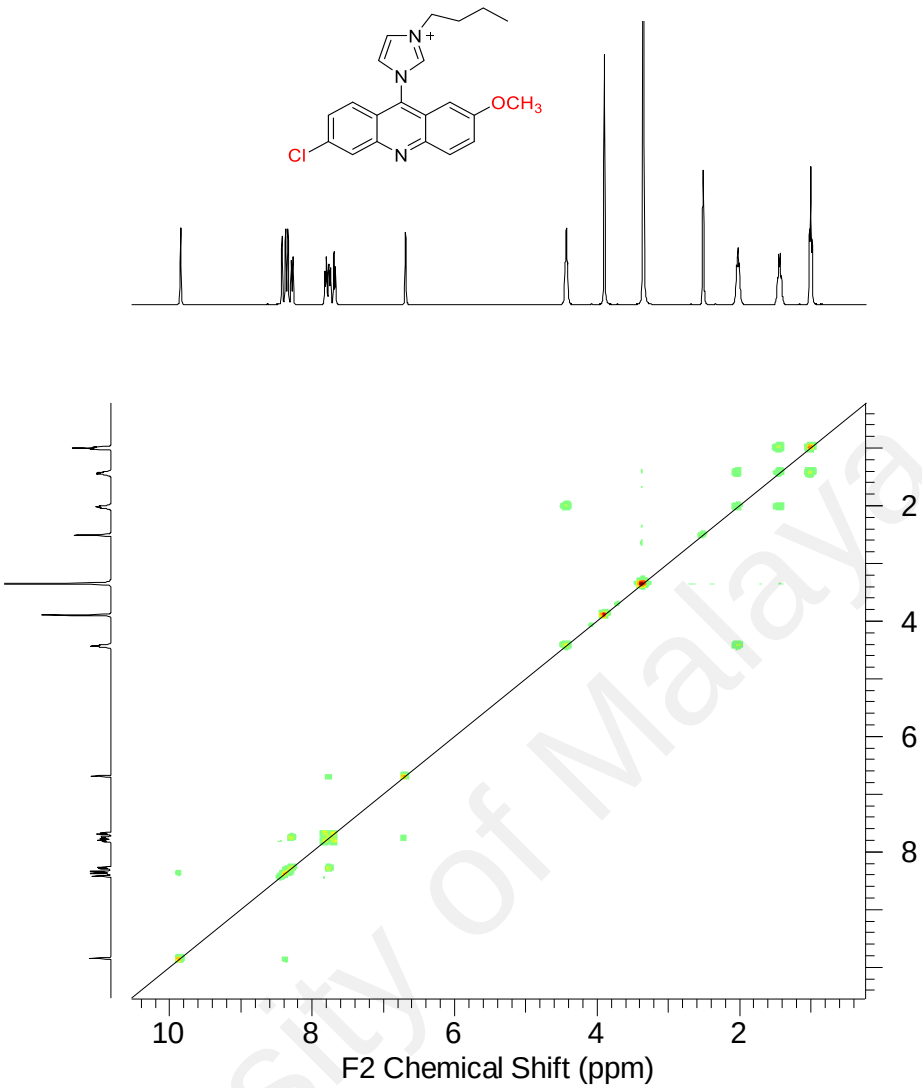

Figure 3.3: **COSY NMR spectrum**

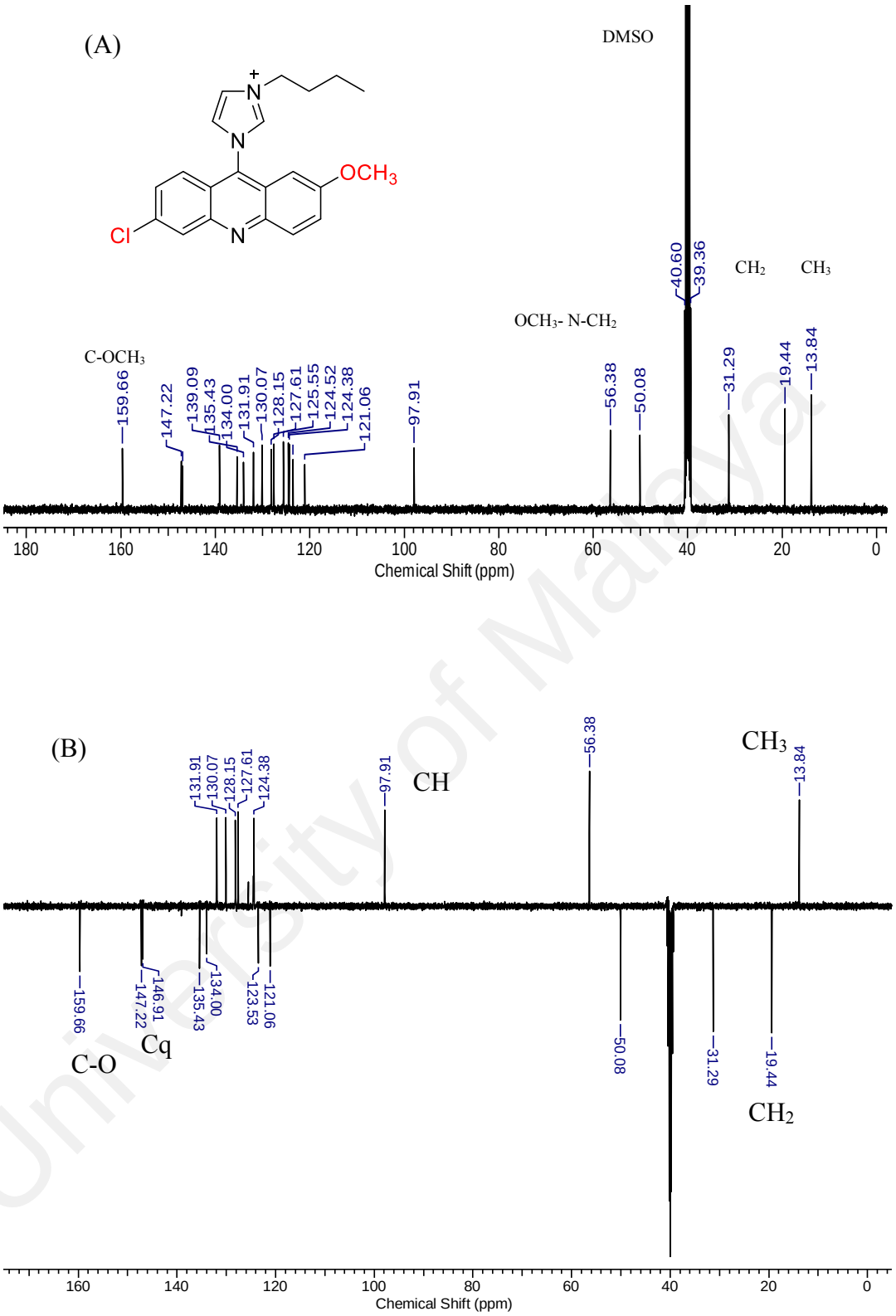

Figure 3.4: ^{13}C NMR (A), APT-C NMR (B) spectra

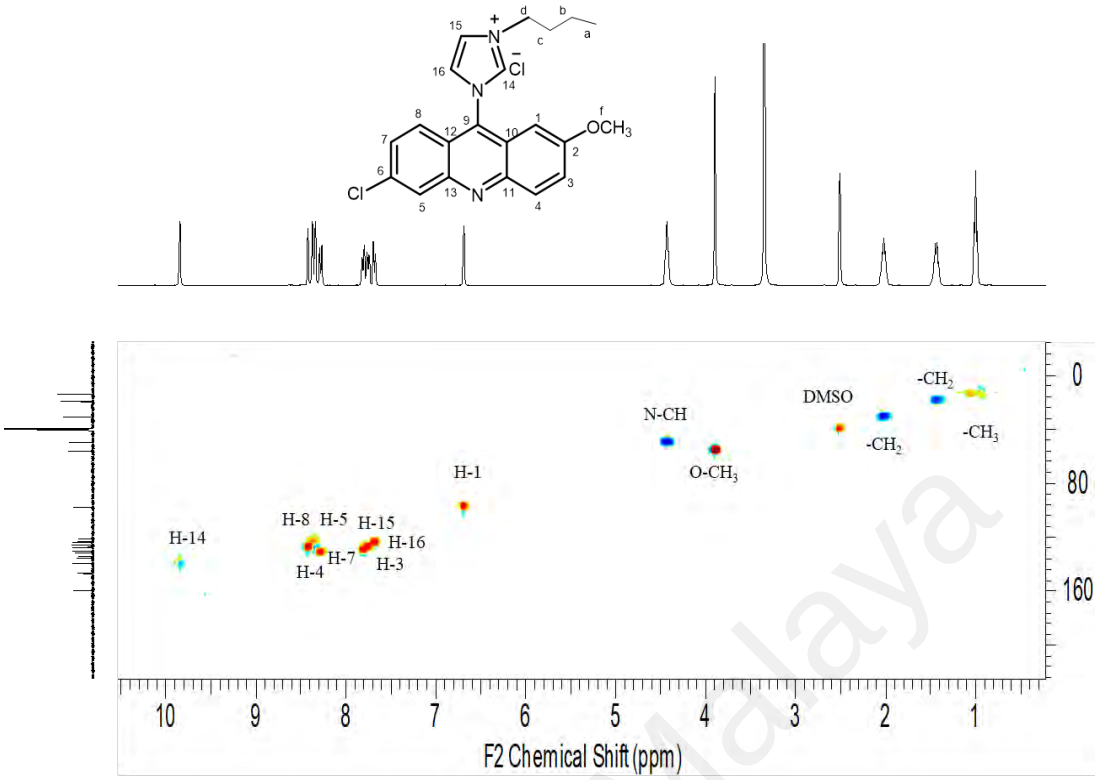

Figure 3.5: HSQC NMR spectra

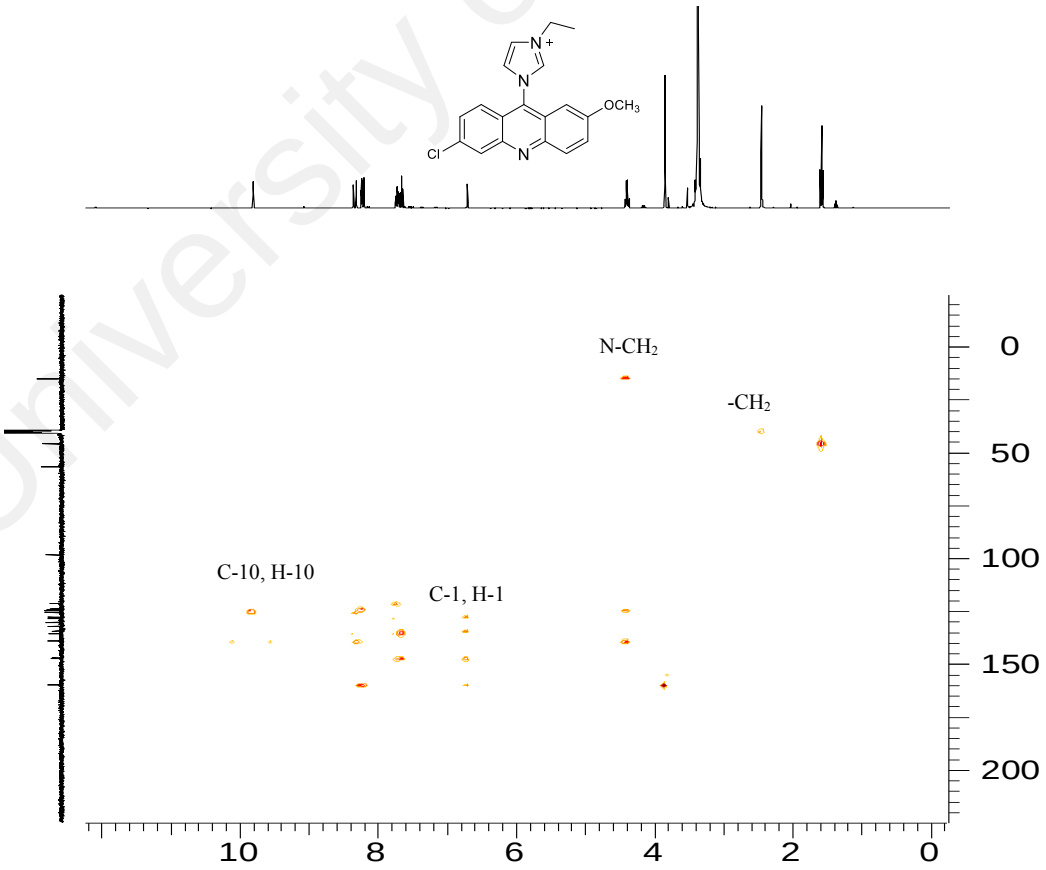

Figure 3.6: HMBC NMR spectra

3.2.3 High Resolution Mass Spectroscopy (HRMS)

Mass spectroscopy analysis can determine the molecular weight of the obtained compounds, as shown in **Figure 3.7**. Mass spectra were recorded for ESI on Triple-Quadrupole systems from Agilent Technologies model A6490 and HRESIMS (High-Resolution Electrospray Ionization Mass Spectroscopy) (ESI-TOF) from Shimadzu were obtained on Agilent 6550 Q-TOF mass spectrometer. The final compounds were dissolved in 1 mL of HPLC grade acetonitrile (pre-filtered CH_3CN). Mass spectra were recorded in the positive mode. The analysis was performed at the Chemistry Department and Centre Lab INFRA Analysis Laboratory, University of Malaya.

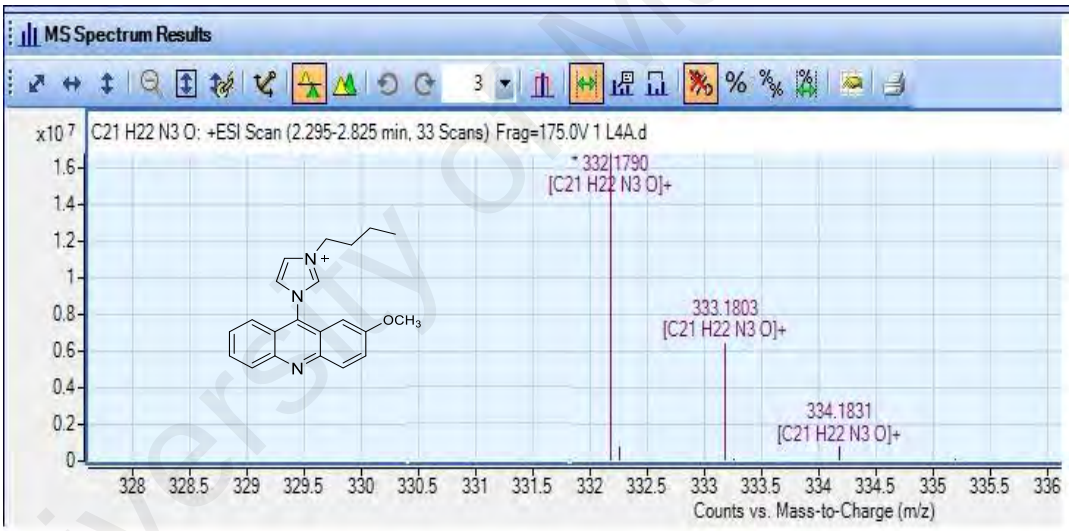

Figure 3.7: HRMS spectrum

3.2.4 Powder X-ray diffraction (PXRD)

X-ray powder diffraction (XRD) is an important analytical technique used to identify and characterize unknown crystalline materials because a crystal lattice diffracts a beam of X-rays into specific directions. Monochromatic X-rays are used within the crystal materials to determine the atomic spacings. Powder X-ray diffraction (PXRD) studies were carried out on a PAN analytical EMPYREAN with monochromator Cu-Kα radiation (λ=15.41874 Å) in the 2θ range of 5° to 50° with a slit size = 0.4785. X-ray single using High Score Plus software. Samples are studied in random orientations as powders with grind to ensure that all crystallographic directions are "sampled" by the beam.

3.2.5 Elemental Analysis

The elemental analysis of carbon, hydrogen and nitrogen elements for all synthesized compounds were done using a Perkin Elmer 2400 II (CHNS/O) elemental analyser. Acetanilide was used as an internal standard for all analyses. All measurements were taken under a constant flow of pure O_2 gas. The weight of the sample used for analysis was~ 1.5-2.0 mg. The experimental data for CHN analyses was found to be in good agreement with the calculated values of the proposed formulae as shown in **Equation 3.1**.

$$\%\,Element(calculted) = \frac{Molar\ mass\ of\ the\ element\ in\ the\ compound}{Molecular\ mass\ of\ the\ entire\ compound}\ X\ 100\ \% \qquad (3.1)$$

3.2.6 Energy Dispersive X-ray Analysis (EDX)

Field emission scanning electron microscopy (FESEM) is a technique that produces largely magnified images by using electrons instead of light. In a typical SEM, a source of electrons is focused on a beam, that penetrates the surface of the specimen. This interaction results in the emission of electrons and photons from the sample, which generate the SEM image. A few milligrams of the dried sample were added into a FESEM cell and subsequently scanned by the electronic microscope. This microscopic investigation was conducted at various magnifications for the samples. FESEM images were obtained on a JEOL JSM-7600F field emission scanning electron microscope. Energy of each X-ray photon is characteristic of the element which produced it. The EDX microanalysis system collects the X-rays, sorts and plots them by energy and automatically identifies and labels the elements responsible for the peaks in this energy distribution. This technique was already used for the analysis of the chemical composition of the material. Selected different areas to determine the distribution of elemental composition.

3.2.7 UV-Vis Spectroscopy

The ultraviolet UV-vis spectra were measured using Shimadzu UV-2600 spectrometer in the range between 300 to 600 nm at a slow scan rate measurement. Each compound was dissolved in acetonitrile and water (v: v,1:1) and its absorption was recorded into UV spectroscopy using a detector at room temperature. All results are presented in terms of absorbance (A) versus wavelength (λ, nm) units.

3.2.8 Fluorescence Spectroscopy

Fluorescence spectroscopy was recorded on Agilent Cary Eclipse spectrometer in 1cm quartz cuvettes at room temperature. Fluorescence spectroscopy measures the light emission of molecules after excitation by a suitable wavelength. The emission spectrum is specific for the chemical compound, while the emission intensity can serve for quantitative analysis. The excitation wavelength was chosen based on the absorption maximum in UV-Vis spectra. Luminescence investigations were performed in acetonitrile/water solution (1:1, v: v) after pre-treatment of the 9-chloroacridine with imidazolium salt. 9-chloroacridine and derivatives-based imidazolium salt were compared with identical optical density for the excitation wavelength.

3.2.9 X-ray Single Crystal

X-ray single-crystal for compounds was collected at 293 K on oxford supernova dual wavelength diffractometer (Oxford, England) (graphite-monochromated Mo-K_α radiation, $\lambda = 0.71073$ Å). The structure was solved using the direct method by SHELXL-2014/7 and refined by the full-matrix least-squares method on F_2 with SHELXL-2014/7. But all data not good because the shape of the crystal is a needle and brittle crystal. XRD could not further support the structures of Ag(I)-NHC complexes as all attempts to get single crystals remained unsuccessful. However, ^{1}H and ^{13}C NMR provided evidence of their successful synthesis. Besides, the sizes of the ligands are also affected by the formation of complexes between metals and ligands. The steric hindrance promotes cyclometallation when the bulky acridine molecule reacts with silver.

3.3 Synthetic methods

3.3.1 General synthetic of ligands

Synthesis of 9-chloroacridine and its derivatives from 2-phenylamino benzoic acid (**2PABA**) and its derivatives.

3.3.1.1 *N*-phenylamino benzoic acids

A mixture of aniline **1** (49 mmol), 2-chlorobenzoic acid **2** (38 mol), potassium iodide (41 mg, 0.25 mmol) and copper powder (2 mmol) in 40 mL dimethylformamide DMF was slowly treated with dry potassium carbonate (K_2CO_3) (6.0 g, 43 mmol), and the reaction was refluxed for 6 to 12 hours. After cooling to room temperature, the reaction mixture was poured into 30 mL of water and decolorized with charcoal. The mixture was filtered through celite and the filtrate was acidified with concentrated hydrochloric acid (HCl, 1 M) (pH was adjusted to 1-2). The precipitate product was filtered and subsequently dissolved in 100 mL of 5% aqueous sodium carbonate solution (stirring 20 min). The solution was filtered through celite and the purified product was obtained by precipitation with acid as described above. 2-phenylamino benzoic acid and its derivatives 2**PABA** were obtained as off-white solids (**3a-3c**), as shown in **Figure 3.8**.

3.3.1.2 9-chloroacridine and derivatives

2**PABA** or its derivative (19 mmol) and phosphorus oxychloride ($POCl_3$) (40 ml) were added into a dried round-bottom flask and heated slowly in a water bath at 85-90 ºC for 15 min. The reaction was monitored carefully; if it turned too violent, the reaction was temporary placed in a cold-water bath until the boiling subsides. After the initial exothermic reaction had seized, the flask was immersed into an oil bath. The temperature was raised to 135-140 ºC and the reaction was kept under reflux for 3 h. Excess of phosphorus oxychloride was subsequently removed by distillation at 140-150 ºC under

vacuum. The cooled reaction mixture was poured into a stirred mixture of 20 ml concentrated aqueous ammonia and 13g of crushed ice. The 9-chloroacridines precipitated within 30 min. They were filtered, washed with saturated sodium carbonate and with water, dried and recrystallized from ethanol to form needle-shaped crystals of **9-chloroacridine** or derivatives **4a-4c**.

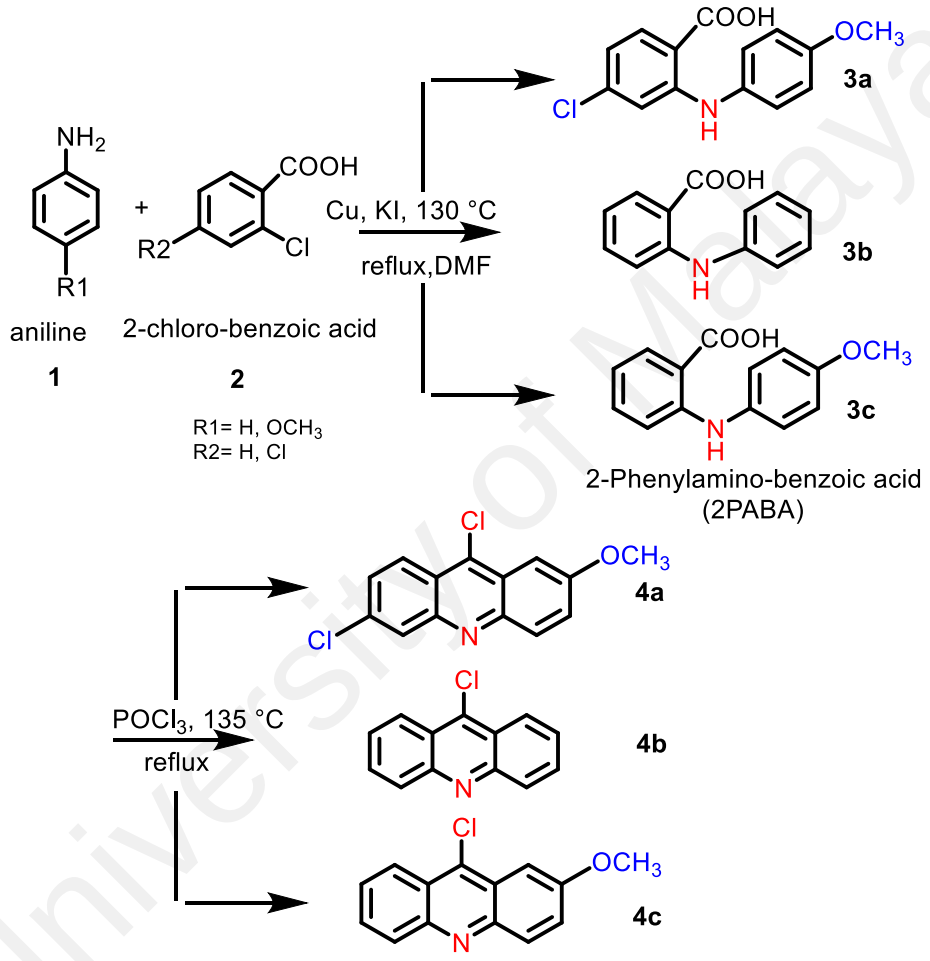

Figure 3.8: Synthesis of 9-chloroacridine and its derivatives

3.3.1.3 *N*-substituted imidazole's

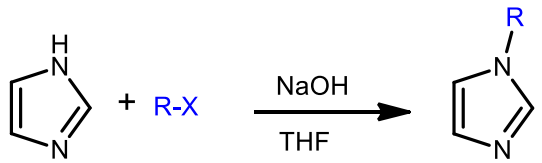

5a, R = C_2H_5, 5b, R= C_6H_{12},
5c, R = C_4H_9, 5d, R= $C_{10}H_{21}$,
5e, R = $C_{12}H_{25}$, 5g, R= $C_{18}H_{37}$

Figure 3.9: Synthesis of *N*-imidazole derivatives (Aryl and Alkyl)

To a solution of imidazole (15.86 mmol) in tetrahydrofuran (THF) 60 mL was added sodium hydroxide NaOH pellets (18.25 mmol) and the reaction was stirred at room temperature for about 2-4 h or reflux 2 h at 60 °C. Alkyl/aryl bromide (14.31 mmol) were added to the mixture and stirring was continued for another 12 h. The reaction mixture was filtered and extracted twice with CH_2Cl_2/H_2O. The organic phase was dried over magnesium sulphate anhydrous $MgSO_4$ and the solvent was removed on a rotary evaporator. The pure *N*-substituted imidazoles **5(a-g)** was obtained as yellow liquids

3.3.1.4 General method for synthesis *N*-substituted imidazolium-acridine salts

1- General procedure A (X=Cl):

A suspension of **4(a-c)** (1.6 mmol) in toluene (20 mL) was treated with *N*-substituted [benz]imidazole **5(a-g)** (1.8 mmol), as illustrated in **Figure 3.17**, and subsequently heated to reflux overnight. A greenish precipitate developed from the initial solution. After cooling, the solid was collected by filtration, washed with hexane (20 mL) and dried under vacuum to provide the [benz]imidazolium-acridine salt as greenish solid.

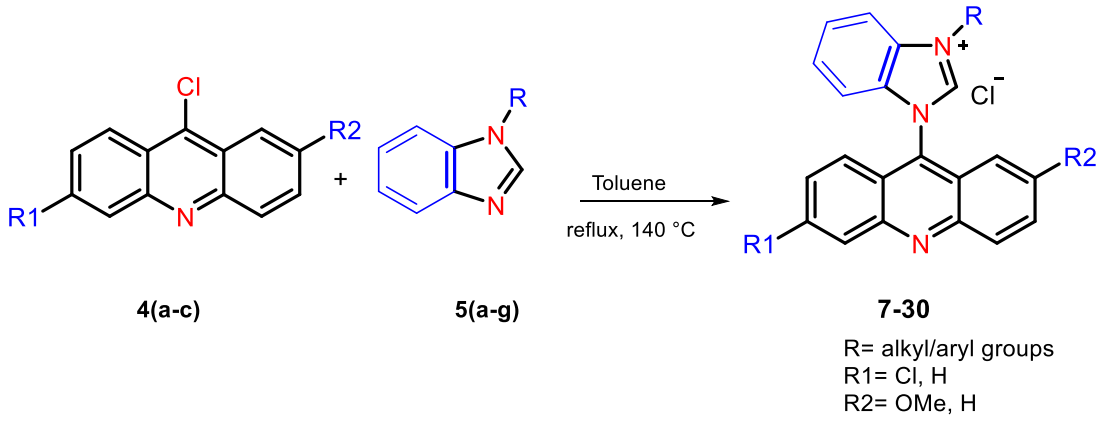

Figure 3.10: Synthesis of [benz]imidazolium-acridine salts

2- General procedure B (X=Br)

A solution of 6 (a-c) (0.25 mmol) and alkyl or aryl bromide (0.75 mmol) in acetonitrile or acetone (25 mL) was refluxed for 12–48 h, as shown in **Figure 3.18**. The [benz]imidazolium salt gradually precipitated. The precipitate was filtered after cooling, washed with acetone or acetonitrile (2x15 mL) and dried to give a yellow solid in a yield of 80-95%.

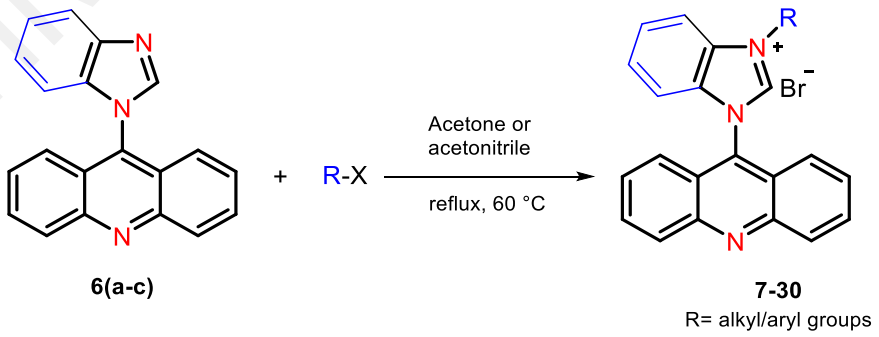

Figure 3.11: Synthesis of [benz]imidazolium-acridine derivatives bromide salts

3.3.2 General method for synthesis Ag(I)-complexes

3.3.2.1 Synthesis [benz]imidazolium-acridine PF_6

The halide precursor (1.0 mmol) was dissolved in methanol and mixed with a solution of KPF_6 (220 mg, 1.2 mmol). The mixture was stirred for 4h and left to stand at room temperature overnight. The yellow solid was filtered and washed several times with water. Drying at vacuum provided [benz]imidazolium-acridine hexafluorophosphate. ^{19}F NMR (376 MHz, Acetonitrile-d_3): δ (ppm) -72.68 (d, $^1J_{P,F}$ = 705 Hz). ^{31}P NMR (162 MHz, Acetonitrile-d_3): δ(ppm) -144.02 (septet,$^1J_{P,F}$ = 705 Hz).

3.3.2.2 Synthesis Ag(I)-complexes

Silver complexes, as shown in **Figure 3.19**, were prepared by the treatment of the [benz]imidazolium-acridine PF_6 (1.0 mmol) with silver oxide Ag_2O (280 mg, 1.2 mmol) in acetonitrile (10 mL) at 60 ºC for 24-48 h with exclusion of light by covering using aluminium foil. The black Ag_2O gradually vanished. The reaction was filtered through celite to remove remaining Ag_2O. The filtrate was concentrated in vacuum to 1 ml and diethyl ether was added to precipitation the complexes as yellow solid. Complexes were purified by repeated precipitation in acetonitrile by the addition of diethyl ether.

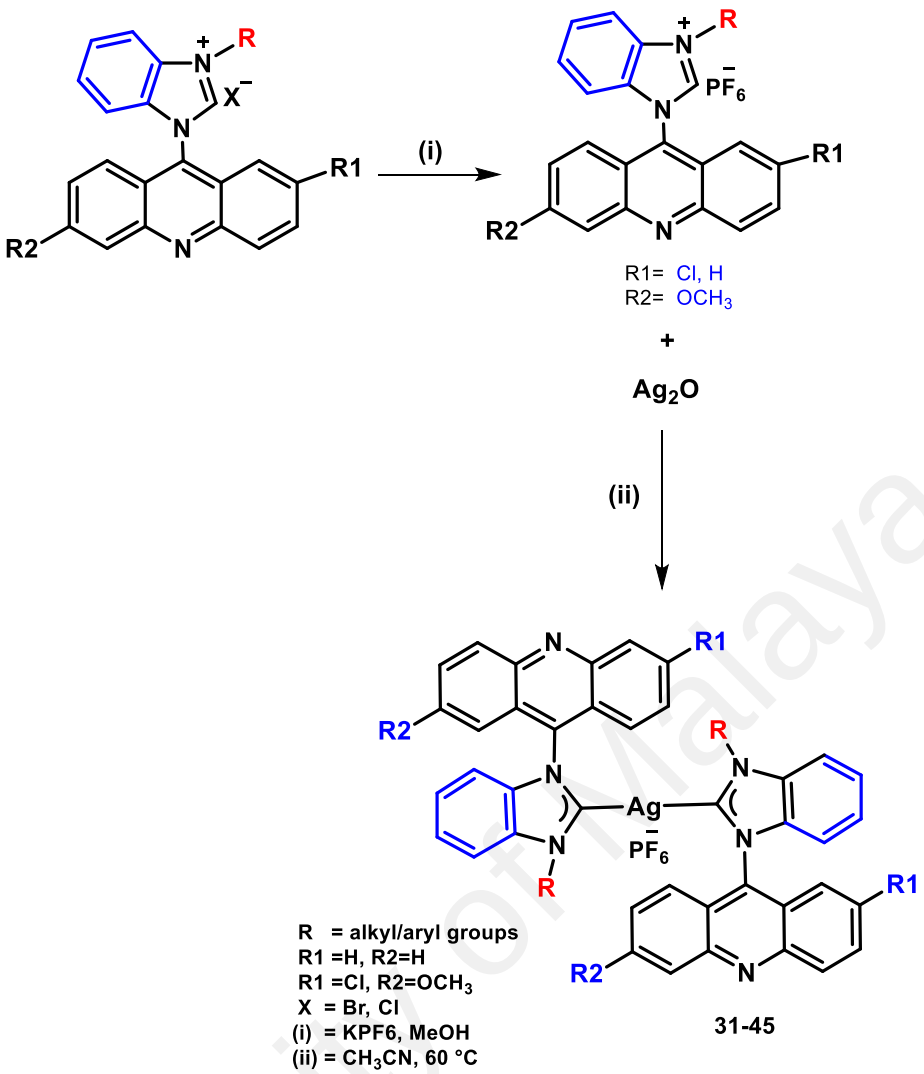

Figure 3.12: Synthesis of Ag(I)-complexes

3.4 Biological Activity

3.4.1 Chemical and instrument

MTT, ascorbic acid and butylated hydroxytoluene **BHT** were obtained from Sigma Aldrich, fetal bovine serum albumin **FBS**, dimethyl sulfoxide **DMSO**, DPPH (1,1-diphenyl-1-picrylhydrazyl), ampicillin, and gentamicin (positive controls for antibacterial assay) were obtained from Merck, while phosphate buffered saline **PBS**, penicillin-streptomycin and RPMI 1640 media were purchased from Nacalai Tesque (Kyoto, Japan), sterilized paper discs (Thermo Fisher, 6mm diameter). Nutrient agar and

nutrient broth (DIFCO, Becton Dickinson, USA). Cell viability was evaluated using ELISA microplate reader (Infinite M200PRO). Centrifugation was done using Hettich Zentrifugen Universal 32, 32R (Germany). Morphological of cells were observed under a fluorescent microscope (Leica attached with Q-Floro software and Olympus BX60, Japan). 5% CO2 incubator (Thermo Fisher Scientific, USA).

3.4.2 Antioxidant

3.4.2.1 DPPH Radical Scavenging Activity

The DPPH (1,1-diphenyl-2-picryl-hydrazyl) assay was performed in a 96-well microtiter plate according to the modified method by Orhan *et al*. (2007), Brem *et al*. (2004), Brand-Williams *et al*. (1995) and Salazar-Aranda *et al*. (2011). A solution of 30 µL DPPH in DMSO (1.5 mg/mL) was treated with 70 µL of tested samples dissolved in DMSO at different concentrations, ranging from 15.6 to 1000 µg/mL. Ascorbic acid (vitamin C) and butylated hydroxytoluene (BHT) were used as the positive control, while the last row of the plate only contained blank samples of DPPH in DMSO as reference. The plate was incubated for 30 min in the dark and the decrease in absorbance at 517 nm was determined using Tecan microplate reader (Infinite M200PRO) (Brand-Williams et al., 1995; Brem et al., 2004; Orhan et al., 2007; Salazar-Aranda et al., 2011).

The radical scavenging activity was calculated using the following **Equation 3.2**:

$$Inhibition = \frac{A0 - A1}{A0} X\ 100\% \qquad (3.2)$$

Where *A0* is the absorbance of the DPPH radical in the blank sample and *A1* is the corresponding absorbance in the presence of the sample. The correlation between each concentration and its scavenging was plotted on a graph, and the IC_{50} was determined from the graph as the concentration required to reduce the DPPH absorption by 50% (Kareem et al., 2015).

3.4.2.2 Ferric Reducing Antioxidant Power Assay (FRAP)

The FRAP assay measured the antioxidant activity of compounds as a reductant to reduce oxidant present in the reagent through a redox-linked colorimetric assay. The determination of the total antioxidant activity followed a modified method of Benzie and Strain (1999) (Benzie & Strain, 1999). The ferric reducing antioxidant power (FRAP) was determined by using freshly prepared reagent based on mixing 300 mM acetate buffer, 10 mM TPTZ (2,4,6-tripyridyl-*s*-triazine) and a solution combining 20 mM iron(III) chloride ($FeCl_3$. $6H_2O$) and 40 mM HCl in a ratio of 10: 1: 1, (v/v), respectively. For measurement, 10 µL of tested samples (1 mg/mL) and 300 µL FRAP reagent were mixed in wells of 96-well plates and readings of the coloured product (ferrous tripyridyltriazine complex) were taken at 593 nm. Ferrous sulphate and ascorbic acid were used as a standard and control, respectively. The FRAP activity was calculated as ferrous equivalents (FE) at a single concentration of 1 mg/mL and the FE was calculated from the standard curve of $FeSO_4$ (Mohammadzadeh et al., 2007). A linear calibration curve covering the range of 100 and 1000 mM $FeSO_4$ was used to convert the absorption readings to FE. The results were expressed as mM Fe(II)/g dry weight of the compound.

3.4.3 Antibacterial

The bacterial stock culture was preserved on nutrient agar, which was stored at 4°C (Ahmad & Aqil, 2007). For the purpose of the antibacterial evaluation, a set of five microorganisms was investigated, covering two Gram-positive bacteria, namely *Staphylococcus aureus* (ATCC 25923) and a clinical isolate of *Staphylococcus epidermidis*, as well as three Gram-negative strains, namely *Pseudomonas aeruginosa* (ATCC27853) and clinical isolates of *Escherichia coli* and *Salmonella typhi*, as shown in **Table. 3.1**. The clinically isolated bacteria were obtained from the University of Malaya

Medical Centre (UMMC), Kuala Lumpur. The antibacterial assay was performed using the disk diffusion method for benzimidazolium-acridine salts and their Ag(I) complexes (Hindi et al., 2009; Wiegand et al., 2008), as shown in **Figure 3.20**. After an incubation period of 24 h at 37 °C the diameter (in mm) of the inhibition zone was determined, reflecting the antibacterial activity. All activity studies of the inhibition zone were performed in triplicates.

Table 3.1: Type of Gram-positive and Gram-negative bacteria.

Strain code	Strain name	Strain type	source
clinical isolated	*Staphylococcus epidermidis*	Gram-positive	University of Malaya Medical Center (UMMC)
ATCC 25923	*Staphylococcus aureus*		American type of culture collection (ATCC)
clinical isolated	*Escherichia coli*	Gram-negative	University of Malaya Medical Center (UMMC)
ATCC27853	*Pseudomonas aeruginosa*		American type of culture collection (ATCC)
clinical isolated	*Salmonella typhi*		University of Malaya Medical Center (UMMC)

Minimal inhibitory concentrations (MIC) were determined in multiwell plates using a twofold broth microdilution approach (Ndi et al., 2007; Ozdemir et al., 2010; Wayne, 2002) starting with compound concentration of (1000–7.81 μg/mL). Ampicillin (10 μg/mL) and gentamicin (1 μg/mL) were used as positive control, while pure DMSO served as a negative control. Samples were incubated for 24 h at 37°C and visually inspected on bacterial growth. The MIC was confirmed by colourization with MTT (20 μL): an aqueous solution (5 mg/mL) of 3-(4,5-dimethyl thiazol-2-yl)-2,5-diphenyl

tetrazolium bromide was added and the samples were subsequently incubated for 1 h at 37°C. A pink colour indicates bacterial growth. Therefore, the MIC value reflected the lowest compound concentration providing a colourless sample (Al-Madhagi et al., 2019; Moulari et al., 2006). The determination of the minimal bactericidal concentration MBC applied all wells near the MIC. 100 µL aliquot were cultured on nutrition agar and incubated at 37 °C for 24h. The presence or absence of bacterial growth was determined by visual inspection. The MBC was considered as the lowest compound concentration at which no bacterial growth was observed (Ndi et al., 2007).

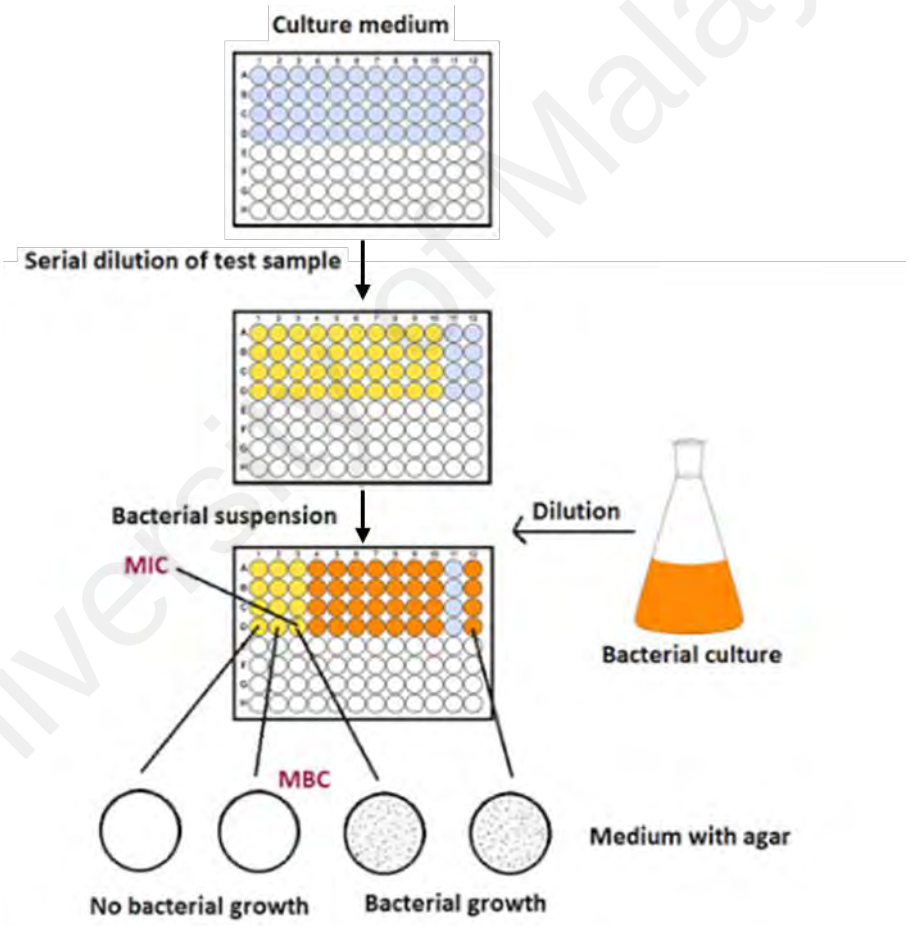

Figure 3.13: A schematic representation of the determination of MIC and MBC (Paiva et al., 2013)

The MIC is the lowest concentration of the active ingredient at which the solution in the well appears as a clear solution. Subsequently, the active ingredient with the concentration range starting from the MIC is tested on cultured on agar and incubated again. The agar plate that shows no bacterial growth (clear zone) is reflected as the MBC of the active ingredient.

3.4.4 Anticancer

3.4.4.1 Cell culture

Five cell lines were used and sub-cultured in the laboratory of the Pharmacy Department, the University of Malaya to perform the preliminary cytotoxicity screening. CAOV-3, MCF-7, MCF-10a, PC-3 and T1074 cell lines were originally obtained from the American Type Culture Collection (ATCC; Manassas, VA), as shown in **Table 3.2.** The cells were cultured in RPMI-1640 medium, supplemented with 10% fetal bovine serum (FBS) and 1% antibiotics (penicillin-streptomycin), and incubated at 37 ^{o}C in a humidified atmosphere containing 5% CO_2. The medium was changed twice a week until confluent cell monolayer was formed and observed under an inverted microscope (Favarin et al., 2019; Jayash et al., 2016).

Table 3.2: Type of cancerous and non-tumorigenic cell lines.

Cell lines	Classification	Company
MCF-7	Breast cancer cells	American Type Culture Collection **(ATCC)**
MCF-10	Non-tumorigenic breast cells	
CAOV-3	Ovarian cancer cells	
T1074	Non-tumorigenic ovarian cells	
PC-3	Prostate adenocarcinoma cells	

3.4.4.2 Cellular viability assay (MTT)

The inhibitory effect of compounds was determined by an MTT assay, in which 5×10^3 of different types of cancer cells per well were seeded in 96-well plates in triplicate and kept for 24 h at 37 °C with 5 % CO_2 saturation to attach. After this incubation, a serial dilution of different concentrations of compounds were prepared and transferred to the 96-well plates containing the seeded cells. The plates were incubated for 24 h and %CO_2 under the culturing conditions prior to addition of the tested compounds in a serial dilution of different concentrations. Subsequently, 20 µL of MTT (3- [4, 5-dimethylthiazol-2-yl]-2, 5-diphenyltetrazolium bromide, 5 mg/mL) was added to the treated cells in a dark place and the plates were incubated for another 4 h under strict light protection by covering with aluminium foil. All media was discharged and a total of 100 µL volume of dimethyl sulfoxide (DMSO) was poured into each well to dissolve the purple formazan crystals. A microplate reader was used to measure the plate at absorbance 570 nm. The experiment was conducted to evaluate the IC_{50} in triplicate. The percentage of cytotoxicity was determined using the following **Equation 3.3**:

$$Cell\ viability\ \% = \left(\frac{X}{Xc}\right) \times 100\% \tag{3.3}$$

where X is the absorbance of treated cells and X_c is the absorbance of the control group (untreated cells). Based on the reference, cytotoxicity responses were qualitatively rated as severe, moderate, slight and non-cytotoxic reflecting cytotoxicity values of < 30%, 30%–59%, 60%–90% and > 90%, respectively (Jayash et al., 2017).

Selectivity index (SI). The degree of selectivity of the composite to the cancer cell line is explored as *SI* ratio as per previous reports (Badisa et al., 2009; Musa et al., 2010). In order to evaluate the selectivity of the potential cancer drugs the selectivity index (*SI*) was determined according to equation according to the following **Equation 3.4**:

$$SI = \frac{IC50\ composite\ on\ normal\ cell\ line}{IC50\ composite\ on\ cancer\ cell\ line} \quad (3.4)$$

where IC_{50} is the concentration of a sample required to kill 50% of the cell population.

3.5 Statistical Analysis

Each test was performed in triplicate and the values were reported as mean ± standard error deviation (SD). Liner regaration was performed in Microsoft Excel 2016 without error analysis and propagation of error for individual measurements. Stock solutions of samples (10 mg/ 2 ml DMSO) and subsequent dilutions were papered once and used for all experiments. The Ferrous Equivalents (FE) was calculated from the standard curve of $FeSO_4$(from the line graphs).

3.6 Molecular Modelling

All computational calculations were carried out in the framework of the Gaussian 09 package. The structure was fully optimized at the ground state using B3LYP correlation functional method with 6-31G + (d, p) basis set for non-metals (C, H, N and O atoms), while LANL2DZ basis set was used for silver atom within density functional theory (DFT) (Bayach et al., 2016; Ramle et al., 2019; Salman et al., 2013b).

CHAPTER 4: RESULT AND DISCUSSION

4.1 Synthesis

4.1.1 Synthesis of [benz]imidazolium acridine ligands

The synthesis of imidazolium salts is following the menshutkin reaction (Menschutkin, 1890a, 1890b), as shown in **Figure 4.1**. Two different procedures were used to synthesize the *N*-substituted imidazolium-acridine salts **7-30**. The first approach applied reaction of *N*-substituted imidazole with 9-chloroacridine to furnish the target compound **7-30** directly. The Menshutkin reaction works well with alkylated imidazoles and benzimidazoles but not with [benz]imidazoles containing aromatic substituents. For these compounds, a reversed approach was used. Here, 9-chloroacridine derivatives **4** was reacted with imidazole and benzimidazole, respectively, to furnish 9-(1-imidazolyl) acridine **6a-6b** and 9-(1-benzimidazolyl) acridine **6c.** The intermates **6a, 6b** and **6c**, respectively, with subsequently alkylated using benzyl or phenacyl bromide. The reason for different approach was low yields and purification problems for compounds **17-26**. **Table 4.1** summarises the synthesis of [benz]imidazolium-acridine ligands. The target compounds were obtained as a yellow solid by crystallization from methanol. The structures of the compounds were confirmed by ^{1}H and ^{13}C NMR.

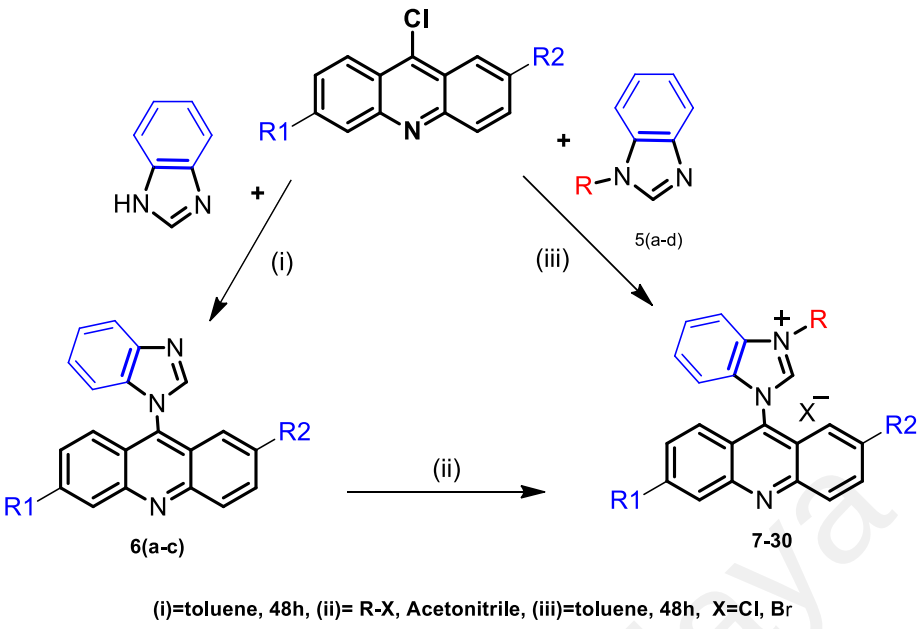

Figure 4.1: **Synthesis of imidazolium-acridine salts derivatives**

The Menshutkin reaction converts an amine with an alkyl halide into a fully substituted ammonium salt. The synthesis of [benz]imidazolium acridine ligands follows a nucleophilic aromatic substitution, comprising the addition of nucleophile at the aromatic ring with subsequent elimination of the leaving groups, as shown in **Figure 4.2**.

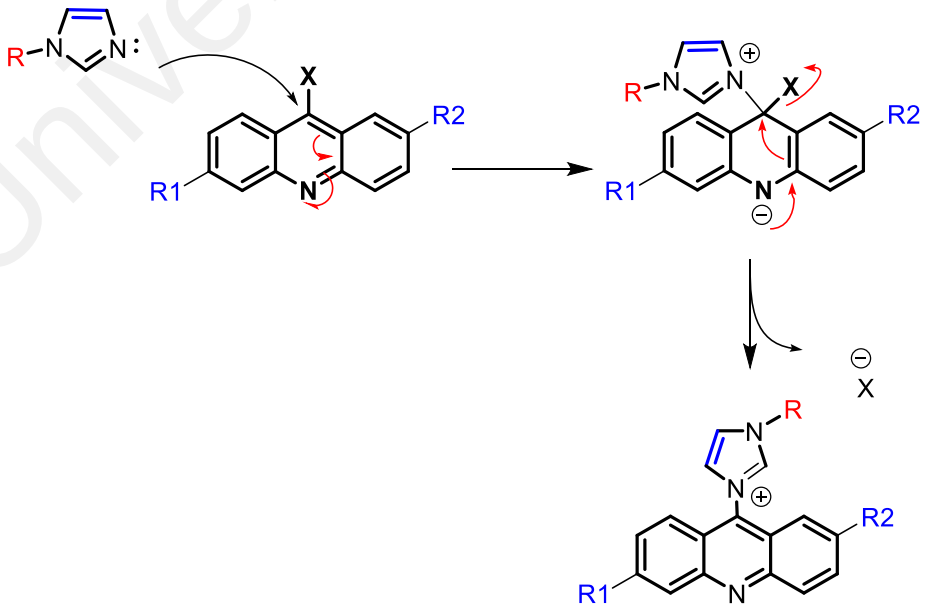

Figure 4.2: Mechanism of reaction between acridine and imidazole

Table 4.1: Structures of the [benz]imidazolium salts.

[benz]imidazolium–based acridine salts						
Compd.	**Precursor**	**R1**	**R2**	**R3**	**X**	**Yield**
6a	IM	H	H	-	-	81%
6b	IM	Cl	OMe	-	-	79%
6c	BIM	H	H	-	-	80%
7	IM	H	H	C_6H_{13}	Cl	75%
8	IM	H	H	$HC{\equiv}CCH_2$	Br	95%
9	IM	H	OMe	Me	Cl	74%
10	IM	H	OMe	C_4H_9	Cl	77%
11	IM	H	OMe	Bn	Cl	77%
12	IM	Cl	OMe	Me	Cl	85%
13	IM	Cl	OMe	C_2H_5	Cl	81%
14	IM	Cl	OMe	C_4H_9	Cl	80%
15	IM	Cl	OMe	C_8H_{17}	Cl	75%
16	IM	H	H	*p* Me-Bn	Cl	85%
17	IM	H	H	*p* Br-Bn	Br	90%
18	IM	H	H	*o*Br-Bn	Br	91%
19	IM	H	H	*p* NO_2-Bn	Br	91%
20	IM	H	H	$BzCH_2$	Br	91%
21	IM	H	H	*p*Br-$BzCH_2$	Br	95%
22	IM	Cl	OMe	Bn	Cl	80%
23	IM	Cl	OMe	$BzCH_2$	Br	90%
24	IM	Cl	OMe	*p*Br-$BzCH_2$	Br	85%
25	IM	H	H	*p*OCH_3-Bz	Br	90%
26	IM	H	H	$C_6H_5COCHCH_3$	Br	85%
27	BIM	H	H	Me	Cl	85**%**
28	BIM	H	H	C_2H_5	Br	85**%**
29	BIM	H	H	Bn	Br	80**%**
30	BIM	Cl	OMe	Me	Cl	80**%**

Bn= benzyl, *P*= para, *o*= ortho, Me= methyl, Bz=phenacyl

Attempts to react 9-chloroacridine with *N*-substituted imidazoles containing long alkyl chain failed to produce the target compounds, as shown in **Figure 4.3** path (i). The failure might be due to the size of long chain, which upon entropic coiling blocks access to the N atom at the imidazole ring. Because of the failure, another route towards the product has been attempted. Acridine imidazole **6** was subjected to Menshutken reaction using corresponding long chain alkyl bromides according to **Figure 4.3** path (ii). However, no reaction was observed. This may be associated with low reactivity of the alkyl halide.

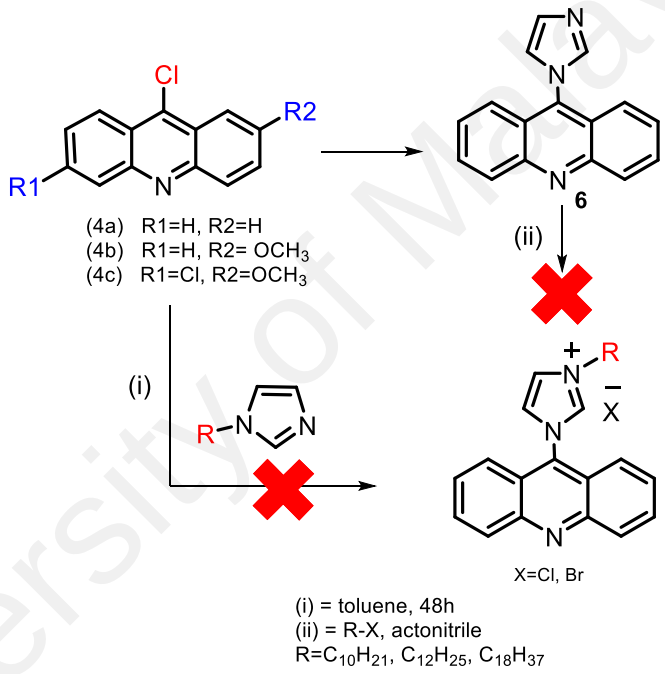

Figure 4.3: Synthesis of *N*-long chain alkyl imidazolium-acridine salts

4.1.2 Synthesis of Ag(I)-NHC complexes

The metalation reaction of the ligands with an excess of silver oxide (Ag_2O) failed. Different solvent, *i.e.* dichloromethane, methanol and acetonitrile, and temperatures (room temperature to 80 ºC) have been investigated over reaction time between one and two days. This failure was attributed to limited solubility of the ligands in the reaction medium (Chen, 2011; Gimeno et al., 2012). Also, the halide counter ions are problematic due to the formation of silver halide bridge complexes affording Ag(I)-complexes (Chen, 2011; Gimeno et al., 2012), as shown in **Figure 4.4**.

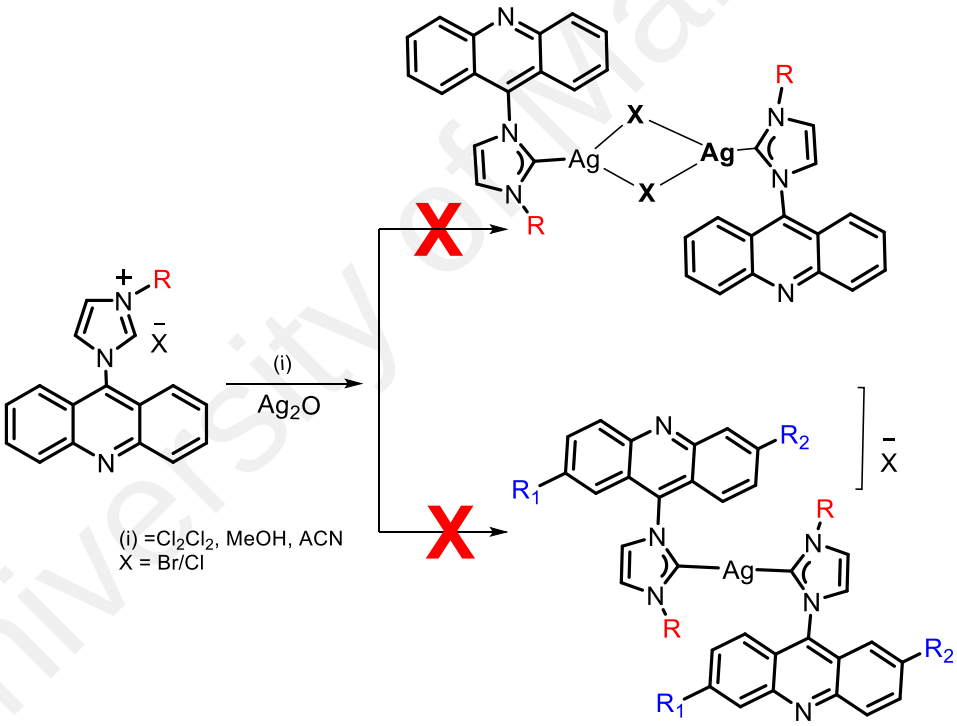

Figure 4.4: Synthesis of Ag(I)-imidazolium Cl/Br complexes

Because of the failure route mentioned above, an alternative approach towards the complexes has been used. Treatment of the imidazolium salts with potassium hexafluorophosphate furnished the corresponding PF_6 ligands in 75-80 % yield. The latter were reacted with Ag_2O under light protection to provide the expected carbene complexes **31-45**, as yellow solids. The sequence is illustrated in **Figure 4.5**, while compounds details can be found in **Table 4.2**. The ion exchange was confirmed by ^{31}P &^{19}F NMR. The Ag(I)-NHC complexes were established based on ^{1}H and ^{13}C NMR spectra. They were soluble in acetonitrile and dimethyl sulfoxide (DMSO) but insoluble in non-polar solvents, and remained stable in the presence of air and moisture at room temperature without evidence of decomposition based on ^{1}H NMR spectra. Moreover, the stability of complex **42** in solution was studied over a period of 7 days by ^{1}H NMR. The investigation, illustrated in **Figure 4.5**, indicated no signs of degradation. The mass spectra indicated a molar ratio of 2:1 for ligands and metal. Besides, isotopic patterns, reflecting the silver atom, were found.

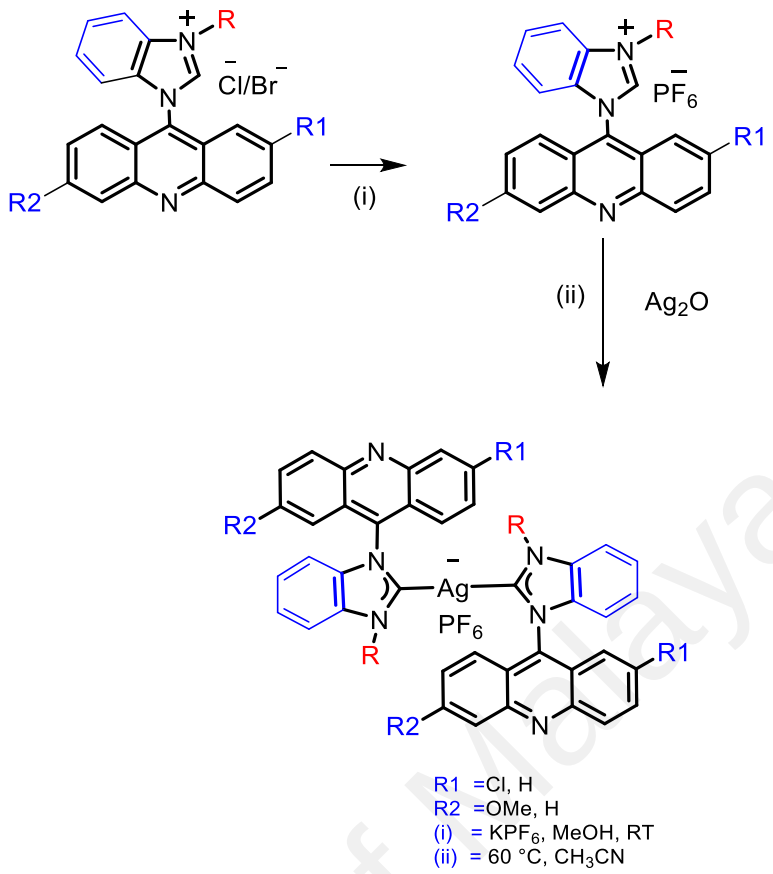

Figure 4.5: Synthesis of Ag(I)-complexes

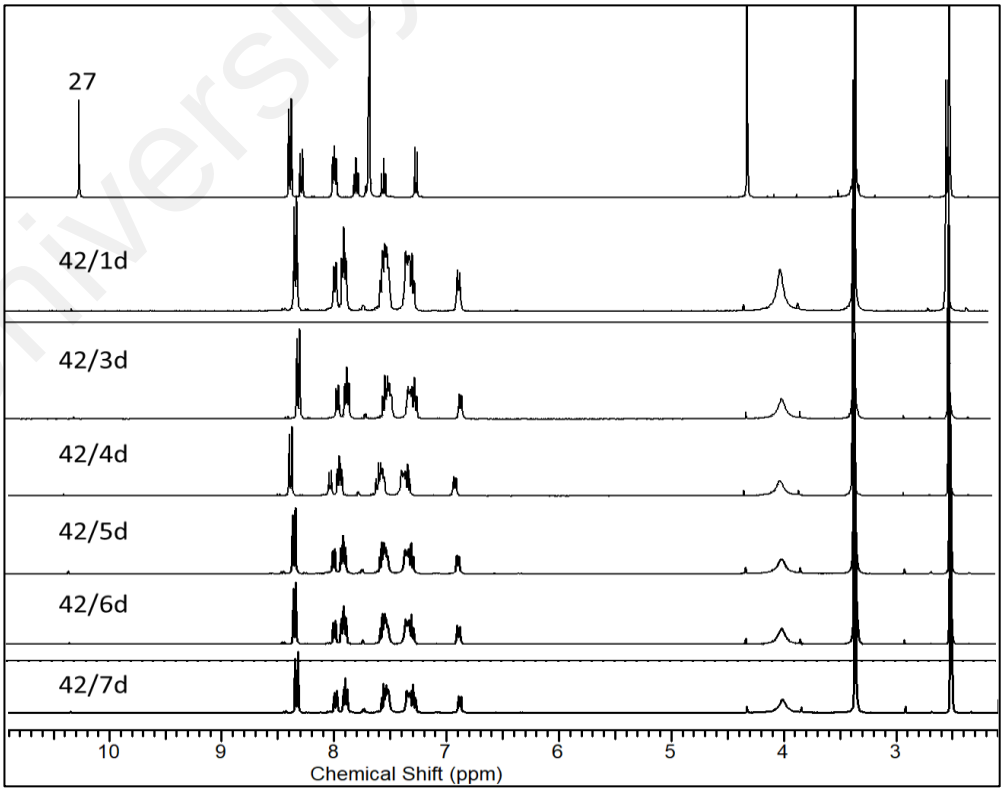

Figure 4.6: Stability of Ag(I)-complexes

Table 4.2: Structures of the Ag(I)-imidazolium complexes.

Ag(I)[benz]imidazolium-acridine complexes					
Compd.	**precursor**	**R1**	**R2**	**R3**	**Yield**
31	IM-7	H	H	C_6H_{13}	54%
32	IM-9	H	OMe	Me	59%
33	IM-10	H	OMe	C_4H_9	65%
34	IM-12	Cl	OMe	Me	70%
35	IM-13	Cl	OMe	C_2H_5	70%
36	IM-14	Cl	OMe	C_4H_9	70%
37	IM-16	H	H	*p* Me-Bn	76%
38	IM-17	H	H	*p* Br-Bn	75%
39	IM-18	H	H	*o*Br-Bn	80%
40	IM-19	H	H	*p* NO_2-Bn	65%
41	IM-22	Cl	OMe	Bn	80%
42	BIM-27	Cl	OMe	Me	70**%**
43	BIM-28	H	H	C_2H_5	70**%**
44	BIM-29	H	H	Bn	65**%**
45	BIM-30	H	H	Me	70**%**

Ligands containing phenacyl substituents could not be converted into complexes, as shown in **Figure 4.7**. Various conditions in terms of solvent and temperature have been applied for the reaction. However, the NMR spectra indicated complex mixtures. The failure may reflect disrupting interaction between carbonyl oxygen with silver leading to a diversity of structures.

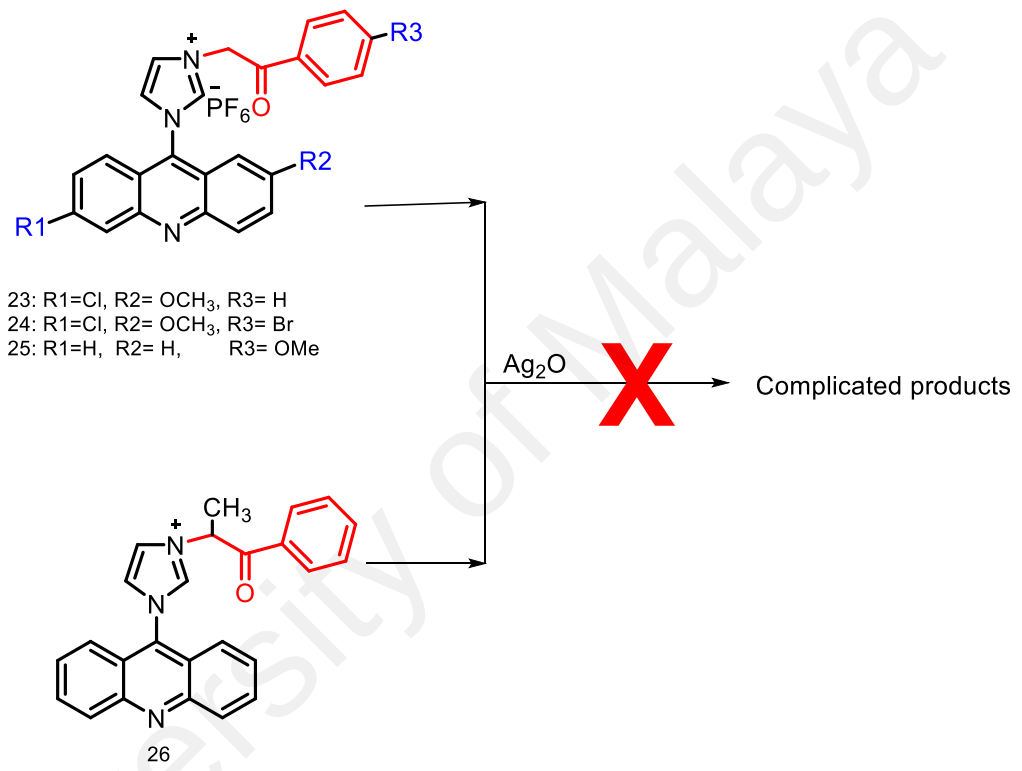

Figure 4.7: Synthesis of Ag(I) complexes with phenyl group

4.2 Spectroscopic analysis

Ligands and complexes were characterized by IR (ATR) spectroscopy in the range of 4000-400 cm^{-1}. The spectra, examples shown in **Figures 4.8-4.9**, were consistent with the proposed structures. The ligands and their Ag(I)-complexes do not have many functional groups. However, there are minor differences between the ligands and complexes which may be used as primary indicators of a successful synthesis (Iqbal et al., 2013a; Iqbal et al., 2013b).

In the spectra, the peaks at 3065-2850 cm^{-1} are assigned to the vibration of aliphatic and aromatic C-H. The bands observed at range 1650-1630 cm^{-1} are ascribed to the imidazole ring C=N stretching vibrations; this observation is in accordance with the previous studies (Budagumpi & Revankar, 2010; Haque et al., 2012; Srivastava, 2011; Tellez et al., 2008). Finally, the bands at around 1566-1422, 1238-1220 cm^{-1} of all compounds are assigned for the other modes of vibrations of C=C, C-N and C-O modules, respectively. This observation is in accordance with the literature (Budagumpi & Revankar, 2010; Haque et al., 2015b; Srivastava, 2011; Wylie et al., 2010). The metal complexes almost reflect the ligand spectra, except for some slight variations in the shifts and significantly reduced intensities due to the dominant metal absorption at about 800 cm^{-1}.

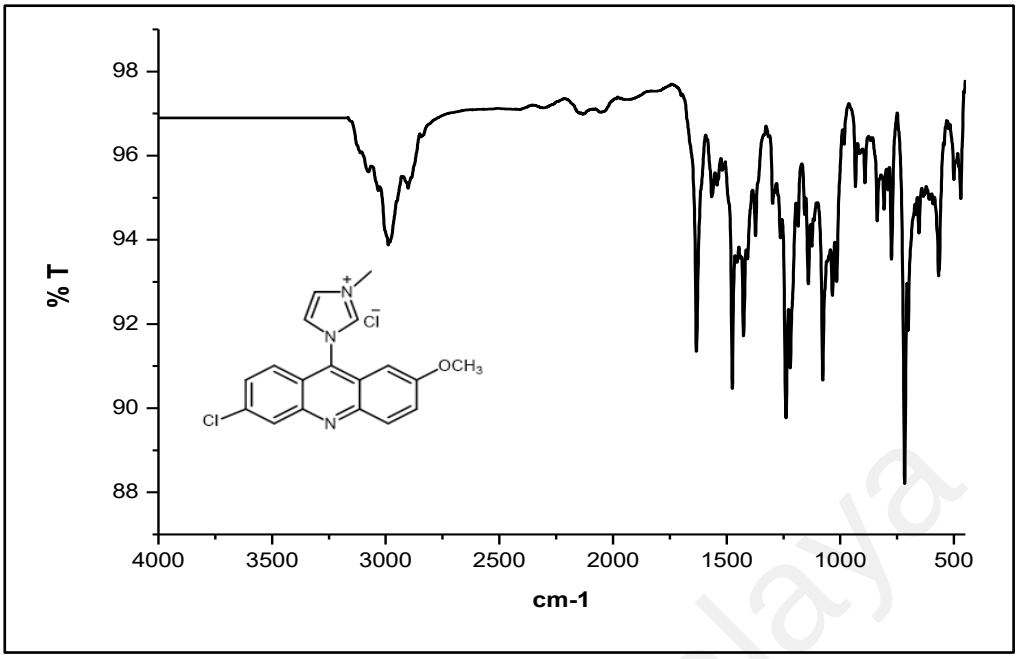

Figure 4.8: IR spectrum of ligand 12

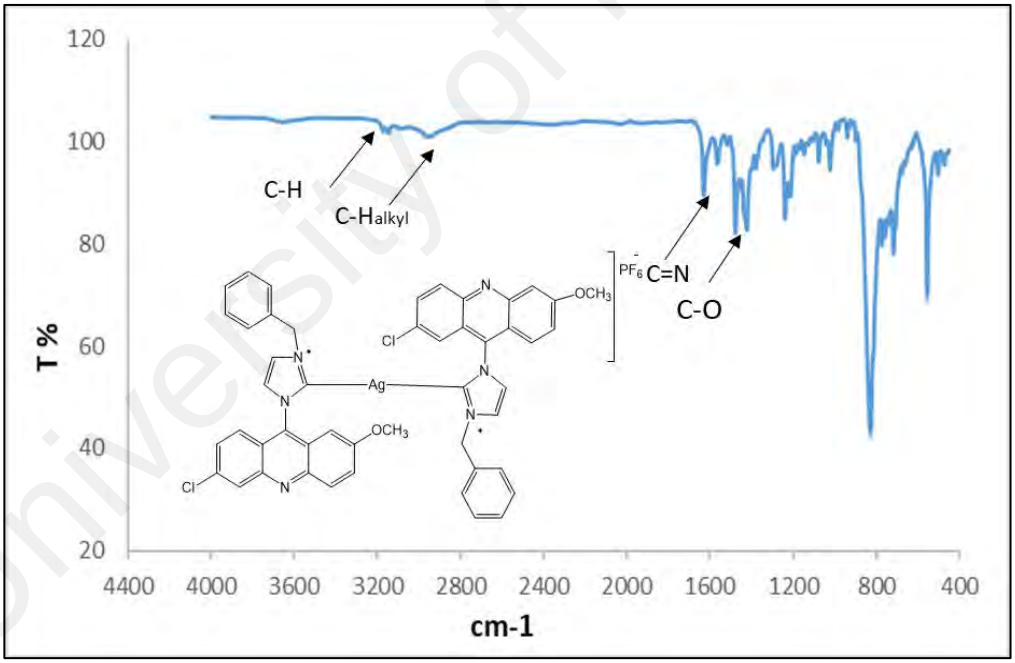

Figure 4.9: IR spectrum of complex 41

NMR spectra of the compounds were analysed in dimethyl sulfoxide (DMSO-d_6), chloroform ($CDCl_3$) and acetonitrile-d_3 deuterium over the scan range 0 to 16 ppm for ^{1}H NMR and 0 to 250 δ ppm for ^{13}C NMR studies. In ^{1}H NMR spectra of the ligands, examples are given in **Figures 4.10-4.12**, the most deshielded signal at δ 9 –11 ppm was observed for acidic imidazolium proton (NC**H**N), which appeared as sharp singlet peak. Its presence indicates the successful formation of the imidazolium salts, while its disappearance upon metal treatment reflects the formation of the carbene complex. The alkyl protons of compounds were seen between 0 – 6 ppm in ^{1}H NMR. The characteristic peaks for methylene protons attached to the imidazole nitrogen appeared at δ 4 - 6 ppm, a triplet peak at δ 0.8-1.00 ppm indicated the terminal methyl group of alkyl chain. The aromatic protons of compounds were found at δ 6.50-8.50 ppm in the ^{1}H NMR spectrum.

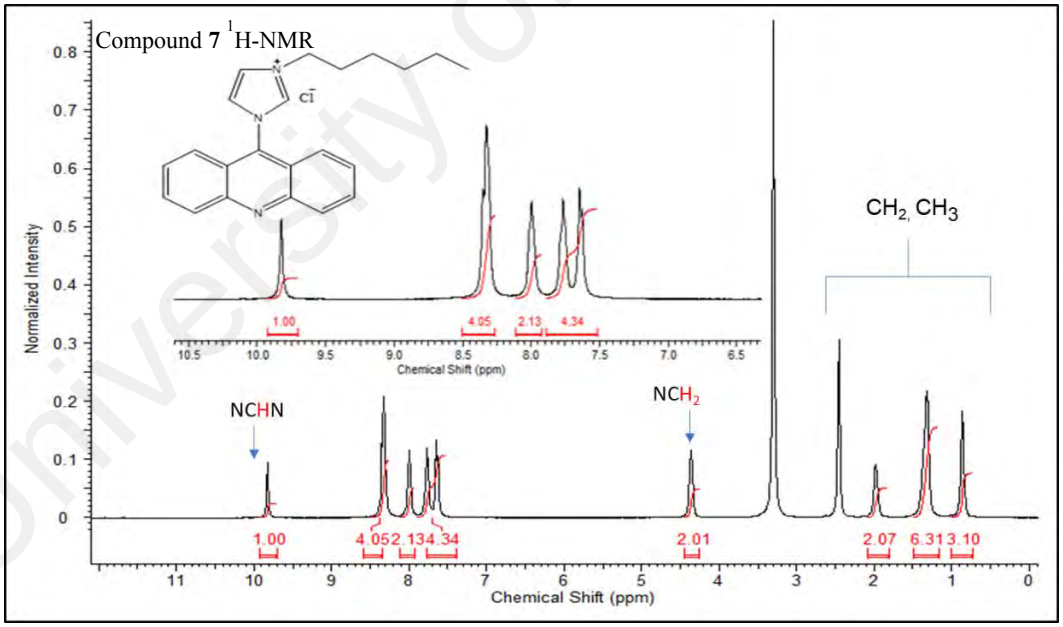

Figure 4.10: ^{1}H NMR of compound 7

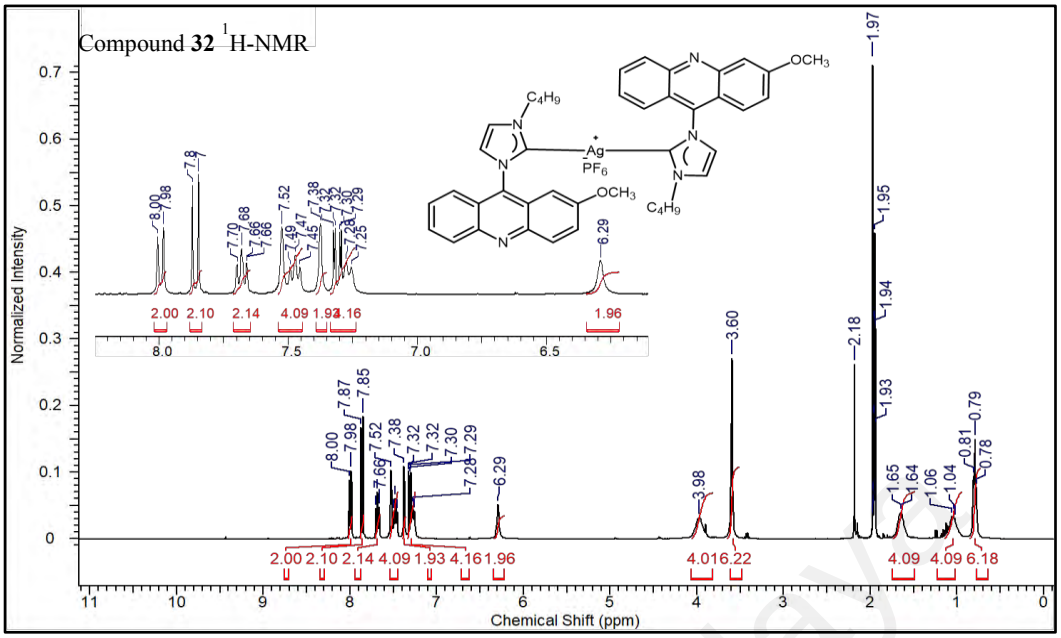

Figure 4.11: ^{1}H NMR of compound 32

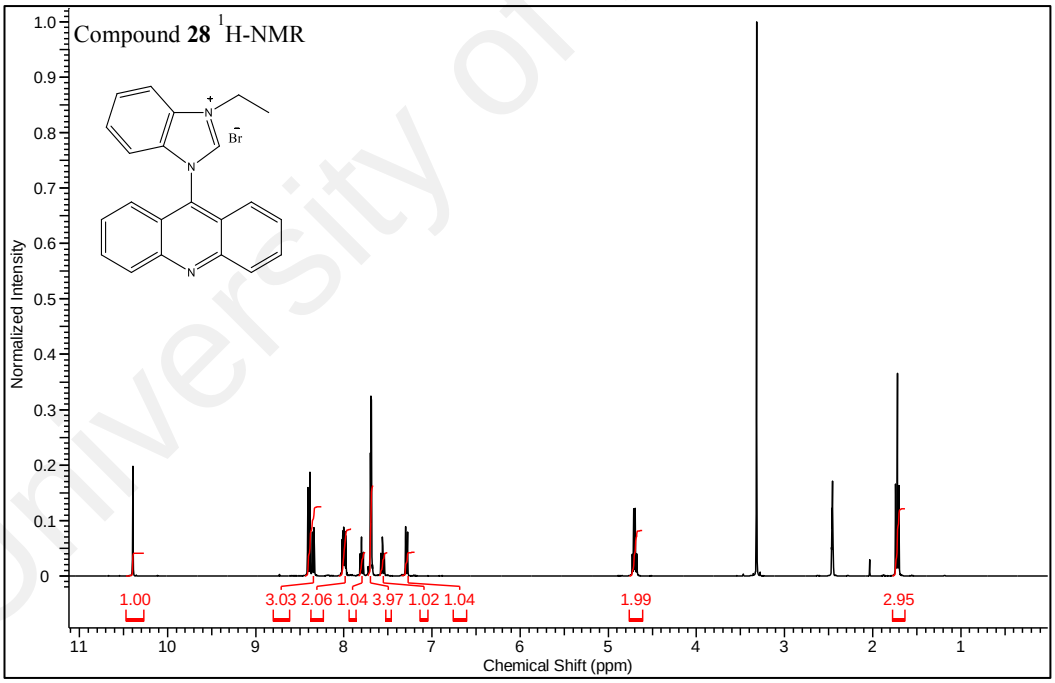

Figure 4.12: ^{1}H NMR of compound 28

Figures 4.13-4.15 show examples for ligands and a complex. The chemical shift of the carbene carbon belonging to Ag(I)-complexes was observed between 170-200 ppm in the ^{13}C NMR spectra, which is in agreement with reported data for similar Ag(I)-complexes (Haque et al., 2013c; Ozdemir et al., 2010). The corresponding carbon peak for the ligands were observed in the range of 133-145 ppm, matching previously reported data for related [benz]imidazolium ligands (Achar et al., 2017b; Haque et al., 2015a). Carbon in position 2 at acridine with Methoxy group resonated at 159-160 ppm for the compounds. The signals caused by Aryl/alkyl group, which connects with [benz]imidazolium units, displayed sharp singlets in the range 40–60 ppm. Also, the alkyl chain carbon resonances were observed in the chemical shift regions δ10–30 ppm.

A comparison between the ^{13}C NMR-spectra of the ligands and Ag(I)-complexes, as shown in **Figures 4.13-4.15**, suggested a successful synthesis as indicated by appearance peak at 170-200 ppm after complexation. To differentiate between quaternary C and methine CH in aromatic regain of the compounds an APT NMR spectrum was recorded, as shown in **Figure 4.16.**

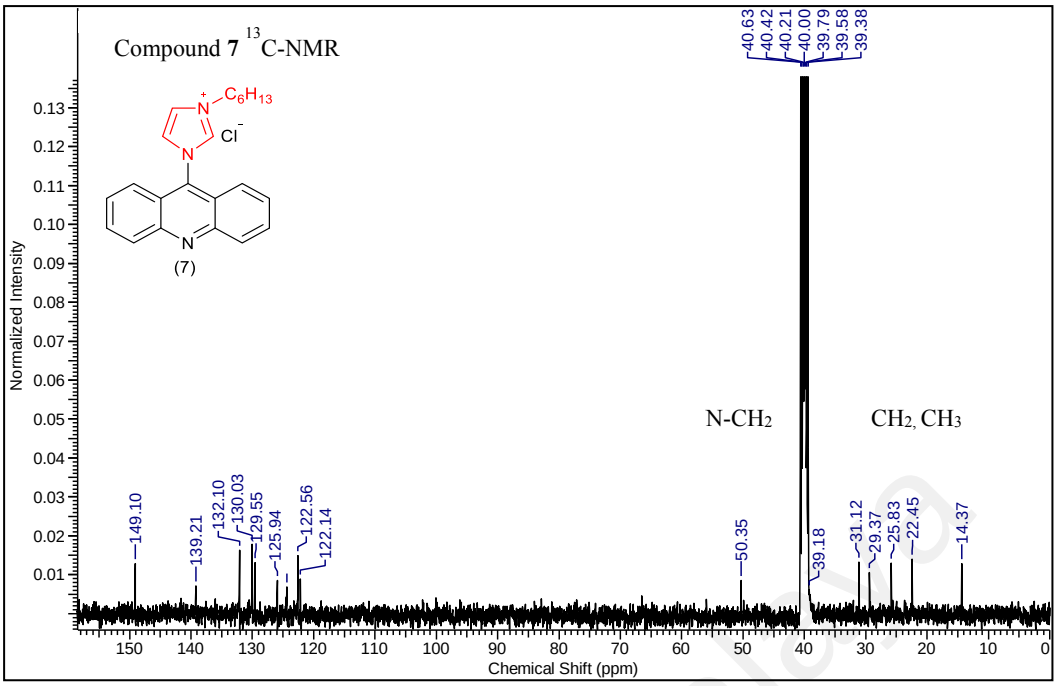

Figure 4.13: ^{13}C NMR of compound 7

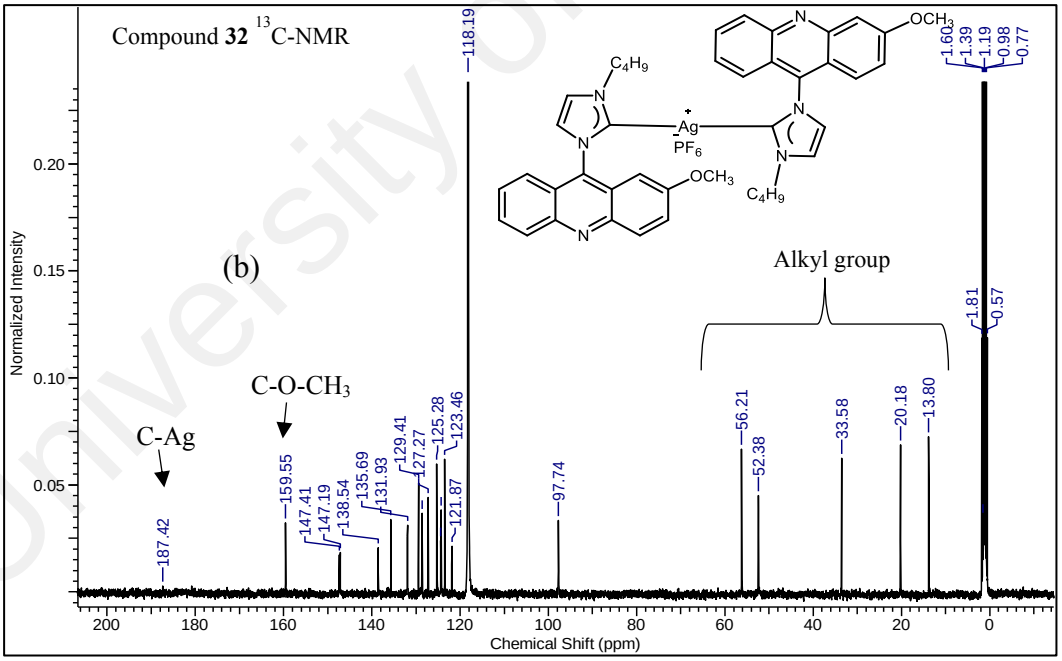

Figure 4.14: ^{13}C NMR of compound 32

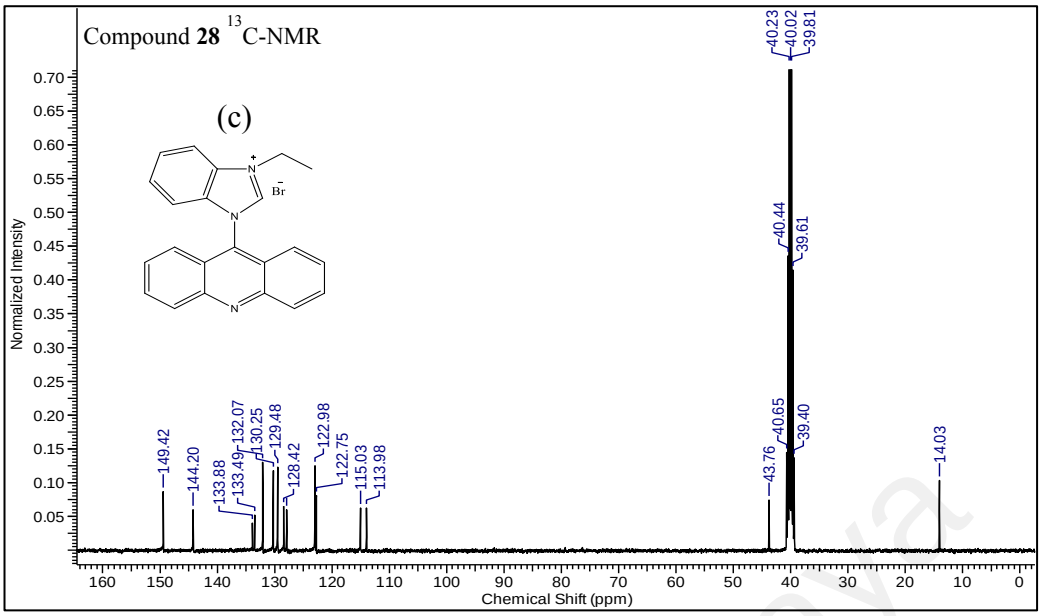

Figure 4.15: ^{13}C NMR of compound 28

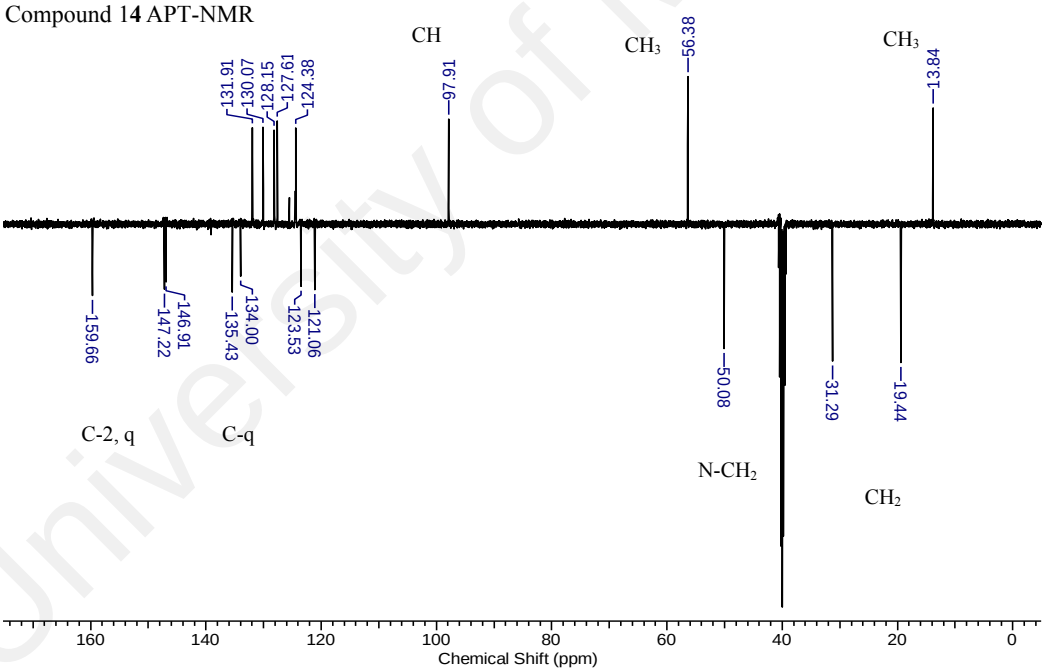

Figure 4.16: APT NMR of compound 14

The elemental analysis data of ligands and their Ag(I) complexes were found to be in good agreement with proposed formulae as the values are approximately similar to each other as shown in synthetic methods. The elemental composition of the compounds was determined using energy dispersive X-ray analysis (EDX) spectroscopy. The appearance of a strong peak around 3 KeV designates the position of elemental silver (Ahmad et al., 2015). In the ligands, it is clearly observed several peaks for C, N, O and Br or Cl in the EDX spectrum of ligands **12** and **29** confirming its successful formation. Meanwhile, EDX spectrum of Ag(I)-complex **36** showed peaks for component elements (Ag, C, N, F, P and Cl); evidence that Ag(I)-complexes were successfully synthesized, a new peak is observed which recognized as Ag atoms, as depicted in **Figure 4.17**, but did not show the characteristic signal of Ag^{+} in ligand spectrum. Furthermore, the presence of P and F, which are confirmed in the ion exchange with Cl or Br. The results of EDX spectra showed that no Br^{-}or Cl^{-} ions could be detected in the complexes, which further confirm the successful anion change. The obtained complexes confirmed the presence of Ag metal in each complex (refer to appendix C).

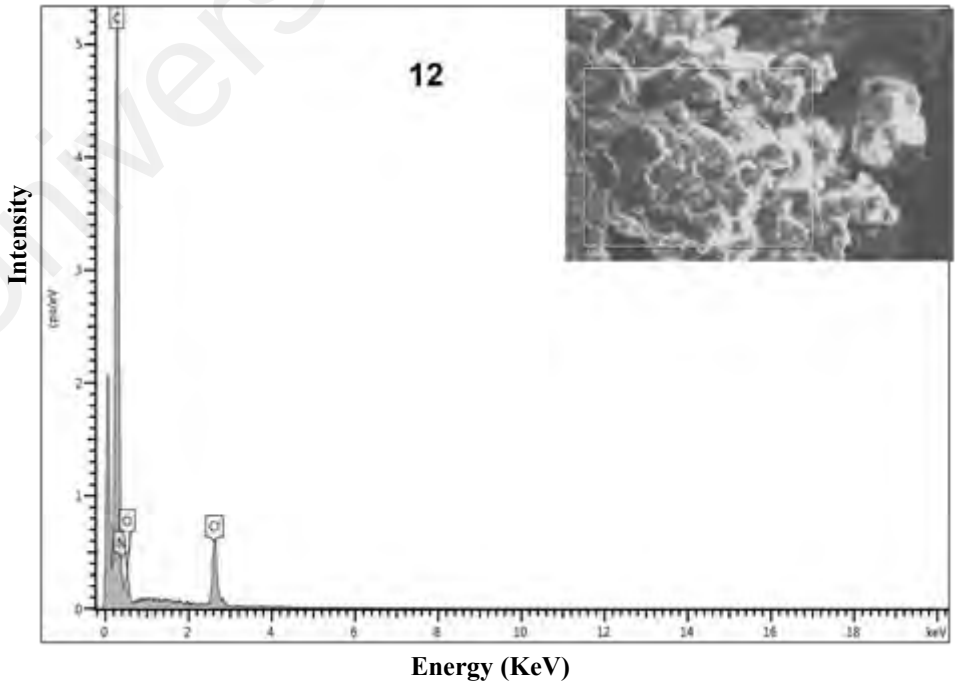

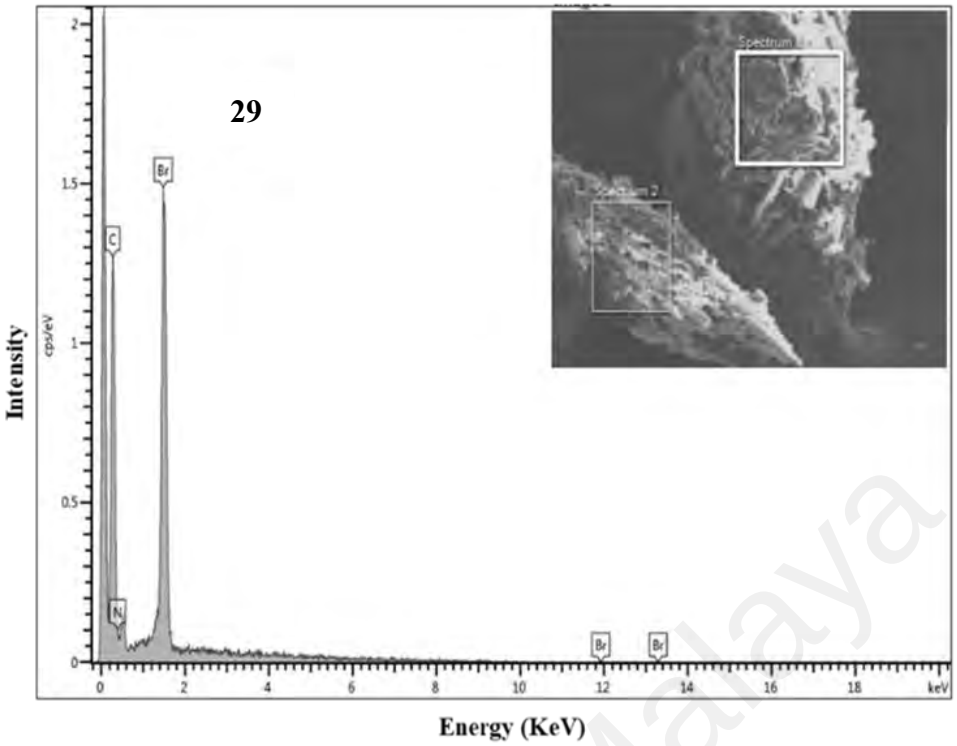

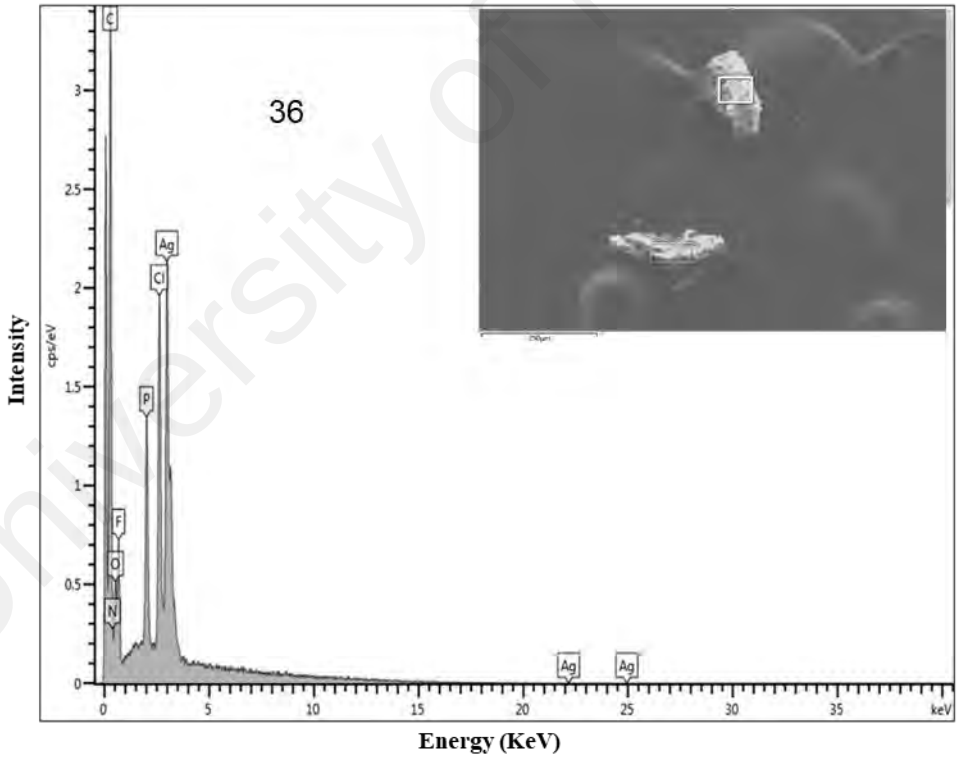

Figure 4.17: Representative EDX spectra

4.3 Optical application

The absorption spectra of the compounds were recorded in aqueous acetonitrile (1:1, v/v) at concentration of $1.2x10^{-6}$ mol L^{-1}. The maximum wavelength was used to indicate the fluorescence application. **Figure 4.18** illustrates the absorption of the compound **12** and their complex **34** at a concentration of $1.2x10^{-6}$ mol L^{-1}. The maximum intensity band at between 300-450 nm for compounds can be ascribed to n-π* transition. The intensity peaks of the complex increased more than the intensity peak of the ligand, which its also due to the interactions between the imidazolium ligand and silver metal.

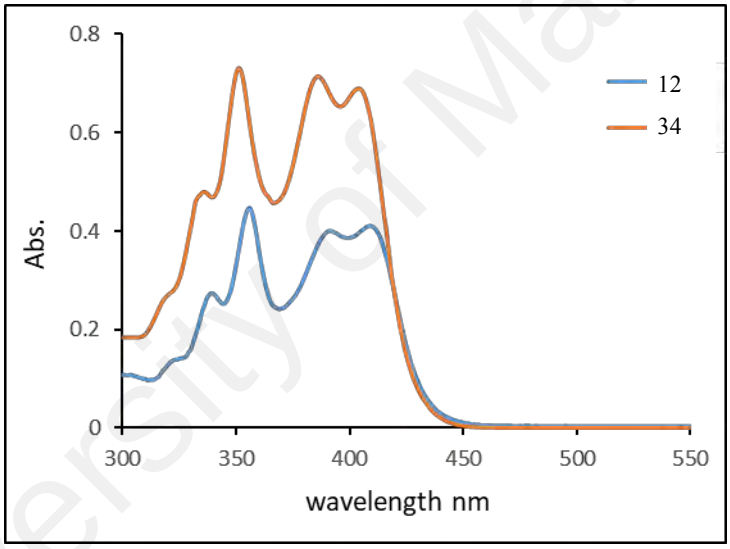

Figure 4.18: **UV-Vis of imidazolium-acridine**

Acridine and its derivatives show high fluorescent activity. This property may enable monitoring of compounds inside a cell to visualise the distribution of drugs. All [benz]imidazolium ligands and their Ag(I) complexes exhibited notable fluorescence upon excitation at 390 nm. The recording of fluorescence spectra followed the conditions use for absorption spectra. The excitation wavelength was chosen to match the maximum for the absorption. The fluorescence spectra of ligands and complexes, as shown in **Figure 4.19**, were almost identical. The comparable fluorescence intensity of ligands and complexes indicates reduced luminescence efficiency for the complexes considering the 1:2 ratio of metal and ligand. Since the complexes contain two of the ligands its fluorescence it is less efficient compared to ligands. Two different shapes, denoted as A & B, were found for the fluorescence spectra. Details are given in **Tables 4.3-4.4**.

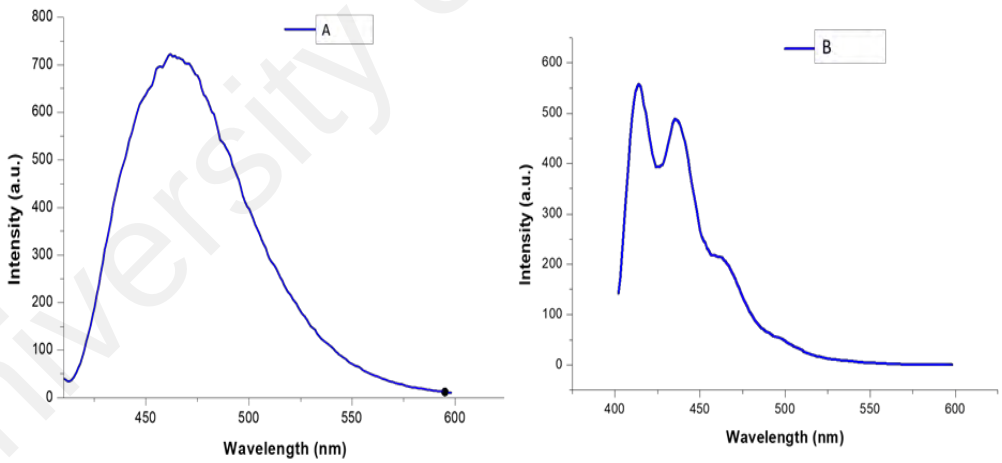

Figure 4.19: Fluorescence spectra shapes

Table 4.3: Fluorescence behaviour for [benz]imidazolium-acridine[x] .

Compd.	$\lambda_{max\ abs}$ λ_{exc} [nm]	$Spect_{em}$	$\lambda_{max\ em}$ [nm]	Int_{em} [AU]
3c	405	A	451	732
6a	389	B	416, 440	493, 462
6b	400	A	455	774
6c	387	A	437	350
7	410	A	458	856
8	400	A	465	714
9	401	B	415, 436	553, 488
10	407	A	450	761
11	411	A	471	456
12	410	A	464	640
13	403	A	464	720
14	392	B	420, 435	319, 323
15	387	B	421, 438	571, 582
16	387	A	461	191
17	386	B	416, 448	427, 409
18	384	B	414, 438	608, 540
19	385	B	416, 440	436, 396
20	408	A	465	756
21	409	A	450	798
22	408	A	443	947
23	386	A	450	600
24	384	A	445	610
25	385	A	442	600
26	387	A	440	558
27	389	B	413, 438	315, 330
28	388	A	438	319
29	387	B	415, 436	534, 528
30	389	A	468	529

[x] c =12 μ mol L^{-1} (acetonitrile/water 1 : 1 v/v)

Table 4.4: Fluorescence behaviour of Ag(I) complexes[x].

Compd.	$\lambda_{max\ abs}$ λ_{exc} [nm]	Spect$_{em}$	$\lambda_{max\ em}$ [nm]	Int$_{em}$ [AU]
31	389	A	460	600
32	400	A	456	700
33	401	A	458	660
34	411	A	460	700
35	405	A	464	610
36	407	A	465	373
37	386	B	416, 433	237, 239
38	387	A	431	262
39	384	B	413, 435	800
40	387	B	416, 434	224, 213
41	408	A	465	843
42	411	A	465	645
43	398	A	464	271
44	391	A	440	712
45	411	A	462	638

[x] c =12 μ mol L^{-1} (acetonitrile/water 1 : 1 v/v)

For excitation, all compounds required low energy UV-light. The blue fluorescence of the sample can easily be visualized using the long wavelength of a standard laboratory UV lamp, as depicted in **Figure 4.20**. The substitutions of acridine with an [benz]imidazole changed the emission spectrum (Raju et al., 2016). This change matched previous reports on documented π*→π and π*→n transitions (Elangovan et al., 2004; Gimeno et al., 2012; He et al., 2015; Lang et al., 2013; Sandeep & Bisht, 2006). [benz]imidazolium-acridine cations containing substituted acridine exhibited double peak fluorescence spectra according to type B, while other compounds showed only a broad single peak emission reflection spectrum type **A**, as shown in **Figure 4.19.** Unlike for *N*-arylated imidazolium cations (Boydston *et al.*, 2008), no significant differences were observed between substituents with and without conjugated systems at the imidazole.

This can be related to the breaking of conjugation due to the methylene linkage. In terms of fluorescence intensity, only a moderate variation was found between the systems. An exception to this, however, is found at compound **18**, which exhibited significantly lower fluorescence intensity. A rational for this unusual behaviour could not be found, unless the effect is related to the non-symmetric aromatic at the imidazole (o-substitution). Compounds 9, 14, 15, 17, 18 and 19 displayed a blue emission with two emission peaks at λ_{max} = 413 and 438 nm, these may be assigned to the π-π* transitions of the delocalized π electrons in the imidazole ring and acridine and the n-π*transitions of the n-electrons of the nitrogen atoms of imidazole and acridine (Cheng *et al.*, 2014). Besides that, compound **6a** showed a broad emission band at λ_{max}= 440 nm, whereas **6c** showed a broad emission band at λ_{max}= 455 nm. *N*-alkyl imidazolium-acridine derivatives and *N*-aryl-imidazolium-acridine exhibited stronger blue emission band at 464 nm upon the excitation values. As stated previously, the emission properties of *N*-substituted-imidazolium-acridine salts are strongly influenced by the nature of its *N*-substituents. The longest wavelength λ_{max} was obtained when *N*-aryl substituents were placed on the imidazole ring (Boydston *et al.*, 2008).

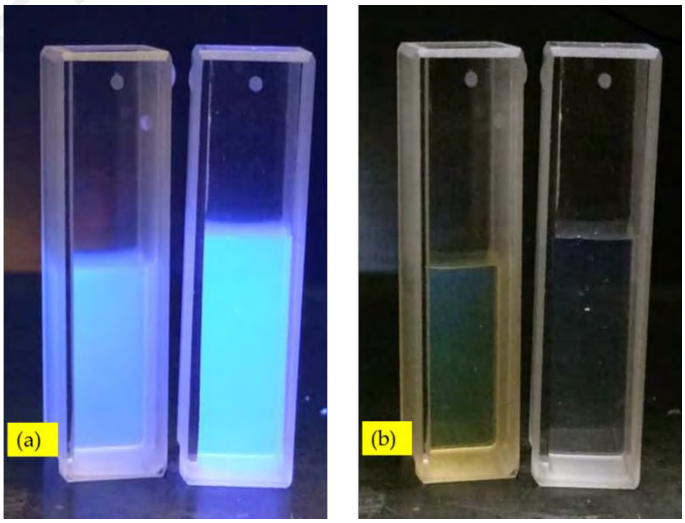

Figure 4.20: Images of samples for 29 (left) and 44 (right) under UV (a) and daylight (b)

4.4 DFT calculations

Attempts to grow single crystals using different methods and solvent have failed. Some compounds led to needle-shaped crystals, which diffraction patterns could not be solve based to the big error in R_{int}~100. A computation study was applied to confirm the structures based on powder XRD patterns with reported analogue crystal structures. Ag(I)-benzimidazolium complex **42** was compared to the imidazolium analogue **47**, for which two crystal structures complexes reported (Gimeno et al., 2012; He et al., 2015). DFT calculations indicated practically identical core structures for benzimidazolium **27** and imidazolium analogue **46**. Upon complexation, the ligands remained unchanged in geometry. The [benz]imidazole ring is perpendicularly aligned to the acridine ring with dihedral angles of 90°, as shown in **Figures 4.21**. This geometry is in agreement with a reported crystal structure (Gimeno et al., 2012).

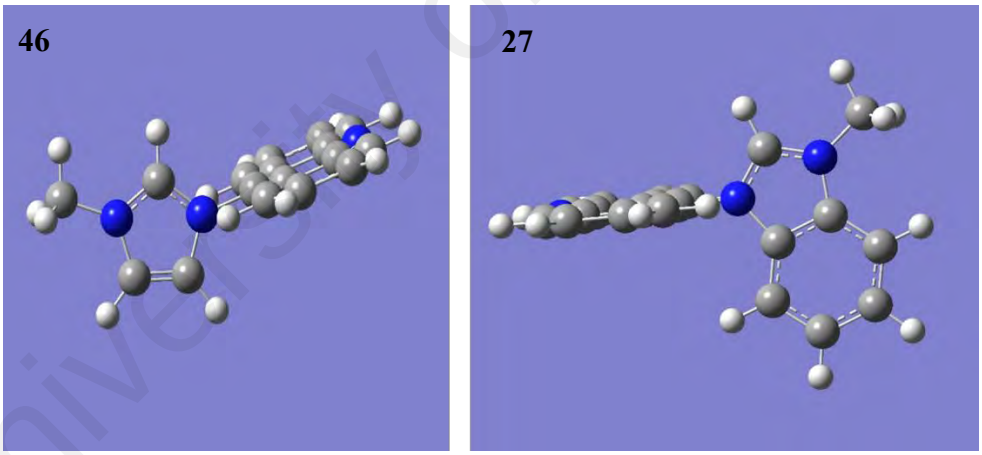

Figure 4.21: Optimized ligand geometry of [benz]imidazolium-acridine-ligands at the B3LYP/GENECP level with 6–31G(d) basis set for non-metals

The DFT result for the Ag(I)-benzimidazolium **42** and imidazolium **47** share the same geometry, as shown in **Figure 4.22**. The simulated structure of **47** matched the crystal structure reported by Gimeno et al. Another crystal structure (He et al. 2015) differed in the dihedral angle between the aromatic rings (84°). More pronounced than the difference in the dihedral angle was the alignment of the two imidazolium ligands around the silver. While the DFT result confirmed a parallel arrangement as energetically favoured confirmation the perpendicular alignment was reported by He et al.

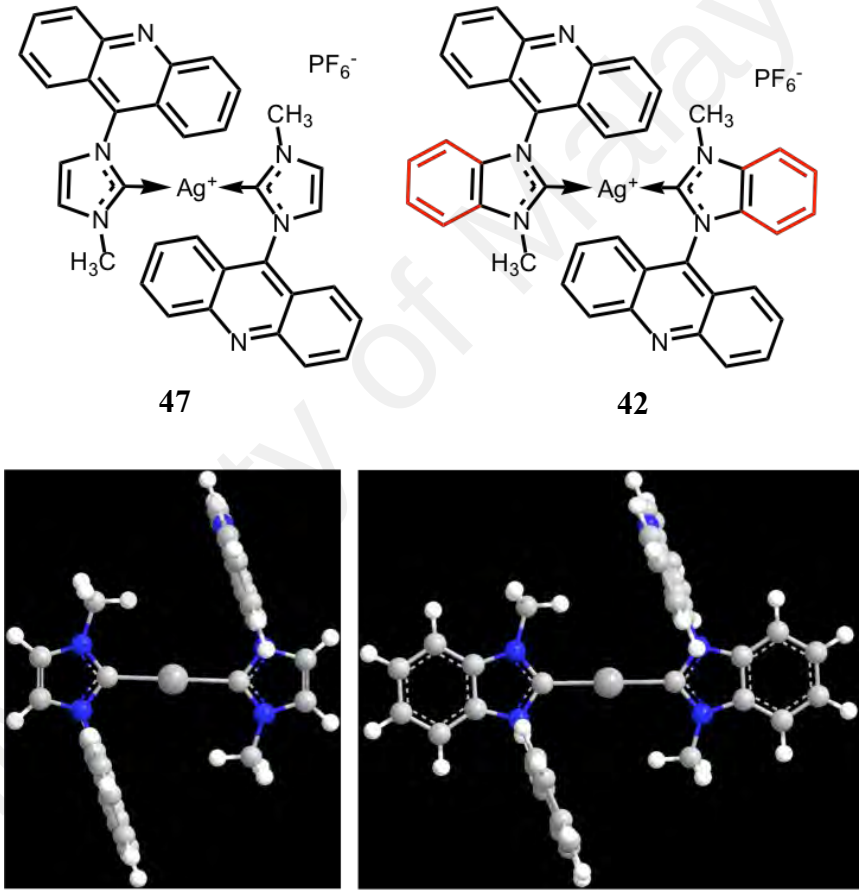

Figure 4.22: Structural analogy of complex 42 and literature reported 47

The XRD pattern of the experimental and crystal structure generated complexes mismatched, as shown in **Figure 4.23**. This may be partially due to the needle shape of the crystals. More importantly, additional peaks in the experimental XRD indicate the presence of other morphologies besides the reported species (Gimeno et al., 2012; He et al., 2015). Because of this constrain, the attempted crystal structure confirmation was abended. Besides, the experimental XRD of **47** and **42** did not show the expected similarity, as can be seen in **Figure 4.23.**

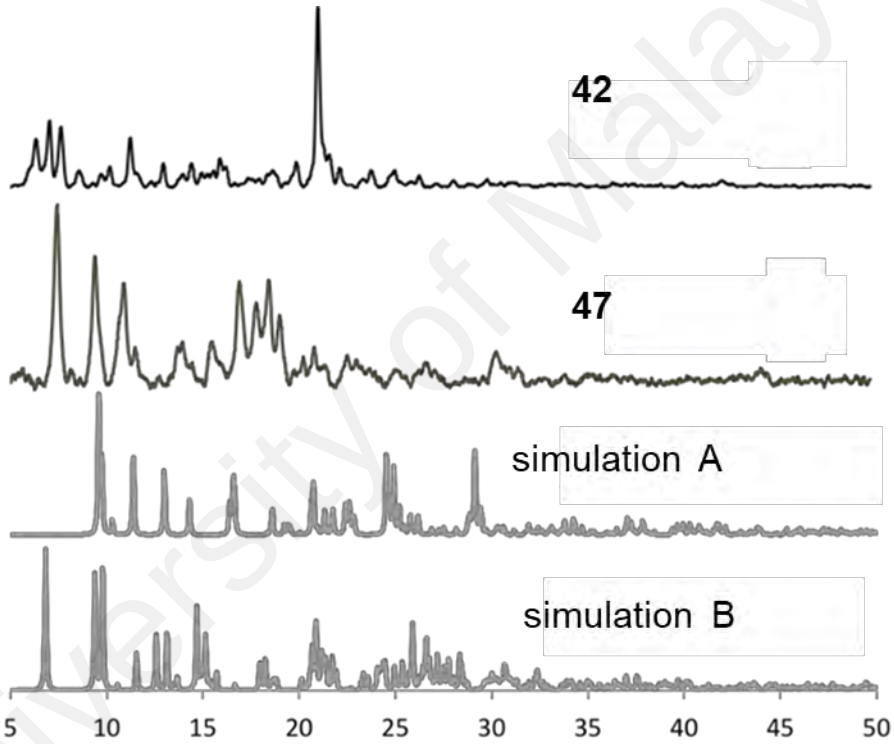

Figure 4.23: Comparison of experimental XRD pattern for 47, 42 with reported crystal structures; A (Gimeno et al., 2012), B (He et al., 2015)

4.5 Biological Activity

A very important aspect in the development of biological-metal complexes is their stability under physiological conditions, which allows a better delivery and transport to tumour cells. Recently, Ag-complexes systematic discovery and development have provided a large number of promising antioxidants, anticancer and antibacterial agents (**Scheme 1**) (Liang et al., 2018).

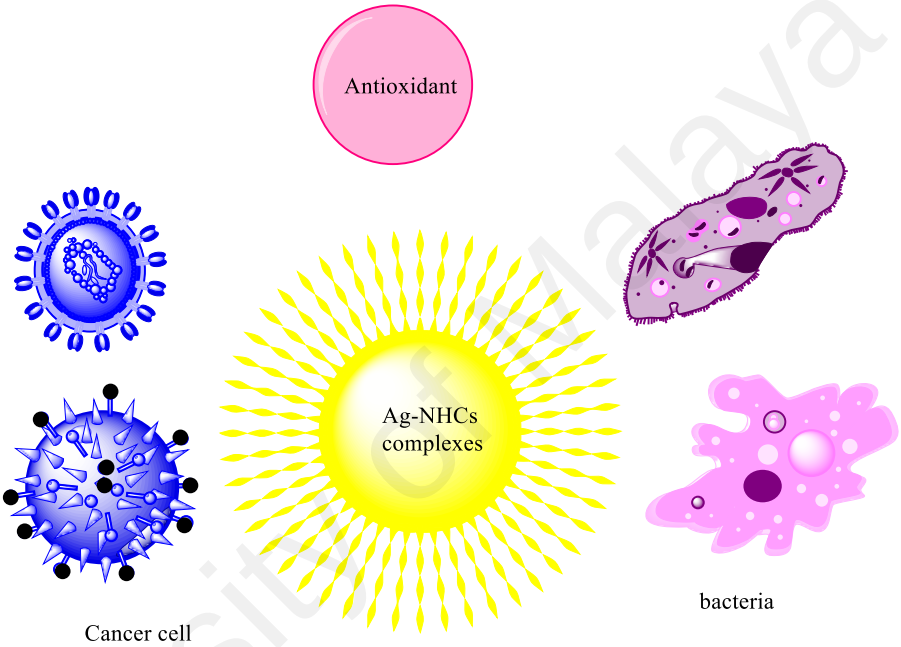

Scheme 1: Application of Ag-NHCs

4.5.1 Antioxidant Activity

Biological effects of the imidazolium compounds have been correlated with antioxidant behaviour (Cai et al., 2010; Radosevic et al., 2013). This led to an investigation of antioxidant activity of the imidazolium-acridines. For this, a DPPH- and FRAP-assays were applied. **Table 4.5** illustrates the IC_{50} values of the ligands and Ag(I)-complexes in comparison to 3,5-bis-tert. butyl-4-hydroxytoluene (BHT) and ascorbic acid (AA) as standard antioxidants. The results revealed differing activities in the two assays.

The non-substituted-acridine imidazolium **7** indicate reasonable, good radical quenching activity, comparable with the standard compound AA. Compound **7** exceeded the radical scavenging ability than the non-ionic precursor **6a.** Good free radical scavenging activities was found for compounds **7**, **8**, **12**, **13**, **14**, **21** and **22**. The increased electron density in the compounds is commonly associated with increasing radical stability. Nevertheless, the addition of a methoxy substituent on acridine in compounds **9** and **10** significantly reduced the antioxidant activity, whereas the subsequent addition of chloride tends to compensate with this influence in compounds **12** (46±4 µg/mL), **13** (47±4µg/mL) and **14** (57±7µg/mL). Compounds **16–24** have an additional methylene-linked π-electron system at the imidazole increase the conjugation system of radical species, if the hydrogen transfer affects the methylene linker. However, IC_{50} values are comparable high, indicated that the hydrogen transfer happens at a different site. All complexes exhibited lower antioxidants activity compared to the respective ligands.

Most of the compounds showed lower reducing activity of Fe^{3+} to Fe^{2+} compared with standard compounds (AA& BHT). Compounds, **16**, **19**, **20**, **24** and **31** exhibited good reducing activity with IC_{50} ranged 145-211 µg/mL compared with standard references, as shown in **Table 4.5**.

Table 4.5: Antioxidant activity of [benz]imidazolium-acridines and Ag(I)-complexes[a].

Antioxidant activity						
Compd.	**DPPH** (IC_{50}, µg/mL)	**FRAP** (Mean ± SD)		**Compd.**	**DPPH** (IC_{50}, µg/mL)	**FRAP** (Mean ± SD)
6a	164 ± 3	<100		**23**	69±5	<100
6b	144±27	<100		**24**	228±12	170
7	49±1	108		**25**	97±2	<100
8	47±1	145		**26**	102±8	<100
9	196 ±16	<100	**Complexes**	**31**	70±2	145
10	133±53	<100		**32**	144±27	<100
11	90±5	<100		**33**	150±2	105
12	46±4	<100		**34**	147±3	<100
13	47±4	<100		**35**	195±9	<100
14	57±1	<100		**36**	133±5	<100
15	216±3	<100		**37**	98±5	<100
16	367±30	211		**38**	86±4	<100
17	103±42	<100		**39**	87±4	<100
18	98±6	<100		**40**	107±7	<100
19	216±41	201		**41**	230±2	<100
20	367±30	211		**A.A**	41±2	337
21	50±2	<100		**BHT**	287±8	860±10
22	43±4	<100				

[a] Data represent mean of 3 measurements; FE =ferric equivalent.
BHT: Butylated hydroxytoluene, AA: ascorbic acid.

4.5.2 Antibacterial activity

The antibacterial effects of benzimidazolium-based acridine ligands and their Ag(I)-complexes were screened along with the positive control drugs (ampicillin and gentamicin) and negative control (dimethyl sulfoxide). Previous studies on *N*-benzimidazolium derivatives without acridine (Gok et al., 2013; Gok et al., 2016; Ozkay et al., 2010) showed effective actions against various strains of bacteria. The preliminary investigation applied a zone inhibition test. No inhibition zone was found for the control DMSO in line with previous investigations (Patil et al., 2011; Shahini et al., 2017). All compounds exhibited potent antibacterial activity against the bacteria tested in this study. It is apparent from the data in **Table 4.6** that the antibacterial activity of Ag(I)-complexes **42-45** was higher than for corresponding ligands **27-30**. This finding is in agreement with previous reports on Ag(I)-complexes by Loh et al. and Ozdemir et al. (Loh et al., 2019; Ozdemir et al., 2010). Ligands **29** and **30** exhibited the highest activity, which may be attributed to the presence of the additional aromatic ring and the methoxy group, respectively.

Table 4.6: Inhibition zone of the antibacterial activity of the ligands and the Ag(I) complexes.

Compd.	Inhibition zones (mm)				
	Gram-negative			Gram-positive	
	E. coli	*S. typhi*	*S. aureus*	*P. aeruginosa*	*S. epidermidis*
6c	8±1	NA	9±0.5	NA	6±1
27	8±1	NA	10±1	NA	8±1
28	8±1	7±1	9±1	NA	6±0.5
29	10±1	8±1	8±1	7±1	9±1
30	9±1	NA	10±1	NA	8±1
42	13±1	14±1	13±1	16±1	13±1
43	12±0.4	14±1	12±1	16±1	15±0.5
44	12±1	15±1	11±1	14±1	13±1
45	12±1	14±1	13±1	16±1	15±1
Ampicillin	16±2	18±0.6	21±1	NA	NA
Gentamicin	29±1	24±0.6	28 ±1	29±0.5	26±2
DMSO	NA	NA	NA	NA	NA

Noted: The antibacterial activity was determined using well diffusion method, each compound (1mg/mL) was dissolved in DMSO, and the mean of inhibition zones was recorded from triplicate tests. *E. coli= Escherichia coli; S. t = Salmonella typhi; S. a = Staphylococcus aureus; P. a = Pseudomonas aeruginosa; S. e = Staphylococcus epidermidis.* NA, no activity, Inhibition zones including the diameter of the well (6 mm). 42-45 = Ag complexes.

The highest antibacterial activity was found for the Ag(I)-complex **44** against *S. typhi*. However, other complexes **42, 43** and **45** exhibited higher activity against *P. aeruginosa* and *S. epidermidis*. Structural activity relationship (SAR) analysis has shown higher activities for compounds containing electron-withdrawing groups compared to those possessing electron-donating groups (Krishnanjaneyulu et al., 2014). The corresponding SAR for benzimidazolium compounds is shown in **Figure.4.24.**

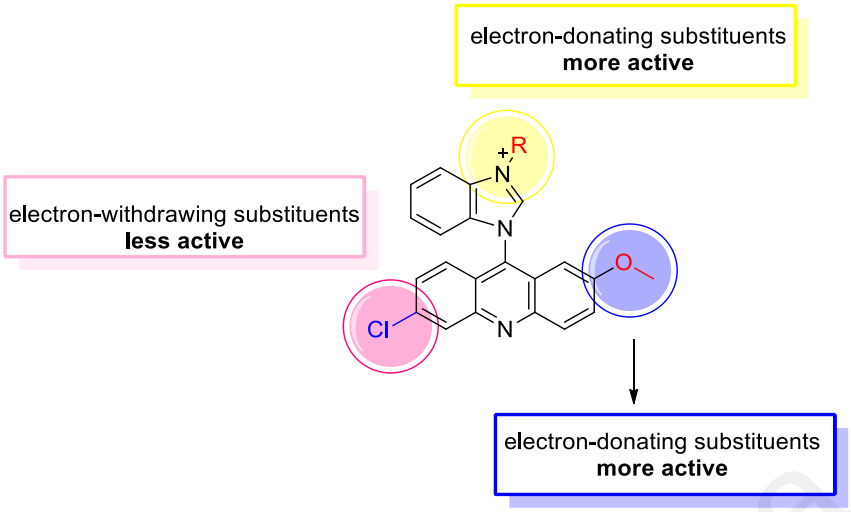

Figure 4.24: Structural activity relationship (SAR) analysis for compounds

The minimum inhibitory concentration **MIC** and minimum bactericidal concentration **MBC** were used to determine the minimum concentration for synthesized compounds that could inhibit the visible growth or kill the tested bacteria. The MIC (the lowest concentrations of compounds that completely inhibited bacterial growth) of the ligands and Ag(I)-complexes against the five bacteria are summarized in **Table 4.7**. Smaller MIC values correspond to higher antibacterial activity. Most of benzimidazolium-acridine ligands and Ag(I) complexes were effective against the five tested bacteria. All complexes exhibited higher activities than the corresponding ligands (Ozdemir et al., 2010; Sarı et al., 2016). Ag(I)-complexes showed antibacterial activity with MIC and MBC values ranging from 250 to 1000 µg/mL. The highest antibacterial activity was recorded from Ag(I)-complexes **42-45** with MIC value 250 µg/mL against all tested bacteria and MBC values of 250-500 µg/mL, this observation is in agreement with the previous report (Gok et al., 2014; Gok et al., 2016; Haziz et al., 2019; He et al., 2015; Sarı et al., 2016). The highest antibacterial activity was observed for complex **45** against *P. aeruginosa, S. typhi* and *S. epidermidis* (250 µg/mL). The activity may be associated to the methoxy-substituted at the acridine ring. The antibacterial activities of complex **44**, which contained the aryl group, exhibited good antibacterial activities against *P. aeruginosa*

with MIC and MBC values of 250 and 500 μg/mL, respectively, well comparable to previously reported MICs between 50 and 250 μg/mL for a variety of non-benzanellated analogues (He et al., 2015). It indicates a low impact of the benzanellation on the antibacterial activity. This may be explained by assuming an interaction at the acridine site rather than the imidazolium.

Table 4.7: The MIC and MBC values of ligands and Ag(I) complexes tested against bacteria.

Samples	*E. coli*		*S. aureus*		*S. epidermidis*		*P. aeruginosa*		*S. typhi*	
	MIC	MBC	MIC	MBC	MIC	MBC	MIC	MBC	MIC	MBC
	(µg/mL)		(µg/mL)		(µg/mL)		(µg/mL)		(µg/mL)	
6c	1000	>1000	>1000	ND	>1000	ND	>1000	ND	>1000	ND
27	500	1000	500	500	500	500	>1000	ND	>1000	ND
28	500	1000	500	1,000	>1000	ND	>1000	ND	500	500
29	1000	1000	500	500	500	500	500	500	>1000	ND
30	500	1000	250	250	1000	1000	>1000	ND	1000	500
42	250	500	250	500	250	500	250	500	250	500
43	250	500	250	500	250	500	250	500	250	500
44	250	250	250	250	250	500	250	500	250	500
45	250	500	250	250	250	500	250	500	250	500
Gentamicin	15.6	31	15.6	31	7.8	32	15.6	31	15.6	31
Ampicillin	125	250	125	250	125	250	250	500	250	500
DMSO	>1000	ND	>1000	ND	>1000	ND	>1000	ND	>1000	ND

E. coli, Escherichia coli; S. typhi, Salmonella typhi; S. aureus, Staphylococcus aureus; P. aeruginosa, Pseudomonas aeruginosa; S. epidermidis, Staphylococcus epidermidis.
ND – no determined.

91

4.5.3 Anticancer studies

The potential cytotoxicity of imidazolium-based acridine derivatives and their Ag(I) complexes were tested *in vitro* against ovarian cancer cells (CAOV-3), prostate adenocarcinoma cells (PC-3), Michigan cancer foundation-7 (breast cancer cells, MCF-7), normal immortalized human ovarian surface epithelial cell line (T1074) and normal epithelial breast cell line (MCF-10a). The investigation applied paclitaxel and tamoxifen as positive control for comparison purpose. **Table 4.8** showed the result. The ligands and Ag(I)-complexes are not toxic for the normal cell lines, as IC_{50} values were about 50 µg/mL or higher. The cytotoxicity results showed that [benz]imidazolium-based acridine and their Ag(I)-complexes potential might be used of cancer therapy.

Ligand **9** revealed higher cytotoxicity activity against CAOV-3 cell with IC_{50} (2.5±0.4 µg/mL) compared to tamoxifen and paclitaxel with IC_{50} (2±1 µg/mL) and (4.8±0.5 µg/ mL), respectively. This is due to the methoxy group in position 2 on acridine. Nevertheless, it was practically inactive against PC-3 and MCF-7 cells with $IC_{50} \geq 40$ µg/mL according to Jayash et al. (Jayash et al., 2017). Similarly, compounds **11**, **14**, **17**, **21** and **23** displayed good activity against CAOV-3 cell with IC_{50} (7±1 µg mL^{-1}), (6±1 µg mL^{-1}), (4.5± 0.7 µg mL^{-1}), (12±2 µg mL^{-1}) and (5±2 µg mL^{-1}), respectively. The structures of these active compounds showed no difference in their main structure, but differ in the substitution on the imidazole and acridine core.

Compounds **7-15** showed moderate cytotoxic against CAOV-3 cells with IC_{50} ~ 2.5-24 µg/mL, due to a medium chain for the imidazole alkylation and single methoxy-substitution of the acridine. Most of the *N*-alkyl imidazolium-2-methoxyacridine derivatives exhibited more cytotoxic activity. The cytotoxicity of compounds **16–26** indicate that the incorporation of aromatic structures at the imidazolium substituent can improve their activity, this matches previous report finding on different systems (Ranke

et al., 2007; Xu et al., 2015; Liu et al., 2015). In addition, the activity of these compounds is sensitive towards any minor change in the substitution at the aromatic ring. The overall activity of these compounds against CAOV-3 cell probably exhibits considerable influence for a medium-sized substituent at the imidazole.

The non-ionic imidazolium-precursor **6a** was the most active against prostate cancer (PC-3**)** cells with IC_{50}= 6±1 µg, while the ligands **11, 16, 18, 19** and **24** showed lower but still reasonable activities with IC_{50}= (12±2 µg mL^{-1}), (9±0.2 µg mL^{-1}), (12±6 µg mL^{-1}), (12±2 µg mL^{-1}) and (24±8 µg mL^{-1}), respectively. However, the other compounds exhibited very weak cytotoxic effect against PC-3 cell.

Compounds **22** exhibited good cytotoxic effect against MCF-7 with IC_{50}=5±0.6 µg mL^{-1}, which was more active than any of the positive controls, tamoxifen (IC_{50}= 11±1 µg mL^{-1}) and paclitaxel (IC_{50}= 6±1 µg mL^{-1}). Also, compound **7** showed a good activity with IC_{50}= 9±1 µg mL^{-1}. To evaluate the selectivity of the potential cancer drugs, the SI was calculated. The data indicate that imidazolium ligands displayed a high degree of cytotoxic selectivity towards specific cancer cell lines with SI higher than 1, as shown in **Table. 4.8**.

Table 4.8: The IC_{50} of the ligands 6-26 in *in vitro* cell toxicity after 24 h[a] incubation.

Compd.	IC_{50} values (μg/mL)							
	Cancer cell lines						non-tumorigenic cell lines	
	CAOV-3	SI	PC-3	SI	MCF-7	SI	T1074	MCF-10a
6a	12± 1	3.3	6 ± 1	6.7	28 ± 2	1.8	40 ± 7	49 ±9
6b	68± 5	1.1	77 ±13	0.9	21 ± 1	3.1	73 ±16	66 ±9
7	80± 2	1.1	71 ± 7	1.3	9 ± 1	7.4	90 ±8	67 ±3
8	50+1	1.6	69 ± 6	1.2	20 ± 3	2.5	81 ±15	>100
9	**2.5** ± 0.4	34.8	68 ± 4	1.3	41 ± 4	1.7	87± 12	70 ±11
10	12 ±2	7.2	62 ± 5	1.4	49 ± 3	1.0	86 ±8	50 ± 1
11	**7**± 1	7.1	12 ±2	4.2	17± 2	2.9	>100	>100
12	77 ± 5	0.9	76±18	0.9	53 ± 5	1.5	66 ±15	82 ±5
13	60 ± 1	1.3	92 ±13	0.8	23 ± 2	4.3	78 ±10	98 ±5
14	**6** ± 1	14.3	75 ±10	1.1	38 ± 5	1.3	86 ± 6	>100
15	24± 12	2.3	28 ±7	1.9	36 ± 7	1.4	54 ±9	>100
16	22± 1	3.8	**9** ± 0.2	9.3	17± 2	5.7	84 ±5	97 ± 2
17	4.5 ± 0.7	14.2	29 ± 1	2.2	24 ± 8	2.1	64 ± 9	>100
18	>100	0.9	12 ± 6	3.8	42 ± 2	2.2	46 ± 5	94 ±2
19	86± 10	1.0	12 ± 2	7.2	56 ±12	1.3	86 ±5	71 ± 14
20	63± 6	1.2	93 ± 7	0.8	43 ±7	1.2	75 ±16	>100
21	12 ± 2	7.3	87± 5	1.0	22 ± 5	2.3	88 ±6	50 ±2
22	27± 2	3.1	99 ± 7	0.8	**5** ± 0.6	17	83 ±11	83 ± 20
23	**5** ± 2	15	79 ± 9	0.9	22 ± 4	3.9	75 ±17	85±10
24	23± 5	3.7	24 ± 8	3.5	20 ± 2	4.4	84 ± 5	87 ± 2
25	25± 1	2	28±1	1.8	28±2	1.8	>100	>100
26	25±0.6	2	31±2	1.6	27±1	2.9	>100	77±2
Tamoxifen	2 ± 1	39	2 ± 1	39	11 ± 1	7.7	78 ± 7	85 ±6
Paclitaxel	4.8±0.5	10.4	5±1	10	6 ± 1	12.5	>100	75± 2

[a] Data represent the mean of three independent determinations.
IC_{50} values (μg/mL) were obtained from the MTT assay.

The Ag(I)-complexes **31-41** are nontoxic with IC_{50} values above 50 µg/mL against non-tumorigenic cell lines MCF-10a and T1047. **Figures 4.25 & 4.26** compare the toxicities of the ligands and complexes against non-tumorigenic. The complexes showed considerable improvement of the anticancer activity towards the ligands against CAOV-3, PC-3 and MCF-7 cells with IC_{50} effects of 5-14, 10-26 and 8-15 µg/mL, respectively. This is possible as a result of bonding of Ag cations to biologically compatible ligands that enhance the bioactivity and ultimately the activity of Ag cations. This finding was in agreement with previous studies reports (Asif et al., 2016; Ghdhayeb et al., 2017; Haque et al., 2013; Johnson et al., 2017; Youngs et al., 2012). The mechanism of Ag cations action is not yet clear; however, it has been shown that Ag cations bind to the cell surfaces and interact with the proteins and nucleic acids that are important for cell. The data for complexes are given in **Table 4.9**. Compounds **32** and **38** showed higher cytotoxicity against CAOV-3 cell with $IC_{50} = 5\pm1$ µg/mL and 7 ± 1 µg/mL, respectively. The variation in the alkylation of the imidazole structure can affect the potency of these complexes as the substituent that produces variation in the lipophilicity of the drugs (Haque et al., 2013c). The selectivity index (SI) of the complexes in the range of 2-10 confirm the potential to be used as a drug.

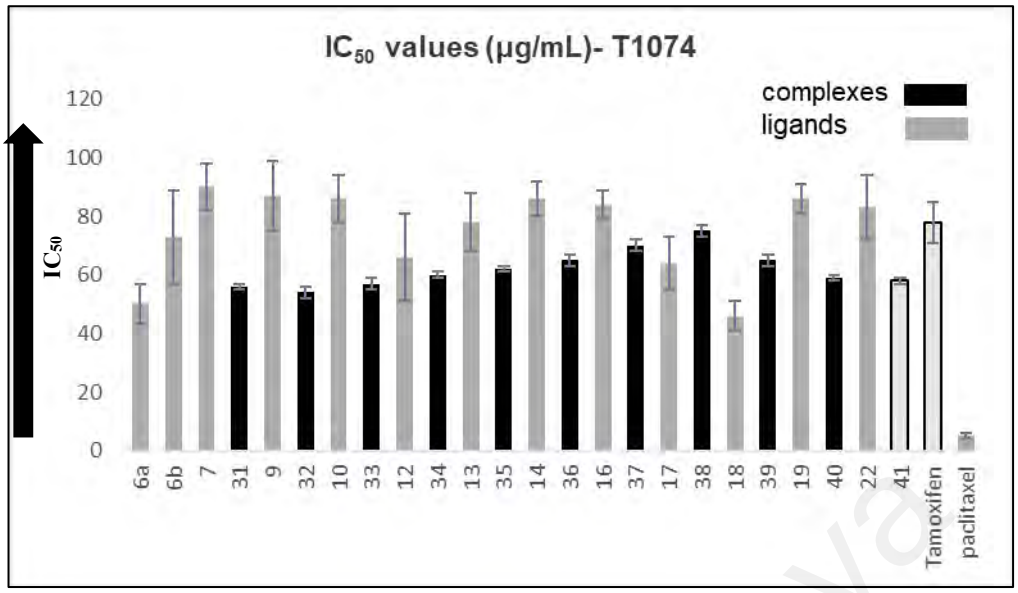

Figure 4.25: The IC_{50} of ligands and Ag(I)-complexes against T1074 cell

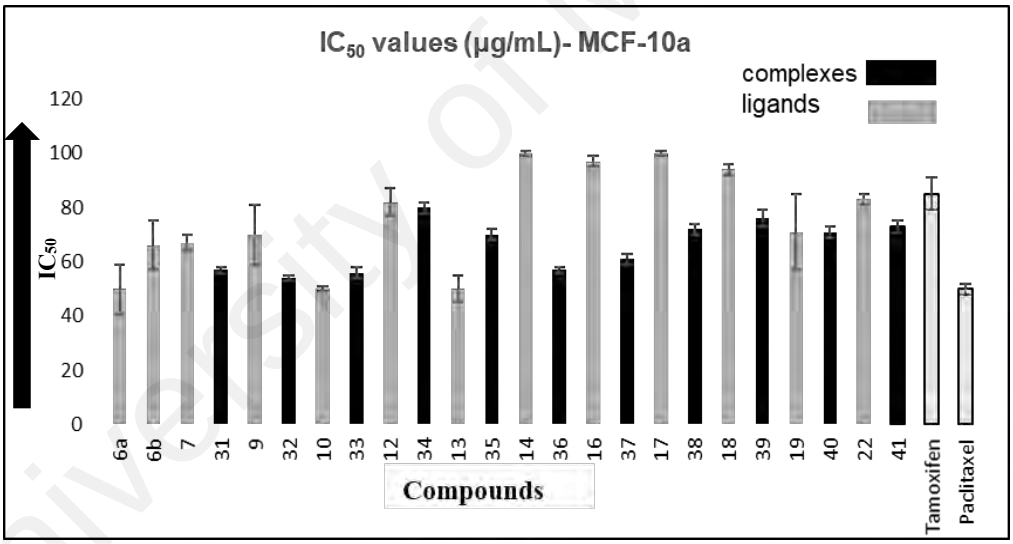

Figure 4.26: The IC_{50} values of ligands and Ag(I)-complexes against MCF-10a cell

Table 4.9: The IC_{50} values of Ag(I)-complexes in *in vitro* cell toxicity after 24 h[a] incubation.

Compd.	IC_{50} values (μg/mL), Cancer cell-lines					
	CAOV-3	SI	PC-3	SI	MCF-7	SI
31	22±1	2.5	25±1	2.2	8±1	7.1
32	5±1	10.8	18±1	3	20±1	2.7
33	18±1	3.2	18±2	3.2	22±1	2.5
34	17±1	3.5	21±1	2.9	18±1	4.4
35	20±1	3.1	18±1	3.4	22±1	3.2
36	9±1	7.2	20±1	3.3	14±1	4
37	9±1	7.8	10±1	7	18±1	3.4
38	7±1	10.7	15±1	5	20±1	3.6
39	20±1	3.3	18±1	3.6	15±1	5.1
40	20±1	3	26±1	2.3	21±1	3.4
41	14±1	4.1	32±3	1.8	8±0.4	9.1
Tamoxifen	2 ± 1	39	2 ± 1	39	11 ± 1	7.7
Paclitaxel	4.8±0.5	10.4	5±1	10	6 ± 1	12.5

IC_{50} values (μg/mL) were obtained from MTT assay.
[a] Data represent the mean of three independent determinations.

The imidazolium-acridine ligands displayed low activity against MCF-7. In the attempt to enhance the activity benzimidazolium analogues ligands **27-30** were synthesised. The ligands and respective Ag(I)-complexes **42-45** were tested against MCF-7. The result in **Table 4.10,** indicated that benzimidazolium-acridine did not improve the cytotoxicity activity against MCF-7 with IC_{50}=40 μg mL^{-1} and above. In contrast, the complexes **42-45** showed a slightly similar cytotoxicity activity compared to the imidazolium complexes.

Table 4.10: The IC_{50} values of the benzimidazolium ligands and Ag(I)-complexes in *in vitro* cell toxicity after 24 h[a] incubation.

Compd.		(IC_{50} ± SEM μg/mL), SI		
		MCF-10a	MCF-7	SI
6c	ligands	87±3	60 ±2	1.4
27		74 ± 2	67 ±5	1.1
28		88± 4	51 ±2	1.7
29		67±2	65± 4	1.03
30		75± 2	44± 3	1.7
42	complexes	69±3	20± 3	3.5
43		74±3	24± 2	3.1
44		80±3	22± 3	3.6
45		78±4	23± 2	3.4
Tamoxifen		85± 6	11± 1	7.7
Paclitaxel		75± 2	6 ±1	12.5

[a] Data represent mean of 3 measurements. Selectivity index (SI).

CHAPTER 5: CONCLUSION

5.1 Conclusion

In this thesis, a series of imidazolium- and benzimidazolium-based acridine ligands and their respective Ag(I)-complexes have been synthesised. Changing the halides in the ligands to hexafluorophosphate enhanced their ability to form complexes. All prepared compounds were characterized by IR, ^{1}H and ^{13}C NMR, elemental analysis and HRMS. Owing to their highly conjugated π-electron system, the fluorescence behaviour of the acridine-based ligand was evaluated for possible application as a fluorescent probe. However, the low water solubility of the compounds has prevented their applicability for fluorescent probing.

The ligands and their Ag(I)-complexes were tested *in vitro* for their biological properties as antioxidant, anticancer and antibacterial agents. All compounds exhibited lower antioxidant activity compared to the standards, *i.e.* ascorbic acid and BHT. The compounds did not show toxic effects on the normal cell lines, MFC-10a and T1047, with IC_{50} values of 50 μg mL^{-1} and above. The imidazolium ligands showed reasonable cytotoxicity activity against CAOV-3, PC-3 and MFC-7 cells. Complexation with silver increased the cytotoxicity against cancer cells. The benzimidazolium ligands did not act as anticancer agents against MCF-7, while their complexes showed better activity towards tested cell.

The benzimidazolium ligands and their Ag(I)-complexes were tested for antibacterial activity. The ligands exhibited moderate activity against a variety of the bacteria, while the complexes showed good activities. The increased activity of complexes is due to the biological effect of silver ion.

5.2 Future outlook

The research has given us preliminary insight into the structural properties of the synthesized Ag(I) complexes. However, there is a lot of advancement work that can be carried out. For plans, it is suggested to synthesise metal complexes using Pd and Pt with emphasis on lipophilic/ hydrophilic balance to develop metallodrugs and grow crystal for complex structure confirmation. Besides, some synthetic compounds have shown good results for biological applications and these warrants for a further depth study. In addition,

5.3 Limitations of the study

The chemicals, solvents and consumables for biological studies assay are quite costly. For this reason, we have just selected some cells and bacterial to test the compounds. Also, number of compounds is 46 that made the biological study is limited.

CHAPTER 6: EXPERIMENTAL DETAILS

6.1 Experimental Data

6, 9-Dichloro-2-methoxyacridine (4a)

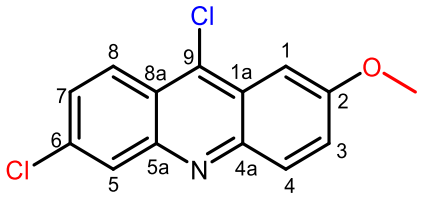

4a

Compound **4a** was prepared according to previous reports (Csuk et al., 2004; Lang et al., 2013; Li et al., 2014; Mironovich et al., 2016). A mixture of 4-chloro-2-(4-methoxyphenylamino)-benzoic acid **3a** (5.21 g, 19 mmol) and $POCl_3$ (40 mL) was heated slowly in oil bath to 85-90 ºC for 15 min. The temperature was subsequently increased to 135-140 ºC, and the reaction was kept at reflux for 3 h. After the completion of the reaction, excess phosphorous oxychloride was removed by vacuum distillation. The reaction mixture was cooled to room temperature and poured into a stirred mixture of 25 ml concentrated ammonia and crushed ice. Crude **4a** precipitated within 30 min. The precipitate was filtered by suction, washed three times with saturated $NaHCO_3$ and subsequently with water. It was dried over phosphorus pentoxide and recrystallized from ethanol to furnished **4a** as a yellow powder. Yield: 92%; mp 160-165 ºC. ^{1}H NMR (400 MHz, $CHCl_3$): δ 8.23 (d, 1H, H-8), 8.13 (s, 1H, H-5), 8.03 (d, 1H, H-4), 7.50-7.45 (2d~t, 2H, H-3, H-7), 7.39 (s, 1H, H-1), 4.01 (s, 3H, OMe); $^3J_{7,8}$=9.0, $^3J_{3,4}$=9.0 Hz; ^{13}C NMR (100 MHz, $CHCl_3$): δ 158.34 (C-2), 146.80 (C-5a), 146.45 (C-4a), 138.38 (C-9), 135.41 (C-6), 131.25 (C-4), 128.14 (C-5), 128.01 (C-7), 126.47 (C-3), 125.54 (C-8), 125.15 (C-1a), 122.69 (C-8a), 99.74 (C-1), 55.69 (O-CH_3).

9-Chloroacridine(4b)

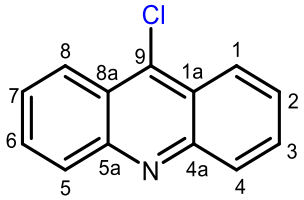

4b

Compounds **4b** was prepared according to previous reports (Csuk et al., 2004; Lang et al., 2013; Li et al., 2014; Mironovich et al., 2016) following the same method that was applied for compound **4a**. A mixture of 2-phenylamino-benzoic acid **3b** (4.0 g, 19 mmol) and $POCl_3$ (40 mL) was heated slowly in an oil bath to 85-90 ºC for 15 min. The temperature was subsequently increased to 135-140 ºC, and the reaction was kept at reflux for 3 hr. After the completion of the reaction, excess phosphorous oxychloride was removed by vacuum distillation. The reaction mixture was cooled to room temperature and poured into a stirred mixture of 25 ml concentrated ammonia and crushed ice. The crude 9-chloroacridine precipitated within 30 min. The precipitate was filtered by suction, washed three times with saturated $NaHCO_3$ and subsequently with water. The precipitate was dried and recrystallized from ethanol to furnished **4b** as pale brown crystals. Yield: 90 %; mp 115-120 ºC. FTIR (ν cm^{-1}): 3057, 2995 (C-H), 1554, 1467 (C=C), 757 (C-Cl). ^{1}H NMR ($CDCl_3$) δ 8.4 (d, 2H, *J*=8 Hz), 8.26 (d, 2H, *J*=8 Hz), 7.85–7.81 (m, 2H), 7.68-7.64 (m, 2H). ^{13}C NMR ($CDCl_3$) δ 148.9(C_{Acri}-4a, C_{Acri}-5a), 141.5 (C_{Acri}-9), 130.8 (C_{Acri}-4, C_{Acri}-5), 129.8(C_{Acri}-3, C_{Acri}-6), 127.1 (C_{Acri}-2, C_{Acri}-7), 124.8(C_{Acri}-1, C_{Acri}-8),124.4 (C_{Acri}-1a, C_{Acri}-8a).

9-Chloro-2-methoxyacridine (4c)

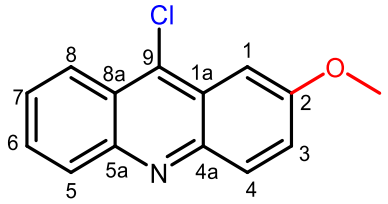

4c

Compound **4c** was prepared according to previous reports (Csuk et al., 2004; Lang et al., 2013; Li et al., 2014) following the same method that was applied for compound **4b**. A mixture of 2-(4-methoxyphenylamino)-benzoic acid **3c** (4.57 g, 19 mmol) and $POCl_3$ (40 mL) was heated slowly in oil bath to 85-90 ºC for 15 min. The temperature was subsequently increased to 135-140 ºC, and the reaction was kept at reflux for 3 h. After the completion of the reaction, excess phosphorous oxychloride was removed by vacuum distillation. The reaction mixture was cooled to room temperature and poured into a stirred mixture of 25 ml concentrated ammonia and crushed ice. Crude **4c** precipitated within 30 min. The precipitate was filtered by suction, washed three times with saturated $NaHCO_3$ and subsequently with water. The precipitate was dried over phosphorus pentoxide and recrystallized from ethanol to furnished **4c** as brown crystals. Yield: 95%; mp 160-165 ºC. ^{1}H NMR ($CDCl_3$) δ 8.40 (d, 1H, *J*=8 Hz), 8.32 (d, 1H, *J*=12 Hz), 8.14 (d, 1H, *J*=8 Hz), 7.79-7.75 (m, 1H), 7.67-7.63 (m, 1H), 7.54–7.49 (m, 2H), 4.05 (s, 3H, OCH_3). ^{13}CNMR ($CDCl_3$) δ 158.2(C-2), 147.3(C-5a), 146.2(C-4a), 138.2(C-9), 131.5 (C-4), 129.8(C-6), 129.4(C-5), 127.1(C-7), 126.0 (C-8), 125.3(C-8a), 124.5(C-3), 124.2 (C-9a), 99.9(C-1), 55.7(O-CH_3).

Synthesis of 1-ethyl imidazole (5a)

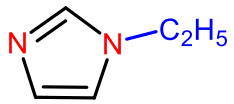

Compound **5a** was prepared according to general procedure **3.3.1.3** (Al-Mohammed et al., 2015b; Rohini et al., 2013; Salman et al., 2015), using 1-bromoethane (1.56 g, 14.31 mmol) to provide **5a** as a yellow liquid. ^{1}H NMR (400 MHz, $CDCl_3$) δ (ppm): 7.47 (s, 1H, NCHN, H-2), 7.06 (s, 1H, CH, H-4), 6.91 (s, 1H, CH, H-5), 3.93 (m, 2H, N-CH_2), 1.40 (t, 3H, CH_3). ^{13}C NMR (100 MHz, $CDCl_3$) δ (ppm): 137.06 (C-2), 129.33 (C-5), 118.77 (C-4), 45.05 (N-CH_2), 16.38 (-CH_3).

Synthesis of 1-butyl imidazole (5b)

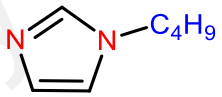

Compound **5b** was prepared according to general procedure **3.3.1.3** using 1-bromobutane (1.96 g, 14.31 mmol) to provide **5b** as a yellow liquid. ^{1}H NMR (400 MHz, $CDCl_3$) δ (ppm): 7.44 (s, 1H, CH, H-2), 7.00 (s, 1H, CH, H-4), 6.88 (s, 1H, CH, H-5), 3.94 (q, 2H, N-CH_2), 1.75-1.73 (m, 2H, CH_2), 1.34-1.28 (m, 2H, CH_2), 0.92 (t, 3H, CH_3). ^{13}C NMR (100 MHz, $CDCl_3$) δ (ppm): 137.04 (C-2), 129.08 (C-5), 118.92(C-4), 46.93 (N-CH_2), 33.13 (-CH_2), 19.80 (-CH_2), 13.58 (-CH_3).

Synthesis of 1-hexyl imidazole (5c)

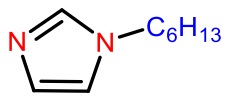

Compound **5c** was prepared according to general procedure **3.3.1.3** using 1-bromo hexane (2.36 g, 14.31 mmol) to provide **5c** as a yellow liquid. ^{1}H NMR (400 MHz, $CDCl_3$) δ (ppm): 7.47 (s, 1H, CH, H-2), 7.06 (s, 1H, CH, H-4), 6.91 (s, 1H, CH, H-5), 3.91 (m, 2H, N-CH_2), 1.74-1.80 (m, 2H, CH_2), 1.26-1.28 (m, 6H, CH_2), 0.87 (t, 3H, CH_3). ^{13}C NMR (100 MHz, $CDCl_3$) δ (ppm): 137.06 (C-2), 129.33 (C-5), 118.77 (C-4), 46.05 (N-CH_2), 33.13 (CH_2), 30.10 (-CH_2), 26.13 (CH_2), 19.80 (CH_2), 14.38 (CH_3).

Synthesis of 1-octyl imidazole (5d)

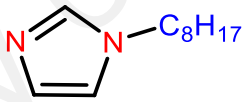

Compound **5d** was prepared according to general procedure **3.3.1.3** using 1-bromooctane (2.76 g, 14.31 mmol) to provide **5d** as a yellow liquid. ^{1}H NMR (400 MHz, $CDCl_3$) δ (ppm):7.47 (s, 1H, CH, H-2), 7.06 (s, 1H, CH, H-4), 6.91 (s, 1H, CH, H-5), 3.93 (m, 2H, NCH_2), 1.72-1.79 (m, 2H, CH_2), 1.26-1.27 (m, 10H, CH_2), 0.87 (t, 3H, CH_3). ^{13}C NMR (100 MHz, $CDCl_3$) δ (ppm): 137.06 (C-2), 129.33 (C-5), 118.77 (C-4), 46.05 (N-CH_2), 33.13 (CH_2), 30.10 (CH_2), 29.58 (-CH_2), 29.51(-CH_2), 29.42 (-CH_2), 26.13 (-CH_2), 14.38 (CH_3).

Synthesis of 1-decyl imidazole (5e)

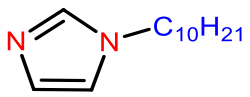

Compound **5e** was prepared according to general procedure **3.3.1.3** using 1-bromodecane (3.16 g, 14.31 mmol) to provide **5e**. ^{1}H NMR (400 MHz, $CDCl_3$) δ (ppm): 7.46 (s, 1H, CH, H-2), 7.05 (s, 1H, CH, H-4), 6.90 (s, 1H, CH, H-5), 3.92 (m, 2H, CH_2), 1.79-1.75 (m, 2H, CH_2), 1.29-1.25 (m, 14H, CH_2), 0.87 (t, 3H, CH_3). ^{13}C NMR (100 MHz, $CDCl_3$) δ (ppm): 137.06 (C-2), 129.33 (C-5), 118.76 (C-4), 47.05 (N-CH_2), 31.86 (-CH_2), 31.07 (-CH_2), 29.58 (-CH_2), 29.51(-CH_2), 29.42 (-CH_2), 29.06 (-CH_2), 26.55 (-CH_2), 22.67 (-CH_2), 14.10 (-CH_3).

Synthesis of 1-dodecyl imidazole (5f)

Compound **5f** was prepared according to general procedure **3.3.1.3** using 1-bromododecane (3.56 g, 14.31 mmol) to provide **5f**. ^{1}H NMR (400 MHz, $CDCl_3$) δ (ppm): 7.45 (s, 1H, CH, H-2), 7.05 (s, 1H, CH, H-4), 6.90 (s, 1H, CH, H-5), 3.92 (m, 2H, N-CH_2), 1.78-1.75 (m, 2H, CH_2), 1.30-1.25 (m, 18H, CH_2), 0.88 (t, 3H, CH_3). ^{13}C NMR (100 MHz, $CDCl_3$) δ (ppm): 137.05 (C-2), 129.32 (C-5), 118.76 (C-4), 47.04 (N-CH_2), 31.89 (-CH_2), 31.08 (-CH_2), 29.58 (-CH_2), 29.51(-CH_2), 29.42 (-CH_2), 29.32 (-CH_2), 29.06 (-CH_2), 26.55 (-CH_2), 22.67 (-CH_2), 14.10 (-CH_3).

Synthesis of 1-octadecyl imidazole (5g)

Compound **5g** was prepared according to general procedure **3.3.1.3** using 1-bromooctadecane (4.77 g, 14.31 mmol) to provide **5g** as a white solid. ^{1}H NMR (400 MHz, $CDCl_3$) δ (ppm): 7.46 (s, 1H, CH, H-2), 7.05 (s, 1H, CH, H-4), 6.90 (s, 1H, CH, H-5), 3.92 (m, 2H, N-CH_2), 1.72-1.79 (m, 2H, CH_2), 1.30-1.26 (m, 30H, CH_2), 0.88 (t, 3H, CH_3). ^{13}C NMR (100 MHz, $CDCl_3$) δ (ppm): 137.05 (C-2), 129.33 (C-5), 118.75 (C-4), 47.04 (N-CH_2), 31.92 (CH_2), 31.08 (CH_2), 29.69 (CH_2), 29.66 (CH_2), 29.63 (CH_2), 29.60 (CH_2), 29.52 (CH_2), 29.42 (CH_2), 29.36 (CH_2), 29.06 (CH_2), 26.55 (CH_2), 22.68 (CH_2), 14.11 (CH_3).

9-(1-Imidazolyl) acridine (6a)

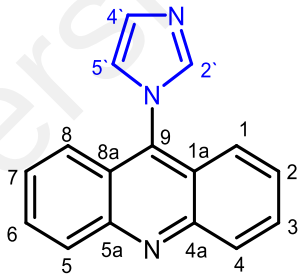

(6a)

The synthesis followed a modified approach of a previous report (Staderini et al., 2015). A solution of **4a** (1.0 g, 4.7 mmol) in toluene (60 mL) was treated with imidazole (369 mg, 5.4 mmol) and the reaction mixture was heated to reflux for 2 d, when TLC indicated complete conversion. After cooling, the yellow solid was collected by filtration, washed with hexane (3×20 mL) and dried under vacuum to provide **6a** (930 mg, 81 %) as yellow powder. mp 210-220 ºC. FTIR: ν (ATR, cm^{-1}) 3090 (C–H), 1629 (C=N), 1555,

1478, 1421 (C=C). ^{1}H NMR (400 MHz, $CDCl_3$): δ 8.35 (t, 1H, *J*=1 Hz, H-1), 8.32 (t, 1H, *J*=1 Hz, H-8), 7.88-7.84 (m, 3H, H-4, H-5, H_{imid}-5`), 7.60-7.59 (m, 4H, H-2, H-7, H-3, H-6), 7.49 (t, 1H, *J*=1 Hz, $H_{imid}$-4`), 7.36 (t, 1H, *J*=1 Hz, H-2`). $^{13}$C NMR (100 MHz, $CDCl_3$): 149.2 ($C_{Acri}$-4a, $C_{Acri}$-5a), 139.0 ($C_{Acri}$-9), 138.3 ($C_{imid}$-2`), 130.7 (C_{Acri}-4, C_{Acri}-5), 130.1 (C_{Acri}-3, C_{Acri}-6), 129.8 (C_{Acri}-2, C_{Acri}-7), 127.6 (C_{Acri}-1, C_{Acri}-8), 122.9 (C_{imid}-5`), 122.5 ($C_{Acri}$-1a, $C_{Acri}$-8a), 122.3($C_{imid}$-4`). Anal. calcd. for $C_{16}H_{11}N_3$: C 78.35, H 4.52, N 17.13 %, found: C 78.31, H 4.54, N 17.15%.

6-Chloro-9-(1-imidazolyl)-2-methoxyacridine (6b)

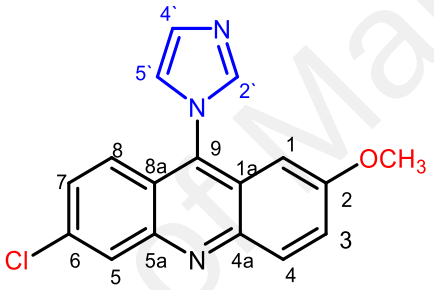

The synthesis followed a modified approach of a previous report (Staderini et al., 2015). A suspension of **4c** (439 mg, 1.6 mmol) in toluene (20 mL) was treated with imidazole (123 mg, 1.8 mmol) and the reaction mixture was heated to reflux for 48 h, when TLC indicated complete conversion. After cooling, the greenish yellow solid was collected by filtration, washed with hexane (20 mL) and then dried under vacuum to provide **6c** (389 mg, 79 %) as yellow powder.mp 211-215 ºC. FTIR: ν (ATR, cm^{-1}) 3095 (C–H), 1633 (C=N), 1560, 1475, 1421 (C=C). ^{1}H NMR (400 MHz, $CDCl_3$): δ 8.33 (d, 1H, *J*= 1 Hz), 8.22 (d, 1H, *J*=8 Hz), 8.04 (s, 1H), 7.59-7.51 (m, 3H), 7.43 (s, 1H), 7.41 (s, 1H), 6.57 (d, 1H, *J*=4 Hz), 3.84 (s, 3H, **OCH_3**). ^{13}C NMR (100 MHz, $CDCl_3$): δ 159.2 (C2-O), 147.3 (C_{Acri}-4a), 147.2 (C_{Acri}-5a), 136.2 (C_{Acri}-9), 135.8 (C_{Acri}-6, C_{imid}-2`), 131.5 ($C_{Acri}$-4, $C_{Acri}$-5), 130.1 ($C_{Acri}$-7), 129.3 ($C_{Acri}$-8), 128.3 ($C_{imid}$-4`), 127.1 (C_{imid}-5`), 124.3

(C_{Acri}-3), 123.4 (C_{Acri}-8a), 121.7 (C_{Acri}-1a), 97.2(C_{Acri}-1), 55.8(**O-CH$_3$**). Anal. calcd. for $C_{17}H_{12}ClN_3O$: C 65.92, H 3.90, N 13.57 %; found: C 65.90, H 3.91, N 13.59 %.

9-(1-benzoimidazolyl) acridine (6c)

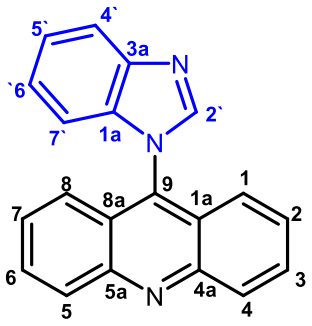

A suspension of 9-chloroacridine **4a** (337 mg, 1.58 mmol) and benzimidazole (213 mg, 1.80 mmol) in toluene (25 mL) was stirred under reflux for 48 h at 140 ºC (monitoring by TLC). The solid was collected and subsequently washed with hexane (20 mL). Recrystallisation from methanol provided off-white solid (420 mg, 90%). mp=300-310 ºC. UV-vis λ_{max}= 387 nm. ^{1}H NMR (400 MHz, DMSO-d$_6$): δ 8.76 (s, 1H, NCHN, C_{bim}-2`), 8.37 (d, 2H, Acr-1/8, J_d= 8.0 Hz), 7.97 (dd~t, 3H, J_t= 8.0 Hz), 7.64 (t, 2H, J_t= 8.0 Hz), 7.38 (dd~t, 3H, J_t= 8.0 Hz, 8.0 Hz), 7.23 (t, 1H, J_t= 8.0 Hz), 6.93 (d, 1H, J_d= 8.0 Hz). ^{13}C NMR (100 MHz, $CDCl_3$) δ (ppm) 149.61(C_{Acri}-4a, C_{Acri}-5a), 143.87 (C_{Acri}-9, C_{Acri}-3a), 136.98 (C_{imid}-2`), 130.88 ($C_{imid}$-1a), 130.11 ($C_{Acri}$-4, $C_{Acri}$-5), 127.87 ($C_{Acri}$-3, $C_{Acri}$-6), 124.33($C_{Acri}$-2, $C_{Acri}$-7), 123.33 ($C_{Acri}$-1, $C_{Acri}$-8), 122.71 ($C_{imid}$-5`, C_{imid}-6`), 120.82($C_{imid}$-4`), 110.72 (C_{Acri}-1a, C_{Acri}-8a, C_{imid}-7`). Anal. calcd. for $C_{20}H_{13}N_3$: C 81.34, H 4.44, N 14.23 %; found: C 81.36, H 4.41, N 14.26 %.

1-(Acridin-9-yl)-3-hexylimidazolium chloride (7)

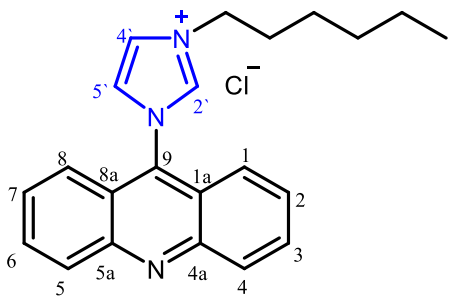

Compound **7** prepared according to general method **A.** 1-Hexylimidazole **5c** (274 mg, 1.8 mmol) and **4a** (337 mg, 1.6 mmol) were reacted to give compound **7** (430 mg, 75 %) as off-white solid. mp 225-230 ºC. FTIR: ν (ATR, cm^{-1}) 3087, 2954, 2858 (C–H), 1628 (C=N), 1542, 1446, 1410 (C=C), 1267, 1135 (C-O), 766 (C-Cl). ^{1}H NMR (400 MHz, DMSO-d_6): δ (ppm) 9.99 (s, 1H, NCHN, H_{imid}-2`), 8.40 (d, 2H *J*= 8 Hz, H-1, H-8), 8.37 (s, 2H, H-4, H-5), 8.04 (dt≈bt, 2H, *J*= 8 Hz, H-3, H-6), 7.80 (dt ≈ bt, 2H, *J*= 9 Hz, H-2, H-7), 7.67 (dd≈bd, 2H, *J*= 9 Hz, $H_{imid}$-4`, H_{imid}-5`), 4.42 (t, 2H, **N-CH$_2$**) 2.01 (mc, 2H, **CH$_2$**), 1.41-1.31 (m, 6H, **CH$_2$**), 0.89 (t, 3H, **CH$_3$**). $^{13}C$ NMR (100 MHz, DMSO-$d_6$): δ (ppm) 149.10 ($C_{Acri}$-4a, $C_{Acri}$-5a), 139.21 ($C_{Acri}$-9), 132.10 ($C_{imid}$-2`), 130.03 (C_{Acri}-4, C_{Acri}-5), 129.55 (C_{Acri}-3, C_{Acri}-6), 125.94 (C_{Acri}-2, C_{Acri}-7), 124.38 (C_{Acri}-1, C_{Acri}-8), 122.55 (C_{imid}-5`), 122.14 ($C_{Acri}$-1a, $C_{Acri}$-8a), 118.79 ($C_{imid}$-4`), 50.35(**N-CH$_2$**), 31.12 (CH_2-), 29.37(**CH$_2$**), 25.83(**CH$_2$**), 22.45(**CH$_2$**), 14.37(**CH$_3$**). Anal. calcd. for $C_{22}H_{24}ClN_3$: C 72.22, H 6.61, N 11.84%; found: C 72.19, H 6.59, N 11.80%. HRMS (ESI^+) *m/z* calcd. for $C_{22}H_{24}N_3$ $[M-Cl]^+$: 330.1970 (100%), 331.2004 (24%); found: 330.1999 (100%), 331.2013 (38%).

1-acridinyl-3-(2-propynyl)-imidazolium chloride salt (8)

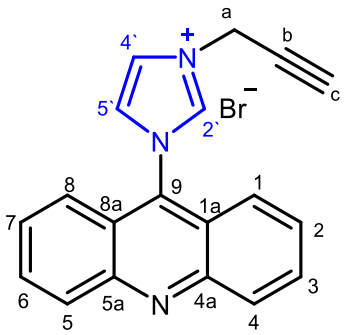

Compound **8** prepared according to general method **B**. A mixture of compound **6a** (61 mg, 0.25 mmol) and propargyl bromide (89 mg, 0.75 mmol) were reacted to give compound **8** (58 mg, 95 %) as off-white solid. mp: 265-270 ºC. FTIR ν (ATR, cm^{-1}): 3124 $(C–H)_{Ar}$, 2120 (C≡C), 1628 (C=N), 1315 (C-N), 765 (C-Cl). ^{1}H NMR (400 MHz, DMSO-d_6): δ (ppm) 9.99 (s, 1H, NCHN, H_{imid}-2`), 8.40-8.35 (m, 4H, H-1, H-8, H-4, H-5), 8.03-8.07 (s, 2H, H-3, H-6), 7.82 (dt≈dd, 2H, *J*=9 Hz, H-2, H-7), 7.72 (s, 1H, $H_{imid}$-4`), 7.70 (s, 1H, H_{imid}-5`), 5.43 (t, 2H, **N-CH₂**), 3.99 (s, H, **CH**). $^{13}C$ NMR (100 MHz, DMSO-$d_6$): δ (ppm) 149.07 ($C_{Acri}$-4a), 141.46 ($C_{Acri}$-5a), 139.46 ($C_{Acri}$-9), 136.07 ($C_{Acri}$-2`), 133.93 (C_{Acri}-4), 132.05 (C_{Acri}-5), 129.96 (C_{Acri}-3), 129.49 (C_{Acri}-6), 126.49 (C_{Acri}-2), 126.17 (C_{Acri}-7), 124.16 (C_{Acri}-1), 122.66 (C_{Acri}-8), 122.19 (C_{Acr}-1a), 121.50 (C_{Acri}-8a), 120.96 (C_{imid}-5`), 117.91 ($C_{imid}$-4`), 80.53 (N-CH_2**C_b**CH), 76.02 (NCH_2C-**CH_c**), 40.02 (N-**CH_2**CCH). Anal. calcd. for $C_{19}H_{14}ClN_3$: C 71.36, H 4.41, N 13.14%. Found: C 71.32, H 4.39, N 13.12%. HRMS (ESI^+) *m/z* calcd. for $C_{19}H_{14}N_3$ $[M–Cl]^+$: 284.1188 (100%), 285.1221 (20%), 286.1255 (2%); found: 284.1188 (100%), 285.1220 (30%), 286.1243 (5%).

1-(2-Methoxyacridin-9-yl)-3-methylimidazolium chloride (9)

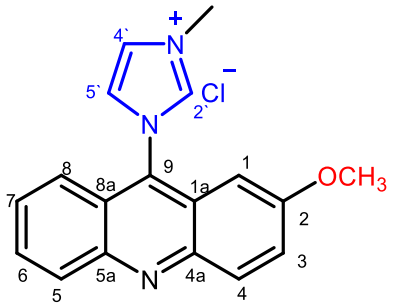

1-Methylimidazole (441 mg, 5.4 mmol) and 9-chloro-2-methylacridine **4b** (1.16 g, 4.8 mmol) were reacted according to general method **A** to give compound **9** (1.15 g, 74 %) as greenish solid. mp 210-215 ºC. FTIR: ν (ATR, cm^{-1}) 3076, 2961 (C–H), 1631 (C=N), 1561, 1477, 1431 (C=C), 1226, 1136, 1023 (C-O), 758 (C-Cl). ^{1}H NMR (400 MHz, DMSO-d_6): δ (ppm) 9.82 (s, 1H, NCHN, H_{imid}-2`), 8.31 (d, 1H, *J*=8 Hz, H-8), 8.29-8.26 (m, 3H, H-4, H-5, H-6), 7.95 (dt, 1H, $J_t$= 9 Hz, $J_d$= 1 Hz, H-3), 7.75 (dt, 1H, $J_t$ =9 Hz, $J_d$ =1 Hz, H-7), 7.70 (dd, 1H, *J*t =9 Hz, $J_d$ =3 Hz, H-4`), 7.62 (d, 1H, *J*= 8 Hz, H_{imid}-5`), 6.80 (d, 1H, *J*= 3 Hz, H-1), 4.12 (s, 3H, **N-CH$_3$**), 3.90 (m, 3H, **OCH$_3$**). $^{13}C$ NMR (100 MHz, DMSO-$d_6$): δ (ppm) 159.44 ($C_{Acri}$-2), 147.10 ($C_{Acri}$-4a), 146.50 ($C_{Acri}$-5a), 139.79 ($C_{Acri}$-9), 133.66 ($C_{imid}$-2`), 132.01(C_{Acri}-4), 130.71 (C_{Acri}-6), 129.97 (C_{Acri}-5), 129.50 (C_{Acri}-7), 126.93 (C_{Acri}-8), 125.67 (C_{Acri}-8a), 125.18 (C_{imid}-5`), 123.47 ($C_{Acri}$-3), 122.57 ($C_{Acri}$-1a), 122.09 ($C_{imid}$-4`), 98.15(C_{Acri}-1), 56.60(**O-CH$_3$**), 37.21 (**CH$_3$**). Anal. calcd. for $C_{18}H_{16}ClN_3O$: C 66.36, H 4.59, N 12.90 %; found: C 66.31, H 4.55, N 12.92%. HRMS (ESI^+) *m/z* calcd. for $C_{18}H_{16}N_3O$ $[M-Cl]^+$: 290.1293 (100%), 291.1327 (20%); found: 290.1302 (100%), 291.1325 (28%).

1-(2-Methoxyacridin-9-yl)-3-butylimidazolium chloride (10)

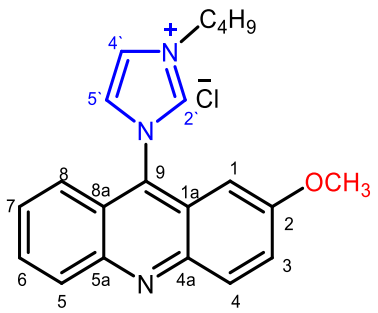

1-Butylimidazole **5b** (448 mg, 3.6 mmol) and compound **4b** (770 mg, 3.2 mmol) were reacted according to general method **A** to give compound **10** (890 mg, 77 %) as greenish solid. mp 212-220 ºC. FTIR: ν (ATR, cm^{-1}) 3080, 2965, 2953, 2875 (C–H), 1632 (C=N), 1563, 1478, 1435(C=C), 1227, 1136, 1022 (C-O), 759 (C-Cl). ^{1}H NMR (400 MHz, DMSO-d_6) δ (ppm) 9.92 (s, 1H, NCHN, H_{imid}-2`), 8.37 (t, 1H, $J_t$ = 1 Hz, H-8), 8.34-8.30 (m, 2H, H-4, H-5), 8.30 (d, 1H, $J_d$ = 9 Hz, H-6), 7.95 (ddd, 1H, *J*= 8/7/1 Hz, H-3), 7.78 (ddd, 1H, *J*= 9/8/1 Hz, H-7), 7.74 (dd, 1H, *J*=9/3 Hz, $H_{imid}$-4`), 7.59 (bd, 1H, *J*=9 Hz, H_{imid}-5`), 6.70 (d, 1H, J_d=3 Hz, H-1), 4.40 (t, 2H, **N-CH$_2$**), 3.84 (s, 3H, **O-CH$_3$**), 1.98 (m, 2H, **CH$_2$**), 1.37 (m, 2H, **CH$_2$**), 0.95 (t, 3H, **CH$_3$**). ^{13}C NMR (100 MHz, DMSO-d_6): δ (ppm) 159.47 (C_{Acri}-2), 147.13 (C_{Acri}-4a), 146.49 (C_{Acri}-5a), 139.23 (C_{Acri}-9), 132.10 (C_{imid}-2`), 130.77 ($C_{Acri}$-4), 130.05 ($C_{Acri}$-6), 129.65 ($C_{Acri}$-5), 126.99 ($C_{Acri}$-7), 125.62 ($C_{Acri}$-8), 124.54 ($C_{Acri}$-8a), 123.39 ($C_{imid}$-5`), 122.45 (C_{Acri}-3), 121.94 (C_{Acri}-1a), 121.95 (C_{imid}-4`), 97.79 (C_{Acri}-1), 56.40 (**N-CH$_2$**), 50.05 (O**CH$_3$**), 31.39 (**CH$_2$**), 19.49 (**CH$_2$**), 13.93 (**CH$_3$**). Anal. calcd. for $C_{21}H_{22}ClN_3O$: C 68.56, H 6.03, N 11.42 %; found: C 68.62, H 6.08, N 11.32%. HRMS (ESI^+) *m/z* calcd. for $C_{21}H_{22}N_3O[M-Cl]^+$: 332.1763 (100%), 333.1796 (23%); found: 332.1790 (100%), 333.1803 (37%).

1-(2-Methoxyacridin-9-yl)-3-benzylimidazolium chloride (11)

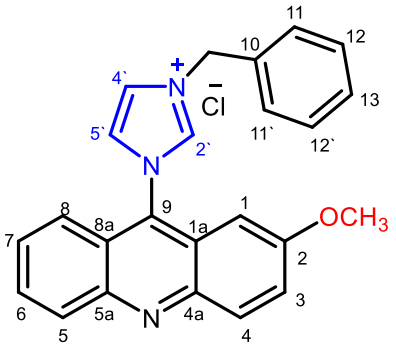

1-Benzylimidazole (570 mg, 3.6 mmol) and compound **4b** (770 mg, 3.2 mmol) were reacted according to general method **A** to give compound **11** (990 mg, 77 %) as greenish solid. mp 230-240 ºC. FTIR: ν (ATR, cm^{-1}) 3071, 2951 (C–H), 1630 (C=N), 1560, 1475, 1430 (C=C), 1226, 1136, 1023 (C-O), 759 (C-Cl). ^{1}H NMR (400 MHz, DMSO-d_6): δ (ppm) 10.16 (s, 1H, NCHN, H-2`), 8.44 (t, 1H, *J*= 1.9 Hz, H-8), 8.38-8.37 (t, 1H, *J*= 2 Hz, H-5), 8.33(d, 1H, *J*= 9 Hz, H-4), 8.28 (d, 1H, *J*= 9 Hz, H-6), 7.97 (dt, 1H, $J_t$=5 Hz, $J_d$=1.5 Hz, H-7), 7.79 (dd, 1H, $J_d$=7 Hz, H-4`), 7.70 (dd, 1H, J_d=7 Hz, H-5`), 7.65 (dd, 2H, $J_d$=9 Hz, H-11, H-11`), 7.59 (d, 1H, *J*= 8 Hz, H-3), 7.53-7.46 (m, 3H, H-12, H-13, H-12`), 6.60 (d, 1H, *J*= 3 Hz, H-1), 5.75 (s, 2H, **N-CH$_2$**), 3.83 (s, 3H, **OCH$_3$**). $^{13}C$ NMR (100 MHz, DMSO-$d_6$): δ (ppm) 159.46 ($C_{Acri}$-2), 147.12 ($C_{Acri}$-4a), 146.45 ($C_{Acri}$-5a), 139.64 ($C_{Acri}$-9), 135.17 ($C_{ph}$-10), 133.53 ($C_{imid}$-2`), 132.08 (C_{Acri}-4), 130.73 (C_{Acri}-6), 130.05 (C_{Acri}-5), 129.68 (C_{ph}-11, C_{ph}-11`), 129.63($C_{ph}$-12, $C_{ph}$-12`), 129.50 (C_{ph}-13), 129.08 (C_{Acri}-8), 126.90 (C_{Acri}-7), 125.90 (C_{Acri}-8a), 124.69 (C_{imid}-4`), 123.33 ($C_{Acri}$-3), 122.31 ($C_{Acri}$-1a), 121.90 ($C_{imid}$-5`), 97.57 (C_{Acri}-1), 56.32 (**N-CH$_2$**), 53.30 (**OCH$_3$**). Anal. calcd. for $C_{24}H_{20}ClN_3O$: C 71.73, H 5.02, N 10.46 %; found: C 71.71, H 5.15, N 10.52%. HRMS (ESI^+) *m/z* calcd. for $C_{24}H_{20}N_3O$ $[M-Cl]^+$: 366.1601 (100%), 367.1635 (26.0%), 368.1668 (3.2%); found: 366.1602 (100%), 367.1622 (26.0%), 368.1651 (3.2%).

1-(6-Chloro-2-methoxyacridin-9-yl)-3-methylimidazolium chloride (12)

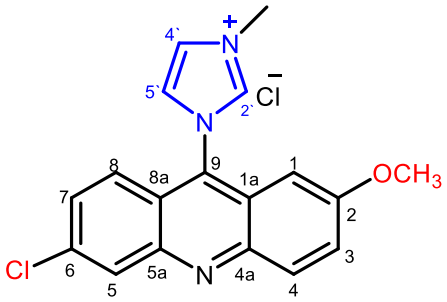

1-Methylimidazole (441 mg, 5.4 mmol) and 6,9-dichloro-2-methoxyacridine **4c** (1.31 g, 4.7 mmol) were reacted according to general procedure **A** to give compound **12** (1.44 g, 85 %) as greenish solid. mp 240-245 ºC. FTIR: ν (ATR, cm^{-1}) 3053 (C-H), 1631 (C=N), 1564, 1476, 1423 (C=C), 1216 (C-O), 832 (C-Cl). ^{1}H NMR (400 MHz, DMSO-d_6): δ (ppm) 9.77 (bs, 1H, NCHN, H_{imid}-2`), 8.35 (dd ≈ bd, 2H, $J$ = 5 Hz, H-8, H-5), 8.27 (bs, 1H, H-4), 8.22 (d, 1H, $J_d$ = 9 Hz, H-7), 7.75(dd, 1 H, $J$ =9/3 Hz, H-4`), 7.71-7.67 (m, 2H, H_{imid}-5`, H-3), 6.80 (d, 1H, $J_d$=3 Hz, H-1), 4.07(s, 3H, **N-CH3**), 3.86 (s, 3H, **OCH3**). $^{13}C$ NMR (100 MHz, DMSO-$d_6$): δ(ppm) 159.67($C_{Acri}$-2), 147.30 ($C_{Acri}$-4a), 146.93 ($C_{Acri}$-5a), 139.38 ($C_{imid}$-2`), 135.93 (C_{Acri}-6), 135.43 (C_{Acri}-9), 134.17 (C_{Acri}-4), 131.89 (C_{Acri}-5), 129.98 (C_{Acri}-7), 128.14 (C_{Acri}-8), 127.66 (C_{imid}-5`), 125.47 ($C_{imid}$-4`), 124.59 (C_{Acri}-3), 123.67 (C_{Acri}-8a), 121.24 (C_{Acri}-1a), 98.35 (C_{Acri}-1), 56.69 (**OCH3**), 37.24 (**N-CH3**). Anal. calcd. for $C_{18}H_{15}Cl_2N_3O$: C 60.01, H 4.20, N 11.66 %; found: C 59.98, H 4.35, N 11.61%. HRMS (ESI^+) *m/z* calcd. for $C_{18}H_{15}ClN_3O$ $[M-Cl]^+$: 324.0904 (100%), 325.0937 (20%), 326.0875 (34%), 327.0908 (7%); found: 324.0898 (100%), 325.0938 (35%), 326.0886 (52%), 327.0906 (10%).

1-(6-Chloro-2-methoxyacridin-9-yl)-3-ethylimidazolium chloride (13)

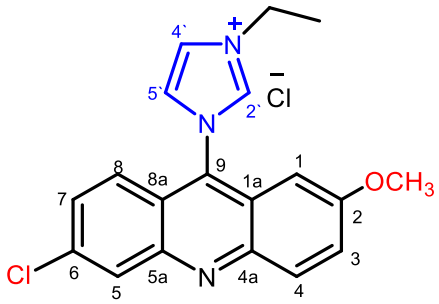

1-Ethylimidazole **5a** (519 mg, 5.4 mmol) was reacted with compound **4c** (1.3 g, 4.7 mmol) according to general method **A** to give compound **13** (1.41 g, 81 %) as greenish solid. mp 214-216 ºC. FTIR: ν (ATR, cm^{-1}) 3053, 2988 (C–H), 1629 (C=N), 1547, 1432, 1408(C=C), 1268, 1140 (C-O), 758 (C-Cl). ^{1}H NMR (400 MHz, DMSO-d_6): δ (ppm) 9.88 (s, 1H, NCHN, H_{imid}-2`), 8.35 (d, 2H, $J_d$ =2 Hz, H-8, H-5), 8.30 (bs, 1H, H-4), 8.27 (d, 1H, $J_d$ =10 Hz, H-7), 7.78-7.66 (m, 3H, $H_{imid}$-4`, H_{imid}-5`, H-3), 6.73 (d, 1H, $J_d$ =2 Hz, H-1), 4.42 (t, 2H, **N-CH$_2$**), 3.86 (s, 3H, **OCH$_3$**), 1.60 (t, 3H, **CH$_3$**). $^{13}$C NMR (100 MHz, DMSO-$d_6$): δ (ppm) 159.69 ($C_{Acri}$-2), 147.32 ($C_{Acri}$-4a), 146.98 ($C_{Acri}$-5a), 138.98 ($C_{imid}$-2`), 135.46 (C_{Acri} -6), 134.72 (C_{Acri} -9), 131.94 (C_{Acri}-4), 130.07 (C_{Acri}-5), 128.18 (C_{Acri}-7), 127.66 (C_{Acri}-8), 125.40 (C_{imid}-5`), 124.66 ($C_{imid}$-4`), 124.33 (C_{Acri}-3), 123.63 (C_{Acri}-8a), 121.19 (C_{Acri}-1a), 98.36 (C_{Acri}-1), 56.62 (**OCH$_3$**), 45.80 (**N-CH$_2$**), 15.02(**CH$_3$**). Anal. calcd. for $C_{19}H_{17}Cl_2N_3O$: C 60.97, H 4.58, N 11.23 %; found: C 60.93, H 4.55, N 11.30%. HRMS (ESI$^+$) *m/z* calcd. for $C_{19}H_{17}ClN_3O[M-Cl]^+$: 338.1060 (100%), 339.1094 (21%), 340.1031 (34%), 341.1065 (7%); found: 338.1064 (100%), 339.1095 (44%), 340.1045 (56%), 341.1062 (10%).

1-(6-Chloro-2-methoxyacridin-9-yl)-3-butylimidazolium chloride (14)

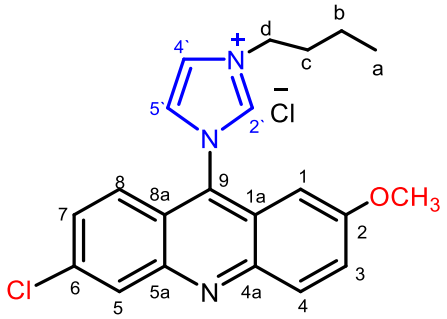

1-Butylimidazole **5b** (672 mg, 5.4 mmol) and compound **4c** (1.3 g, 4.7 mmol) were reacted according to general method **A** to give compound **14** (1.52 g, 80 %) as greenish solid. mp 220-225 ºC. FTIR: ν (ATR, cm^{-1}) 3079, 2956 (C–H), 1631 (C=N), 1542, 1480, 1426 (C=C), 1238, 1127 (C-O), 830 (C-Cl). ^{1}H NMR (400 MHz, DMSO-d_6): δ (ppm) 10.00 (s, 1H, NCHN, H_{imid}-2`), 8.42 (bs, 1H, H-8), 8.38 (d, 1H, $J_d$=2 Hz, H-5), 8.33 (d, 1H, $J_d$=1 Hz, H-4), 8.25 (d, 1 H, $J_d$=9 Hz, H-7), 7.80 (dd, 1H, *J*=10/2 Hz, H-4`), 7.75 (dd, 1H, *J*=10/3 Hz, H-5`), 7.68 (d, 1H, J_d=9 Hz, H-3), 6.69 (d, 1H, J_d=3 Hz, H-1), 4.46 (t, 2H, **N-CH₂**), 3.89 (s, 3H, **OCH₃**), 2.02 (m, 2H, **CH₂**), 1.42 (m, 2H, **CH₂**), 0.99 (t, 3H, **CH₃**). ^{13}C NMR (100 MHz, DMSO-d_6): δ (ppm) 159.47 (C_{Acri}-2), 147.30 (C_{Acri}-4a), 146.99 (C_{Acri}-5a), 139.23 (C_{imid}-2`), 135.49 ($C_{Acri}$-6), 134.10 ($C_{Acri}$-9), 131.99 ($C_{Acri}$-4), 130.15 ($C_{Acri}$-5), 128.23 ($C_{Acri}$-7), 127.71 ($C_{Acri}$-8), 125.59 ($C_{imid}$-5`), 124.59 (C_{imid}-4`), 124.49 (C_{Acri}-3), 123.60 (C_{Acri}-8a), 121.13 (C_{Acri}-1a), 98.00 (C_{Acri}-1), 56.48 (**OCH₃**), 50.10 (**N-CH₂**, d), 31.36 (**CH₂**, c), 19.50 (**CH₂**, b), 13.92(**CH₃**, a). Anal. calcd. for $C_{21}H_{21}Cl_2N_3O$: C 62.69, H 5.26, N 10.44 %; found: C 62.51, H 5.25, N 10.31%. HRMS (ESI+) *m/z* calcd. for $C_{21}H_{21}ClN_3O[M-Cl]^+$: 366.1373 (100%), 367.1407 (23%), 368.1344 (35%), 369.1378 (8%); found: 366.1418 (100%), 367.1409 (53%), 368.1361 (66%), 369.1374 (19%).

1-(6-Chloro-2-methoxyacridin-9-yl)-3-octylimidazolium chloride (15)

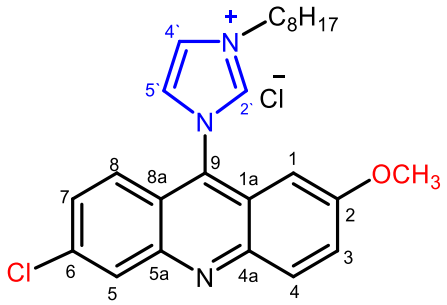

1-Octylimidazole **5d** (324 mg, 1.8 mmol) and compound **4c** (439 mg, 1.6 mmol) were reacted according to general method **A** to give compound **15** (545 mg, 75 %) as yellow solid. mp 320-330 ºC. FTIR: ν (ATR, cm^{-1}) 3069, 2954, 2924, 2854 (C–H), 1631 (C=N), 1595, 1561, 1476 (C=C), 1281(C-N), 1233, 1154, 1030 (C-O), 818, 747 (C-Cl). ^{1}H NMR (400 MHz, DMSO-d_6): δ (ppm) 9.86 (s, 1H, NCHN, H_{imid}-2`), 8.33 (bs, 1H, H-8), 8.31 (s, 1H, H-5), 8.28 (d, 1H, $J_d$=10 Hz, H-4), 7.95 (dt, 1H, $J_t$= 7 Hz, $J_d$= 2 Hz, H-7), 7.77 (dt, 1H, $J_t$=7 Hz, $J_d$ = 1 Hz, $H_{imid}$-4`), 7.71 (dd, 1H, J= 9/3 Hz, H_{imid}-5`), 7.56 (d, 1H, J_d =9 Hz, H-3), 6.69 (d, 1H, J_d = 3 Hz, H-1), 4.42 (t, 2H, **N-CH₂**), 3.87 (s, 3H, **OCH₃**), 2.00 (m, 2H, **CH₂**), 1.36- 1.26 (m, 10H, **CH₂**), 0.85 (t, 3H, **CH₃**). ^{13}C NMR (100 MHz, DMSO-d_6): δ (ppm) 159.47 (C_{Acri}-2), 147.14 (C_{Acri}-4a), 146.50 (C_{Acri}-5a), 139.22 (C_{imid}-2`), 133.58 ($C_{Acri}$-6), 132.11 ($C_{Acri}$-9), 130.76 ($C_{Acri}$-4), 130.08 ($C_{Acri}$-5), 129.61 ($C_{Acri}$-7), 126.96 ($C_{Acri}$-8), 125.62 ($C_{imid}$-5`), 124.53 (C_{imid}-4`), 123.40 (C_{Acri}-3), 122.47 (C_{Acri}-8a), 121.91 (C_{Acri}-1a), 97.86 (C_{Acri}-1), 56.39 (**OCH₃**), 50.32 (**N-CH₂**), 31.70 (**CH₂**), 29.39 (**CH₂**), 29.07 (**CH₂**), 28.91(**CH₂**), 26.15 (**CH₂**), 22.62 (**CH₂**), 14.49 (**CH₃**). Anal. calcd. For $C_{25}H_{29}Cl_2N_3O$: C 65.50, H 6.38, N 9.17%; found: C 65.52, H 6.35, N 9.19%. HRMS (ESI^+) *m/z* calcd. for $C_{25}H_{29}ClN_3O[M-Cl]^+$: 422.1999 (100%), 423.2033 (28%), 424.1970 (34%), 425.2004 (10%); found: 422.1992 (100%), 423.2543 (%), 424.1968 (46%).

1-(Acridin-9-yl)-3-(4-methylbenzyl)-imidazolium chloride (16)

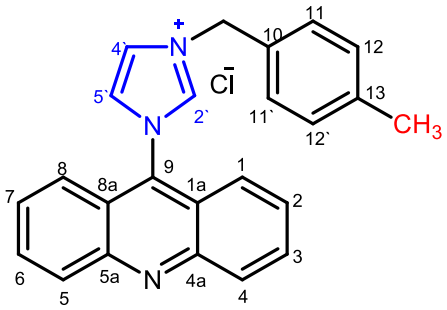

Compound **4a** (337 mg, 1.6 mmol) and 1-(4-Methylbenzyl)-imidazole (310 mg, 1.8 mmol) were reacted according to general method **A** to give compound **16** (520 mg, 85 %) as white solid. mp 205-210 ºC. FTIR: ν (ATR, cm^{-1}) 3020, 2946 (C–H), 1626 (C=N), 1536, 1520, 1439 (C=C), 1259 (C-N), 1132 (C-C), 770 (C–Cl). ^{1}H NMR (400 MHz, DMSO-d_6): δ (ppm) 9.95 (s, 1H, NCHN, H_{imid}-2`), 8.34-8.28 (m, 4H, H-1, H-8, H-4, H-5), 7.99 (bt, 2H, *J*= 8 Hz, H-3, H-6), 7.77 (dt, 2H, $J_t$= 6 Hz, $J_d$=1 Hz, H-2, H-7), 7.60 (d, 2H, $J_d$= 9 Hz, $H_{imid}$-4`, H_{imid}-5`), 7.48 (d, 2H, $J_d$= 8 Hz, H-12, H-12`), 7.27 (d, 2H, J_d= 8 Hz, H-11, H-11`), 5.59 (s, 2H, **N-CH$_2$**), 2.30 (s, 3H, **Ar-CH$_3$**). $^{13}$C NMR (100 MHz, DMSO-$d_6$): δ (ppm) 149.06 ($C_{Acri}$-4a, $C_{Acri}$-5a), 139.46 ($C_{Acri}$-9), 139.04 ($C_{ph}$-13), 136.02 ($C_{imid}$-2`), 132.05 (C_{ph}-10), 131.65 (C_{Acri}-3, C_{Acri}-6), 130.25 (C_{Acri}-4, C_{Acri}-5), 130.01 (C_{ph}-11, C_{ph}-11`), 129.57 ($C_{ph}$-12, $C_{ph}$-12`), 129.39 (C_{Acri}-2, C_{Acri}-7), 126.18 (C_{Acri}-1, C_{Acri}-8), 124.39 (C_{imid}-4`), 122.51 ($C_{Acri}$-1a, $C_{Acri}$-8a), 122.08 ($C_{imid}$-5`), 53.26 (**N-CH$_2$**), 21.32 (**Ar-CH$_3$**). Anal. calcd. For $C_{24}H_{20}ClN_3$: C 74.70, H 5.22, N 10.89 %; found: C 74.80, H 5.20, N 10.90 %. HRMS (ESI$^+$) *m/z* calcd. for $C_{24}H_{20}N_3$[M-Cl]$^+$: 350.1657 (100%), 351.1691 (27%); found: 350.1650 (100%), 351.1682 (74%).

1-(Acridin-9-yl)-3-(4-bromobenzyl)-imidazolium bromide (17)

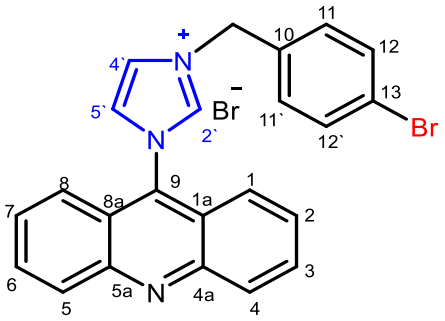

4-Bromobenzyl bromide (748 mg, 3.0 mmol) and compound **6a** (244 mg, 1.0 mmol) were reacted according to general method **B** to give compound **17** (445 mg, 90 %) as yellow solid. mp 280-290 ºC. FTIR: ν (ATR, cm^{-1}) 3010, 2950 (C–H), 1633 (C=N), 1534, 1425 (C=C), 1137, 1030 (C-O), 750 (C-Br). ^{1}H NMR (400 MHz, DMSO-d_6): δ (ppm) 9.93 (s, 1H, NCHN, H_{imid}-2`), 8.39-8.33 (m, 4H, H-1, H-8, H-4, H-5), 8.03 (dt, 2H, $J_t$=7 Hz, $J_d$=1 Hz, H-3, H-6), 7.81 (dt, 2H, $J_t$= 6 Hz, $J_d$=1 Hz, H-12, H-12`), 7.72 (d, 2H, J_d=8 Hz, H-2, H-7), 7.68 (d, 2H, J_d=8 Hz, H_{imid}-4`, $H_{imid}$-5`), 7.60 (d, 2H, J_d=8 Hz, H-11, H-11`), 5.67 (s, 2H, **N-CH$_2$**). $^{13}C$ NMR (100 MHz, DMSO-$d_6$): δ (ppm) 149.05 ($C_{Acri}$-4a, $C_{Acri}$-5a), 139.59 ($C_{Acri}$-9), 135.98 ($C_{ph}$-10), 133.88 ($C_{imid}$-2`), 132.62 (C_{ph}-11, C_{ph}-11`), 132.07 ($C_{ph}$-12, $C_{ph}$-12`), 131.77 (C_{Acri}-3, C_{Acri}-6), 129.98(C_{Acri}-4, C_{Acri}-5), 129.57 (C_{Acri}-2, C_{Acri}-7), 126.23 (C_{Acri}-1, C_{Acri}-8), 124.47 (C_{imid}-4`), 123.01 ($C_{ph}$-13), 122.60 ($C_{Acri}$-1a, $C_{Acri}$-8a), 122.06 ($C_{imid}$-5`), 52.76 (**N-CH$_2$**). Anal. calcd. for $C_{23}H_{17}Br_2N_3$: C 55.78, H 3.46, N 8.49 %; found: C 55.77, H 3.47, N 8.51%. HRMS (ESI^+) *m/z* calcd. for $C_{23}H_{17}BrN_3$ $[M-Br]^+$: 414.0606 (100%), 415.0639 (26%), 416.0605 (97%), 417.0638 (26%); found: 414.0626 (100%), 415.0641 (35%), 416.0608 (99%), 417.0621 (35%).

1-(Acridin-9-yl-3-(2-bromobenzyl)-imidazolium bromide (18)

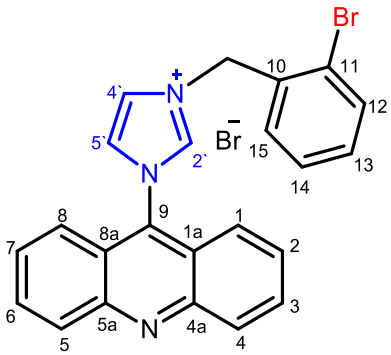

Compound **6a** (244 mg, 1.0 mmol) and 2-Bromobenzyl bromide (748 mg, 3.0 mmol) were reacted according to general method **B** to give compound **18** (449 mg, 91 %) as yellow solid. mp 276-278 ºC. FTIR: ν (ATR, cm^{-1}) 3023, 2960 (C–H), 1632 (C=N), 1518, 1423 (C=C), 1269, 1135 (C-O), 750, 806 (C-Br). ^{1}H NMR (400 MHz, DMSO-d_6): δ (ppm) 9.93 (s, 1H, NCHN, H_{imid}-2`), 8.43 (t, 1H, $J_t$ =2 Hz, H-1), 8.38 (bd, 2H, $J$ =10Hz, H-8, H-4), 8.32 (t, 1H, $J_t$ =2 Hz, H-5), 8.04 (dt, 2H, $J_t$ = 6 Hz, $J_d$= 1 Hz, H-3, H-6), 7.84-7.80 (m, 3H, H-2, H-7, H-12), 7.70 (dd ≈ bd, 1H, $J$= 8 Hz, H-14), 7.67 (bd, 2H, $J$=8 Hz, H-4`, H-5`), 7.57 (dt, 1H, $J_t$ =7 Hz, $J_d$ = 2 Hz, H-13), 7.45 (dt, 1H, $J_t$= 7 Hz, $J_d$= 2 Hz, H-15), 5.77 (s, 2H, **N-CH₂**). $^{13}C$ NMR (100 MHz, DMSO-$d_6$): δ (ppm) 149.08 ($C_{Acri}$-4a, $C_{Acri}$-5a), 140.18 ($C_{Acri}$-9), 135.93 ($C_{ph}$-10), 133.93 ($C_{imid}$-2`), 133.30 (C_{ph}-12), 132.40 (C_{ph}-15), 132.08 (C_{Acri}-3, C_{Acri}-6), 130.05 (C_{Acri}-4, C_{Acri}-5), 129.60 (C_{ph}-13), 129.25 (C_{ph}-14), 126.35 (C_{Acri}-2, C_{Acri}-7), 124.69 (C_{Acri}-1, C_{Acri}-8), 124.14 (C_{ph}-11), 122.45 (C_{imid}-4`), 122.15 ($C_{Acri}$-1a, $C_{Acri}$-8a), 100.00 ($C_{imid}$-5`), 53.97 **(N-CH₂)**. Anal. calcd. for $C_{23}H_{17}Br_2N_3$: C 55.78, H 3.46, N 8.49 %; found: C 55.79, H 3.49, N 8.52 %. HRMS (ESI^+) *m/z* calcd. for $C_{23}H_{17}BrN_3[M\text{-}Br]^+$: 414.0606 (100%), 415.0639 (26%), 416.0605 (97%), 417.0638 (26%); found: 414.0621 (100%), 415.0642 (32%), 416.0603 (98%), 417.0622 (32%).

1-(Acridin-9-yl)-3-(4-nitrobenzyl)-imidazolium bromide (19)

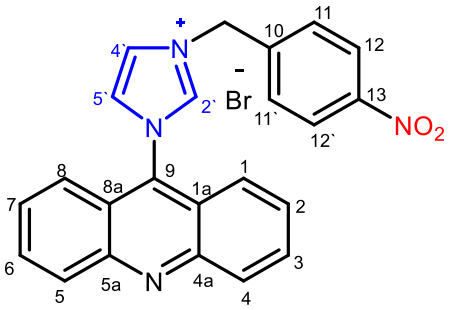

According to general method **B**, 4-Nitrobenzyl bromide (486 mg, 2.3 mmol) and **6a** (183 mg, 0.75 mmol) were reacted to give compound **19** (315 mg, 91 %) as yellow solid. mp 220-230 ºC. FTIR: ν (ATR, cm^{-1}) 3064, 2928 (C–H), 1605 (C=N), 1542, 1513, 1428, 1349 (C=C), 1271, 1140 (C-O), 757 (C-Br). ^{1}H NMR (400 MHz, DMSO-d_6): δ (ppm) 9.97 (s, 1H, NCHN, H_{imid}-2`), 8.44-8.35 (m, 6H, H-1, H-8, H-4, H-5, H-12, H-12`), 8.04 (bt, 2H, J_t=8 Hz, H-3, H-6), 7.89 (d, 2H, J_d=8 Hz, H-2, H-7), 7.82 (t, 2H, J_t=8 Hz, H-11, H-11`), 7.72 (d, 2H, $J_d$=8 Hz, $H_{imid}$-4`, H_{imid}-5`), 5.85 (s, 2H, **N-CH$_2$**). $^{13}C$ NMR (100 MHz, DMSO-$d_6$): δ (ppm) 149.08 ($C_{Acri}$-4a, $C_{Acri}$-5a), 148.33($C_{ph}$-13, C-$NO_2$), 141.87 ($C_{Acri}$-9), 140.00 ($C_{ph}$-10), 135.95 ($C_{imid}$-2`), 132.08 (C_{Acri}-3, C_{Acri}-6), 130.64 (C_{Acri}-4, C_{Acri}-5), 130.01 (C_{ph}-11, C_{ph}-11`), 129.58 ($C_{Acri}$-2, $C_{Acri}$-7), 126.39 ($C_{Acri}$-1, $C_{Acri}$-8), 124.70 ($C_{ph}$-12, $C_{ph}$-12`), 122.67 (C_{imid}-4`, $C_{imid}$-5`), 122.05 (C_{Acri}-8a, C_{Acri}-1a), 52.59 (**N-CH$_2$**). Anal. calcd. for $C_{23}H_{17}BrN_4O_2$: C 59.88, H 3.71, N 12.15; found: C 59.90, H 3.79, N 12.20%. HRMS (ESI^+) *m/z* calcd. for $C_{23}H_{17}N_4O_2[M-Br]^+$: 381.1352 (100%), 382.1385 (25%); found 381.1383 (100%), 382.139 (40%).

1-(Acridin-9-yl)-3-(phenacyl)-imidazolium bromide (20)

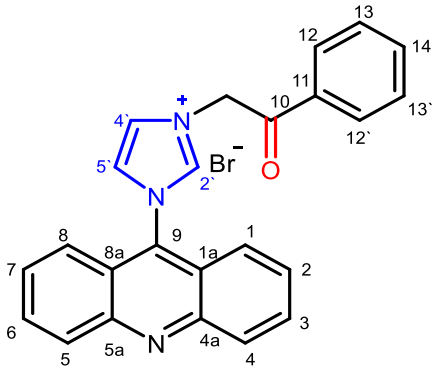

2-Bromo-acetophenone (596 mg, 3.0 mmol) and compound **6a** (244 mg, 1.0 mmol) were reacted according to general method **B** to give compound **20** (401 mg, 91 %) as yellow solid. mp 190-200 ºC. FTIR: ν (ATR, cm^{-1}) 3064, 2928 (C–H), 1689 (C=O), 1633 (C=N), 1540, 1426, 1424, 1347 (C=C), 1224, 1146 (C-O), 752 (C-Br). ^{1}H NMR (DMSO-d_6): δ (ppm) 9.82 (s, 1H, NCHN, H_{imid}-2`), 8.44 (dd≈bs, 1H, H-1), 8.41 (d, 2H, $J_d$= 8 Hz, H-8, H-4), 8.25 (t, 1H, $J_t$ = 3 Hz, H-5), 8.16 (d, 2H, $J_d$= 8 Hz, H-3, H-6), 8.06 (dt, 2H, $J_t$ = 9 Hz, *J*d=1 Hz, H-2, H-7), 7.88 (bd, 2H, $J_d$ = 9 Hz, $H_{imid}$-4`, H_{imid}-5`), 7.82 (t, 1H, $J_t$ = 7 Hz, H-14), 7.71-7.67 (m, 4H, H-12, H-12`, H-13, H-13`), 6.32 (s, 2H, **N-CH₂**). $^{13}$C NMR (DMSO-$d_6$): δ (ppm) 191.73 (C-10, **C=O**), 149.06 ($C_{Acri}$-4a, $C_{Acri}$-5a), 140.96 ($C_{ph}$-11), 135.98 ($C_{imid}$-2`), 135.22 (C_{Acri}-9), 134.09 (C_{ph}-14), 132.04 (C_{Acri}-3, C_{Acri}-6), 130.07 (C_{Acri}-4, C_{Acri}-5), 129.68 (C_{ph}-12, C_{ph}-12`), 129.64 ($C_{ph}$-13, $C_{ph}$-13`), 128.83 (C_{Acri}-2, C_{Acri}-7), 125.81 (C_{Acri}-1, C_{Acri}-8), 125.52 (C_{imid}-4`), 122.17 ($C_{Acri}$-1a, $C_{Acri}$-8a), 122.14 ($C_{imid}$-5`), 56.65 (**N-CH₂**). Anal. calcd. for $C_{24}H_{18}BrN_3O$: C 64.88, H 4.08, N 9.46 %; found: C 64.86, H 4.05, N 9.51%. HRMS (ESI^+) *m/z* calcd. for $C_{24}H_{18}N_3O$ $[M- Br]^+$: 364.1450 (100%), 365.1483 (27%); found: 364.1433 (100%), 265.1463 (36%).

1-(Acridin-9-yl)-3-(4-bromophenacyl)-imidazolium bromide (21)

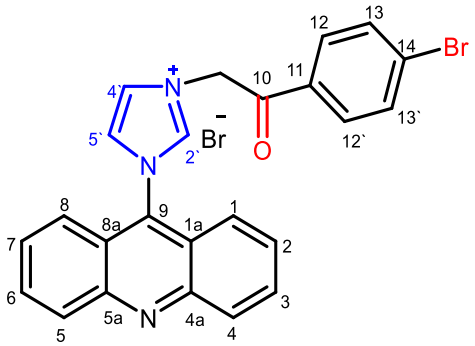

2,4`-Dibromo-acetophenone (624 mg, 2.2 mmol) and compound **6a** (183 mg, 0.75 mmol) were reacted according to general method **B** to give compound **21** (372 mg, 95 %) as yellow solid.mp 220-230 ºC. FTIR: ν (ATR, cm^{-1}) 3081, 2966 (C–H), 1698 (C=N), 1585, 1423, 1393 (C=C), 1269, 1135 (C-O), 987, 749 (C-Br). ^{1}H NMR (DMSO-d_6): δ (ppm) 9.81 (t≈, 1H, NCHN, H_{imid}-2`), 8.44 (d, 1H, *J*= 2 Hz, H-1), 8.41 (bd, 2H, *J*= 8 Hz, H-5, H-8), 8.24 (t, 1H, $J_t$= 2 Hz, H-4), 8.09 (d, 2H, $J_d$= 8 Hz, H-3, H-6), 8.08-8.06 (m, 2H, H-12, H-12`), 7.92 (d, 2H, J_d= 8 Hz, H-2, H-7), 7.91-7.86 (m, 2H, H_{imid}-4`, $H_{imid}$-5`), 7.68 (d, 2H, J_d= 8 Hz, H-13, H-13`), 6.29 (s, 2H, **N-CH$_2$**). $^{13}$C NMR (DMSO-$d_6$): δ (ppm) 191.22 (C-10, **C=O**), 149.12 ($C_{Acri}$-4a, $C_{Acri}$-5a), 140.99 ($C_{ph}$-11), 136.05 ($C_{imid}$-2`), 133.23 (C_{Acri}-9, C-N), 132.84 (C_{ph}-13, C_{ph}-13`), 132.10 ($C_{Acri}$-3, $C_{Acri}$-6), 130.84 ($C_{ph}$-12, $C_{ph}$-12`), 130.13 (C_{Acri}-4, C_{Acri}-5), 129.68 (C_{Acri}-2, C_{Acri}-7, C_{bz}-14), 129.40 (C_{Acri}-1, C_{Acri}-8), 125.85 (C_{imid}-4`), 125.60 ($C_{imid}$-5`), 122.22 (C_{Acri}-8a, C_{Acri}-1a), 56.65 (**N-CH$_2$**). Anal. calcd. for $C_{24}H_{17}Br2N_3$ O: C 55.09, H 3.27, N 8.03; found: C 55.07, H 3.30, N 8.05%. HRMS (ESI$^+$) *m/z* calcd. for $C_{24}H_{17}BrN_3O[M-Br]^+$: 442.0555 (100%), 443.0589 (27%), 444.0535 (98%), 445.0569 (26%); found 442.1206 (100%), 443.1237 (27%), 444.1186 (31%), 445.1207 (10%).

1-(6-Chloro-2-methoxyacridin-9-yl)-3-benzylimidazolium chloride (22)

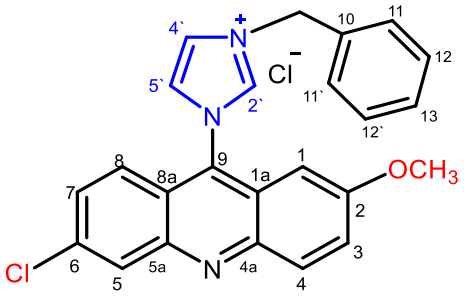

1-Benzylimidazole (570 mg, 3.6 mmol) and compound **4c** (878 mg, 3.2 mmol) were reacted according to general method **A** to give compound **22** (1.1 g, 80 %) as greenish solid. mp 245-250 ºC. FTIR: ν (ATR, cm^{-1}) 2960 (C–H), 1627 (C=N), 1556, 1440, 1409 (C=C), 1141, 1030 (C-O), 763 (C-Br). ^{1}H NMR (DMSO-d_6): δ (ppm) 9.92 (s, 1H, NCHN, H_{imid}-2`), 8.43 (d, 1H, $J_d$=2 Hz, H-8), 8.35 (d, 2H, $J_d$=1 Hz, H-5, H-4), 8.27 (d, 1H, $J_d$=10 Hz, H-7), 7.82 (dd, 1H, $J$=10/2 Hz, $H_{imid}$-4`), 7.74 (dd, 1H, J=10/3 Hz, H_{imid}-5`), 7.68 (d, 1H, $J_d$=10 Hz, H-3), 7.60 (d, 2H, $J_d$=7 Hz, H-11, H-11`), 7.53-7.46 (m, 3H, H-12, H-12`, H-13), 6.58 (d, 1H, $J_d$=3 Hz, H-1), 5.72-5.63 (AB-syst., 2H, **N-$CH_2$**), 3.83 (s, 3H, **$OCH_3$**). $^{13}C$ NMR (DMSO-$d_6$): δ(ppm) 159.70 ($C_{Acri}$-2), 147.26 ($C_{Acri}$-4a), 146.98 ($C_{Acri}$-5a), 139.61 ($C_{imid}$-2`), 135.48 (C_{Acri}-6), 134.98 (C_{Acri}-9), 134.09 (C_{ph}-10), 131.99 (C_{Acri}-4), 130.15 (C_{Acri}-5), 129.70 (C_{Acri}-7), 129.53 (C_{ph}-11, C_{ph}-11`), 129.10 ($C_{ph}$-12, $C_{ph}$-12`), 128.22 (C_{ph}-13), 127.69 (C_{Acri}-8), 125.90 (C_{imid}-5`), 124.75 ($C_{imid}$-4`), 124.46 (C_{Acri}-3), 123.56 (C_{Acri}-8a), 121.02 (C_{Acri}-1a), 97.76 (C_{Acri}-1), 56.38 (**OCH_3**), 53.41 (**N-CH_2**). Anal. calcd. for $C_{24}H_{19}C_{l2}N_3O$: C 66.06. H 4.39, N 9.63 %; found: C 66.09, H 4.41, N 9.60%. HRMS (ESI^+) *m/z* calcd. for $C_{24}H_{19}ClN_3O[M-Cl]^+$: 400.1217 (100%), 401.1250 (27%), 402.1188 (35%), 403.1221 (8%); found: 400.1214 (100%), 401.1241 (27%), 402.1189 (33%), 403.1215 (8%).

1-(6-Chloro-2-methoxyacridin-9-yl)-3-(phenacyl) imidazolium bromide (23)

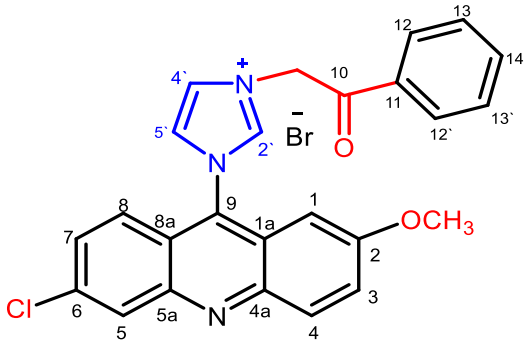

2-Bromoacetophenone (298 mg, 1.5 mmol) and compound **6b** (154 mg, 0.50 mmol) were reacted according to general method **B** to give compound **23** (227 mg, 90 %) as yellow solid. mp 250-260 ºC. FTIR: ν (ATR, cm^{-1}) 3064, 2996 (C–H), 1683 (C=O), 1633 (C=N), 1562, 1477, 1424 (C=C), 1234, 1074 (C-O), 757 (C-Br). ^{1}H NMR (DMSO-d_6): δ (ppm) 9.81 (s, 1H, NCHN, H_{imid}-2`), 8.43 (dd≈bd, 1H, *J*= 2 Hz, H-8), 8.39 (t, 1H, $J_t$ =1 Hz, H-5), 8.28 (d, 1, $J_d$= 10 Hz, H-4), 8.25 (t, 1H, $J_t$ = 3 Hz, H-7), 8.16 (dd, 2H, *J*= 8/1 Hz, H-12, H-12`), 7.87 (dd, 1H, *J*= 9/2 Hz, H-14), 7.82 (t, 1H, *Jt*= 8/1 Hz, H-3), 7.76 (dd, 1H, *J*= 8/3 Hz, H_{imid}-4`), 7.73 (d, 1H, $J_d$ =10 Hz, $H_{imid}$-5`), 7.69 (t, 2H, J_t =8 Hz, H-13, H-13`), 6.78 (d, 1H, $J_d$=2 Hz, H-1), 6.41-6.26 (AB-syst., 2H, **N-CH₂**), 3.98 (s, 3H, **OCH₃**). $^{13}C$ NMR (DMSO-$d_6$): δ (ppm) 191.97 (**C=O**, $C_{bz}$-10), 159.91 ($C_{Acri}$-2), 147.29 ($C_{Acri}$-4a), 147.0 ($C_{Acri}$-5a), 141.23 ($C_{Acri}$-6), 135.51 ($C_{Acri}$-9), 135.32 ($C_{imid}$-2`), 134.09 (C_{ph}-11), 132.02 (C_{ben}-14), 130.23 (C_{Acri}-4), 129.75 (C_{Acri}-5), 128.90 (C_{ph}-12, C_{ph}-12`), 128.29 ($C_{ph}$-13, $C_{ph}$-13`), 127.78 (C_{Acri}-7), 126.03 (C_{Acri}-8), 125.21 (C_{imid}-4`), 124.21 ($C_{Acri}$-8a), 123.86 ($C_{Acri}$-3), 121.10 ($C_{Acri}$-1a), 100.01 ($C_{imid}$-5`), 97.56 (C_{Acri}-1), 56.76 (**N-CH₂**), 56.54 (**OCH₃**). Anal. calcd. For $C_{25}H_{19}BrClN_3O_2$: C 59.02, H 3.76, N 8.26%; found: C 59.21, H 3.78, N 8.31%. HRMS (ESI^+) *m/z* calcd. for $C_{25}H_{19}ClN_3O_2$ $[M-Br]^+$: 428.1166 (100%), 429.1199 (28%), 430.1137 (34%), 431.1170 (10%); found: 428.1194 (100%), 429.1207 (39%), 430.1157 (45%), 431.1178 (13%).

1-(6-Chloro-2-methoxyacridin-9-yl)-3-(4-bromophenacyl)-imidazolium bromide (24)

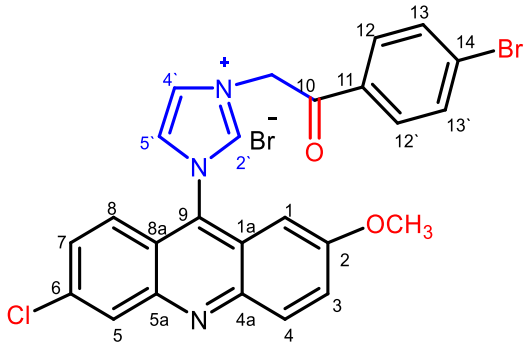

2,4'-Dibromoacetophenone (624 mg, 2.2 mmol) and compound **6b** (231 mg, 0.83 mmol) were reacted according to general method **B** to give compound **24** (414 mg, 85 %) as yellow solid. mp 260-270 ºC. FTIR: ν (ATR, cm^{-1}) 3072, 2983 (C-H), 1693 (C=N), 1634, 1584, 1477 (C=C), 1425, 1235, 1067 (C-O), 812 (C-Br). ^{1}H NMR (DMSO-d_6): δ (ppm) 9.78 (s, 1H, NCHN, H_{imid}-2`), 8.44 (d, 1H, $J_d$ = 2 Hz, H-8), 8.39 (t, 1H, $J$= 1 Hz, H-5), 8.29 (d, 1H, $J_d$= 10 Hz, H-4), 8.23 (t, 1H, $Jt$= 2 Hz, H-7), 8.08 (d, 2H, $J_d$= 8 Hz, H-12, H-12`), 7.92 (d, 2H, J_d= 8 Hz, H-13, H-13`), 7.86 (dd, 1H, $J$= 10/2 Hz, H-3), 7.76 (dd, 1H, $J$= 8/2 Hz, $H_{imid}$-4`), 7.73 (d, 1H, J_d= 8 Hz, H_{imid}-5`), 6.76 (d, 1H, $J_d$= 3 Hz, H-1), 6.36-6.22 (AB-syst, 2H, **N-CH$_2$**), 3.97 (s, 3H, **CH$_3$**). $^{13}C$ NMR (DMSO-$d_6$): δ (ppm) 191.38 (**C=O**, C-10), 159.89($C_{Acri}$-2), 147.30($C_{Acri}$-4a), 147.01($C_{Acri}$-5a), 141.20($C_{Acri}$-6), 135.50 ($C_{Acri}$-9), 134.16 ($C_{imid}$-2`), 133.18 (C_{ph}-11), 132.84 (C_{ph}-13, C_{ph}-13`), 132.03 ($C_{Acri}$-4), 130.84 ($C_{ph}$-12, $C_{ph}$-12`), 130.84 (C_{Acri}-5), 129.45 (C_{Acri}-7), 128.29 (C_{Acri}-8), 127.76 (C_{ph}-14), 126.01 (C_{imid}-4`), 125.23 ($C_{Acri}$-8a), 124.22 ($C_{Acri}$-3), 123.87 ($C_{Acri}$-1a), 121.11 ($C_{imid}$-5`), 97.56(C_{Acri}-1), 56.70(**OCH$_3$**), 56.53(**N-CH$_2$**). Anal. calcd. for $C_{25}H_{18}Br_2ClN_3O_2$: C 51.09, H 3.09, N 7.15%; found: C 51.11, H 3.05, N 7.31%. HRMS (ESI^+) *m/z* calcd. for $C_{25}H_{18}BrClN_3O_2[M-Br]^+$: 506.0271 (75%), 507.0304 (21%), 508.0270 (100%), 509.0294 (27%), 510.0232 (27%), 511.0265 (8%); found: 506.0282

(85%), 507.0306 (28%), 508.0267 (100%), 509.0285 (33%), 510.0238 (31%), 511.0261 (7%).

1-acridinyl-3-(4-methoxyphenacyl)-imidazolium bromide (25)

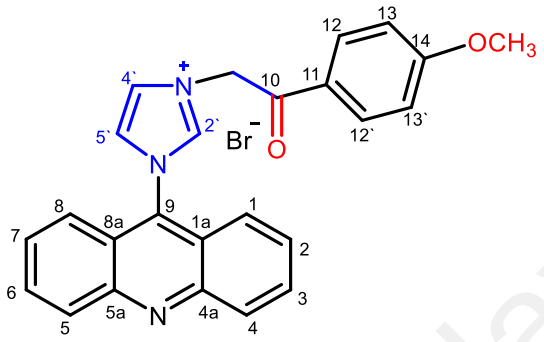

4-Methoxybenzyl bromide (151 mg, 0.75mmol) and compound **6a** (61 mg, 0.25mmol) were reacted according to general method **B** to give compound **25** (0.305g, 90 %) as a yellow solid. mp: 220-230 ºC. FTIR: ν (ATR, cm^{-1}) 3072 $(C–H)_{Ar}$, 2983$(C–H)_{Aliph}$, 1693(C=O), 1634(C=N), 1584, 1478 $(C=C)_{Ar}$, 1425, 1235(C-O), 812 (C-Br).^{1}H NMR (400 MHz, DMSO-d_6): δ (ppm) 9.79 (s, 1H, NCHN, H_{imid}-2`), 8.39-8.35 (m, 3H, H-1, H-8, H-2), 8.22 (s, 1H, H-7), 8.10 (d, 2H, $J_d$= 8 Hz, H-3, H-6), 8.04-8.01 (m, 2H, H-12, H-12`), 7.85-7.81 (m, 2H, H-4, H-5), 7.65 (d, 2H, J_d= 8 Hz, H_{imid}-4`, $H_{imid}$-5`), 7.16 (d, 2H, J_d= 8 Hz, H-13, H-13`), 6.23 (s, 2H, **N-CH$_2$**), 3.87 (s, 3H, **Ar-OCH$_3$**). $^{13}$C NMR (100 MHz, DMSO-$d_6$): δ (ppm) 190.20 (**C=O**, C-10), 146.63 ($C_{ph}$-14-**OCH$_3$**), 141.41 ($C_{Acri}$-4a, $C_{Acri}$-5a), 137.24 ($C_{Acri}$-9), 134.0 ($C_{imid}$-2`), 131.10 (C_{Acri}-3, C_{Acri}-6), 127.06 (C_{ph}-12, C_{ph}-12`), 126.52 ($C_{ph}$-11), 124.52 ($C_{Acri}$-4, $C_{Acri}$-5), 122.20 ($C_{Acri}$-2, $C_{Acri}$-7), 121.55 ($C_{Acri}$-1, $C_{Acri}$-8), 119.91 ($C_{imid}$-4`), 117.85 (C_{Acri}-8a, C_{Acri}-1a), 114.89 (C_{ph}-13, C_{ph}-13`), 114.89 ($C_{imid}$-5`), 56.34 (N-**CH$_2$**), 55.26 (Ar-OCH_3). Anal. calcd. for $C_{25}H_{20}BrN_3O_2$: C 63.30, H 4.25, N 8.86; Found: C 63.40, H 4.20, N 8.80%. HRMS (ESI^+) *m/z* calcd for $C_{25}H_{20}N_3O_2[M–Br]^+$: 394.1551 (100%), 395.1584 (27%), 396.1618 (4%); found: 394.1541 (90%), 395.1574 (29%), 396.1618 (3%).

1-(acridinyl)-3-(1-oxo-1-phenylpropanyl)-imidazolium bromide (26)

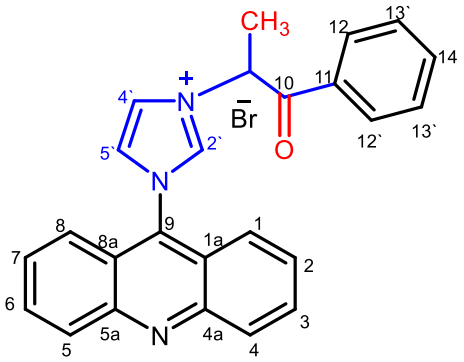

2-Bromopropiophenone (160 mg, 0.75mmol) and compound **6a** (61 mg, 0.25mmol) were reacted according to method **B** to give Compound **26** (52 mg, 85 %) as a yellow solid. mp: 240-245 ºC. FTIR: ν (ATR, cm^{-1}) 3075 $(C–H)_{Ar}$, 2985$(C–H)_{Aliph}$, 1683(C=N), 1635, 1580, 1470$(C=C)_{Ar}$, 1425, 1230(C-O), 815 (C-Br). ^{1}H NMR (400 MHz, DMSO-d_6): δ (ppm) 10.09(s,1H, NCHN, H_{imid}-2`), 8.42-8.35 (m, 4H, H-1, H-8, H-4, H-5), 8.17-8.15 (d, 2H, H-3, H-6), 8.06-8.01 (m, 2H, H-4`, H-5`), 7.88-7.76 (m, 3H, H-14, H-12, H-12`), 7.70-7.64 (m, 4H, H-2, H-7, H-13, H-13`), 6.83-6.85 (m, 1H, **N-CH**), 1.93-1.91 (m, 3H, **$CH_3$**). $^{13}C$ NMR (100 MHz, DMSO-$d_6$): δ (ppm) 195.20 (**C=O**, C-10), 149.05 ($C_{Acri}$-4a, $C_{Acri}$-5a), 140.18($C_{Acri}$-9), 136.06 ($C_{imid}$-2`), 135.28 (C_{ph}-14), 134.00 (C_{ph}-11), 133.36 (C_{Acri}-3, C_{Acri}-6), 132.21 (C_{Acri}-4, C_{Acri}-5), 130.08 (C_{Acri}-12), 129.82 (C_{ph}-12`), 129.72 ($C_{ph}$-13), 129.64($C_{ph}$-13`), 125.38(C_{Acri}-2, C_{Acri}-7), 124.72 (C_{Acri}-1, C_{Acri}-8), 122.63 (C_{imid}-4`), 122.10 ($C_{Acri}$-8a, $C_{Acri}$-1a), 117.85 ($C_{imid}$-5`), 61.63 (**N-CH**), 18.55 (**CH_3**). Anal. calcd for $C_{25}H_{20}BrN_3O$: C 65.51, H 4.40, N 9.17 %; found: C 65.55, H 4.44, N 9.20%. HRMS (ESI^+) *m/z* calcd for $C_{25}H_{20}N_3O$ $[M–Br]^+$ 378.1606 (100 %), 379.1640 (27 %), 380.1673 (3 %); found: 378.1606 (100 %), 379.1637 (27 %), 380.1668 (4 %).

1-(acridin-9-yl)-3-methyl-benzo[d]imidazolium chloride (27)

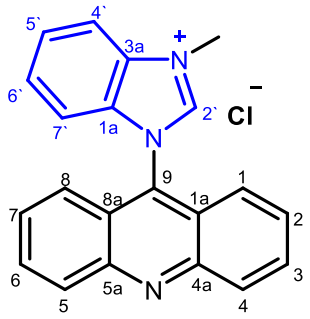

A suspension of 9-chloroacridine **4a** (337 mg, 1.58 mmol) and 1-methylbenzimidazole (238 mg, 1.80 mmol) were reacted according to method **A** to give Compound **27** (435 mg, 80%) as a yellow powder. mp = 280-290 ºC. FTIR: ν (ATR, cm^{-1}) 3023 $(C–H)_{Ar}$, 2891 $(C-H)_{Aliph}$, 1645 (C=N), 1550, 1491, 1466 (C=C), 1261(C-N). ^{1}H NMR (400 MHz, DMSO-d_6): δ (ppm) 10.33 (s, 1H, NCHN, H_{bim}-2`), 8.43 (d, 2H, $J_d$ = 8.0 Hz, H-1, H-8), 8.33 (d, 1H, $J_d$ = 8.0 Hz, $H_{bim}$-4`), 8.06-8.02 (m, 2H, H-4, H-5), 7.84 (t, 1H, J_t = 8.0 Hz, H_{bim}-5`), 7.73-7.71 (m, 4H, H-2, H-7, H-3, H-6), 7.59 (t, 1H, $J_t$ = 8.0 Hz, $H_{bim}$-6`), 7.30 (d, 1H, J_d = 8.0 Hz, H_{bim}-7`), 4.32 (s, 3H, **$CH_3$**). $^{13}C$ NMR (100 MHz, DMSO-$d_6$): δ (ppm) 149.42 ($C_{Acri}$-4a, $C_{Acri}$-5a), 145.25 ($C_{bim}$-2`), 133.81 (C_{Acri}-9), 133.20 (C_{bim}-3a), 132.68 (C_{Acri}-3, C_{Acri}-6), 132.06 (C_{bim}-1a), 130.25 (C_{Acri}-4, C_{Acri}-5), 129.44 (C_{Acri}-2, C_{Acri}-7), 128.28 (C_{Acri}-1, C_{Acri}-8), 127.84 (C_{bim}-5`), 122.92 ($C_{bim}$-6`), 122.74 (C_{Acri}-1a, C_{Acri}-8a), 114.89 (C_{bim}-7`), 113.82 ($C_{bim}$-4`), 34.79 (**N-CH_3**). Anal. calcd. for $C_{21}H_{16}ClN_3$: C 72.93, H 4.66, N 12.15 %; found: C 72.81, H 4.61, N 12.31%. HRMS (ESI^+) *m/z* calcd for $C_{21}H_{16}N_3[M–Cl]^+$: 310.1344 (100%), 311.1378 (23%), 312.1411 (3%), found: 310.1340 (100%), 311.1370 (21%), 312.1397 (3%).

1-(acridin-9-yl)-3-ethyl-benzo[d]imidazolium bromide (28)

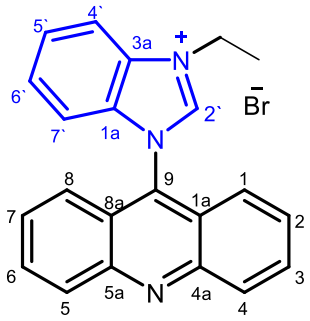

A solution of 9-(1-benzoimidazolyl) acridine **6c** (740 mg, 0.25 mmol) and bromoethane (820 mg, 0.6 mL, 0.75 mmol) were reacted according to method **B** to give compound **28** (710 mg, 72%) as a yellow solid. mp = 290-300 ºC. FTIR: ν (ATR, cm^{-1}) 3109 $(C–H)_{Ar}$, 2948 $(C-H)_{Aliph}$, 1628 (C=N), 1552, 1471, 1346 (C=C), 1240 (C-N). ^{1}H NMR (400 MHz, DMSO-d_6): δ (ppm) 10.44 (s, 1H, NCHN, H_{bim}-2`), 8.44 (d, 2H, $J_d$ = 8.0 Hz, H-1, H-8), 8.39 (d, 1H, $J_d$ = 8.0 Hz, $H_{bim}$-4`), 8.06-8.02 (m, 2H, H-4, H-5), 7.84 (t, 1H, J_t = 8.0 Hz, H_{bim}-5`), 7.74-7.73 (m, 4H, H-2, H-7, H-3, H-6), 7.60 (t, 1H, $J_t$ = 8.0 Hz, $H_{bim}$-6`), 7.33 (d, 1H, J_d = 8.0 Hz, H_{bim}-7`), 4.77-4.72 (m, 2H, **N-CH$_2$**), 1.76 (t, 3H, **CH$_3$**). $^{13}C$ NMR (100 MHz, DMSO-$d_6$): δ (ppm) 149.42 ($C_{Acri}$-4a, $C_{Acri}$-5a), 144.20 ($C_{bim}$-2`), 133.88 (C_{Acri}-9), 133.49 (C_{bim}-3a), 131.97(C_{Acri}-3, C_{Acri}-6), 131.92 (C_{bim}-1a), 130.15 (C_{Acri}-4, C_{Acri}-5), 129.38 (C_{Acri}-2, C_{Acri}-7), 128.32 (C_{Acri}-1, C_{Acri}-8), 127.78 (C_{bim}-5`), 121.88 ($C_{bim}$-6`), 121.69 (C_{Acri}-1a, C_{Acri}-8a), 114.93 (C_{bim}-7`), 113.88 ($C_{bim}$-4`), 43.76 (N-**CH$_2$**), 14.03 (NCH$_2$**CH$_3$**). Anal. calcd. for $C_{22}H_{18}BrN_3$: C 65.36, H 4.49, N 10.39 %; found: C 65.46, H 4.54, N 10.45 %. HRMS (ESI^+) *m/z* calcd. for $C_{22}H_{18}N_3[M–Br]^+$: 324.1496 (100%), 325.1529 (24%), 326.1563 (3%), found: 324.1492 (100%), 325.1520 (28%), 326.1547 (2%).

1-(acridin-9-yl)-3-benzyl-benzo[d]imidazolium bromide (29)

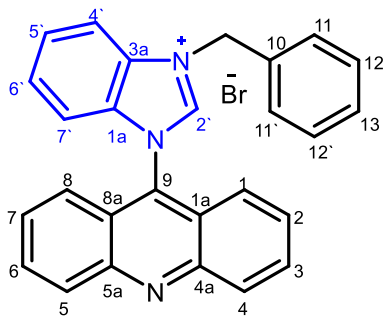

A solution of **6c** (740 mg, 0.25 mmol) and benzyl bromide (0.9 mL, 1.3 g, 0.75 mmol) were reacted according to method **B** to give compound **29** (930 mg, 80 %) as a yellow solid. mp = 230-240 ºC. FTIR: ν (ATR, cm^{-1}) 3138 $(C–H)_{Ar}$, 2989 $(C-H)_{Aliph}$, 1630 (C=N), 1538, 1471, 1386 (C=C), 1268 (C-N). UV-vis λ_{max}=389 nm. ^{1}H NMR (400 MHz, DMSO-d_6): δ (ppm) 10.45 (s, 1H, NCHN, H_{bim}-2`), 8.43(d, 2H, $J_d$ = 8.0 Hz, H-1, H-8), 8.25 (d, 1H, $J_d$ = 8.0 Hz, $H_{bim}$-4`), 8.06-8.02 (m, 2H, H-4, H-5), 7.81 (t, 1H, J_t = 8.0 Hz, H_{bim}-5`), 7.77-7.72 (m, 4H, H-2, H-7, H-3, H-6), 7.67 (d, 2H, $J_d$ = 8.0 Hz, $H_{ph}$-11, $H_{ph}$-11`), 7.61(t, 1H, J_t = 8.0 Hz, H_{bim}-6`), 7.52 (m, 3H, $H_{ph}$-12, $H_{ph}$-12`, H_{ph}-13), 7.36 (d, 1H, J_d = 8.0 Hz, H_{bim}-7`), 6.00 (s, 2H, **N-CH$_2$**). $^{13}$C NMR (100 MHz, DMSO-$d_6$): δ (ppm) 149.39 ($C_{Acri}$-4a, $C_{Acri}$-5a), 145.02 ($C_{bim}$-2`), 133.76 (C_{Acri}-9), 133.68(C_{ph}-10), 133.60 (C_{bim}-3a), 132.05 (C_{Acri}-3, C_{Acri}-6), 131.84 (C_{ph}-11, C_{ph}-11`), 130.28 ($C_{Acri}$-4, $C_{Acri}$-5), 129.74 ($C_{ph}$-12, $C_{ph}$-12`), 129.59 (C_{bim}-1a), 129.41 (C_{Acri}-2, C_{Acri}-7), 128.68 (C_{Acri}-1, C_{Acri}-8), 128.20 (C_{bim}-5`, $C_{bim}$-6`), 122.73 (C_{ph}-13), 122.64 (C_{Acri}-1a, C_{Acri}-8a), 115.19 (C_{bim}-7`), 114.25 ($C_{bim}$-4`), 51.65 (**N-CH$_2$**). Anal. calcd. for $C_{27}H_{20}BrN_3$: C 69.53, H 4.32, N 9.01 %; found: C 69.49, H 4.35, N 9.11%. HRMS (ESI$^+$) *m/z* calcd. for $C_{27}H_{20}N_3[M–Br]^+$: 386.1652 (100%), 387.1686 (29%), 388.1719 (4%), found: 386.1638 (100%), 387.1668 (31%), 388.1405 (6%).

1-(6-chloro-2-methoxyacridinyl)-3-methylbenzoimidazolum chloride (30)

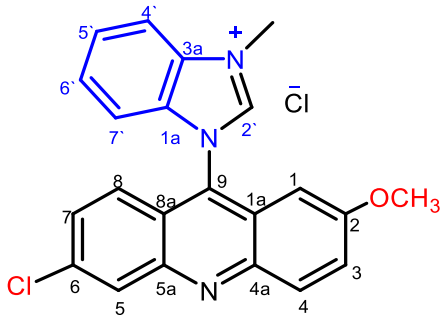

A suspension of 6,9-dichloro-2-methoxyacridine **4c** (439 mg, 1.6 mmol) and 1-methyl benzimidazole (238 mg, 1.80 mmol) were reacted according to method **A** to give compound **30** (520 mg, 80%) as a yellow powder. mp = 280-285 ºC. FTIR: ν (ATR, cm^{-1}) 3025$(C–H)_{Ar}$, 2892 $(C-H)_{Aliph}$, 1645 (C=N), 1550, 1491, 1466(C=C), 1261 (C-N). ^{1}H NMR (400 MHz, DMSO-d_6): δ (ppm) 10.32 (s, 1H, NCHN, H_{bim}-2`), 8.45 (d, 1H, $J_d$ = 4.0 Hz, H-8 ), 8.36-8.30 (m, 2H, H-5, $H_{bim}$-4`), 7.85 (t, 1H, J_t = 8.0 Hz, H-4), 7.76-7.61 (m, 4H, H-3, H_{bim}-5`, $H_{bim}$-6`, H_{bim}-7`), 7.35 (d, 1H, $J_d$ = 8.0 Hz, H-7), 6.82 (d, 1H, $J_d$ = 1.0 Hz, H-1), 4.33 (s, 3H, **N-$CH_3$**), 3.74 (s, 3H, **$OCH_3$**). $^{13}C$ NMR (100 MHz, DMSO-$d_6$): δ (ppm) 159.80 ($C_{Acri}$-2), 147.53 ($C_{Acri}$-4a), 147.23 ($C_{Acri}$-5a), 145.12 ($C_{bim}$-2`), 135.36 (C_{Acri}-9), 132.76(C_{Acri}-6), 132.68 (C_{bim}-3a), 132.14 (C_{Acri}-4), 131.75 (C_{Acri}-5), 129.91 (C_{Acri}-7), 128.38 (C_{bim}-1a), 128.18 (C_{bim}-5`), 127.80 ($C_{bim}$-6`), 127.51 (C_{Acri}-8), 124.68 (C_{bim}-8a), 124.22 (C_{Acri}-3), 121.64 (C_{bim}-1a), 114.88 (C_{bim}-7`), 113.90 ($C_{bim}$-4`), 98.73(C_{Acri}-1), 56.75 (**OCH_3**), 34.84 (**N-CH_3**). Anal. calcd. for $C_{22}H_{17}Cl_2N_3O$: C 64.40, H 4.18, N 10.24 %; found: C 64.33, H 4.21, N 10.29%. HRMS (ESI^+) *m/z* calcd. for $C_{22}H_{17}ClN_3O[M–Cl]^+$: 374.1055 (100%), 375.1089 (24%), 376.1026 (32%); found: 374.1044 (100%), 375.1070 (20%), 376.1020 (29%).

Ag [1-acridinyl-3-hexylimidazolydiene]2(PF6) (31)

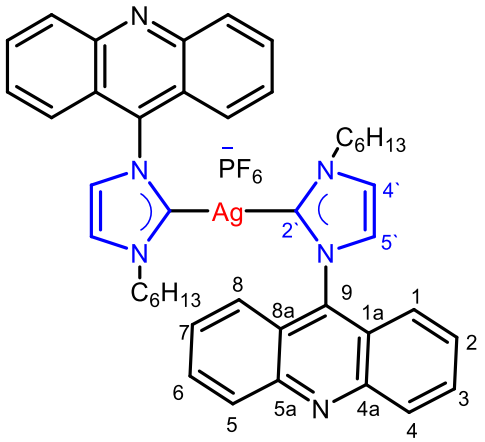

Compound **31** was prepared according to general method **3.3.4**. A suspension of compound **7** ($C_{22}H_{24}N_3PF_6$, 457 mg, 1 mmol) and Ag_2O (280 mg, 1.2 mmol) was reacted to give compound **31** (575 mg, 64%) as a yellow solid. mp: 305-310 ºC. FTIR: ν (ATR, cm^{-1}) 3060 $(C–H)_{Ar}$, 2936 $(C-H)_{Aliph}$, 1615 (C=N), 1568, 1479, 1440 (C=C), 1283(C-N). ^{1}H NMR (400 MHz, Acetonitrile-d_3): δ (ppm) 8.17 (d, 4H, J_d= 9 Hz), 7.83-7.79 (m, 4H), 7.54-7.50 (m, 6H), 7.44 (d, 2H, J_d= 2 Hz), 7.37 (d, 4H, J_d= 9.5 Hz), 3.92 (s, 4H, **N-CH₂**), 1.67-1.69 (m, 4H, **CH₂**), 1.23-1.07 (m, 12H, **CH₂**), 0.86 (t, 6H, **CH₃**). ^{13}C NMR (100 MHz, Acetonitrile-d_3): δ (ppm) 183.05 (**C2`-Ag**), 148.93 ($C_{Acri}$-4a, $C_{Acri}$-5a), 140.51 ($C_{Acri}$-9, C-N), 131.26 ($C_{Acri}$-4, $C_{Acri}$-5), 129.61 ($C_{Acri}$-3, $C_{Acri}$-6), 128.10 ($C_{Acri}$-2, $C_{Acri}$-7), 124.85 ($C_{Acri}$-1, $C_{Acri}$-8), 122.52 ($C_{imid}$-5`), 122.34 (C_{Acri}-8a, C_{Acri}-1a), 121.60 (C_{imid}-4`), 52.7 (**N-CH₂**), 32.0(**CH₂**), 31.65 (**CH₂**), 26.71 (**CH₂**), 23.28 (**CH₂**), 14.37(**-CH₃**). ^{19}F NMR (376 MHz, Acetonitrile-d_3): δ (ppm) -72.68 (d, $^1J_{P,F}$ = 705 Hz). ^{31}P NMR (162 MHz, Acetonitrile-d_3): δ(ppm) -144.02 (septet, $^1J_{P,F}$ = 705 Hz). HRMS (ESI$^+$) *m/z* calcd. for $C_{44}H_{46}AgN_6$ $[M-PF_6]^+$ m/z: 765.2835 (100%), 766.2868 (47%), 767.2832 (92%), 768.2865 (44%), 769.2899 (10%); found: 765.2834 (92%), 766.2863 (47%), 767.2838 (100%), 768.2865 (44%), 769.2899 (10%).

Ag[1-(2-methoxyacridinyl)-3-methylimidazolydiene]2(PF6) (32)

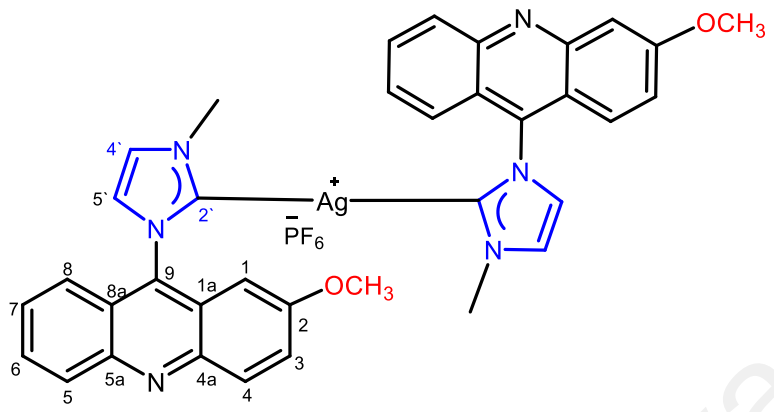

Compound **32** was obtained according to the general procedure **3.3.4** described using compound **9** ($C_{18}H_{16}ON_3PF_6$, 435 mg, 1 mmol) to furnish compound **32** (555 mg, 67%) as a yellow powder. mp: 190-200 ºC. FTIR: (ATR, cm^{-1}) 3080 $(C–H)_{Ar}$, 2948 $(C-H)_{Aliph}$, 1632 (C=N), 1566, 1479, 1430 (C=C), 1280 (C-N), 1232 (C-O). ^{1}H NMR (400 MHz, Acetonitrile-d_3): δ (ppm) 7.99 (d, 2H, J_d= 8 Hz, CHCH), 7.90 (d, 2H, J_d = 8 Hz), 7.70-7.66 (dt, 2H, Jt = 9 Hz, J_d =1 Hz, CHCH), 7.61-7.60 (d, 2H, J_d = 8 Hz), 7.50 (t, 2H, J_t =9 Hz, J_d =1 Hz, Acri-H), 7.42 (d, 2H, J_d= 1.2 Hz, Acri-H), 7.37-7.33 (m, 4H, Acri-H), 6.50 (d, 2H, J_d= 3 Hz, Acri-H), 3.98 (s, 6H, **OCH_3**), 3.77 (s, 6H, **N-CH_3**). ^{13}C NMR (100 MHz, Acetonitrile-d_3): δ (ppm) 184.22 (**C2`-Ag**), 158.61 ($C_{Acri}$-2), 147.53 ($C_{Acri}$-4a), 146.77 ($C_{Acri}$-5a), 139.15 ($C_{Acri}$-9), 132.13 ($C_{Acri}$-4), 130.84 ($C_{Acri}$-6), 130.32 ($C_{Acri}$-5), 128.98 ($C_{Acri}$-7), 127.07 ($C_{Acri}$-8), 125.31 ($C_{Acri}$-8a), 124.88 ($C_{imid}$-5`), 124.74 (C_{Acri}-3), 123.94 (C_{Acri}-1a), 122.77(C_{imid}-4`), 98.56 (C_{Acri}-1), 56.69 (**OCH_3**), 39.45 (**N-CH_3**). ^{19}F NMR (376 MHz, Acetonitrile-d_3): δ (ppm) -72.68 (d, $^1J_{P,F}$ = 705 Hz). ^{31}P NMR (162 MHz, Acetonitrile-d_3): δ(ppm)-144.02 (septet,$^1J_{P,F}$ = 705 Hz). HRMS (ESI^+) *m/z* calcd. for $C_{36}H_{30}AgN_6O_2[M-PF_6]^+$:685.1481 (100%), 686.1515 (38%), 687.1478 (92%), 688.1511 (36%), 689.1545 (7%); found 685.1496 (95%), 686.1525 (37%), 687.1499 (100%), 688.1524 (36%), 689.1551 (6%).

Ag [1-(2-methoxyacridinyl)-3-butylimidazolydiene]2(PF6) (33)

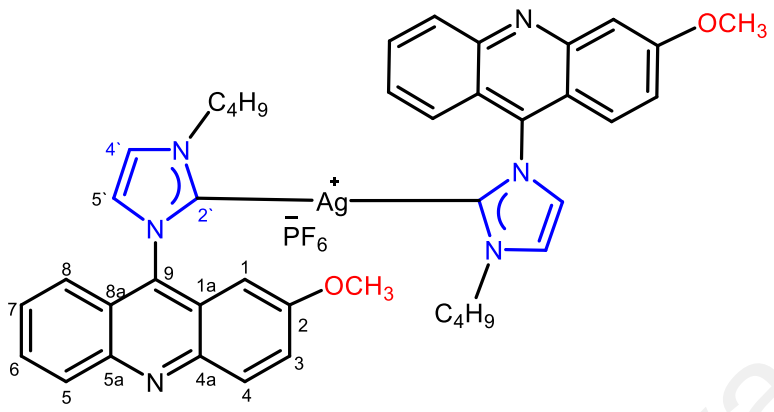

Compound **33** was obtained according to the general procedure **3.3.4** described using compound **10** ($C_{21}H_{22}ON_3PF_6$, 477 mg, 1 mmol) to provide compound **33** (580 mg, 64 %) as a yellow powder. mp: 225-230 ºC. FTIR: ν (ATR, cm^{-1}) 3083 $(C–H)_{Ar}$, 2962 $(C-H)_{Aliph}$, 1631 (C=N), 1562, 1478, 1428 (C=C), 1235(C-N), 1216(C-O). ^{1}H NMR (400 MHz, Acetonitrile-d_3) δ (ppm) 7.99 (d, 2H, J_d= 8 Hz), 7.86 (d, 2H, J_d= 8 Hz), 7.68 (t, 2H, J_t= 8 Hz), 7.52-7.46 (m, 4H), 7.38 (s, 2H), 7.32-7.25 (m, 4H), 6.29 (s, 2H), 3.98 (s, 4H, **N-CH$_2$**), 3.60 (s, 6H, **O-CH$_3$**), 1.65 (s, 4H, CH_2), 1.06-1.02 (s, 4H, CH_2), 0.79 (t, 3H, CH_3). ^{13}C NMR (100 MHz, Acetonitrile-d_3): δ (ppm) 187.42 (**C2`-Ag**), 159.55 ($C_{Acri}$-2), 147.41 ($C_{Acri}$-4a), 147.19 ($C_{Acri}$-5a), 138.54 ($C_{Acri}$-6), 135.69 ($C_{Acri}$-9), 131.93 ($C_{Acri}$-4), 129.41 ($C_{Acri}$-5), 128.59 ($C_{Acri}$-7), 127.27 ($C_{Acri}$-8), 125.28 ($C_{imid}$-5`), 124.39 (C_{imid}-4`), 124.26 (C_{Acri}-3), 123.46 (C_{Acri}-8a), 121.87 (C_{Acri}-9a), 97.74 (C_{Acri}-1), 56.38 (O-**CH$_3$**), 52.38 (N-**CH$_2$**), 33.58 (**CH$_2$**CH_2CH_2), 20.18 (CH_2**CH$_2$**CH_3), 13.80 (CH_2**CH$_3$**). ^{19}F NMR (376 MHz, Acetonitrile-d_3): δ (ppm) -72.68 (d, $^1J_{P,F}$ = 705 Hz). ^{31}P NMR (162 MHz, Acetonitrile-d_3): δ(ppm) -144.02 (septet,$^1J_{P,F}$ = 705 Hz). HRMS(ESI$^+$) *m/z* calcd. for $C_{42}H_{42}AgN_6O_2$ $[MPF_6]^+$: 769.2420 (100%), 770.2454 (45%), 771.2417 (92%), 772.2450 (42%), 773.2484 (9%), 774.2517 (1%); found: 769.2425 (92%), 770.2454 (50%), 771.2430 (100%), 772.2452 (45%), 773.2483 (9%), 774.2506 (1%).

Ag[1-(6-chloro-2-methoxyacridinyl)-3-methylimidazolydiene]2(PF6) (34)

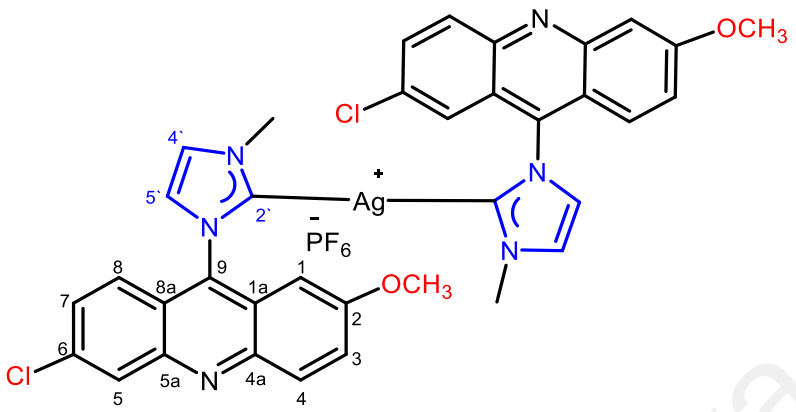

Compound **34** was obtained according to the general procedure **3.3.4** described using compound **12** ($C_{18}H_{15}ON_3ClPF_6$, 470 mg, 1 mmol) to provide compound **34** (580 mg, 64%) as a yellow powder. mp: 290-300 ºC. FTIR: ν(ATR, cm^{-1}) 3163$(C–H)_{Ar}$, 2953 $(C-H)_{Aliph}$, 1630 (C=N), 1566, 1476, 1422 (C=C), 1278 (C-N), 1238 (C-O). ^{1}H NMR (400 MHz, Acetonitrile-d_3): δ (ppm) 7.57 (d, 4H, J_d= 4 Hz, CHCH), 7.49 (d, 2H, J_d= 8 Hz, NCHN), 7.32 (s, 2H, H_{imid}), 7.24 (d, 2H, J_d = 8 Hz), 7.15-7.10 (m, $4H_{Acri}$), 6.26 (s, 2H), 4.05 (s, 6H, **OCH_3**), 3.67 (m, 6H, **CH_3**). ^{13}C NMR (100 MHz, Acetonitrile-d_3): δ (ppm) 184.81 (**C2`-Ag**), 159.88 ($C_{Acri}$-2), 147.23 ($C_{Acri}$-4a), 147.04 ($C_{Acri}$-5a), 139.54 ($C_{Acri}$-6), 136.26 ($C_{Acri}$-9), 131.86 ($C_{Acri}$-4), 129.63 ($C_{Acri}$-5), 128.41 ($C_{Acri}$-7), 127.88 ($C_{Acri}$-8), 126.76 ($C_{imid}$-5`), 125.20 (C_{imid}-4`), 125.01 (C_{Acri}-3), 124.82 (C_{Acri}-8a), 122.48 (C_{Acri}-1a), 98.63 (C_{Acri}-1), 56.74 (**O-CH_3**), 39.63(**N-CH_3**). ^{19}F NMR (376 MHz, Acetonitrile-d_3): δ (ppm) -72.68 (d, $^1J_{P,F}$ = 705 Hz). ^{31}P NMR (162 MHz, Acetonitrile-d_3): δ (ppm) -144.02 (septet,$^1J_{P,F}$ =705 Hz). HRMS (ESI^+) *m/z* calcd. for $C_{36}H_{28}AgCl_2N_6O_2[M-PF_6]^+$: 753.0697 (100%), 754.0730 (38%), 755.0693 (92.%), 756.0701 (24%), 757.0664 (59%), 758.0697 (23%), 759.0634 (10%), 760.0668 (4%); found:753.0678 (92%), 754.0709 (38%), 755.0670 (100%), 756.0698 (25%), 757.0657 (59%), 758.0679 (23%), 759.0652 (10%). 760.0633 (4%).

Ag[1-(6-chloro-2-methoxyacridinyl)-3-ethylimidazolydiene]2(PF6) (35)

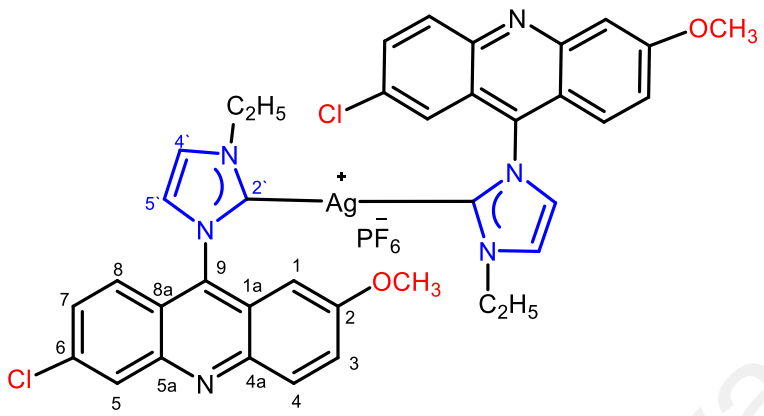

Compound **35** was obtained according to the general procedure **3.3.4** described using compound **13** ($C_{19}H_{17}ClN_3OPF_6$, 484 mg, 1 mmol) to provide compound **35** (600 mg, 65 %) as a yellow powder. mp: 230-240 ºC. FTIR: ν(ATR, cm^{-1}) 3160$(C–H)_{Ar}$, 2963 $(C-H)_{Aliph}$, 1633 (C=N), 1560, 1478, 1422 (C=C), 1280 (C-N), 1235 (C-O). ^{1}H NMR (400 MHz, DMSO-d_6): δ (ppm) 8.23 (s, 2H, H-8), 8.11 (d, 2H, J_d= 8 Hz, H-5), 7.91 (s, 2H, H-4), 7.82 (s, 2H), 7.58-7.55 (m, 4H, Acri-H), 7.28 (d, 2H, J_d= 12 Hz), 6.34 (s, 2H, H-1), 3.95 (s, 4H, N-C**H₂**), 3.67 (s, 6H, O-C**H₃**), 1.2(s, 6H, **CH₃**). ^{13}C NMR (100 MHz, DMSO-d_6): δ (ppm) 184.22 (**C2`-Ag**), 158.85 ($C_{Acri}$-2), 148.29 ($C_{Acri}$-4a), 147.0 ($C_{Acri}$-5a), 146.81 ($C_{Acri}$-6), 138.68 ($C_{Acri}$-9), 135.01 ($C_{Acri}$-4), 131.79 ($C_{Acri}$-5), 129.23 ($C_{Acri}$-7), 128.09 ($C_{Acri}$-8), 126.96 ($C_{imid}$-5`), 125.27 (C_{imid}-4`), 124.49 (C_{Acri}-3), 123.08 (C_{Acri}-8a), 121.41 (C_{Acri}-1a), 98.02 (C_{Acri}-1), 56.07 (O-**C**H₃), 46.76 (**N-CH₂**), 17.14 (**C**H₃). ^{19}F NMR (376 MHz, Acetonitrile-d_3): δ (ppm) -72.68 (d, $^1J_{P,F}$ = 705 Hz). ^{31}P NMR (162 MHz, Acetonitrile-d_3): δ(ppm) -144.02 (septet,$^1J_{P,F}$ = 705 Hz). HRMS (ESI$^+$) *m/z* calcd. for $C_{38}H_{32}AgCl_2N_6O_2[M-PF_6]^+$: 781.1015 (100%), 782.1048 (41%), 783.1011 (92%), 784.1019 (26%), 785.0982 (59%), 786.1015 (24%), 787.0952 (9%), 788.0986 (4%); found: 781.1015 (92%), 782.1043 (38%), 783.1010 (100%), 784.1033 (41%), 785.0994 (59%), 786.1015 (24%), 787.0993 (9%), 788.0986 (4%).

Ag[1-(6-chloro-2-methoxyacridinyl)-3-butylimidazolydiene]2(PF6) (36)

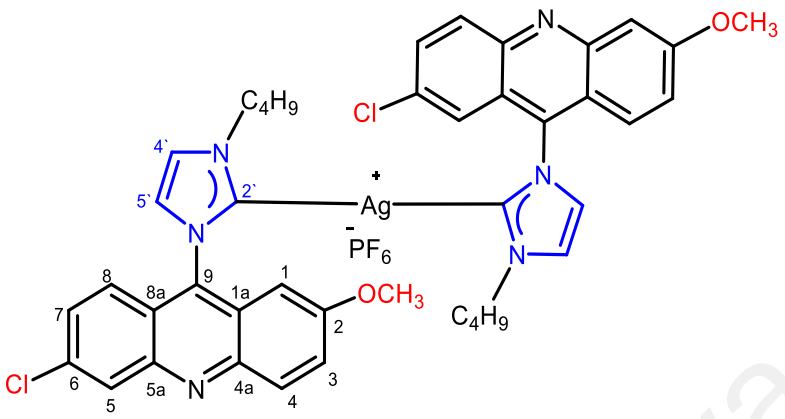

Compound **36** was obtained according to the general procedure **3.3.4** described using compound **14** ($C_{21}H_{21}ClN_3OPF_6$, 512 mg, 1 mmol) to furnish compound **36** (610 mg, 62 %) as a yellow powder. mp: 235-245 ºC. FTIR: ν (ATR, cm^{-1}) 3141, 3094 $(C–H)_{Ar}$, 2945 $(C-H)_{Aliph}$, 1632 (C=N), 1562, 1474, 1422(C=C), 1280(C-N), 1234(C-O). ^{1}H NMR (400 MHz, Acetonitrle-d_3): δ (ppm) 7.88 (sb, 2H), 7.76 (d, 2H, J_d= 8 Hz), 7.49 (s, 2H), 7.49-7.27 (m, 6H), 7.13 (sb, 2H), 6.12 (s, 2H), 3.97 (sb, 4H, **N-CH$_2$**), 3.55 (s, 6H, **O-CH$_3$**), 1.64 (s, 4H, **CH$_2$**), 1.05-102 (m, 4H, **CH$_2$**), 0.81 (t, 6H, **CH$_3$**). ^{13}C NMR (100 MHz, Acetonitrle-d_3): δ (ppm) 159.75 (C_{Acri}-2), 147.61 (C_{Acri}-4a), 147.40 (C_{Acri}-5a), 138.74 (C_{Acri}-6), 135.89 (C_{Acri}-9), 132.13(C_{Acri}-4), 129.6 (C_{Acri}-5), 128.79 (C_{Acri}-7), 127.47 (C_{Acri}-8), 125.48 (C_{imid}-5`), 124.59 ($C_{imid}$-4`), 124.46 (C_{Acri}-3), 123.67 (C_{Acri}-8a), 122.07 (C_{Acri}-1a), 97.94 (C_{Acri}-1), 56.41 (O-**CH$_3$**), 52.58 (N-**CH$_2$**CH$_2$), 33.78 (**CH$_2$**CH$_2$ CH$_2$), 20.38 (CH$_2$**CH$_2$**CH$_3$), 14.00 (CH$_2$**CH$_3$**). ^{19}F NMR (376 MHz, Acetonitrile-d_3): δ (ppm) -72.68 (d, $^1J_{P,F}$ = 705 Hz). ^{31}P NMR (162 MHz, Acetonitrile-d_3): δ(ppm) -144.02 (septet,$^1J_{P,F}$ = 705 Hz). HRMS (ESI$^+$) *m/z* calcd for $C_{42}H_{40}AgCl_2N_6O_2[M-PF_6]^+$: 837.1641 (100%), 838.1674 (45%), 839.1637 (92%), 840.1659 (42%), 841.1623 (59%), 842.1642 (27%), 843.1624 (6%), 844.1626 (4.3%); found: 837.1640 (92 %), 838.1670 (35%), 839.1636 (100%), 840.1671 (42%), 841.1608 (59%), 842.1641 (27%), 843.1675 (6%), 844.1612 (4%).

Ag[1-acridinyl-3-(4-methylbenzylimidazolydiene)]2(PF6) (37)

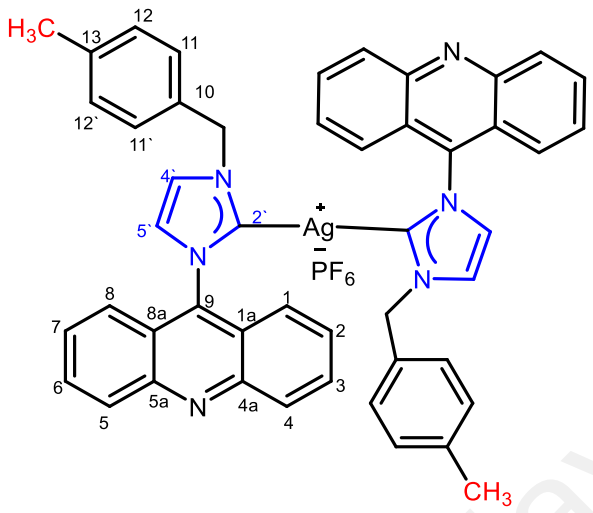

Compound **37** was obtained according to the general procedure **3.3.4** described using compound **16** ($C_{24}H_{20}N_3PF_6$, 495 mg, 1 mmol) to provide compound **37** (595 mg, 64%) as a yellow powder. mp: 220-230 ºC. FTIR: ν (ATR, cm^{-1}) 3055$(C–H)_{Ar}$, 2948 $(C-H)_{aliph}$, 1632 (C=N), 1566, 1488, 1439 (C=C), 1282 (C-O). ^{1}H NMR (400 MHz, Acetonitrile-d_3): δ (ppm) 8.01 (d, 4H, J_d= 8 Hz), 7.72 (t, 4H, J_t=8 Hz), 7.49-7.39 (m, 8H, CHCH), 7.28 (d, 4H, J_d= 8 Hz, Ar-H), 7.12 (d, 4H, J_d= 8 Hz), 7.0 (m, 4H), 5.04 (s, 4H, **N-CH$_2$**), 2.3 (s, 6H, **CH$_3$**). ^{13}C NMR (100 MHz, Acetonitrile-d_3): δ (ppm) 149.34 (C_{Acri}-4a, C_{Acri}-5a), 140.76 (C_{Acri}-9), 139.03 (C_{ph}-13), 133.86 (C_{ph}-10), 131.71 (C_{Acri}-3, C_{Acri}-6), 130.27 (C_{ph}-11, C_{ph}-11`), 130.15 ($C_{ph}$-12, $C_{ph}$-12`), 128.67 (C_{Acri}-1, C_{Acri}-8), 128.19 (C_{Acri}-2, C_{Acri}-7), 125.76 (C_{Acri}-8a, C_{Acri}-1a), 123.43 (C_{Acri}-4, C_{Acri}-5), 123.06 (C_{imid}-4`), 122.72 ($C_{imid}$-5`), 55.38 (**-NCH$_2$**), 20.86 (**Ar-CH$_3$**). ^{19}F NMR (376 MHz, Acetonitrile-d_3): δ (ppm) -72.68 (d, $^1J_{P,F}$ = 705 Hz). ^{31}P NMR (162 MHz, Acetonitrile-d_3): δ(ppm) -144.02 (septet,$^1J_{P,F}$ = 705 Hz). HRMS (ESI$^+$) *m/z* calcd. for $C_{48}H_{38}AgN_6[M-PF_6]^+$: 805.2209 (100%), 806.2242 (51%), 807.2206 (92%), 808.2239 (48.2%), 809.2273 (12.3%); found: 805.2206 (100%), 806.2235 (60%), 807.2212 (95%), 808.2235 (60 %), 809.2261 (15%).

Ag[1-acridinyl-3-(4-bromobenzylimidazolydiene)]2(PF6) (38)

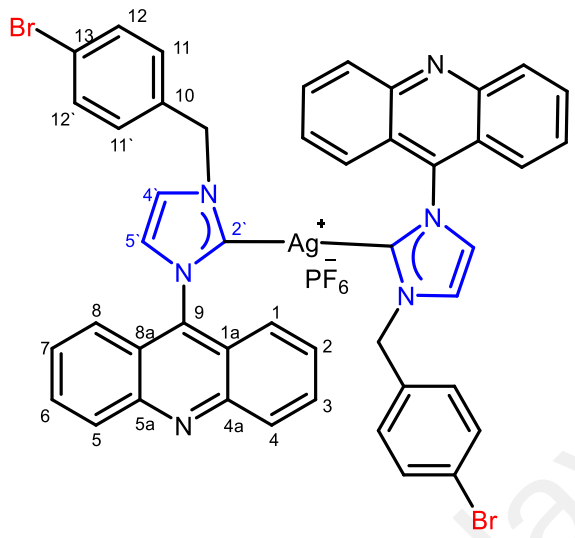

Compound **38** was obtained according to the general procedure **3.3.4** described using compound **17**($C_{23}H_{17}BrN_3PF_6$, 560 mg, 1 mmol) to provide compound **38** (660 mg, 75 %) as a yellow powder. mp: 300-305 ºC. FTIR: ν (ATR, cm^{-1}) 3062 $(C–H)_{Ar}$, 2938 $(C-H)_{Aliph}$, 1614 (C=N), 1566, 1479, 1440 (C=C), 1283 (C-N), 1215 (C-O). ^{1}H NMR (400 MHz, Acetonitrile-d_3): δ (ppm) 8.12 (d, 4H, J_d= 8.5 Hz), 7.78 (t, 4H, J_t= 8 Hz), 7.47-7.41 (m, 12H, Ar-H), 7.30 (d, 4H, J_d= 9.5 Hz), 6.98 (s, 4H), 4.99 (s, 4H, **NCH_2**). ^{13}C NMR (100 MHz, Acetonitrile-d_3): δ (ppm) 148.96 (C_{Acri}-4a, C_{Acri}-5a), 139.93(C_{Acri}-9), 135.54 (C_{ph}-10), 132.05 (C_{ph}-12, C_{ph}-12`), 131.01 ($C_{ph}$-11, $C_{ph}$-11`), 129.69 (C_{Acri}-3, C_{Acri}-6), 129.48 (C_{Acri}-1, C_{Acri}-8), 128.08 (C_{Acri}-2, C_{Acri}-7), 125.31 (C_{ph}-13), 122.86 (C_{Acri}-4, C_{Acri}-5), 122.46 (C_{imid}-4`), 122.14 ($C_{Acri}$-8a, $C_{Acri}$-1a), 122.92 ($C_{imid}$-5`), 54.16 (N**CH_2**). ^{19}F NMR (376 MHz, Acetonitrile-d_3): δ (ppm) -72.68 (d, $^1J_{P,F}$ = 705 Hz). ^{31}P NMR (162 MHz, Acetonitrile-d_3): δ(ppm) -144.02 (septet,$^1J_{P,F}$ = 705 Hz). HRMS (ESI^+) *m/z* calcd. for $C_{46}H_{32}AgBr_2N_6[M-PF_6]^+$: 933.0106 (51%), 934.0140 (26%), 935.0086 (100%), 936.0119 (49%), 937.0082 (92%), 938.0116 (46%), 939.0062 (45%), 940.0032 (22%); found: 933.0103 (40%), 934.0134 (26%), 935.0093 (100%), 936.0121 (49%), 937.0085 (97%), 938.0108 (46%), 939.0083 (40%), 940.0100 (22%).

Ag [1-acridinyl-3-(2-bromobenzylimidazolydiene)]2(PF6) (39)

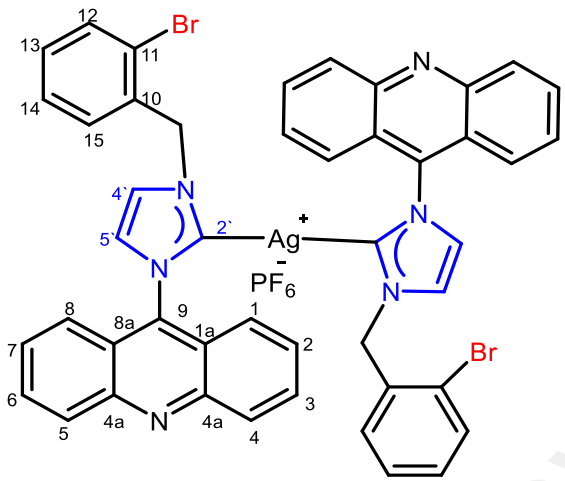

Compound **39** was obtained according to the general procedure **3.3.4** described using compound **18** ($C_{23}H_{17}BrN_3PF_6$, 560 mg, 1 mmol) to provide compound **39** (670 mg, 62%) as a yellow powder. mp: 290-300 ºC. FTIR: ν (ATR, cm^{-1}) 3065$(C–H)_{Ar}$, 2960 $(C-H)_{Aliph}$, 1630 (C=N), 1556, 1480, 1431(C=C), 1213(C-O). ^{1}H NMR (400 MHz, DMSO-d_6): δ (ppm) 8.26 (d, 4H, J_d= 8 Hz, CHCH), 7.95-7.85 (m, 8H, Ar-H), 7.68-7.58 (m, 6H), 7.43-7.31 (m, 10H), 5.40 (s, 4H, **N-CH₂**). ^{13}C NMR (100 MHz, DMSO-d_6): δ (ppm) 148.60 (C_{Acri}-4a, C_{Acri}-5a), 139.91 (C_{Acri}-9), 135.09 (C_{ph}-10), 133.18 (C_{ph}-12, C_{ph}-12`), 131.08 ($C_{Acri}$-3, $C_{Acri}$-6), 130.67 ($C_{ph}$-13), 130.61 ($C_{Acri}$-1, $C_{Acri}$-8), 129.45 ($C_{ph}$-14), 128.50 ($C_{Acri}$-2, $C_{Acri}$-7), 128.17 ($C_{ph}$-11), 125.50 ($C_{Acri}$-4, $C_{Acri}$-5), 123.32 ($C_{imid}$-4`), 123.10 (C_{Acri}-8a, C_{Acri}-1a), 122.09 (C_{imid}-5`), 54.54 (N-**CH₂**). ^{19}F NMR (376 MHz, Acetonitrile-d_3): δ (ppm) -72.68 (d, $^1J_{P,F}$ = 705 Hz). ^{31}P NMR (162 MHz, Acetonitrile-d_3): δ(ppm) -144.02 (septet, $^1J_{P,F}$ = 705 Hz). HRMS (ESI^+) *m/z* calcd. for $C_{46}H_{32}AgBr_2N_6$ $[M-PF_6]^+$:933.0106 (51%), 934.0140 (26%), 935.0086 (100%), 936.0119 (49%), 937.0082 (92%), 938.0116 (46%), 939.0062 (45%), 940.0032 (22%); found: 933.0106 (40%), 934.0135 (26%), 935.0093 (100%), 936.0123 (49%), 937.0085 (97%), 938.0109 (46%), 939.0087 (40%), 940.0099 (22%).

Ag [1-acridinyl-3-(4-Nitrobenzylimidazolydiene)]2(PF6) (40)

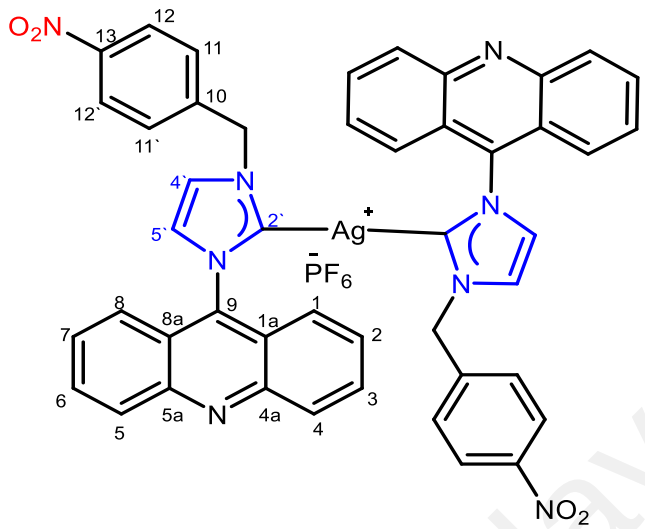

Compound **40** was obtained according to the general procedure **3.3.4** described using compound **19** ($C_{23}H_{17}O_2N_4PF_6$, 562 mg, 1 mmol) to provide compound **40** (680 mg, 70%) as a yellow powder. mp: 240-250 ºC. FTIR: ν (ATR, cm^{-1}) 3048 $(C–H)_{Ar}$, 2956 $(C-H)_{Aliph}$, 1605 (C=N), 1517, 1439 (C=C), 1343, 1283 (C-O). ^{1}H NMR (400 MHz, Acetonitrile-d_3): δ (ppm) 8.09 (d, 4H, J_d= 9 Hz), 8.00 (d, 4H, J_d= 8 Hz), 7.71 (t, 4H, J_t = 7 Hz), 7.50 (s, 2H), 7.43 (t, 6H, J_t = 9 Hz, Ar-H), 7.30 (d, 4H, J_d= 8 Hz), 7.18 (s, 4H), 5.30 (s, 4H, **N-CH$_2$**), ^{13}C NMR (100 MHz, Acetonitrile-d_3):δ (ppm) 149.91 (C_{Acri}-4a, C_{Acri}-5a), 149.02 (C_{Acri}-9), 144.59 (C_{ph}-13, **C-NO$_2$**), 141.12 (C_{ph}-10), 132.34 (C_{Acri}-3, C_{Acri}-6), 130.73 (C_{ph}-11, C_{ph}-11`), 129.37 ($C_{Acri}$-1, $C_{Acri}$-8), 129.25 ($C_{Acri}$-2, $C_{Acri}$-7), 126.75 ($C_{ph}$-12, $C_{ph}$-12`), 125.22 (C_{Acri}-4, C_{Acri}-5), 124.35(C_{imid}-4`), 123.60 ($C_{Acri}$-8a, $C_{Acri}$-1a), 123.33 ($C_{imid}$-5`), 55.14 (**N-CH$_2$**). ^{19}F NMR (376 MHz, Acetonitrile-d_3): δ (ppm) -72.68 (d, $^1J_{P,F}$ = 705 Hz). ^{31}P NMR (162 MHz, Acetonitrile-d_3): δ(ppm) -144.02 (septet,$^1J_{P,F}$ = 705 Hz). HRMS (ESI^+) *m/z* calcd. for $C_{46}H_{32}AgN_8O_4[M-PF_6]^+$: 867.1597 (100%), 868.1631 (49%), 869.1594 (92%), 870.1628 (46%), 871.1661 (11%), 872.1695 (2%); found: 867.1590 (100%), 868.1620 (49%), 869.1595 (80%), 870.1620 (46%), 871.1679 (11%), 872.1693 (2%).

Ag[1-(6-chloro-2-methoxyacridinyl)-3-benzylimidazolydiene]2(PF6) (41)

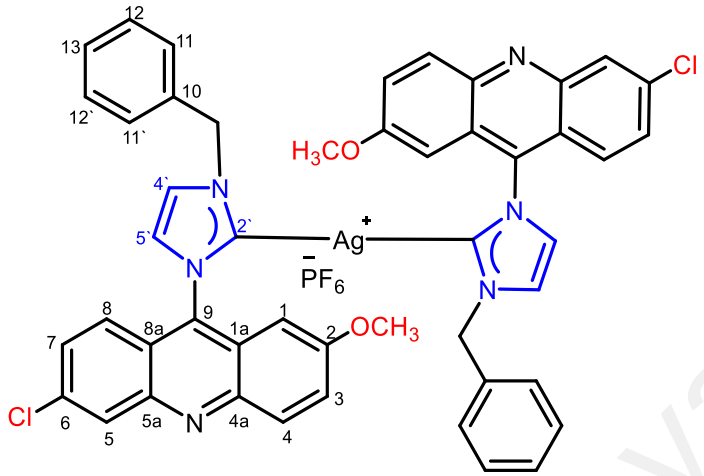

Compound **41** was obtained according to the general procedure **3.3.4** described using compound **22** ($C_{24}H_{19}ON_3ClPF_6$, 546 mg, 1 mmol) to provide compound **38** (650 mg, 62 %) as a yellow powder. mp: 260-270 ºC. FTIR: ν (ATR, cm^{-1}) 3150$(C–H)_{Ar}$, 2954 $(C-H)_{Aliph}$, 1631 (C=N), 1565, 1478, 1424(C=C), 1240 (C-O). ^{1}H NMR (400 MHz, Acetonitrile-d_3):δ (ppm) 7.79 (s, 2H), 7.67 (d, 2H, J_d= 8 Hz), 7.55 (s, 2H, CHCH), 7.39-7.30 (m, 10H, Ar-H), 7.25-7.13 (m, 8H), 6.08 (sb, 2H), 5.31 (s, 4H, **N-CH$_2$**), 3.51 (s, 6H, **OCH$_3$**), ^{13}C NMR (100 MHz, Acetonitrile-d_3): δ (ppm) 160.26 (C_{Acri}-2), 147.80 (C_{Acri}-4a), 147.60 (C_{Acri}-5a), 139.30 (C_{Acri}-6), 138.28 (C_{Acri}-9), 136.51 (C_{ph}-10), 132.46 (C_{Acri}-4), 130.66 (C_{Acri}-5), 130.22 (C_{Acri}-7), 130.04 (C_{ph}-11, C_{ph}-11`), 129.13 ($C_{ph}$-12, $C_{ph}$-12`), 128.84 (C_{ph}-13), 128.07 (C_{Acri}-8), 126.37 (C_{imid}-5`), 125.08 ($C_{imid}$-4`), 124.93 (C_{Acri}-3), 124.77 (C_{Acri}-8a), 122.49 (C_{Acri}-1a), 98.40 (C_{Acri}-1), 56.94 (O-**CH$_3$**), 56.64 (N-**CH$_2$**). ^{19}F NMR (376 MHz, Acetonitrile-d_3): δ (ppm) -72.68 (d, $^1J_{P,F}$ = 705 Hz). ^{31}P NMR (162 MHz, Acetonitrile-d_3): δ(ppm) -144.02 (septet,$^1J_{P,F}$ = 705 Hz). HRMS (ESI$^+$) *m/z* calcd. for $C_{48}H_{36}AgCl_2N_6O_2[M-PF_6]^+$:905.1328 (100%), 906.1361 (51%), 907.1324 (92%), 908.1358 (48%), 909.1295 (59%), 910.1328 (30%); found: 905.1328 (93%), 906.1361 (60%), 907.1324 (100%), 908.1358 (70%), 909.1295 (68%), 910.1328 (39%).

Ag (1-acridinyl-3-methylbenzimidazolydiene)2(PF6) (42)

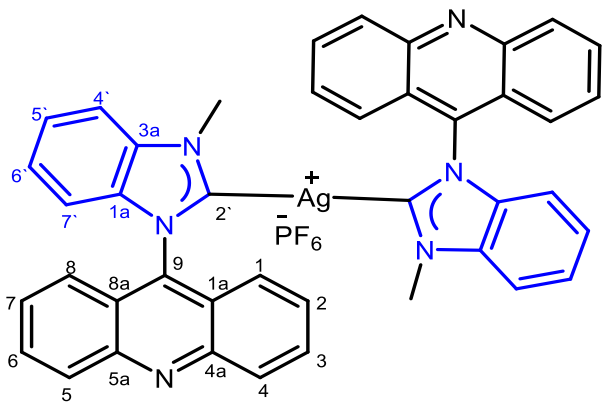

Compound **42** was obtained according to the general procedure **3.3.4** described using compound **27** ($C_{21}H_{16}N_3PF_6$, 460 mg, 1 mmol) to provide compound **42** (560 mg, 63%) as a yellow powder. mp: 290-300 ºC. UV-vis λ_{max}= 411 nm. FTIR: ν (ATR, cm^{-1}) 3065 $(C–H)_{Ar}$, 2957 $(C-H)_{Aliph}$, 1627 (C=N), 1557, 1439, 1391 (C=C), 1214(C-N). ^{1}H NMR (400 MHz, Acetonitrile-d_3): δ (ppm) 8.10 (d, 4H, J_d=8.0 Hz), 7.84 (d, 2H, J_d =8.0 Hz), 7.72 (dt, 4H, J_t =8.0 Hz, J_d = 4.0 Hz), 7.54 (t, 2H, J_t= 8.0 Hz), 7.38 (t, 4H, J_t= 8.0 Hz), 7.30-7.25 (m, 6H), 6.77 (d, 2H, J_d= 8.0 Hz), 4.06 (s, 6H, **CH_3**). ^{13}C NMR (100 MHz, Acetonitrile-d_3): δ (ppm) 192.43 (**C_{bim}-2`-Ag**), 149.95 ($C_{Acri}$-4a, $C_{Acri}$-5a), 139.48 ($C_{Acri}$-9), 136.67 ($C_{bim}$-3a), 135.17 ($C_{Acri}$-3, $C_{Acri}$-6), 132.36 ($C_{bim}$-1a), 130.70 ($C_{Acri}$-4, $C_{Acri}$-5), 129.10 ($C_{Acri}$-2, $C_{Acri}$-7), 126.16 ($C_{Acri}$-1, $C_{Acri}$-8), 124.09 ($C_{bim}$-4`, C_{bim}-5`), 123.35 ($C_{Acri}$-1a, $C_{Acri}$-8a), 113.49 ($C_{bim}$-6`), 112.87 (C_{bim}-3`), 36.68 (**N-CH_3**). ^{19}F NMR (376 MHz, Acetonitrile-d_3): δ (ppm) -72.68 (d, $^1J_{P,F}$ = 705 Hz). ^{31}P NMR (162 MHz Acetonitrile-d_3): δ(ppm) -144.02 (septet,$^1J_{P,F}$ = 705 Hz). Anal. calcd. for $C_{42}H_{30}AgF_6N_6P$: C, 57.88; H, 3.47; N, 9.64; found: C, 57.92; H, 3.51; N, 9.71; %. HRMS (ESI^+) *m/z* calcd. for $C_{42}H_{30}AgN_6[M-PF_6]^+$: 725.1583 (100%), 726.1616 (45%), 727.1579 (93%), 728.1610 (42%); found: 725.1581 (100%), 726.1609 (42%), 727.1584 (95%), 728.1609 (42%).

Ag [1-acridinyl-3-ethylbenzimidazolydiene]2(PF6) (43)

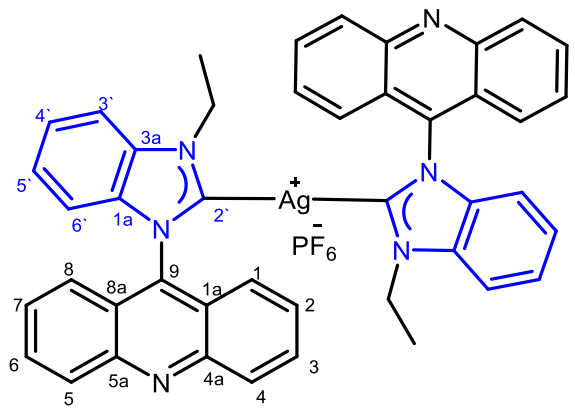

Compound **43** was obtained according to the general procedure **3.3.4** described using compound **28** ($C_{22}H_{18}N_3PF_6$, 470 mg, 1 mmol) to provide compound **42** (555 mg, 62%) as a yellow powder. Mp = 300-305 ºC. FTIR: ν (ATR, cm^{-1}) 3109$(C–H)_{Ar}$, 2948 $(C\text{-}H)_{Aliph}$, 1628 (C=N), 1552, 1471, 1346 (C=C), 1211 (C-N). UV-vis λ_{max}= 398 nm. ^1H NMR (400 MHz, Acetonitrile-d_3): δ (ppm) 8.20 (d, 4H, J_d= 8.0 Hz), 7.85-7.77 (m, 6H), 7.52 (t, 2H, J_t=8.0 Hz), 7.43 (t, 4H, J_t=8.0 Hz), 7.27 (t, 6H, J_t= 8.0 Hz), 6.81 (d, 2H, J_d= 8.0 Hz), 4.27 (q, 4H, **N-CH$_2$**), 1.33 (s, 6H, **-CH$_3$**). ^{13}C NMR (100 MHz, DMSO-d_6): δ (ppm) 191.21 (**C$_{bim}$-2`- Ag**), 149.95 ($C_{Acri}$-4a, $C_{Acri}$-5a), 139.30 ($C_{Acri}$-9), 136.6 ($C_{bim}$-3a), 133.72 ($C_{Acri}$-3, $C_{Acri}$-6), 132.15 ($C_{bim}$-1a), 130.54 ($C_{Acri}$-4, $C_{Acri}$-5), 128.97 ($C_{Acri}$-2, $C_{Acri}$-7), 126.01 ($C_{Acri}$-1, $C_{Acri}$-8), 125.92 ($C_{bim}$-4`), 123.94 (C_{bim}-5`), 123.24 ($C_{Acri}$-1a, $C_{Acri}$-8a), 113.27 ($C_{bim}$-6`), 112.87 (C_{bim}-3`), 45.45 (**N-CH$_2$**), 16.04 (NCH_2**CH$_3$**). ^{19}F NMR (376 MHz, Acetonitrile-d_3): δ (ppm) -72.68 (d, $^1J_{P,F}$ = 705 Hz). ^{31}P NMR (162 MHz, Acetonitrile-d_3): δ(ppm) -144.02 (septet, $^1J_{P,F}$ = 705 Hz). Anal. calcd. for $C_{44}H_{34}AgF_6N_6P$: C 58.74, H 3.81, N 9.34 %; found: C 58.79, H 3.89, N 9.38 %. HRMS (ESI^+) *m/z* calcd. for $C_{44}H_{34}AgN_6$ $[M–PF_6]^+$: 753.1896 (100%), 754.1929 (47%), 755.1893 (93%), 756.1926 (44%); found 753.1896 (100%), 754.1923 (48%), 755.1898 (83%), 756.1923 (17%).

Ag (1-acridinyl-3-benzylbenzimidazolydiene)2(PF6) (44)

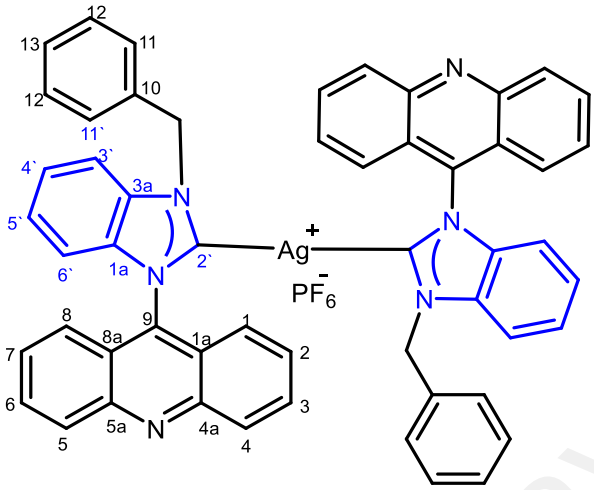

Compound **44** was obtained according to the general procedure **3.3.4** described using compound **29** (531 mg, 1.0 mmol) to furnish **44** (650 mg, 64%) as yellow solid. mp= 255-260 ºC. FTIR: ν (ATR, cm^{-1}) 3094 $(C–H)_{Ar}$, 2970 $(C-H)_{Aliph}$, 1633 (C=N), 1492, 1476, 1410 (C=C), 1262 (C-N). ^{1}H NMR (400 MHz, Acetonitrile-d_3): δ (ppm) 7.96 (d, 4H, J_d= 8.0 Hz), 7.70-7.65 (m, 6H), 7.46-7.22 (m, 22H), 6.77 (d, 2H, J_d= 8.0 Hz), 5.60 (s, 4H, **N-CH$_2$**). ^{13}C NMR (100 MHz, Acetonitrile-d_3): δ (ppm) 191.86 (**C_{bim}-2`-Ag**), 141.68 ($C_{Acri}$-4a, $C_{Acri}$-5a), 138.68 ($C_{Acri}$-9), 136.04 ($C_{bim}$-3a), 135.47 ($C_{ph}$-10), 133.30 ($C_{Acri}$-3, $C_{Acri}$-6), 131.72 ($C_{bim}$-1a), 129.40 ($C_{bim}$-4`), 129.20 (C_{Acri}-4, C_{Acri}-5), 128.54 (C_{ph}-12, C_{ph}-12`), 128.37 ($C_{bim}$-5`), 127.39 (C_{Acri}-2, C_{Acri}-7), 125.47 (C_{Acri}-1, C_{Acri}-8), 125.39 (C_{ph}-11, C_{ph}-11`), 123.07 ($C_{ph}$-13), 122.33 ($C_{Acri}$-1a, $C_{Acri}$-8a), 112.94 ($C_{bim}$-6`), 112.20 (C_{bim}-3`), 53.03 (**N-CH$_2$**). ^{19}F NMR (376 MHz, Acetonitrile-d_3): δ (ppm) -72.68 (d, $^{1}J_{P,F}$ = 705 Hz). ^{31}P NMR (162 MHz, Acetonitrile-d_3): δ(ppm) -144.02 (septet,$^{1}J_{P,F}$ = 705 Hz). Anal. calcd. for $C_{54}H_{38}AgF_6N_6P$: C 63.35, H 3.74, N 8.21 %; found: C 63.41, H 3.89, N 8.27%. HRMS (ESI^+) *m/z* calcd. for $C_{54}H_{38}AgN_6[M-PF_6]^+$: 877.2209 (100%), 878.2242 (58%), 879.2206 (93%), 880.2239(53%); found: 877.2240 (100%), 878.2257 (80%), 879.2241 (90%), 880.2243 (28%).

Ag(1-(6-chloro-2-methoxyacridinyl))-3-methylbenzimidazolydiene)2(PF6) (45)

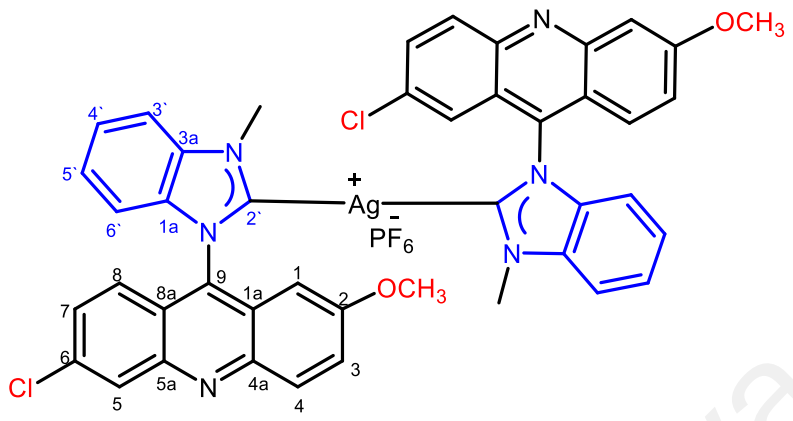

Compound **45** was obtained according to the general procedure **3.3.4** described using compound **30** (520 mg, 1.0 mmol) to furnish compound **45** (625 mg, 62%) as yellow solid. mp= 290-295 ºC. UV-vis λ_{max}=411 nm. FTIR: ν (ATR, cm^{-1}) 3065 $(C–H)_{Ar}$, 2957 $(C-H)_{Aliph}$, 1627 (C=N), 1557, 1439, 1391 (C=C), 1214(C-N). ^{1}H NMR (400 MHz, Acetonitrile-d_3): δ (ppm) 7.90 (d, 2H, *J*= 8.0 Hz), 7.86 (d, 2H, J_d= 8.0 Hz), 7.76 (s, 1H), 7.74 (s, 1H), 7.58 (dt, 2H, J_d = 2.0 Hz, J_t= 8.0 Hz), 7.33-7.28 (m, 4H), 7.24-7.17 (m, 4H), 6.87 (d, 2H, J_d= 8.0 Hz), 6.41 (d, 2H, J_d= 8.0 Hz), 4.31(s, 6H, **-OCH3**), 3.62 (s, 6H, **N-CH3**). ^{13}C NMR (100 MHz, Acetonitrile-d_3): δ (ppm) 192.04 (**C_{bim}-2`-Ag**), 159.07 ($C_{Acri}$-2-O**C**$H_3$), 146.38 ($C_{Acri}$-4a), 146.16 ($C_{Acri}$-5a), 136.73 ($C_{Acri}$-9), 135.4 ($C_{Acri}$-6), 135.32 ($C_{bim}$-3a), 134.45 ($C_{Acri}$-4), 130.87 ($C_{Acri}$-5), 128.82 ($C_{Acri}$-7), 127.45 ($C_{bim}$-1a), 126.88 ($C_{bim}$-4`), 125.12 (C_{bim}-5`), 125.03 ($C_{Acri}$-8), 124.60 ($C_{Acri}$-1a), 123.96 ($C_{Acri}$-3), 122.00 ($C_{Acri}$-8a), 112.57 ($C_{bim}$-6`), 111.89 (C_{bim}-3`), 97.86 (C_{Acri}-1), 55.87 (**O-CH3**), 36.23 (**N-CH3**). ^{19}F NMR (376 MHz, Acetonitrile-d_3): δ (ppm) -72.68 (d, $^{1}J_{P,F}$ = 705 Hz). ^{31}P NMR (162 MHz, Acetonitrile-d_3): δ(ppm) -144.02 (septet,$^{1}J_{P,F}$ =705 Hz). Anal. calcd. For $C_{44}H_{32}AgCl_2F_6N_6O_2P$: C 52.82, H 3.22, N,8.40%; found: C 52.76, H 3.35, N 8.62%. HRMS (ESI^+) *m/z* calcd. for $C_{44}H_{32}AgCl_2N_6O_2[M-PF_6]^+$: 853.1015 (100%), 854.1048 (48%), 855.1011 (93%), 856.1045 (44%), found: 853.1016 (90%), 854.1045 (45%), 855.1010 (100%), 856.1035 (35%).

REFERENCES

Achar, G., Hokrani, P. P., Brinda, K. N., Małecki, J. G., & Budagumpi, S. (2019). Synthesis, characterization, crystal structure and antibacterial properties of N– and O–functionalized (benz)imidazolium salts and their N–heterocyclic carbene silver(I) complexes. *Journal of Molecular Structure, 1196*, 627-636.

Achar, G., Shahini, C., Patil, S. A., & Budagumpi, S. (2017a). Synthesis, structural characterization, crystal structures and antibacterial potentials of coumarin–tethered N–heterocyclic carbene silver(I) complexes. *Journal of Organometallic Chemistry, 833*, 28-42.

Achar, G., Uppendranath, K., Ramya, V. C., Biffis, A., Keri, R. S., & Budagumpi, S. (2017b). Synthesis, characterization, crystal structure and biological studies of silver(I) complexes derived from coumarin-tethered N-heterocyclic carbene ligands. *Polyhedron, 123*, 470-479.

Adjei, A. A. (1999). Current status of pyrazoloacridine as an anticancer agent. *Investigational New Drugs, 17*(1), 43-48.

Afzal, A., Sarfraz, M., Wu, Z., Wang, G., & Sun, J. (2016). Integrated scientific data bases review on asulacrine and associated toxicity. *Critical Reviews in Oncology /Hematology, 104*, 78-86.

Ahmad, A., Syed, F., Shah, A., Khan, Z., Tahir, K., Khan, A. U., & Yuan, Q. (2015). Silver and gold nanoparticles from sargentodoxa cuneata: Synthesis, characterization and antileishmanial activity. *RSC Advances, 5*(90), 73793-73806.

Ahmad, I., & Aqil, F. (2007). *In vitro* efficacy of bioactive extracts of 15 medicinal plants against ESβL-producing multidrug-resistant enteric bacteria. *Microbiological Research, 162*(3), 264-275.

Ahmad, R., Wani, A., & Ahsan, H. (2013). Role of antioxidants in pathophysiology. *Journal of Medical Erudite, 1*(2), 9-15.

Al-Madhagi, W., Hashim, N., Ali, N., & Othman, R. (2019). Phytochemical screening, cytotoxic and antimicrobial activities of limonium socotranum and peperomia blanda extracts. *Tropical Biomedicine, 36*(1), 11-21.

Al-Mohammed, N. N., Alias, Y., & Abdullah, Z. (2015a). Bis-imidazolium and benzimidazolium based gemini-type ionic liquids structure: Synthesis and antibacterial evaluation. *RSC Advances, 5*(112), 92602-92617.

Al-Mohammed, N. N., Hussen, R. S. D., Alias, Y., & Abdullah, Z. (2015b). Tris-imidazolium and benzimidazolium ionic liquids: A new class of biodegradable surfactants. *RSC Advances, 5*(4), 2869-2881.

Alfadda, A. A., & Sallam, R. M. (2012). Reactive oxygen species in health and disease. *Journal of Biomedicine and Biotechnology*, *2012*, 1-14.

Alfarouk, K. O., Stock, C.-M., Taylor, S., Walsh, M., Muddathir, A. K., Verduzco, D., Bashir, A. H. H., Mohammed, O. Y., Elhassan, G. O., Harguindey, S., Reshkin, S. J., Ibrahim, M. E., & Rauch, C. (2015). Resistance to cancer chemotherapy: failure in drug response from ADME to P-gp. *Cancer Cell International, 15*(1), 71-82.

Alotaibi, S. H., & Momen, A. A. (2019). Anticancer Drugs' Deoxyribonucleic Acid (DNA) Interactions. In Biophysical Chemistry-Advance Applications, 1-23. IntechOpen. DOI: 10.5772/intechopen.85794.

Antonini, I., Polucci, P., Magnano, A., & Martelli, S. (2001). Synthesis, antitumor cytotoxicity, and DNA-binding of novel *N*-5, 2-Di (ω-aminoalkyl)-2, 6-dihydropyrazolo [3, 4, 5-kl] acridine-5-carboxamides. *Journal of Medicinal Chemistry, 44*(20), 3329-3333.

Apak, R., Guclu, K., Demirata, B., Ozyurek, M., Celik, S. E., Bektasoglu, B., Berker, K. I., & Ozyurt, D. (2007). Comparative evaluation of various total antioxidant capacity assays applied to phenolic compounds with the CUPRAC assay. *Molecules (Basel, Switzerland), 12*(7), 1496-1547.

Apak, R., Ozyurek, M., Guclu, K., & Capanoglu, E. (2016). Antioxidant activity/capacity measurement. 3. Reactive oxygen and nitrogen species (ROS/RNS) scavenging assays, oxidative stress biomarkers, and chromatographic/chemometric assays. *Journal of Agricultural and Food Chemistry, 64*(5), 1046-1070.

Arduengo, A. J., Krafczyk, R., Schmutzler, R., Craig, H. A., Goerlich, J. R., Marshall, W. J., & Unverzagt, M. (1999). Imidazolylidenes, imidazolinylidenes and imidazolidines. *Tetrahedron, 55*(51), 14523-14534.

Arduengo III, A. J., Harlow, R. L., & Kline, M. (1991). A stable crystalline carbene. *Journal of the American Chemical Society, 113*(1), 361-363.

Asekunowo, P. O., Haque, R. A., & Razali, M. (2017). A comparative insight into the bioactivity of mono-and binuclear silver (I)-N-heterocyclic carbene complexes: Synthesis, lipophilicity and substituent effect. *Reviews in Inorganic Chemistry, 37*(1), 29-50.

Asif, M., Iqbal, M. A., Hussein, M. A., Oon, C. E., Haque, R. A., Khadeer Ahamed, M. B., Abdul Majid, A. S., & Abdul Majid, A. M. S. (2016). Human colon cancer targeted pro-apoptotic, anti-metastatic and cytostatic effects of binuclear silver(I)–N-heterocyclic carbene (NHC) complexes. *European Journal of Medicinal Chemistry, 108*, 177-187.

Badisa, R. B., Darling-Reed, S. F., Joseph, P., Cooperwood, J. S., Latinwo, L. M., & Goodman, C. B. (2009). Selective cytotoxic activities of two novel synthetic drugs on human breast carcinoma MCF-7 cells. *Anticancer Research, 29*(8), 2993-2996.

Baguley, B. C., Denny, W. A., Atwell, G. J., Finlay, G. J., Rewcastle, G. W., Twigden, S. J., & Wilson, W. R. (1984). Synthesis, antitumor activity, and DNA binding properties of a new derivative of amsacrine, *N*-5-dimethyl-9-[(2-methoxy-4-methylsulfonylamino) phenylamino]-4-acridinecarboxamide. *Cancer Research, 44*(8), 3245-3251.

Bandow, J. E., & Metzler-Nolte, N. (2009). New ways of killing the beast: Prospects for inorganic–organic hybrid nanomaterials as antibacterial agents. *Chemical Biology and Biological Chemistry, 10*(18), 2847-2850.

Baron, M., Bellemin-Laponnaz, S., Tubaro, C., Basato, M., Bogialli, S., & Dolmella, A. (2014). Synthesis and biological assays on cancer cells of dinuclear gold complexes with novel functionalised di (N-heterocyclic carbene) ligands. *Journal of Inorganic Biochemistry, 141*, 94-102.

Barry, C. G., Baruah, H., & Bierbach, U. (2003). Unprecedented monofunctional metalation of adenine nucleobase in guanine- and thymine-containing dinucleotide sequences by a cytotoxic platinum−acridine hybrid agent. *Journal of the American Chemical Society, 125*(32), 9629-9637.

Baruah, H., Rector, C. L., Monnier, S. M., & Bierbach, U. (2002). Mechanism of action of non-cisplatin type DNA-targeted platinum anticancer agents: DNA interactions of novel acridinylthioureas and their platinum conjugates. *Biochemical Pharmacology, 64*(2), 191-200.

Baruah, H., Wright, M. W., & Bierbach, U. (2005). Solution structural study of a dna duplex containing the guanine-n7 adduct formed by a cytotoxic platinum−acridine hybrid agent. *Biochemistry, 44*(16), 6059-6070.

Bayach, I., Manickam Achari, V., Wan Iskandar, W., Sugimura, A., & Hashim, R. (2016). Computational insights into octyl-D-xyloside isomers towards understanding the liquid crystalline structure: Physico-chemical features. *Liquid Crystals, 43*(10), 1503-1513.

Baydar, N. G., Ozkan, G., & Yasar, S. (2007). Evaluation of the antiradical and antioxidant potential of grape extracts. *Food Control, 18*(9), 1131-1136.

Beckford, F., Thessing, J., Woods, J., Didion, J., Gerasimchuk, N., Gonzalez-Sarrias, A., & Seeram, N. P. (2011). Synthesis and structure of [(η6-p-cymene) Ru (2-anthracen-9-ylmethylene-*N*-ethylhydrazinecarbothioamide) Cl] Cl; biological evaluation, topoisomerase II inhibition and reaction with DNA and human serum albumin. *Metallomics, 3*(5), 491-502.

Belmont, P., Bosson, J., Godet, T., & Tiano, M. (2007). Acridine and acridone derivatives, anticancer properties and synthetic methods: Where are we now? *Anti-Cancer Agents in Medicinal Chemistry (Formerly Current Medicinal Chemistry-Anti-Cancer Agents), 7*(2), 139-169.

Belmont, P., & Dorange, I. (2008). Acridine/acridone: a simple scaffold with a wide range of application in oncology. *Expert Opinion on Therapeutic Patents, 18*(11), 1211-1224.

Benoit, A. R., Schiaffo, C., Salomon, C. E., Goodell, J. R., Hiasa, H., & Ferguson, D. M. (2014). Synthesis and evaluation of *N*-alkyl-9-aminoacridines with antibacterial activity. *Bioorganic & Medicinal Chemistry Letters, 24*(14), 3014-3017.

Benzie, I. F., & Strain, J. (1999). [2] Ferric reducing/antioxidant power assay: Direct measure of total antioxidant activity of biological fluids and modified version for simultaneous measurement of total antioxidant power and ascorbic acid concentration. *Methods in Enzymology,* 299, 15-27.

Bernthsen, A. (1884). Die acridine. *Justus Liebigs Annalen der Chemie, 224*(1-2), 1-56.

Bongarzone, S., & Bolognesi, M. L. (2011). The concept of privileged structures in rational drug design: Focus on acridine and quinoline scaffolds in neurodegenerative and protozoan diseases. *Expert Opinion on Drug Discovery, 6*(3), 251-268.

Brand-Williams, W., Cuvelier, M.-E., & Berset, C. (1995). Use of a free radical method to evaluate antioxidant activity. *LWT-Food Science and Technology, 28*(1), 25-30.

Bray, F., Ferlay, J., Soerjomataram, I., Siegel, R. L., Torre, L. A., & Jemal, A. (2018). Global cancer statistics 2018: Globocan estimates of incidence and mortality worldwide for 36 cancers in 185 countries. *CA: A Cancer Journal for Clinicians, 68*(6), 394-424.

Bray, F., Lortet-Tieulent, J., Ferlay, J., Forman, D., & Auvinen, A. (2010). Prostate cancer incidence and mortality trends in 37 European countries: An overview. *European Journal of Cancer, 46*(17), 3040-3052.

Brem, B., Seger, C., Pacher, T., Hartl, M., Hadacek, F., Hofer, O., Vajrodaya, S., & Greger, H. (2004). Antioxidant dehydrotocopherols as a new chemical character of Stemona species. *Phytochemistry, 65*(19), 2719-2729.

Browning, C. H., Cohen, J. B., Gaunt, R., & Gulbransen, R. (1922). Relationships between antiseptic action and chemical constitution with special reference to compounds of the pyridine, quinoline, acridine and phenazine series. *Proceedings of the Royal Society of London. Series B, Containing Papers of a Biological Character, 93*(653), 329-366.

Bu, X.-H., Tong, M.-L., Chang, H.-C., Kitagawa, S., & Batten, S. R. (2004). A neutral 3d copper coordination polymer showing 1d open channels and the first interpenetrating nbo-type network. *Angewandte Chemie International Edition, 43*(2), 192-195.

Budagumpi, S., & Revankar, V. K. (2010). Interaction of E. coli DNA with diazine-bridged late first row transition metal complexes derived from hexadentate compartmental ligands: An approach to DNA cleavage/binding studies. *Transition Metal Chemistry, 35*(6), 649-658.

Byvaltsev, V. A., Bardonova, L. A., Onaka, N. R., Polkin, R. A., Ochkal, S. V., Shepelev, V. V., Aliyev, M. A., & Potapov, A. A. (2019). Acridine orange: A review of novel applications for surgical cancer imaging and therapy. *Frontiers in Oncology, 9*, 925-925.

Cai, M., Liang, Y., Yao, M., Xia, Y., Zhou, F., & Liu, W. (2010). Imidazolium ionic liquids as antiwear and antioxidant additive in poly(ethylene glycol) for steel/steel contacts. *ACS Applied Materials & Interfaces, 2*(3), 870-876.

Cano, A., Alcaraz, O., Acosta, M., & Arnao, M. B. (2002). On-line antioxidant activity determination: comparison of hydrophilic and lipophilic antioxidant activity using the $ABTS^{\bullet+}$ assay. *Redox Report, 7*(2), 103-109.

Carocho, M., & Ferreira, I. C. (2013). A review on antioxidants, prooxidants and related controversy: natural and synthetic compounds, screening and analysis methodologies and future perspectives. *Food and Chemical Toxicology, 51*, 15-25.

Charmantray, F., & Martelli, A. (2001). Interest of acridine derivatives in the anticancer chemotherapy. *Current Pharmaceutical Design, 7*(17), 1703-1724.

Chen, K.-M., Sun, Y.-W., Tang, Y.-W., Sun, Z.-Y., & Kwon, C.-H. (2005). Synthesis and antitumor activity of sulfur-containing 9-anilinoacridines. *Molecular Pharmaceutics, 2*(2), 118-128.

Chen, X.-M. (2011). Chapter 10 - Assembly chemistry of coordination polymers. In R. Xu, W. Pang & Q. Huo (Eds.), *Modern Inorganic Synthetic Chemistry* (pp. 207-225). Amsterdam: Elsevier.

Cheng, Z., Yang, B., Yang, M., & Zhang, B. (2014). Structural study and fluorescent property of a novel organic microporous crystalline material. *Journal of the Brazilian Chemical Society, 25*(1), 112-118.

Chianese, A. R., Li, X., Janzen, M. C., Faller, J., & Crabtree, R. H. (2003). Rhodium and iridium complexes of N-heterocyclic carbenes via transmetalation: structure and dynamics. *Organometallics, 22*(8), 1663-1667.

Chifotides, H. T., & Dunbar, K. R. (2005). Interactions of metal−metal-bonded antitumor active complexes with DNA fragments and DNA. *Accounts of Chemical Research, 38*(2), 146-156.

Chilin, A., Marzaro, G., Marzano, C., Dalla Via, L., Ferlin, M. G., Pastorini, G., & Guiotto, A. (2009). Synthesis and antitumor activity of novel amsacrine analogs: The critical role of the acridine moiety in determining their biological activity. *Bioorganic & Medicinal Chemistry, 17*(2), 523-529.

Cholewinski, G., Dzierzbicka, K., & Kołodziejczyk, A. M. (2011). Natural and synthetic acridines/acridones as antitumor agents: Their biological activities and methods of synthesis. *Pharmacological Reports, 63*(2), 305-336.

Cholody, W. M., Martelli, S., & Konopa, J. (1990). 8-Substituted 5-[(aminoalkyl) amino]-6H-v-triazolo [4, 5, 1-de] acridin-6-ones as potential antineoplastic agents: ynthesis and biological activity. *Journal of Medicinal Chemistry, 33*(10), 2852-2856.

Chopra, I., & Roberts, M. (2001). Tetracycline antibiotics: mode of action, applications, molecular biology, and epidemiology of bacterial resistance. *Microbiology and Molecular Biology Reviews*, 65(2), 232-260.

Coban, G., Zencir, S., Zupko, I., Rethy, B., Gunes, H. S., & Topcu, Z. (2009). Synthesis and biological activity evaluation of 1H-benzimidazoles via mammalian DNA topoisomerase I and cytostaticity assays. *European Journal of Medicinal Chemistry, 44*(5), 2280-2285.

Csuk, R., Barthel, A., & Raschke, C. (2004). Convenient access to substituted acridines by a Buchwald–Hartwig amination. *Tetrahedron, 60*(27), 5737-5750.

De Almeida, M. S., Lafayette, A. E., Da Silva, P. L., Amorim, A. C., De Oliveira, B. T., Ruiz, L. A., De Carvalho, E. J., De Moura, O. R., Beltrao, I. E., De Lima, D. M., & Junior, B. L. (2015). Synthesis, DNA binding, and antiproliferative activity of novel acridine-thiosemicarbazone derivatives. *International Journal of Molecular Sciences, 16*(6), 13023-13042.

De Fremont, P., Marion, N., & Nolan, S. P. (2009). Carbenes: synthesis, properties, and organometallic chemistry. *Coordination Chemistry Reviews, 253*(7), 862-892.

Deen, K. I., Silva, H., Deen, R., & Chandrasinghe, P. C. (2016). Colorectal cancer in the young, many questions, few answers. *World Journal of Gastrointestinal Oncology, 8*(6), 481-488.

Delhaes, L., Biot, C., Berry, L., Delcourt, P., Maciejewski, L. A., Camus, D., Brocard, J. S., & Dive, D. (2002). Synthesis of ferroquine enantiomers: first investigation of effects of metallocenic chirality upon antimalarial activity and cytotoxicity. *Chemical Biology and Biological Chemistry, 3*(5), 418-423.

Demeunynck, M. (2004). Antitumour acridines. *Expert Opinion on Therapeutic Patents, 14*(1), 55-70.

Dickens, B. F., Weglicki, W. B., Boehme, P. A., & Mak, T. I. (2002). Antioxidant and lysosomotropic properties of acridine-propranolol: Protection against oxidative endothelial cell injury. *Journal of Molecular and Cellular Cardiology, 34*(2), 129-137.

Dogan, O., Demir, S., Ozdemir, İ., & Cetinkaya, B. (2011). Palladium (II)-NHC complexes containing benzimidazole ligand as a catalyst for C-N bond formation. *Applied Organometallic Chemistry, 25*(3), 163-167.

Dudonne, S., Vitrac, X., Coutiere, P., Woillez, M., & Merillon, J.-M. (2009). Comparative study of antioxidant properties and total phenolic content of 30 plant extracts of industrial interest using DPPH, ABTS, FRAP, SOD, and ORAC assays. *Journal of Agricultural and Food Chemistry, 57*(5), 1768-1774.

Edwards, C. L., Scales, M. T., Loughlin, C., Bennett, G. G., Harris-Peterson, S., De Castro, L. M., Whitworth, E., Abrams, M., Feliu, M., & Johnson, S. (2005). A brief review of the pathophysiology, associated pain, and psychosocial issues in sickle cell disease. *International Journal of Behavioral Medicine, 12*(3), 171-179.

Elangovan, A., Chiu, H.-H., Yang, S.-W., & Ho, T.-I. (2004). Arylethynylacridines: electrochemiluminescence and photophysical properties. *Organic &Biomolecular Chemistry, 2*(21), 3113-3118.

Farghadani, R., Rajarajeswaran, J., Hashim, N. B. M., Abdulla, M. A., & Muniandy, S. (2017). A novel β-diiminato manganese III complex as the promising anticancer agent induces G 0/G 1 cell cycle arrest and triggers apoptosis via mitochondrial-dependent pathways in MCF-7 and MDA-MB-231 human breast cancer cells. *RSC Advances, 7*(39), 24387-24398.

Fatima, T., Haque, R. A., Razali, M. R., Ahmad, A., Iqbal, M. A., Asif, M., Ahamed, M. B. K., & Abdul Majid, A. M. S. (2016). Synthesis, crystal structure, *in vitro* anticancer and *in vivo* acute oral toxicity studies of tetramethylene linked bis-benzimidazolium salts and their respective dinuclear Ag(I)–NHC complexes. *Journal of Coordination Chemistry, 69*(22), 3367-3383.

Favarin, L. R., Oliveira, L. B., Silva, H., Micheletti, A. C., Pizzuti, L., Machulek-Júnior, A., ... & Duarte, L. F. B. (2019). Sonochemical synthesis of highly luminescent silver complexes: Photophysical properties and preliminary in vitro antitumor and antibacterial assays. *Inorganica Chimica Acta*, 492, 235-242.

Feio, M. J., Sousa, I., Ferreira, M., Cunha-Silva, L., Saraiva, R. G., Queiros, C., Alexandre, J. G., Claro, V., Mendes, A., & Ortiz, R. (2014). Fluoroquinolone–metal complexes: A route to counteract bacterial resistance. *Journal of Inorganic Biochemistry, 138*, 129-143.

Ferlay, J., Soerjomataram, I., Dikshit, R., Eser, S., Mathers, C., Rebelo, M., Parkin, D. M., Forman, D., & Bray, F. (2015). Cancer incidence and mortality worldwide: Sources, methods and major patterns in globocan 2012. *International Journal of Cancer, 136*(5), E359-E386.

Fichtner, I., Cinatl, J., Michaelis, M., C Sanders, L., Hilger, R., N Kennedy, B., L Reynolds, A., Hackenberg, F., Lally, G., & J Quinn, S. (2012). *In vitro* and *in vivo* investigations into the carbene silver acetate anticancer drug candidate SBC1. *Letters in Drug Design & Discovery, 9*(9), 815-822.

Forman, H. J., Maiorino, M., & Ursini, F. (2010). Signaling functions of reactive oxygen species. *Biochemistry, 49*(5), 835-842.

Galdino-Pitta, M. R., Pitta, M. G. R., Lima, M. C. A., Galdino, S. L., & Pitta, I. R. (2013). Niche for acridine derivatives in anticancer therapy. *Mini-Reviews in Medicinal Chemistry, 13*(9), 1256-1271.

Gamage, S. A., Figgitt, D. P., Wojcik, S. J., Ralph, R. K., Ransijn, A., Mauel, J., Yardley, V., Snowdon, D., Croft, S. L., & Denny, W. A. (1997). Structure−activity relationships for the antileishmanial and antitrypanosomal activities of 1 '-substituted 9-anilinoacridines. *Journal of Medicinal Chemistry, 40*(16), 2634-2642.

Gandin, V., Pellei, M., Marinelli, M., Marzano, C., Dolmella, A., Giorgetti, M., & Santini, C. (2013). Synthesis and *in vitro* antitumor activity of water soluble sulfonate-and ester-functionalized silver (I) N-heterocyclic carbene complexes. *Journal of Inorganic Biochemistry, 129*, 135-144.

Gao, C., Li, B., Zhang, B., Sun, Q., Li, L., Li, X., Chen, C., Tan, C., Liu, H., & Jiang, Y. (2015). Synthesis and biological evaluation of benzimidazole acridine derivatives as potential DNA-binding and apoptosis-inducing agents. *Bioorganic & Medicinal Chemistry, 23*(8), 1800-1807.

García, C., Leon, L. G., Pungitore, C. R., Ríos-Luci, C., Daranas, A. H., Montero, J. C., Pandiella, A., Tonn, C. E., Martin, V. S., & Padron, J. M. (2010). Enhancement of antiproliferative activity by molecular simplification of catalpol. *Bioorganic & Medicinal Chemistry, 18*(7), 2515-2523.

Garrison, J. C., & Youngs, W. J. (2005). Ag (I) N-heterocyclic carbene complexes: synthesis, structure, and application. *Chemical Reviews, 105*(11), 3978-4008.

Gasser, G., Ott, I., & Metzler-Nolte, N. (2011). Organometallic anticancer compounds. *Journal of Medicinal Chemistry, 54*(1), 3-25.

Gautier, A., & Cisnetti, F. (2012). Advances in metal–carbene complexes as potent anti-cancer agents. *Metallomics, 4*(1), 23-32.

Ghdhayeb, M. Z., Haque, R. A., Budagumpi, S., Ahamed, M. B. K., & Majid, A. M. A. (2017). Mono-and bis-N-heterocyclic carbene silver (I) and palladium (II) complexes: synthesis, characterization, crystal structure and *in vitro* anticancer studies. *Polyhedron, 121*, 222-230.

Gimeno, M. C., Laguna, A., & Visbal, R. (2012). N-heterocyclic carbene coinage metal complexes as intense blue-green emitters. *Organometallics, 31*(20), 7146-7157.

Gniazdowski, M., & Szmigiero, L. (1995). Nitracrine and its congeners-an overview. *General Pharmacology: The Vascular System, 26*(3), 473-481.

Gok, Y., Akkoc, S., Albayrak, S., Akkurt, M., & Tahir, M. N. (2014). N-phenyl-substituted carbene precursors and their silver complexes: Synthesis, characterization and antimicrobial activities. *Applied Organometallic Chemistry, 28*(4), 244-251.

Gok, Y., Akkoc, S., Celikal, O. O., Ozdemir, I., Gunal, S., & Sayin, E. (2013). *N*-functionalized benzimidazol-2-ylidene silver complexes: Synthesis, characterization, and antimicrobial studies. *Turkish Journal of Chemistry, 37*(6), 1007-1013.

Gok, Y., Akkoc, S., Erdogan, H., & Albayrak, S. (2016). *In vitro* antimicrobial studies of new benzimidazolium salts and silver N-heterocyclic carbene complexes. *Journal of Enzyme Inhibition and Medicinal Chemistry, 31*(6), 1322-1327.

Goftar, M., Kor, N., & Kor, Z. (2014). DNA intercalators and using them as anticancer drugs. *International Journal of Advanced Biological and Biomedical Research*, *2*(3), 811-822.

Goodell, J. R., Ougolkov, A. V., Hiasa, H., Kaur, H., Remmel, R., Billadeau, D. D., & Ferguson, D. M. (2008). Acridine-based agents with topoisomerase II activity inhibit pancreatic cancer cell proliferation and induce apoptosis. *Journal of Medicinal Chemistry, 51*(2), 179-182.

Graham, C. (2005). The role of silver in wound healing. *British Journal of Nursing, 14*(Sup5), S22-S28.

Graham, L. A., Suryadi, J., West, T. K., Kucera, G. L., & Bierbach, U. (2012). Synthesis, aqueous reactivity, and biological evaluation of carboxylic acid ester-functionalized platinum–acridine hybrid anticancer agents. *Journal of Medicinal Chemistry, 55*(17), 7817-7827.

Gram, C. (1884). Ueber die isolirte farbung der schizomyceten in schnittundtrockenpraparaten. *Fortschritte der Medicin*, 2, 185-189.

Guerret, O., Solé, S., Gornitzka, H., Teichert, M., Trinquier, G., & Bertrand, G. (1997). 1, 2, 4-Triazole-3, 5-diylidene: a building block for organometallic polymer synthesis. *Journal of the American Chemical Society, 119*(28), 6668-6669.

Gunanathan, C., Shimon, L. J., & Milstein, D. (2009). Direct conversion of alcohols to acetals and H_2 catalyzed by an acridine-based ruthenium pincer complex. *Journal of the American Chemical Society, 131*(9), 3146-3147.

Guo, C., Gasparian, A., Zhuang, Z., Bosykh, D., Komar, A., Gudkov, A., & Gurova, K. (2009). 9-Aminoacridine-based anticancer drugs target the PI3K/AKT/mTOR, NF-κB and p53 pathways. *Oncogene, 28*(8), 1151-1161.

Guo, L., Song, X.-Z., Lin, C.-X., Li, Q.-S., Liu, C., Wang, W.-H., & Xu, F.-B. (2015). Synthesis of multi-imidazolium salt ligands containing calixarene fragments and their N-heterocyclic carbene Ag(I) macrocyclic complexes. *Polyhedron, 85*, 732-739.

Gupta, R., Sharma, M., Lakshmy, R., Prabhakaran, D., & Reddy, K. S. (2009). Improved method of total antioxidant assay. *Indian Journal of Biochemistry & Biophysics, 46,* 126-129.

Hackenberg, F., & Tacke, M. (2014). Benzyl-substituted metallocarbene antibiotics and anticancer drugs. *Dalton Transactions, 43*(22), 8144-8153.

Hadei, N., Kantchev, E. A. B., O'Brie, C. J., & Organ, M. G. (2005). Electronic nature of N-heterocyclic carbene ligands: Effect on the suzuki reaction. *Organic letters, 7*(10), 1991-1994.

Hadjikakou, S. K., Ozturk, I. I., Xanthopoulou, M. N., Zachariadis, P. C., Zartilas, S., Karkabounas, S., & Hadjiliadis, N. (2008). Synthesis, structural characterization and biological study of new organotin(IV), silver(I) and antimony(III) complexes with thioamides. *Journal of Inorganic Biochemistry, 102*(5), 1007-1015.

Haider, M. R., Ahmad, K., Siddiqui, N., Ali, Z., Akhtar, M. J., Fuloria, N., Fuloria, S., Ravichandran, M., & Yar, M. S. (2019). Novel 9-(2-(1-arylethylidene) hydrazinyl)acridine derivatives: Target topoisomerase 1 and growth inhibition of HeLa cancer cells. *Bioorganic Chemistry, 88*, Article#102962.

Hamblin, M. R., & Hasan, T. (2004). Photodynamic therapy: a new antimicrobial approach to infectious disease. *Photochemical & Photobiological Sciences, 3*(5), 436-450.

Han, X., Zhou, Y., & Liu, W. (2017). Precision cardio-oncology: Understanding the cardiotoxicity of cancer therapy. *NPJ Precision Oncology, 1*(1), 31-37.

Hanahan, D., & Weinberg, R. A. (2011). Hallmarks of cancer: The next generation. *Cell, 144*(5), 646-674.

Haque, R. A., Asekunowo, P. O., & Razali, M. R. (2014). Dinuclear silver (I)-N-heterocyclic carbene complexes of *N*-allyl substituted (benz) imidazol-2-ylidenes with pyridine spacers: Synthesis, crystal structures, nuclease and antibacterial studies. *Transition Metal Chemistry, 39*(3), 281-290.

Haque, R. A., Choo, S. Y., Budagumpi, S., Abdullah, A. A.-A., Khadeer Ahamed, M. B., & Abdul Majid, A. M. S. (2015a). Synthesis, crystal structures, characterization and biological studies of nitrile-functionalized silver(I) N-heterocyclic carbene complexes. *Inorganica Chimica Acta, 433*, 35-44.

Haque, R. A., Choo, S. Y., Budagumpi, S., Iqbal, M. A., & Al-Ashraf Abdullah, A. (2015b). Silver(I) complexes of mono- and bidentate N-heterocyclic carbene ligands: Synthesis, crystal structures, and *in vitro* antibacterial and anticancer studies. *European Journal of Medicinal Chemistry, 90*, 82-92.

Haque, R. A., Ghdhayeb, M. Z., Budagumpi, S., Salman, A. W., Ahamed, M. B. K., & Majid, A. M. S. A. (2013). Non-symmetrically substituted N-heterocyclic carbene–Ag (I) complexes of benzimidazol-2-ylidenes: Synthesis, crystal structures, anticancer activity and transmetallation studies. *Inorganica Chimica Acta, 394*, 519-525.

Haque, R. A., Ghdhayeb, M. Z., Salman, A. W., Budagumpi, S., Ahamed, M. B. K., & Majid, A. M. A. (2012). Ag (I)-N-heterocyclic carbene complexes of *N*-allyl substituted imidazol-2-ylidenes with ortho-, meta-and para-xylyl spacers: Synthesis, crystal structures and *in vitro* anticancer studies. *Inorganic Chemistry Communications, 22*, 113-119.

Haque, R. A., Hasanudin, N., Iqbal, M. A., Ahmad, A., Hashim, S., Abdul Majid, A., & Ahamed, M. B. K. (2013a). Synthesis, crystal structures, *in vitro* anticancer, and *in vivo* acute oral toxicity studies of bis-imidazolium/benzimidazolium salts and respective dinuclear Ag(I)-N-heterocyclic carbene complexes. *Journal of Coordination Chemistry, 66*(18), 3211-3228.

Haque, R. A., Haziz, U. F. M., Abdullah, A. A.-A., Shaheeda, N., & Razali, M. R. (2016). New non-functionalized and nitrile-functionalized benzimidazolium salts and their silver(I) complexes: Synthesis, crystal structures and antibacterial studies. *Polyhedron, 109*, 208-217.

Haque, R. A., Iqbal, M. A., Asekunowo, P., Majid, A. M. S. A., Khadeer Ahamed, M. B., Umar, M. I., Al-Rawi, S. S., & Al-Suede, F. S. R. (2013b). Synthesis, structure, anticancer, and antioxidant activity of para-xylyl linked bis-benzimidazolium salts and respective dinuclear Ag(I) N-heterocyclic carbene complexes (Part-II). *Medicinal Chemistry Research, 22*(10), 4663-4676.

Haque, R. A., Iqbal, M. A., Mohamad, F., & Razali, M. R. (2018). Antibacterial and DNA cleavage activity of carbonyl functionalized N-heterocyclic carbene-silver(I) and selenium compounds. *Journal of Molecular Structure, 1155*, 362-370.

Haque, R. A., Nasri, S. F., Iqbal, M. A., Al-Rawi, S. S., Jafari, S. F., Ahamed, M. B. K., & Abdul Majid, A. (2013c). Synthesis, characterization, and crystal structures of bis-imidazolium salts and respective dinuclear Ag (I) N-heterocyclic carbene complexes: *In vitro* anticancer studies against "human colon cancer" and "breast cancer". *Journal of Chemistry, 2013*, 1-11.

Haque, R. A., Salman, A. W., Budagumpi, S., Abdullah, A. A. A., Abdul Hameed Al-Mudaris, Z. A., & Abdul Majid, A. M. (2013d). Silver (I)-N-heterocyclic carbene complexes of bis-imidazol-2-ylidenes having different aromatic-spacers: Synthesis, crystal structure, and *in vitro* antimicrobial and anticancer studies. *Applied Organometallic Chemistry, 27*(8), 465-473.

Hartinger, C. G., & Dyson, P. J. (2009). Bioorganometallic chemistry-from teaching paradigms to medicinal applications. *Chemical Society Reviews, 38*(2), 391-401.

Haziz, U. F. M., Haque, R. A., Amirul, A. A., Aidda, O. N., & Razali, M. R. (2019). New class of non-symmetrical homo-dibenzimidazolium salts and their dinuclear silver(I) di-NHC complexes. *Journal of Organometallic Chemistry, 899*, 120914.

Haziz, U. F. M., Haque, R. A., Amirul, A. A., Shaheeda, N., & Razali, M. R. (2016). Synthesis, structures and antibacterial studies of non-functionalized and nitrile-functionalized bis-benzimidazolium salts and respective dinuclear silver(I)-N-heterocyclic carbene complexes. *Polyhedron, 117*, 628-636.

He, Z., Huang, K., Xiong, F., Zhang, S.-F., Xue, J.-R., Liang, Y., Jing, L.-H., & Qin, D.-B. (2015). Self-assembly of imidazoliums salts based on acridine with silver oxide as coordination polymers: synthesis, fluorescence and antibacterial activity. *Journal of Organometallic Chemistry, 797*, 67-75.

Hindi, K. M., Panzner, M. J., Tessier, C. A., Cannon, C. L., & Youngs, W. J. (2009). The medicinal applications of imidazolium carbene−metal complexes. *Chemical Reviews, 109*(8), 3859-3884.

Hindi, K. M., Siciliano, T. J., Durmus, S., Panzner, M. J., Medvetz, D. A., Reddy, D. V., Hogue, L. A., Hovis, C. E., Hilliard, J. K., & Mallet, R. J. (2008). Synthesis, stability, and antimicrobial studies of electronically tuned silver acetate N-heterocyclic carbenes. *Journal of Medicinal Chemistry, 51*(6), 1577-1583.

Holmstrom, K. M., & Finkel, T. (2014). Cellular mechanisms and physiological consequences of redox-dependent signalling. *Nature Reviews Molecular Cell Biology, 15*(6), 411-421.

Hopkinson, M. N., Richter, C., Schedler, M., & Glorius, F. (2014). An overview of N-heterocyclic carbenes. *Nature, 510*(7506), 485-496.

Huang, D., Ou, B., & Prior, R. L. (2005). The chemistry behind antioxidant capacity assays. *Journal of Agricultural and Food Chemistry, 53*(6), 1841-1856.

Huang, M., Duan, S., Ma, X., Cai, B., Wu, D., Li, Y., Li, L., Zhang, H., & Yang, X. (2019). Synthesis and antitumor activity of aza-brazilan derivatives containing imidazolium salt pharmacophores. *Medicinal Chemistry Communications, 10*(6), 1027-1036.

Hussaini, S. Y., Haque, R. A., & Razali, M. R. (2019). Recent progress in silver(I)-, gold(I)/(III)- and palladium(II)-N-heterocyclic carbene complexes: A review towards biological perspectives. *Journal of Organometallic Chemistry, 882*, 96-111.

Iqbal, M. A., Haque, R. A., Ahamed, M. B. K., Majid, A. M. S. A., & Al-Rawi, S. S. (2013a). Synthesis and anticancer activity of para-xylyl linked bis-benzimidazolium salts and respective Ag(I) N-heterocyclic carbene complexes. *Medicinal Chemistry Research, 22*(5), 2455-2466.

Iqbal, M. A., Haque, R. A., Budagumpi, S., Khadeer Ahamed, M. B., & Abdul Majid, A. M. S. (2013b). Short metal–metal separations and *in vitro* anticancer studies of a new dinuclear silver(I)-N-heterocyclic carbene complex of para-xylyl-linked bis-benzimidazolium salt. *Inorganic Chemistry Communications, 28*, 64-69.

Ismail, N. A., Salman, A. A., Mohd Yusof, M. S., Che Soh, S. K., Kadir Pahirulzaman, K. A., Ali, H. M., & Sarip, R. (2019). Synthesis, cytotoxicity and antineoplastic activities of novel acridine-based platinum(II) organometallic complexes. *Journal of Organometallic Chemistry, 897*, 42-49.

Janssen-Muller, D., Schlepphorst, C., & Glorius, F. (2017). Privileged chiral N-heterocyclic carbene ligands for asymmetric transition-metal catalysis. *Chemical Society Reviews, 46*(16), 4845-4854.

Jayash, S. N., Hashim, N. M., Misran, M., & Baharuddin, N. (2016). *In vitro* evaluation of osteoprotegerin in chitosan for potential bone defect applications. *PeerJ, 4*, Article#e2229.

Jayash, S. N., Hashim, N. M., Misran, M., & Baharuddin, N. A. (2017). Formulation and *in vitro* and *in vivo* evaluation of a new osteoprotegerin–chitosan gel for bone tissue regeneration. *Journal of Biomedical Materials Research Part A, 105*(2), 398-407.

John, A., & Ghosh, P. (2010). Fascinating frontiers of N/O-functionalized N-heterocyclic carbene chemistry: From chemical catalysis to biomedical applications. *Dalton Transactions, 39*(31), 7183-7206.

Johnson, N. A., Southerland, M. R., & Youngs, W. J. (2017). Recent developments in the medicinal applications of silver-NHC complexes and imidazolium salts. *Molecules, 22*(8), Article#1263.

Kalinowska-Lis, U., Felczak, A., Chęcinska, L., Zawadzka, K., Patyna, E., Lisowska, K., & Ochocki, J. (2015). Synthesis, characterization and antimicrobial activity of water-soluble silver (I) complexes of metronidazole drug and selected counter-ions. *Dalton Transactions, 44*(17), 8178-8189.

Kalirajan, R., Kulshrestha, V., Sankar, S., & Jubie, S. (2012). Docking studies, synthesis, characterization of some novel oxazine substituted 9-anilinoacridine derivatives and evaluation for their antioxidant and anticancer activities as topoisomerase II inhibitors. *European Journal of Medicinal Chemistry, 56*, 217-224.

Kalirajan, R., Rafick, M. H. M., Sankar, S., & Jubie, S. (2012). Docking studies, synthesis, characterization and evaluation of their antioxidant and cytotoxic activities of some novel isoxazole-substituted 9-anilinoacridine derivatives. *The Scientific World Journal, 2012*, Article#165258.

Kaloglu, M., Kaloglu, N., Ozdemir, I., Gunal, S., & Ozdemir, I. (2016). Novel benzimidazol-2-ylidene carbene precursors and their silver (I) complexes: Potential antimicrobial agents. *Bioorganic & Medicinal Chemistry, 24*(16), 3649-3656.

Kareem, H. S., Ariffin, A., Nordin, N., Heidelberg, T., Abdul-Aziz, A., Kong, K. W., & Yehye, W. A. (2015). Correlation of antioxidant activities with theoretical studies for new hydrazone compounds bearing a 3,4,5-trimethoxy benzyl moiety. *European Journal of Medicinal Chemistry, 103*(Supplement C), 497-505.

Kerru, N., Singh, P., Koorbanally, N., Raj, R., & Kumar, V. (2017). Recent advances (2015–2016) in anticancer hybrids. *European Journal of Medicinal Chemistry, 142*, 179-212.

Klotz, L. (2012). Active surveillance for favorable-risk prostate cancer: Background, patient selection, triggers for intervention, and outcomes. *Current Urology Reports, 13*(2), 153-159.

Kohanski, M. A., Dwyer, D. J., & Collins, J. J. (2010). How antibiotics kill bacteria: from targets to networks. *Nature Reviews Microbiology*, 8(6), 423-435.

Kora, A. J., & Rastogi, L. (2013). Enhancement of antibacterial activity of capped silver nanoparticles in combination with antibiotics, on model gram-negative and gram-positive bacteria. *Bioinorganic Chemistry and Applications, 2013*, 7-14.

Krishnanjaneyulu, I. S., Saravanan, G., Vamsi, J., Supriya, P., Bhavana, J. U., & Sunil Kumar, M. V. (2014). Synthesis, characterization and antimicrobial activity of some novel benzimidazole derivatives. *Journal of Advanced Pharmaceutical Technology & Research, 5*(1), 21-27.

Kudryavtseva, T., Sysoev, P., Popkov, S., & Klimova, L. (2017). Synthesis and antimicrobial activity of 10-(5-arylamino-1, 3, 4-oxadiazol-2-ylmethyl) acridin-9 (10H)-ones. *Russian Journal of General Chemistry, 87*(8), 1702-1706.

Kumar, P., Kumar, R., & Prasad, D. N. (2013a). Synthesis and biological evaluation of new 9-aminoacridine-4-carboxamide derivatives as anticancer agents: 1st cancer update. *Arabian Journal of Chemistry, 6*(1), 59-65.

Kumar, R., Kaur, M., & Kumari, M. (2012). Acridine: A versatile heterocyclic nucleus. *Acta Poloniae Pharmaceutica, 69*(1), 3-9.

Kumar, R., Kaur, M., & Silakari, O. (2013b). Chemistry and biological activities of thioacridines/thioacridones. *Mini Reviews in Medicinal Chemistry, 13*(8), 1220-1230.

Kumar, R., Sharma, A., Sharma, S., Silakari, O., Singh, M., & Kaur, M. (2017). Synthesis, characterization and antitumor activity of 2-methyl-9-substituted acridines. *Arabian Journal of Chemistry, 10*, S956-S963.

Lang, X., Li, L., Chen, Y., Sun, Q., Wu, Q., Liu, F., Tan, C., Liu, H., Gao, C., & Jiang, Y. (2013). Novel synthetic acridine derivatives as potent DNA-binding and apoptosis-inducing antitumor agents. *Bioorganic & Medicinal Chemistry, 21*(14), 4170-4177.

Li, B., Gao, C.-M., Sun, Q.-S., Li, L.-L., Tan, C.-Y., Liu, H.-X., & Jiang, Y.-Y. (2014). Novel synthetic acridine-based derivatives as topoisomerase I inhibitors. *Chinese Chemical Letters, 25*(7), 1021-1024.

Li, Y.-H., Zhou, B., Shi, Y.-M., Xun, Y.-P., Yang, Y.-H., & Yang, L.-J. (2018). Novel 3-substituted *N*-methylcarbazole–imidazolium salt derivatives: Synthesis and cytotoxic activity. *Chemical Biology & Drug Design, 92*(1), 1206-1213.

Li, Y., Chen, X., Song, Y., Fang, L., & Zou, G. (2011). Well-defined N-heterocyclic carbene silver halides of 1-cyclohexyl-3-arylmethylimidazolylidenes: Synthesis, structure and catalysis in a 3-reaction of aldehydes, amines and alkynes. *Dalton Transactions, 40*(9), 2046-2052.

Liang, X., Luan, S., Yin, Z., He, M., He, C., Yin, L., Zou, Y., Yuan, Z., Li, L., & Song, X. (2018). Recent advances in the medical use of silver complex. *European Journal of Medicinal Chemistry, 157*, 62-80.

Liang, X., Wu, Q., Luan, S., Yin, Z., He, C., Yin, L., Zou, Y., Yuan, Z., Li, L., Song, X., He, M., Lv, C., & Zhang, W. (2019). A comprehensive review of topoisomerase inhibitors as anticancer agents in the past decade. *European Journal of Medicinal Chemistry, 171*, 129-168.

Lin, I. J., & Vasam, C. S. (2007). Preparation and application of N-heterocyclic carbene complexes of Ag (I). *Coordination Chemistry Reviews, 251*(5-6), 642-670.

Liu, C.-S., Chen, P.-Q., Yang, E.-C., Tian, J.-L., Bu, X.-H., Li, Z.-M., Sun, H.-W., & Lin, Z. (2006). Silver(I) complexes in coordination supramolecular system with bulky acridine-based ligands: Syntheses, crystal structures, and theoretical investigations on C−H···Ag close Interaction. *Inorganic Chemistry, 45*(15), 5812-5821.

Liu, L.-X., Wang, X.-Q., Zhou, B., Yang, L.-J., Li, Y., Zhang, H.-B., & Yang, X.-D. (2015). Synthesis and antitumor activity of novel *N*-substituted carbazole imidazolium salt derivatives. *Scientific Reports, 5*, 13101-131120.

Liu, W., & Gust, R. (2013). Metal N-heterocyclic carbene complexes as potential antitumor metallodrugs. *Chemical Society Reviews, 42*(2), 755-773.

Lobo, V., Patil, A., Phatak, A., & Chandra, N. (2010). Free radicals, antioxidants and functional foods: Impact on human health. *Pharmacognosy Reviews, 4*(8), 118-126.

Loh, Y. L., Haziz, U. F. M., Haque, R. A., Amirul, A. A., Aidda, O. N., & Razali, M. R. (2019). The effect of short alkane bridges in stability of bisbenzimidazole-2-ylidene silver(I) complexes: Synthesis, crystal structure and antibacterial activity. *Journal of Coordination Chemistry, 72*(5-7), 894-907.

Makhaeva, G. F., Lushchekina, S. V., Boltneva, N. P., Serebryakova, O. G., Rudakova, E. V., Ustyugov, A. A., Bachurin, S. O., Shchepochkin, A. V., Chupakhin, O. N., Charushin, V. N., & Richardson, R. J. (2017). 9-Substituted acridine derivatives as acetylcholinesterase and butyrylcholinesterase inhibitors possessing antioxidant activity for alzheimer's disease treatment. *Bioorganic & Medicinal Chemistry, 25*(21), 5981-5994.

Matsuda, N., Wang, X., Lim, B., Krishnamurthy, S., Alvarez, R. H., Willey, J. S., Parker, C. A., Song, J., Shen, Y., & Hu, J. (2018). Safety and efficacy of panitumumab plus neoadjuvant chemotherapy in patients with primary her2-negative inflammatory breast cancer. *JAMA Oncology, 4*(9), 1207-1213.

McGuinness, D. S., Green, M. J., Cavell, K. J., Skelton, B. W., & White, A. H. (1998). Synthesis and reaction chemistry of mixed ligand methylpalladium–carbene complexes1. *Journal of Organometallic Chemistry, 565*(1–2), 165-178.

McGuire, S. (2016). World cancer report 2014. Geneva, Switzerland: World Health Organization, international agency for research on cancer, WHO Press, 2015: Oxford University Press. *Advances in Nutrition, 7*(2), 418-419.

Medeiros, G. M. M., Leitão, M. F., & Costa, S. M. (1993). Fluorescence of acridine and acridine 9-carboxylic acid in anionic micelles. *Journal of Photochemistry and Photobiology A: Chemistry*, *72*(3), 225-233.

Medici, S., Peana, M., Nurchi, V. M., Lachowicz, J. I., Crisponi, G., & Zoroddu, M. A. (2015). Noble metals in medicine: latest advances. *Coordination Chemistry Reviews, 284*, 329-350.

Menschutkin, N. (1890a). Beitrage zur kenntnis der affinitatskoeffizienten der alkylhaloide und der organischen amine. *Zeitschrift fur Physikalische Chemie, 5U*(1), 589-600.

Menschutkin, N. (1890b). Uber die affinitatskoeffizienten der alkylhaloide und der amine. *Zeitschrift fur Physikalische Chemie, 6U*(1), 41-57.

Mercs, L., & Albrecht, M. (2010). Beyond catalysis: N-heterocyclic carbene complexes as components for medicinal, luminescent, and functional materials applications. *Chemical Society Reviews, 39*(6), 1903-1912.

Mironovich, L. M., Ageeva, L. S., & Podol'nikova, A. Y. (2016). Nucleophilic substitution of chlorine in 9-chloroacridine with amino(hydrazine, thioxo)-1,2,4-triazines. *Russian Journal of General Chemistry, 86*(2), 420-422.

Morones-Ramirez, J. R., Winkler, J. A., Spina, C. S., & Collins, J. J. (2013). Silver enhances antibiotic activity against gram-negative bacteria. *Science Translational Medicine, 5*(190), Article#190ra181.

Mottais, A., Berchel, M., Le Gall, T., Sibiril, Y., d'Arbonneau, F., Laurent, V., Jaffrès, P.-A., & Montier, T. (2019). Antibacterial and transfection activities of nebulized formulations incorporating long n-alkyl chain silver N-heterocyclic carbene complexes. *International Journal of Pharmaceutics, 567*, 118500.

Moulari, B., Pellequer, Y., Lboutounne, H., Girard, C., Chaumont, J.-P., Millet, J., & Muyard, F. (2006). Isolation and *in vitro* antibacterial activity of astilbin, the bioactive flavanone from the leaves of *Harungana* madagascariensis Lam. ex Poir.(Hypericaceae). *Journal of Ethnopharmacology, 106*(2), 272-278.

Movahedi, E., & Rezvani, A. R. (2018). Multispectroscopic DNA-binding studies and antimicrobial evaluation of new mixed-ligand silver(I) complex and nanocomplex: A comparative study. *Journal of Molecular Structure, 1160*, 117-128.

Musa, M. A., Badisa, V. L., Latinwo, L. M., Waryoba, C., & Ugochukwu, N. (2010). *In vitro* cytotoxicity of benzopyranone derivatives with basic side chain against human lung cell lines. *Anticancer Research, 30*(11), 4613-4617.

Mutee, A., Salhimi, S., Yam, M., Lim, C., Abdullah, G., Ameer, O., Abdulkarim, M., & Asmawi, M. (2010). *In vivo* anti-inflammatory and *in vitro* antioxidant activities of peperomia pellucida. *International Journal of Pharmacology, 6*(5), 686-690.

Nadaraj, V., Selvi, S. T., & Mohan, S. (2009). Microwave-induced synthesis and anti-microbial activities of 7, 10, 11, 12-tetrahydrobenzo [c] acridin-8 (9H)-one derivatives. *European Journal of Medicinal Chemistry, 44*(3), 976-980.

Ndi, C. P., Semple, S. J., Griesser, H. J., Pyke, S. M., & Barton, M. D. (2007). Antimicrobial compounds from Eremophila serrulata. *Phytochemistry, 68*(21), 2684-2690.

Newman, D. J., Cragg, G. M., & Snader, K. M. (2003). Natural products as sources of new drugs over the period 1981− 2002. *Journal of Natural Products, 66*(7), 1022-1037.

Nguyen, T. (2015). Food and cancer: a guide to understanding the secondary causes of cancer. *The Committee on Diet, Nutrition, and Cancer, EnCognitive. com, 1*, 100-200.

Nicolaou, K. C., Chen, J. S., Edmonds, D. J., & Estrada, A. A. (2009). Recent advances in the chemistry and biology of naturally occurring antibiotics. *Angewandte Chemie International Edition, 48*(4), 660-719.

Nowak, K. (2017). Chemical structures and biological activities of bis-and tetrakis-acridine derivatives: A review. *Journal of Molecular Structure, 1146*, 562-570.

Nunez, C., Fernandez-Lodeiro, A., Fernandez-Lodeiro, J., Carballo, J., Capelo, J. L., & Lodeiro, C. (2014). Synthesis, spectroscopic studies and *in vitro* antibacterial activity of Ibuprofen and its derived metal complexes. *Inorganic Chemistry Communications, 45*, 61-65.

Oehninger, L., Rubbiani, R., & Ott, I. (2013). N-heterocyclic carbene metal complexes in medicinal chemistry. *Dalton Transactions, 42*(10), 3269-3284.

Ofele, K. (1968). 1, 3-Dimethyl-4-imidazolinyliden-(2)-pentacarbonylchrom ein neuer ubergangsmetall-carben-komplex. *Journal of Organometallic Chemistry, 12*(3), P42-P43.

Olszewska, P., Mikiciuk-Olasik, E., Błaszczak-Swiatkiewicz, K., Szymanski, J., & Szymanski, P. (2014). Novel tetrahydroacridine derivatives inhibit human lung adenocarcinoma cell growth by inducing G1 phase cell cycle arrest and apoptosis. *Biomedicine & Pharmacotherapy, 68*(8), 959-967.

Orhan, I., Kartal, M., Naz, Q., Ejaz, A., Yilmaz, G., Kan, Y., Konuklugil, B., Sener, B., & Choudhary, M. I. (2007). Antioxidant and anticholinesterase evaluation of selected Turkish salvia species. *Food Chemistry, 103*(4), 1247-1254.

Ou, B., Hampsch-Woodill, M., & Prior, R. L. (2001). Development and validation of an improved oxygen radical absorbance capacity assay using fluorescein as the fluorescent probe. *Journal of Agricultural and Food Chemistry, 49*(10), 4619-4626.

Ozdemir, I., Gurbuz, N., Dogan, O., Gunal, S., & Ozdemir, I. (2010). Synthesis and antimicrobial activity of Ag(I)-N-heterocyclic carbene complexes derived from benzimidazol-2-ylidene. *Applied Organometallic Chemistry, 24*(11), 758-762.

Ozkay, Y., Tunalı, Y., Karaca, H., & Isıkdag, I. (2010). Antimicrobial activity and a SAR study of some novel benzimidazole derivatives bearing hydrazone moiety. *European Journal of Medicinal Chemistry, 45*(8), 3293-3298.

Paiva, P. M., Pontual, E. V., Coelho, L., & Napoleao, T. H. (2013). Protease inhibitors from plants: Biotechnological insights with emphasis on their effects on microbial pathogens. *Microbial Pathogens and Strategies for Combating Them: Science, Technology and Education, 1*, 641-649.

Patil, S., Deally, A., Gleeson, B., Muller-Bunz, H., Paradisi, F., & Tacke, M. (2011). Novel benzyl-substituted N-heterocyclic carbene-silver acetate complexes: Synthesis, cytotoxicity and antibacterial studies. *Metallomics, 3*(1), 74-88.

Patrick, G. L. (2013). An introduction to medicinal chemistry: Oxford University Press. *Illustratedd, OUP Oxford*, 15-85.

Peacock, A. F., & Sadler, P. J. (2008). Medicinal organometallic chemistry: designing metal arene complexes as anticancer agents. *Chemistry–An Asian Journal, 3*(11), 1890-1899.

Pereira, E., Do Quental, L., Palma, E., Oliveira, M. C., Mendes, F., Raposinho, P., Correia, I., Lavrado, J., Di Maria, S., & Belchior, A. (2017). Evaluation of acridine orange derivatives as DNA-targeted radiopharmaceuticals for auger therapy: Influence of the radionuclide and distance to DNA. *Scientific Reports, 7*, 42544-42560.

Perez, S. A., de Haro, C., Vicente, C., Donaire, A., Zamora, A., Zajac, J., Kostrhunova, H., Brabec, V., Bautista, D., & Ruiz, J. (2017). New acridine thiourea gold (I) anticancer agents: Targeting the nucleus and inhibiting vasculogenic mimicry. *ACS Chemical Biology, 12*(6), 1524-1537.

Philippe, B., Johann, B., Thomas, G., & Martin, T. (2007). Acridine and acridone derivatives, anticancer properties and synthetic methods: Where are we now? *Anti-Cancer Agents in Medicinal Chemistry, 7*(2), 139-169.

Potgieter, K., Engelbrecht, Z., Naganagowda, G., Cronje, M. J., & Meijboom, R. (2017). Anticancer activity of silver(I) cyclohexyldiphenylphosphine complexes toward SNO cancer cells. *Journal of Coordination Chemistry, 70*(15), 2644-2658.

Prasad, A., Raju, G., Sivalingam, V., Girdhar, A., Verma, M., Vats, A., Taneja, V., Prabusankar, G., & Patel, B. K. (2016). An acridine derivative, [4,5-bis{(*N*-carboxy methyl imidazolium)methyl}acridine] dibromide, shows anti-TDP-43 aggregation effect in ALS disease models. *Scientific Reports, 6*, 39490-39499.

Radosevic, K., Cvjetko, M., Kopjar, N., Novak, R., Dumic, J., & Srcek, V. G. (2013). *In vitro* cytotoxicity assessment of imidazolium ionic liquids: Biological effects in fish channel catfish ovary (CCO) cell line. *Ecotoxicology and Environmental Safety, 92*(Supplement C), 112-118.

Rakesh, K. P., Kumara, H. K., Manukumar, H. M., & Gowda, D. C. (2019). Anticancer and DNA binding studies of potential amino acids based quinazolinone analogs: Synthesis, SAR and molecular docking. *Bioorganic Chemistry*, 87, 252-264.

Raju, G., Vishwanath, S., Prasad, A., Patel, B. K., & Prabusankar, G. (2016). Imidazolium tagged acridines: synthesis, characterization and applications in DNA binding and anti-microbial activities. *Journal of Molecular Structure, 1107*, 291-299.

Ramachandran, E., Raja, D. S., Bhuvanesh, N. S., & Natarajan, K. (2012). Mixed ligand palladium (II) complexes of 6-methoxy-2-oxo-1, 2-dihydroquinoline-3-carbaldehyde 4 *N*-substituted thiosemicarbazones with triphenylphosphine co-ligand: synthesis, crystal structure and biological properties. *Dalton Transactions, 41*(43), 13308-13323.

Ramle, A. Q., Khaledi, H., Hashim, A. H., Mingsukang, M. A., Arof, A. K. M., Ali, H. M., & Basirun, W. J. (2019). Indolenine–dibenzotetraaza [14] annulene Ni(II) complexes as sensitizers for dye-sensitized solar cells. *Dyes and Pigments, 164*, 112-118.

Ranke, J., Stolte, S., Störmann, R., Arning, J., & Jastorff, B. (2007). Design of sustainable chemical productsthe example of ionic liquids. *Chemical Reviews, 107*(6), 2183-2206.

Rastogi, K., Chang, J.-Y., Pan, W.-Y., Chen, C.-H., Chou, T.-C., Chen, L.-T., & Su, T.-L. (2002). Antitumor AHMA linked to DNA minor groove binding agents: Synthesis and biological evaluation. *Journal of Medicinal Chemistry, 45*(20), 4485-4493.

Ray, S., Mohan, R., Singh, J. K., Samantaray, M. K., Shaikh, M. M., Panda, D., & Ghosh, P. (2007). Anticancer and antimicrobial metallopharmaceutical agents based on palladium, gold, and silver N-heterocyclic carbene complexes. *Journal of the American Chemical Society, 129*(48), 15042-15053.

Ribeiro, A. G., Almeida, S. M. V. d., de Oliveira, J. F., Souza, T. R. C. d. L., Santos, K. L. d., Albuquerque, A. P. d. B., Nogueira, M. C. d. B. L., Carvalho Junior, L. B. d., Moura, R. O. d., da Silva, A. C., Pereira, V. R. A., Castro, M. C. A. B. d., & Lima, M. d. C. A. d. (2019). Novel 4-quinoline-thiosemicarbazone derivatives: synthesis, antiproliferative activity, *in vitro* and in silico biomacromolecule interaction studies and topoisomerase inhibition. *European Journal of Medicinal Chemistry, 182*, Article#111592.

Rice-Evans, C. A., Miller, N. J., & Paganga, G. (1996). Structure-antioxidant activity relationships of flavonoids and phenolic acids. *Free Radical Biology and Medicine, 20*(7), 933-956.

Rippe, J. M. (2013). *Lifestyle Medicine, Second Edition*: CRC Press, 3th, illustrated, 1435.

Rohini, R., Lee, C. K., Lu, J. T., & Lin, I. J. (2013). Symmetrical 1, 3-dialkylimidazolium based ionic liquid crystals. *Journal of the Chinese Chemical Society, 60*(7), 745-754.

Sahin-Bolukbasi, S., & sahin, N. (2019). Novel silver-NHC complexes: Synthesis and anticancer properties. *Journal of Organometallic Chemistry, 891*, 78-84.

Salazar-Aranda, R., Pérez-Lopez, L. A., Lopez-Arroyo, J., Alanís-Garza, B. A., & Waksman de Torres, N. (2011). Antimicrobial and antioxidant activities of plants from northeast of mexico. *Evidence-Based Complementary and Alternative Medicine, 2011,*1-6.

Salman, A. A., Tabandeh, M., Heidelberg, T., Hussen, R. S. D., & Ali, H. M. (2015). Alkyl-imidazolium glycosides: non-ionic—cationic hybrid surfactants from renewable resources. *Carbohydrate Research, 412*, 28-33.

Salman, A. W., Haque, R. A., Budagumpi, S., & Zulikha, H. Z. (2013a). Coordination diversity of Ag(I) and Hg(II) towards symmetrically and non-symmetrically substituted imidazol-2-ylidenes: Synthesis, crystal structures, nitrile reactivity, and Hofmann-type elimination studies. *Polyhedron, 49*(1), 200-206.

Salman, S. M., Heidelberg, T., & Tajuddin, H. A. B. (2013b). N-linked glycolipids by staudinger coupling of glycosylated alkyl diazides with fatty acids. *Carbohydrate Research, 375*, 55-62.

Sandeep, P., & Bisht, P. B. (2006). Photophysics of 9-amino acridine hydrochloride hydrate single microcrystals. *Chemical Physics, 326*(2), 521-526.

Sarı, Y., Akkoc, S., Gok, Y., Sifniotis, V., Ozdemir, I., Gunal, S., & Kayser, V. (2016). Benzimidazolium-based novel silver N-heterocyclic carbene complexes: synthesis, characterisation and *in vitro* antimicrobial activity. *Journal of Enzyme Inhibition and Edicinal Chemistry, 31*(6), 1527-1530.

Sarı, Y., Aktas, A., Celepci, D. B., Gok, Y., & Aygun, M. (2017). Synthesis, characterization and crystal structure of new 2-morpholinoethyl-substituted bis-(NHC) Pd(II) complexes and the catalytic activity in the direct arylation reaction. *Catalysis Letters, 147*(9), 2340-2351.

Shahini, C. R., Achar, G., Budagumpi, S., Müller–Bunz, H., Tacke, M., & Patil, S. A. (2018). Benzoxazole and dioxolane substituted benzimidazole–based N–heterocyclic carbene–silver(I) complexes: Synthesis, structural characterization *and in vitro* antimicrobial activity. *Journal of Organometallic Chemistry, 868*, 1-13.

Shahini, C. R., Achar, G., Budagumpi, S., Tacke, M., & Patil, S. A. (2017). Synthesis, structural investigation and antibacterial studies of non–symmetrically p–nitrobenzyl substituted benzimidazole N–heterocyclic carbene–silver(I) complexes. *Inorganica Chimica Acta, 466*, 432-441.

Sharma, O. P., & Bhat, T. K. (2009). DPPH antioxidant assay revisited. *Food Chemistry, 113*(4), 1202-1205.

Siegel, R. L., Miller, K. D., & Jemal, A. (2015). Cancer statistics, 2015. *CA: A Cancer Journal for Clinicians, 65*(1), 5-29.

Singh, M. S., & Chowdhury, S. (2012). Recent developments in solvent-free multicomponent reactions: a perfect synergy for eco-compatible organic synthesis. *RSC Advances, 2*(11), 4547-4592.

Slimani, I., Mansour, L., Abutaha, N., Harrath, A. H., Al-Tamimi, J., Gürbüz, N., Özdemir, I., & Hamdi, N. (2019). Synthesis, structural characterization of silver(I)-NHC complexes and their antimicrobial, antioxidant and antitumor activities. *Journal of King Saud University - Science*. *32*(2), 1544-1554.

Sondhi, S. M., Kumar, S., Rani, R., Chakraborty, A., & Roy, P. (2013). Synthesis of bis-acridine derivatives exhibiting anticancer and anti-inflammatory activity. *Journal of Heterocyclic Chemistry, 50*(2), 252-260.

Sorrenti, V., Salerno, L., Di Giacomo, C., Acquaviva, R., Siracusa, M. A., & Vanella, A. (2006). Imidazole derivatives as antioxidants and selective inhibitors of nNOS. *Nitric Oxide, 14*(1), 45-50.

Srivastava, A. (2011). Synthesis and structural investigations of co-ordination compounds of palladium(II) with uracil, uracil 4 carboxylic acid and 4-amino uracil. *Journal of Bioscience and Bioengineering*, *2*, 213-219.

Staderini, M., Bolognesi, M. L., & Menéndez, J. C. (2015). Lewis acid-catalyzed generation of c-c and c-n bonds on π-deficient heterocyclic substrates. *Advanced Synthesis & Catalysis, 357*(1), 185-195.

Streciwilk, W., Cassidy, J., Hackenberg, F., Muller-Bunz, H., Paradisi, F., & Tacke, M. (2014). Synthesis, cytotoxic and antibacterial studies of p-benzyl-substituted NHC–silver(I) acetate compounds derived from 4, 5-di-p-diisopropylphenyl-or 4, 5-di-p-chlorophenyl-1H-imidazole. *Journal of Organometallic Chemistry, 749*, 88-99.

Subramanya Prasad, T., Shahini, C., Patil, S. A., Huang, X., Bugarin, A., & Patil, S. A. (2017). Non-symmetrically p-nitrobenzyl-and p-cyanobenzyl-substituted N-heterocyclic carbene-silver(I) complexes: Synthesis, characterization and antibacterial studies. *Journal of Coordination Chemistry, 70*(4), 600-614.

Tacke, M. (2015). Benzyl-substituted carbene–metal complexes: potential for novel antibiotics and anticancer drugs. *Journal of Organometallic Chemistry, 782*, 17-21.

Tan, S. J., Yan, Y. K., Lee, P. P. F., & Lim, K. H. (2010). Copper, gold and silver compounds as potential new anti-tumor metallodrugs. *Future Medicinal Chemistry, 2*(10), 1591-1608.

Tang, J., Chu, B., Wang, J., Song, B., Su, Y., Wang, H., & He, Y. (2019). Multifunctional nanoagents for ultrasensitive imaging and photoactive killing of Gram-negative and Gram-positive bacteria. *Nature Communications*, 10(1), 1-14.

Tellez, F., Lopez-Sandoval, H., Castillo-Blum, S. E., & Barba-Behrens, N. (2008). Coordination behavior of benzimidazole, 2-substituted benzimidazoles and benzothiazoles towards transition metal ions. *ChemInform, 39*(40), 245-275.

Teyssot, M.-L., Jarrousse, A.-S., Manin, M., Chevry, A., Roche, S., Norre, F., Beaudoin, C., Morel, L., Boyer, D., & Mahiou, R. (2009). Metal-NHC complexes: a survey of anti-cancer properties. *Dalton Transactions, 35*, 6894-6902.

Thaipong, K., Boonprakob, U., Crosby, K., Cisneros-Zevallos, L., & Byrne, D. H. (2006). Comparison of ABTS, DPPH, FRAP, and ORAC assays for estimating antioxidant activity from guava fruit extracts. *Journal of Food Composition and Analysis, 19*(6-7), 669-675.

Turrens, J. F. (2003). Mitochondrial formation of reactive oxygen species. *The Journal of Physiology, 552*(2), 335-344.

Ullmann, F. (1903). On a new formation of diphenylamine derivatives. *Berichte der Deutschen Chemischen Gesellschaft, 36*, 2382-2384.

Ullmann, F., Racovitza, N., & Rozenband, M. (1902). Ueber phenylnaphtacridinderivate. *Berichte der Deutschen Chemischen Gesellschaft, 35*(1), 316-325.

Valko, M., Rhodes, C., Moncol, J., Izakovic, M., & Mazur, M. (2006). Free radicals, metals and antioxidants in oxidative stress-induced cancer. *Chemico-Biological Interactions, 160*(1), 1-40.

Wainwright, M. (2001). Acridine—a neglected antibacterial chromophore. *Journal of Antimicrobial Chemotherapy, 47*(1), 1-13.

Wang, C. C., Chu, C. Y., Chu, K. O., Choy, K. W., Khaw, K. S., Rogers, M. S., & Pang, C. P. (2004). Trolox-equivalent antioxidant capacity assay versus oxygen radical absorbance capacity assay in plasma. *Clinical Chemistry, 50*(5), 952-954.

Wang, H. M. J., & Lin, I. J. B. (1998). Facile synthesis of silver(I)−carbene complexes. useful carbene transfer agents. *Organometallics, 17*(5), 972-975.

Wang, Y., Gao, D., Chen, Z., Li, S., Gao, C., Cao, D., Liu, F., Liu, H., & Jiang, Y. (2013). Acridone derivative 8a induces oxidative stress-mediated apoptosis in CCRF-CEM leukemia cells: Application of metabolomics in mechanistic studies of antitumor agents. *PloS One, 8*(5), Article#e63572.

Wang, Z., Wen, J., Bi, Q.-W., Xu, X.-Q., Shen, Z.-Q., Li, X.-X., & Chen, Z. (2014). Oxirane synthesis from diazocarbonyl compounds via NHC-Ag^+ catalysis. *Tetrahedron Letters, 55*(18), 2969-2972.

Wanzlick, H.-W., & Schonherr, H.-J. (1968). Direct synthesis of a mercury salt-carbene complex. *Angewandte Chemie International Edition in English, 7*(2), 141-142.

Wayne, P. (2002). National committee for clinical laboratory standards. *Performance Standards for Antimicrobial Disc Susceptibility Testing, 12*, 01-53.

Wesierska-Gadek, J., Schloffer, D., Gueorguieva, M., Uhl, M., & Skladanowski, A. (2004). Increased susceptibility of poly (ADP-Ribose) polymerase-1 knockout cells to antitumor triazoloacridone C-1305 is associated with permanent G~ 2 cell cycle arrest. *Cancer Research, 64*(13), 4487-4497.

Weskamp, T., Bohm, V. P., & Herrmann, W. A. (2000). N-heterocyclic carbenes: state of the art in transition-metal-complex synthesis. *Journal of Organometallic Chemistry, 600*(1), 12-22.

Wiegand, I., Hilpert, K., & Hancock, R. E. (2008). Agar and broth dilution methods to determine the minimal inhibitory concentration (MIC) of antimicrobial substances. *Nature Protocols, 3*(2), 163-175.

Wylie, W., Lough, A. J., & Morris, R. H. (2010). Palladium(II) and platinum(II) complexes featuring a nitrile-functionalized N-heterocyclic carbene ligand. *Organometallics, 3*(29), 570-581.

Xu, X.-L., Yu, C.-L., Chen, W., Li, Y.-C., Yang, L.-J., Li, Y., Zhang, H.-B., & Yang, X.-D. (2015). Synthesis and antitumor activity of novel 2-substituted indoline imidazolium salt derivatives. *Organic & Biomolecular Chemistry, 13*(5), 1550-1557.

Yehye, W. A., Rahman, N. A., Ariffin, A., Hamid, S. B. A., Alhadi, A. A., Kadir, F. A., & Yaeghoobi, M. (2015). Understanding the chemistry behind the antioxidant activities of butylated hydroxytoluene (BHT): A review. *European Journal of Medicinal Chemistry, 101*, 295-312.

Youngs, W. J., Knapp, A. R., Wagers, P. O., & Tessier, C. A. (2012). Nanoparticle encapsulated silver carbene complexes and their antimicrobial and anticancer properties: a perspective. *Dalton Transactions, 41*(2), 327-336.

Zhang, B., Li, X., Li, B., Gao, C., & Jiang, Y. (2014a). Acridine and its derivatives: a patent review (2009 - 2013). *Expert Opinion on Therapeutic Patents, 24*(6), 647-664.

Zhang, L., Peng, X. M., Damu, G. L., Geng, R. X., & Zhou, C. H. (2014b). Comprehensive review in current developments of imidazole-based medicinal chemistry. *Medicinal Research Reviews, 34*(2), 340-437.

Zhong, R., Lindhorst, A. C., Groche, F. J., & Kuhn, F. E. (2017). Immobilization of N-heterocyclic carbene compounds: A synthetic perspective. *Chemical Reviews, 117*(3), 1970-2058.

Zhang, W., Zhang, B., Yang, T., Wang, N., Gao, C., Tan, C., Liu, H., & Jiang, Y. (2016). Synthesis and antiproliferative activity of 9-benzylamino-6-chloro-2-methoxy-acridine derivatives as potent DNA-binding ligands and topoisomeraseII inhibitors. *European Journal of Medicinal Chemistry, 116*, 59-70.

Zhou, B., Liu, Z.-F., Deng, G.-G., Chen, W., Li, M.-Y., Yang, L.-J., Li, Y., Yang, X.-D., & Zhang, H.-B. (2016a). Synthesis and antitumor activity of novel *N*-substituted tetrahydro-β-carboline–imidazolium salt derivatives. *Organic & Biomolecular Chemistry, 14*(39), 9423-9430.

Zhou, L., Lokman Hossain, M., & Xiao, T. (2016b). Synthesis of N-containing heterocyclic compounds using visible-light photoredox catalysis. *The Chemical Record, 16*(1), 319-334.

Zugic, A., Dordevic, S., Arsic, I., Markovic, G., Zivkovic, J., Jovanovic, S., & Tadic, V. (2014). Antioxidant activity and phenolic compounds in 10 selected herbs from Vrujci Spa, Serbia. *Industrial Crops and Products, 52*(Supplement C), 519-527.

Zugic, A., Jeremic, I., Isakovic, A., Arsic, I., Savic, S., & Tadic, V. (2016). Evaluation of anticancer and antioxidant activity of a commercially available CO_2 supercritical extract of old man's beard (usnea barbata). *PloS One, 11*(1), Article#e0146342.

LIST OF PUBLICATIONS AND PAPERS PRESENTED

List of publications:

Sharhan, O., Heidelberg, T., Hashim, N. M., Salman, A. A., Ali, H. M., & Jayash, S. N. (2018). Synthesis and biological study of acridine-based imidazolium salts. *RSC Advances, 8*(68), 38995-39004.

Sharhan, O., Heidelberg, T., Hashim, N. M., & Al-Madhagi, M., W., Ali, H. M., (2020). Benzimidazolium-acridine-based silver N-heterocyclic carbene complexes as potential anti-bacterial and anti-cancer drug. *Inorganica Chimica Acta, 8*(68), 38995-39004.

Al-Madhagi, W. M., Hashim, N. M., Awadh Ali, N. A., Taha, H., Alhadi, A. A., Abdullah, A. A., **Sharhan, O**., & Othman, R. (2019). Bioassay-guided isolation and in silico study of antibacterial compounds from petroleum ether extract of Peperomia blanda (Jacq.) Kunth. *Journal of Chemical Information and Modeling*, *59*(5), 1858-1872.

Papers Presented

1- Olla Sharhan, Thorsten Heidelberg, Najihah Mohd Hashim, Synthesis, characterization and biological study of acridine imidazolium salt, The 31st International conference of analytical science 2018 (SKAM31), 17-19 August 2018, Vistana Hotel, Kuantan, Pahang, Malaysia. (best poster presenter).

2- Olla Sharhan, Thorsten Heidelberg, Najihah Mohd Hashim, Synthesis, characterization and biological activity of acridine derivatives and their complexes, 1st Mini symposium and workshop on Chemical Crystallography (2019), 5-6 August 2018, University of Malaya, Kuala Lumpur, Malaysia. (Oral presenter).